TOTAL SYNTHESIS OF ARGYRIN A AND ANALOGUES THEREOF

By Chou-Hsiung Chen, BSc

Thesis submitted to the University of Nottingham

for the degree of Doctor of Philosophy

January 2013

Abstract

The cyclin dependent kinase inhibitor p27 is one of the most frequently dysregulated tumour suppressor protein in human cancers. A reduction in the level of cellular p27 is frequently due to increased proteasome-dependent degradation. Recently, studies show that the macrocyclic octapeptide argyrin A induced an increase in cellular p27 levels by preventing the turnover of the protein *via* inhibition of proteasome function.

In order to investigate this interesting biological property, this project embarked on the total synthesis of argyrin A, a naturally occurring macrocyclic peptide originally isolated from myxobacteria *Archangium gephyra*. Argyrin A is a non-ribosomal octapeptide containing four standard amino acids and three unusual amino acid-based subunits.

The synthesis of these three unusual amino acid components was established. In particular, a novel generic synthetic route to access the optically pure *N*-Fmoc-4-methoxy-tryptophan and analogues thereof was developed. Key features of the synthetic route include the use of chiral Strecker amino acid synthesis and mild conditions to hydrolyse α-amino nitrile to α-amino acid.

Furthermore, the total synthesis of argyrin A and analogues was accomplished by the application of modern solid-phase chemistry and macrocyclisation strategies. This platform technology will enable the robust total chemical synthesis of a focused library of argyrin analogues, which will facilitate a comprehensive SAR study.

Additionally, the synthesised argyrin A and analogues thereof comprising unique tryptophan analogues were tested in a cytotoxicity assay against HCT-117 human colon cell line. The results showed that all synthetic argyrin derivatives display growth inhibitory effects at nanomolar concentrations. The best result was obtained for the argyrin A and (5-methoxy-Trp^4)argyrin with GI_{50} value at 1.8 and 3.8 nM, respectively. In summary, it became apparent that the methoxy group at 4- or 5-position of tryptophan-5 residue is essential for the biological activity of argyrin.

Acknowledgements

I would like to thank my supervisors Prof. Peter Fischer and Dr. Weng Chan to their continued support, guidance and encouragement throughout my Ph.D study. In this three year, they were dedicated to teach me. Not only did they provide helpful advice concerning my project, but also patiently guide my language learning and understanding of chemical reactions and their mechanism. Many thanks also to Tracey Bradshaw who provided invaluable help and advice during the biological study. In addition, I would also like to thank the CS Bio. for the partial funding of my study.

I am especially grateful to all of the present and past members of the chemistry corridor in CBS for their friendship as well as their assistants. I would especially like to express my thanks to Sivaneswary Genapathy for helping me with bioassay and looking out for grammatical errors of my thesis throughout the write-up year of my PhD study. I would also like to thank Cillian Byrne, Chris Gordon and Fabio Rui who always willing to offer invaluable suggestion and help every time when reaction doesn't work.

During my time in Nottingham, I am extremely grateful for all of the help from so many people who have contributed to my growth as a chemist and as a person. I would like to thank Christophe Fromont and Fadi Soukarieh for bringing bright, enjoyable working atmosphere to me. I would also like to thank Gavin Hackett, Rob Hampson and Alex Disney who bring me to authentic British culture. Also thank to my three-year housemate Mo Tian for supporting me when things were difficult. I am especially grateful to my girlfriend Polly Hu, her presence in my life makes my PhD journey feel complete.

Finally, my study would not have been possible without the confidence, endurance and financial support of my family. I deeply express my sincere thanks to my parents to support me during my life trip and my PhD.

Abbreviations

AcOH	Acetic acid
Ala	Alanine
APC	Anaphase-promoting complex
Bn	Benzyl
Boc	*tert*-Butoxycarbonyl
CAN	Ceric ammonium nitrate
CBz	Carbobenzyloxy
C-L	Caspase-like
CT-L	Chymotrypsin-like
CAK	CDK-activating kinase
CDK	Cyclin dependant kinase
CKI	Cyclin-dependant kinase inhibitor
m-CPBA	*m*-Chloroperoxybenzoic acid
COSY	Correlation spectroscopy
DABCO	1,4-Diazabicyclo[2.2.2]octane
DCC	1,3-Dicyclohexylcarbodiimide
DBU	1,8-Diazabicyclo[5.4.0]undec-7-ene
DCM	Dichloromethane
DDQ	2,3-Dichloro-5,6-dicyano-1,4-benzoquinone
Dha	Dehydroalanine
DIAD	Diisopropyl azodicarboxylate
DEAD	Diethyl azodicarboxylate
DME	Dimethoxyethane
DIC	1,3-Diisopropylcarbodiimde
DIPEA	*N*,*N*-Diisopropylethylamine
DMF	*N*,*N*-Dimethylformamide
DMSO	Dimethylformamide
$DMSO_2$	Dimethyl sulfone
DNA	Deoxyribose nucleic acid
DUBs	Deubiquitylation enzymes
ER	Endoplasmic reticulum
Et_2O	Diethyl ether

Abbreviations

EtOAc	Ethyl acetate
Fmoc	9-Fluorenylmethoxycarbonyl
FDA	Food and drug administration
FT-IR	Fourier-transform infra-red
GI_{50}	50 % maximal growth inhibition
Gly	Glycine
HATU	*N*-[(Dimethylamino)-1H-1,2,3-triazolo-[4,5-b]pyridin-1-ylmethylene]-*N*-methylmethanaminium hexafluorophosphate *N*-oxide
HOAt	1-Hydroxy-7-azabenzotriazole
HOBt	1-Hydroxybenzotriazole
IC_{50}	50 % maximal inhibitory concentration
IκB	Nuclear factor kappa-light-chain-enhancer of activated B cells
IPA	Isopropyl alcohol
*K*i	Inhibition constant between a proteasome and its inhibitor
KPC	Kip1 ubiquitylation-promoting complex
mp	Melting point
MeOH	Methanol
MM	Multiple myeloma
MS	Mass spectrometry
MTPA	Methoxy-α-trifluoromethylphenylacetic acid
MTT	3-(4,5-Dimethythiazol- 2-yl)-2,5-diphenyl tetrazolium bromide
M.W.	Microwave irradiation
NBS	*N*-Bromosuccinimide
NF-κB	Nuclear factor kappa B
NMR	Nuclear magnetic resonance
Ph(Se)	Phenylselenocysteine
PMB	*p*-Methoxybenzyl
PLP	Pyridoxal 5'-phosphate cofactor
PPh_3	Triphenylphosphine
PyBOP	Benzotriazolyloxy-tris[pyrrolidino]-phosphonium hexafluorophosphate
PyOxim	(Ethyl cyano(hydroxyimino)acetato)-tri-(1-pyrrolidinyl)-phosphonium hexafluorophosphate
Rb	Retinoblastoma protein
RP-HPLC	Reverse phased high-performance liquid chromatography

rt	Room temperature
SAR	Structure-activity relationship
Sar	Sarcosine
SCF	Skp, Cullin, F-box containing complex
SKP2	S-phase kinase-associated protein 2
SPPS	Solid phase peptide synthesis
TFA	Trifluoroacetic acid
TFAA	Trifluoroacetic acid anhydride
TGF-β	Transforming growth factor-beta
THF	Tetrahydrofuran
TIPS	Triisopropylsilane
T-L	Trypsin-like
TLC	Thin-layer chromatography
Thr	Threonine
Thz	Thiazole
t_R	Retention time
Trp	Tryptophan
Trp(X)	Tryptophan derivatives
UP	Ubiquitin-proteasome
UV	Ultra violet
v/v	Volume per volume

Contents

Chapter 1
Introduction

The proteasome is responsible for the degradation of most intracellular proteins, including those crucial for the cell cycle regulation and induction of apoptosis. With the increasing understanding of the ubiqutin-proteasome pathway, the proteasome has become an attractive drug target for anti-cancer therapy.

Several types of proteasome inhibitors have been developed. Bortezomib (**13**), currently as the first-line treatment of multiple myeloma, has demonstrated the clinical value of proteasome inhibition. There are currently five proteasome inhibitors in clinical development, belonging to three different structural classes.[1]

Apart from those, recent studies have revealed that the cyclic octapeptide argyrin A, a secondary metabolite of myxobacteria, can be regarded as a potential alternative to bortezomib.[2] Its anti-tumour activity is believed to depend on the stabilisation of the tumour suppressor p27.[3]

The major goal of this project is the total synthesis of the naturally occurring proteasome inhibitor argyrin A and analogues. This chapter outlines the rationales for targeting the proteasome in cancer therapy, followed by the literature review on the existing proteasome inhibitors.

1.1 Cyclin-dependent kinase inhibitor p27

As a cyclin-dependent kinase inhibitors (CKIs), p27 is a broad-spectrum inhibitor that binds and inhibits cyclinD-CDK4, cyclinE-CDK2, and cyclinA-CDK2, where the former two complexes are important for G1 progression and the latter is essential for the S phase (Figure 1-1). The CDK-inhibiting activity of p27 in the cell cycle can be explained by two aspects: its concentration and the phosphorylation status.[4]

1.1.1 Cell cycle

The cell cycle, also known as cell division cycle, is a process by which one cell divides into two daughter cells. In eukaryotic cells, the division frequency and the division time vary considerably according to cell types. For example, skin cells divide more frequently than liver cells. The latter only divide when damaged cells need to be repaired. In addition, specialised cell (*e.g.* nerve cells and muscle cells) cease to divide when the body reaches maturity.[5]

The cell cycle consists of two phases, the interphase and the mitosis phase. Prior to the cycle, the cells stop dividing or they are at rest, which is called the quiescent state (G0). During the interphase, which accounts for ninety percent of the cycle duration, the cells grow, duplicate their DNA and accumulate nutrients needed for mitosis. Mitosis is a relatively short period of the cycle. During this time, the chromosomes separate into two identical sets, followed by division of the nuclei, cytoplasm and cell membranes into two identical cells.[6]

The interphase can be divided into three distinct phases; the gap phase (G1), synthesis phase (S) and the second gap phase (G2) (Figure 1-1). Normally, a cell cycle begins with the G1 phase during which the cells increase in size. Significant

biosynthesis of enzymes required for DNA replication also takes place during this phase. During the S phase, the chromosomal DNA and centrosome duplication are mediated by several enzymes. During the G2 phase, the cell continues to grow and prepares microtubules for mitosis.[6]

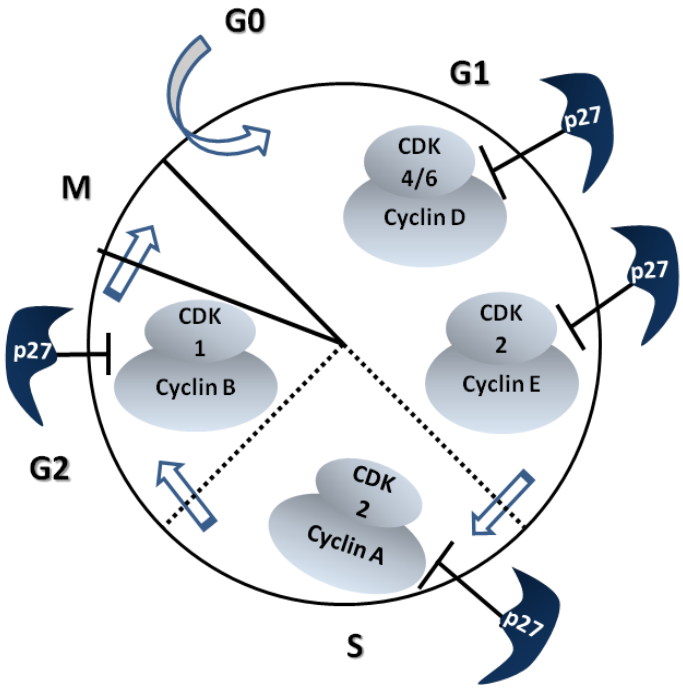

Figure 1-1 p27 in cell cycle control.

1.1.2 Cell cycle regulation

To ensure a precise cell division, there are several sensoring mechanisms, known as the cell cycle checkpoints. There are three checkpoints that ensure genomic integrity, namely the G1, G2 and mitotic spindle checkpoints.[7] They are regulated by several types of regulatory proteins cooperatively, such as cyclins, cyclin dependent kinases (CDKs) and cyclin dependent kinase inhibitors (CKIs).[8]

The cyclins regulate the cell cycle *via* their cyclical increase and decrease in levels. Regulation is mediated by the phosphorylation of the substrates by the functional heterodimeric complexes formed by cyclins and CDKs. However, during the G1 phase, the kinase activity of CDK is usually inactivated by CKI. For example, p27, one of the CKIs, can block the active site of cyclinE-CDK2 during the G1 phase. Once a cell progresses from the G1 to S phase, p27 is removed from cyclinE-CDK2, releasing the kinase activity.[9]

The G1 check point, also known as the restriction point, is located at the end of the G1 phase to check if the DNA is undamaged.[10] In response to DNA damages, the G1 checkpoint stops the cell cycle by increasing the level of two CKIs, p27 and p21. This inactivates the CDKs and prevents the cell from entering into the S phase.

When the cell passes the G1 checkpoint, cyclinD-CDK4/6 complexes can inactivate the tumour suppressor retinoblastoma protein (Rb) by phosphorylation and partially release the transcription factor E2F (Figure 1-2).[11] The partially released E2F induces the expression of cyclin E which forms a complex with CDK2. The cyclinE-CDK2 complex then fully releases E2F by further phosphorylation of Rb. The fully released E2F triggers the expression of downstream cyclins (*e.g.* cyclin A) and other proteins required for DNA synthesis in the S phase.[12]

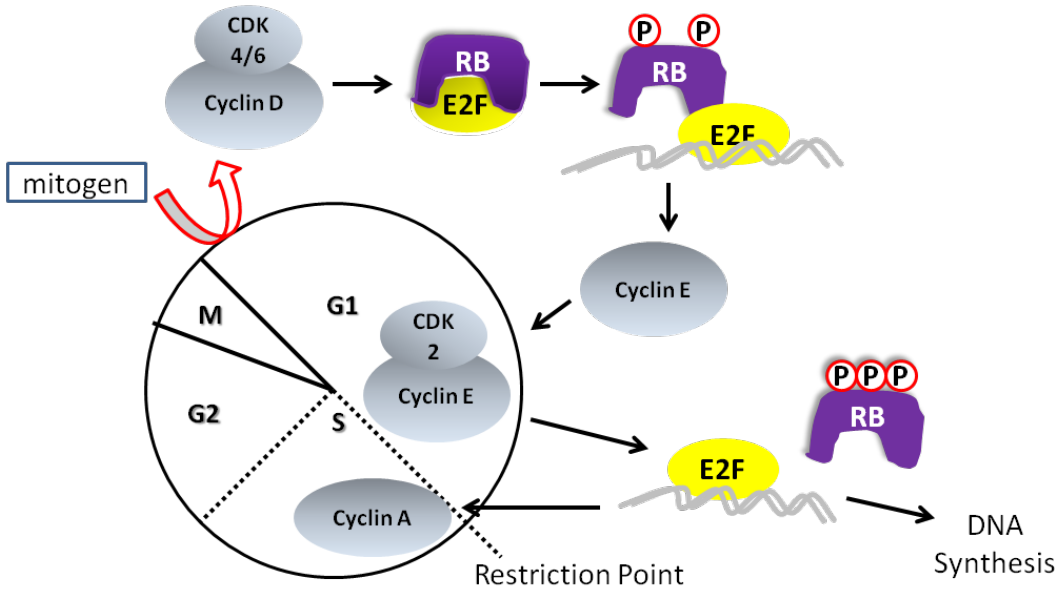

Figure 1-2 Regulation of G1 and the G1/S transition. (Adapted from Malumbres *et al.*)[12]

The G2 checkpoint at the end of the G2 phase prevents a damaged genome from entering mitotic phase. Cyclin B-CDK1 complex is required for G2-M transition. In response to the damaged or unrepaired DNA, two kinases Myt1 and Wee1 phosphorylate cyclin B-CDK1 complex, which results in deactivation of CDK1 activity. During the mitosis transition, CDK1 is activated by the phosphatase cdc25, which then triggers the initiation of mitosis (Figure 1-3).[13]

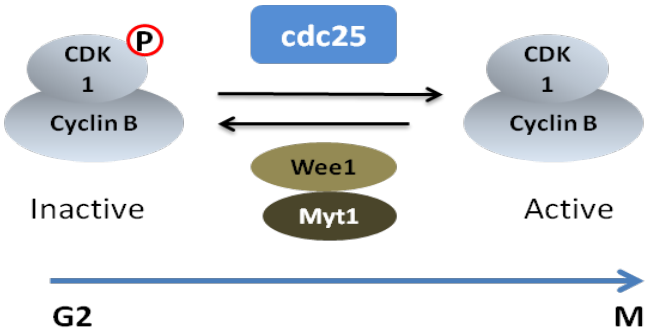

Figure 1-3 The G2 checkpoint.

The mitotic spindle checkpoint, the checkpoint at mitosis phase, ensures precise chromosome transmission. It stops the cell cycle progression if spindle damage and /or unattached kinetochores were present.[14] Its signalling cascade is mediated by several cell cycle arrest proteins, including Bub3, Mad2, Mad3 and cdc20.[15] In response to unattached kinetochores, the spindle checkpoint stops the cycle by inhibiting the anaphase-promoting complex (APC) of which the APC activator cdc20 is further blocked by the interaction of Bub3, Mad2 and Mad3 (Figure 1-4). When the last kinetochore is attached to the microtubules of the spindle, Bub3, Mad2 and Mad3 dissociate from APC, activating APC-cdc20 for the anaphase.

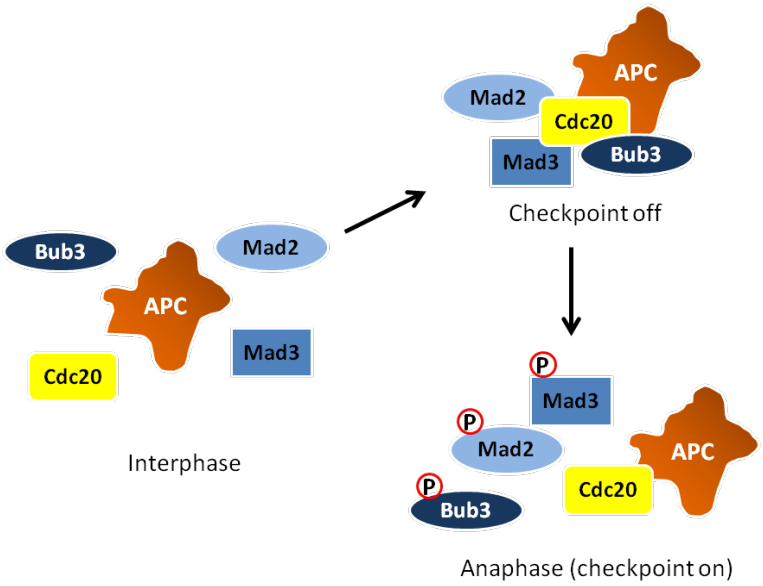

Figure 1-4 Inhibition of APC-cdc20 complex by combined action of Bub3, Mad2 and Mad3. (Adapted from Hardwick *et al.*)[15]

1.1.3 **Cyclin dependent kinase inhibitors (CKIs)**

The cyclin and CDK themselves do not have kinase activity unless they bind to each other by forming non-covalent complexes. Cyclin-CDK complexes are essential for regulating and timing the cell cycle progressions from one phase to the next. The activation of a cyclin-CDK is a two-step process.[16] In the first step, the CDK is bound by cyclin with the assistance of the cyclin-binding motif, resulting in it an active configuration. In the second step, the CDK is phosphorylated at Thr-160 by CDK-activating kinase (CAK), which further change the CDK conformation that allows cyclin-CDK to bind its substrates.[17]

The activity of cyclin-CDK complexes can be controlled in several ways. They can be directly inhibited by the phosphorylation of their CDK catalytic sites. Alternatively, one can control the abundance of cyclin-CDK through the expression and degradation of cyclins since the concentration of CDKs do not fluctuate during the cell cycle.[18]

Recent studies have found that the activity of cyclin-CDK is also constrained by cyclin dependent kinase inhibitors (CKIs), which regulate the cell cycle especially during phase transitions. The effectiveness of CKIs are controlled by three ways; their concentrations, the distribution of bound- and unbound-CDK complexes and their subcellular localisation.[19]

In mammalian cells, CKIs are grouped into two families based on their sequence alignments and the specificity of cyclin-CDK targets. One family is the inhibitors of cyclin-dependent kinase 4 family (INK4) that are named for their specific ability to inhibit the catalytic sites of CDK4 and CDK6. The proteins of this family, including $p15^{INK4B,\ MTS2}$, $p16^{INK4,\ MTS1}$, $p18^{INK4c}$ and $p19^{INK4D}$ act as tumour suppressor proteins during the G1 phase.[20] In particular, they are induced by the extracellular anti-proliferative signals such as growth factors (TGF-β) and hormones, and hence block the active subunit of cyclinD-CDK4. The cell cycle then arrests at the G1 phase. Interestingly, it has been found that the INK4 tumour suppressor protein is mutated in a wide range of human cancers.[21]

The other family of CKIs is the Kip/Cip family, including $p27^{kip1}$, $p21^{cip1, WAF-1}$, and $p57^{kip2}$. They are able to bind to and hence inhibit various classes of cyclin-CDK complexes such as cyclinD-CDK4/6 and cylcinE-CDK2 complexes at the G1 phase, cyclinA-CDK2 complex at the S phase and cyclinA-CDK1 at the G2 phase.[22-24] Therefore, cyclin-CDK complexes are activated and phase transitions can occur when CKIs are effectively removed through the ubiquitin-proteasome degradation process. For example, p27 reaches its highest level during the G0 and early G1 phase. During late G1 and S phases the level rapidly declines due to its degradation by the proteasome.

Unlike INK4, the genes of those proteins in the Kip/Cip family are rarely mutated, but their levels are reduced in many cancer cells due to the over-degradation or the relocation from nucleus to the cytoplasm.[25] Therefore, one of the possible cancer therapies, on which is this thesis focus, is to stabilise Kip/Cip protein levels.

1.1.4 **p27, a multifunctional CKI**

As one of Kip/Cip inhibitors, p27 governs the transition from the G0 to G1 and the G1 to S phase. It was discovered in 1994. Thus, the treatment of the mink lung cell with the anti-proliferative signal, transforming growth factor (TGF-β), triggered the accumulation of p27 and consequently induced cell cycle arrest.[22] This indicates that it is the extracellular proliferative signals that are responsible for the reduction of p27, although the signalling pathway was not elucidated. Moreover, throughout the cell cycle, the p27 mRNA level remained constant while the p27 level varied, implying that the level of p27 is modulated through translational and posttranslational regulations.

Figure 1-5 illustrates the level of p27 during the cell cycle. During the G0 phase when the p27 level is high, the activities of CDKs are low. However, during the transitions from the G0 to G1 phase and from the G1 to S phase, the p27 level decreases and the CDK activity is increased.[4]

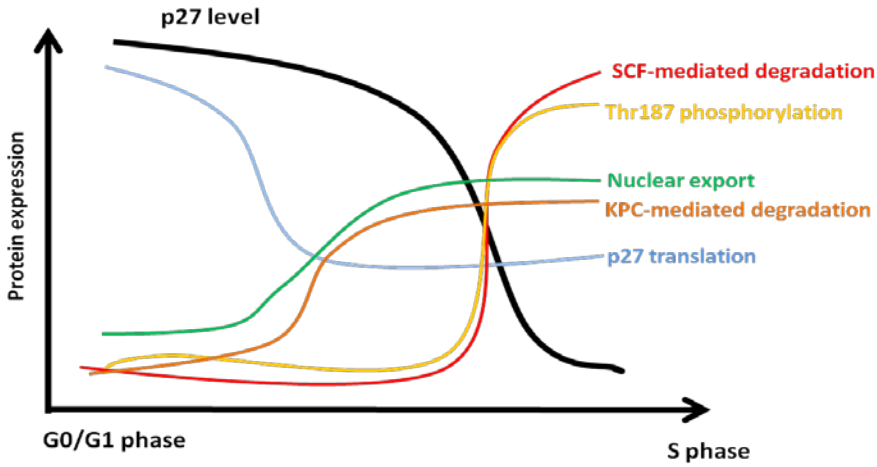

Figure 1-5 p27 levels and regulation during G0/G1 to S phase. (Reproduced from Hardwick *et al.*)[4]

1.1.4.1 The role of p27 in the G0/G1 transition

During the G0 to early G1 phase, most p27 binds to the cyclinE-CDK2 complex and inhibits its activity. During the G1 phase, the growth factors, such as fibroblast growth factors (FGFs), trigger the phosphorylation of p27 at Ser10 by kinases-interacting stathmin (KIS) or the arginine-directed serine/threonine kinase Mirk/DYRK (Figure 1-6 (a)).[26, 27] The phosphorylated S10-p27 is recognised by the exportin CRM1 which then targets and interacts with nuclear export signal (NES). This enables the dissociation of p27 from the cyclinE-CDK2 and for the nuclear exportation. The exportation begins with the binding of the transport protein RanGTP to the exportin CRM1, forming a RanGTP-exportin-p27 complex.[28] This ternary complex is then transported to cytoplasm through the nuclear pore embedded in the nuclear envelope. In the cytoplasm, RanGTP is hydrolysed to RanGDP by Ran GTPase activating protein, changing the exportin's conformation to dissociate from p27.

The monomeric p27 in the cytoplasm has two destinations that depend on the concentration of mitogenic signals (Figure 1-6 (b)); In the absence of the signals, p27 is directly ubiquitinated by the ubiquitin ligase KPC (kip1 ubiquitylation promoting complex).[29] This leads to the degradation of p27 by the 26S proteasome (see Section 1.2.3 for details). With the presence of the signals, p27 is phosphorylated at both T157 and T198 by AGC kinase. This results in the

promotion of the assembly the p27-cyclinD-CDK complexes but without activating it.[30, 31]

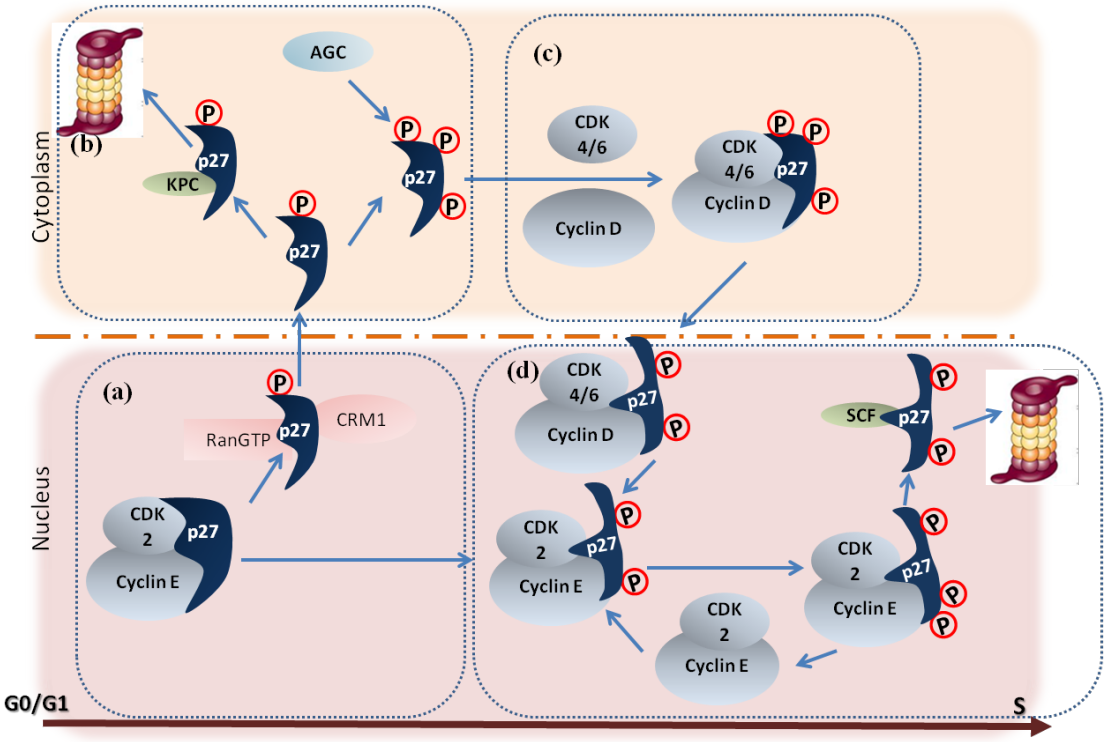

Figure 1-6 Model of signalling pathway that regulate p27. (Modified from Chu *et al.*)[4]

1.1.4.2 The role of the p27 in the G1/S transition

The p27-cyclinD-CDK4/6 complex is essential for the cell progressing from the G1 to S phase (Figure 1-6 (c)).[32,33] The assembly process is triggered by extracellular mitogen *via* the Ras-MEK-MAPK signal pathway.[34] Generally, the Ras signal firstly promotes the expression of cyclin D. p27 then binds to both cyclin D and CDK4/6, acting as an assembly factor for cyclinD-CDK4/6. However, the nature of this ternary-complex interaction remains unclear.

In order to activate the cyclinD-CDK4/6, the complex is transported to the nucleus and the p27 has to be removed from the active sites of cyclinD-CDK4/6. Studies have shown that the phosphorylation of p27 at the key tyrosine residue at position 88 (Y88) involves two kinases, the Src and Bcr-abl kinase.[35, 36] This results in the inhibitory domain 3_{10}-helix of p27 to be ejected from the ATP-binding pocket of CDK4/6 (see Figure 1-7).[37 38]

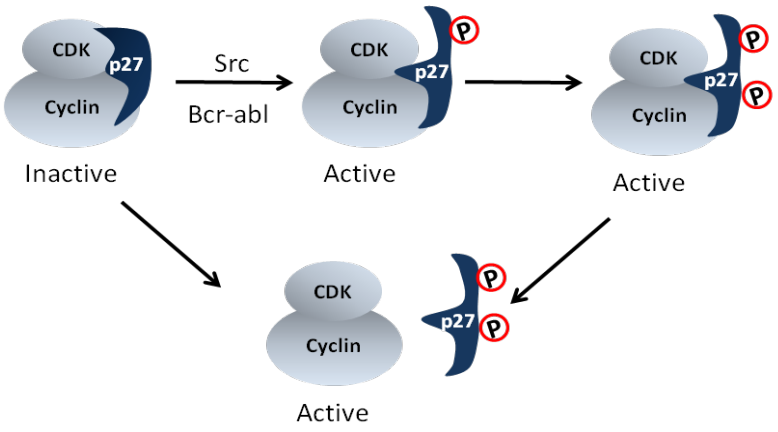

Figure 1-7 p27 binding to cyclin D-CDK4/6 complexes. (Adapted from Kaldis *et al.*)[38]

To start the importation of p27-cyclinD-CDK4 into the nucleus, the phosphorylated residues T157, T198 and S10 of p27 need to be dephosphorylated (Figure 1-6 (c)), though the mechanism is poorly understood.[39] The p27-cyclinD-CDK4 complex is imported to the nucleus during the late G1 phase (Figure 1-6 (d)). Similarly to its exportation in the early G1 phase, the p27 complex is recognised by an importin α and bound to the importin β through the nuclear localisation signal region (NLS).[40]

Studies have shown that the nucleus p27-cyclinD-CDK4/6 are involved in two activities in the G1/S transition (see Figure 1-8).[41] The first one is the phosphorylation of Rb, which triggers the two-step releasing of E2F after the G1 checkpoints. This result in the E2F transcription of cyclin E and cyclin A as mentioned Section 1.1.2 (see also Figure 1-8 (a)). The second activity involves transferring p27 to cyclinE-CDK2 for its degradation (see Figure 1-8 (b)). However, the transferring mechanism is less understood.

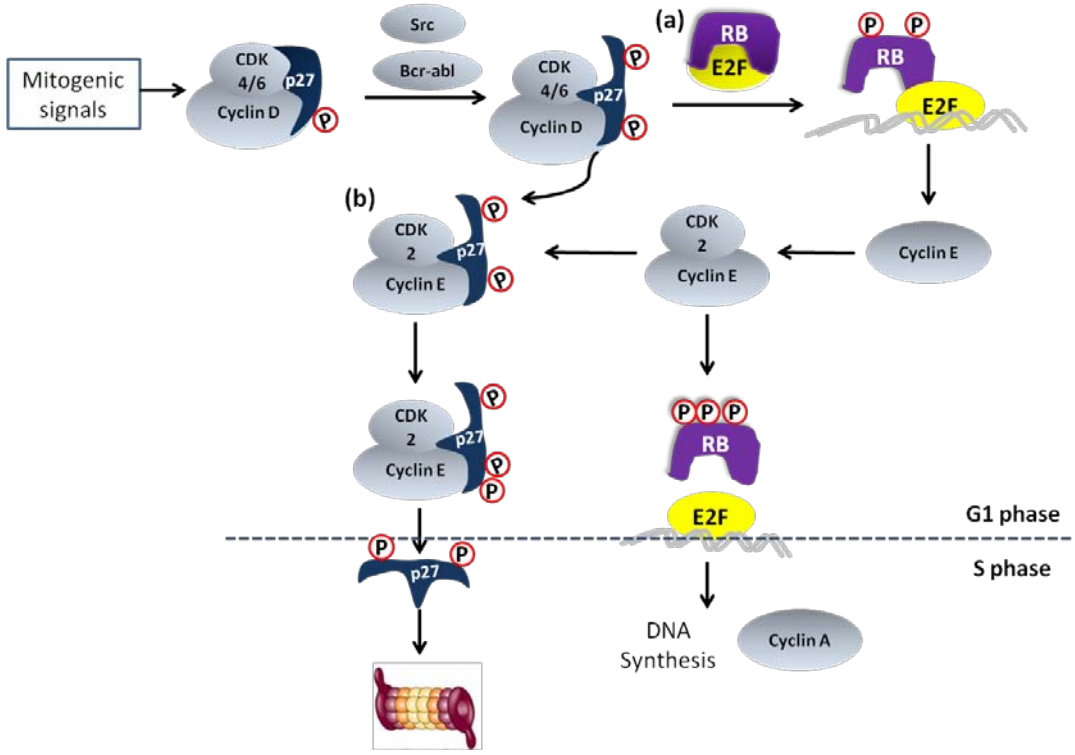

Figure 1-8 Regulation of the G1/S transition.

As a potent CDK2 inhibitor, the level of p27 in the nucleus needs to be reduced to enable the transition from the G1 to S phase. Unlike the KPC-mediated proteolysis in the cytoplasm during the G0 to G1 phase, the degradation of p27 in the nucleus during the G1 to S phase is mediated by the SCF^{Skp2} (see Figure 1-6 (d)).[42]

Specifically, SCF^{Skp2} only function in the nucleus and it requires the phosphorylation of the Thr 187 residue of cyclinE-CDK2-bound p27. The latter process generates a binding site for the SCF. This E3 ligase polyubiquitinates p27 and targets it for the further degradation by the 26S proteasome.[43] Recently, Nguyen *et al.* have also reported that even in the absence of cyclinE-CDK2, the Y88-phosphorylated p27 can still be phosphorylated on the Thr 187 for the SCF mediated ubiqutination.[44]

1.1.5 **p27 and cancer**

Following the above discussions, the tumour suppressor p27 is regarded as a possible candidate for chemotherapy development since (1) p27 is not a classic

tumour suppressor like p53, as it is rarely mutated or lost at the gene level;[45] (2) the mislocated p27 can be targeted for translocation back to the nucleus;[45, 46] (3) p27 can be a powerful diagnostic marker since it indicates the involvement of different pathways in the development of tumours.[47]

In human tumour cells, it has been observed that p27 levels and its activity are decreased because of the anomalous increase in its degradation and cytoplasmic mislocalisation.[48] Specifically, studies have shown that excessive level of SCF^{Skp2} have been observed in human tumours and correlated with a wide range of malignancies.[49] On the other hand, the p27 in the cytoplasm of colon, ovarian, breast and thyroid tumours is suggested to be mislocated from its nuclear cyclin-CDK targets, though the mechanism is unknown.[50, 51] The accelerated proteolysis and mislocation lead to the deregulation of its downstream substrates, such as cyclinE-CDK2 and cyclinD-CDK4, and consequently promote the cell cycle, *i.e.* the tumour cell proliferates.

The project outlined in this thesis aimed to overcome the over-degradation of p27. Typically, it is well known that the ubiqutin-proteasome pathway accounts for the degradation of regulatory proteins. Hence the unregulated degradation of p27 is believed to be a result of the enhanced SCF-mediated proteasome pathway.

1.2 **The ubiquitin-proteasome pathway**

Cells have robust mechanisms in place to regulate their intracellular protein stability and degradation. Two major routes of protein degradation have been identified. One is through the endocytosis pathway by lysosomes. This is only involved in the degradation of membrane-associated proteins and extracellular proteins. The other channel, through which the majority of proteins are degraded, is the ubiquitin–proteasome (UP) pathway.[52]

The ubiquitin-proteasome (UP) pathway, operating both in nucleus and cytosol, can be explained in two sequential steps: (1) A series of ubiquitin molecules are attached successively to a target protein *via* covalent bonding. (2) The proteasome

complex then degrades the polyubiquitylated protein and recycles the ubiquitins (see Figure 1-9).[52]

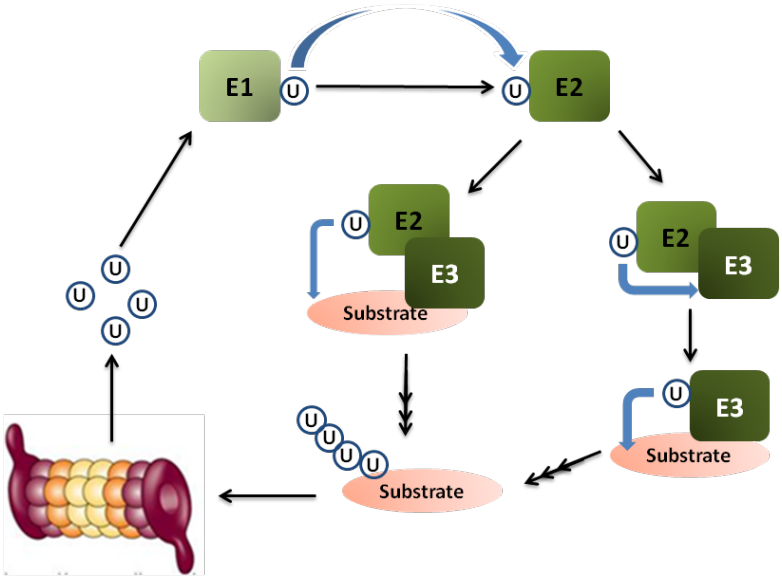

Figure 1-9 Overview of the ubiquitin-proteasome pathway.

The UP pathway is crucially related to the cell-cycle regulations. For example, the degradation of the key short-lived cellular processes such as the synchronised degradation of CKIs are mediated through the UP pathway.[44] The turnover of a broad range of transcription factors that regulate the cell proliferation, such as IκB, p53 and Bcl-2, have also been shown to be modulated by the UP pathway. Therefore, the idea of disrupting the UP pathway can profoundly influences both the aetiology and treatment of cancer.[53]

1.2.1 The ubiquitin system

In the UP pathway, the targeted proteins need to be firstly polyubiquitinated. This was discovered by Ciechanover, Hershko and Rose, who were awarded the Chemistry Nobel prize in 2004.[54] Successive ubiquitination occurs through the sequential actions of three enzymes (see Figure 1-9). Initially, the ubiquitin-activating enzyme (E1), consumes one ATP and forms a thioester bond between its active site of cysteine and the carboxyl terminal of ubiquitin. Then, the ubiquitin-conjugating enzyme (E2) takes the ubiquitin with the high-energy thioester from E1 and transfers to an ubiquitin-protein ligase protein (E3) which is responsible for

determining the substrate specificity. There are two major types of E3:[55] the unbound HECT-type E3, which will subsequently bind to the target protein, and the RING-type E3 which is already bound with the target protein. Both of these E3s will facilitate the attachment of the ubiquitin, by forming a covalent peptide bond with the Lys residue of the target protein. The iterative actions of E1, E2 and E3 finally results in a chain of (usually more than four) ubiquitin moieties. *i.e.* a polyubiquitin, being attached to the target protein. This allows the target protein to be recognised and degraded by the proteasome.[54]

1.2.2 **The proteasome: a proteolytic enzyme**

Proteasomes are highly conserved and compartmentalised protease complexes that can be found in the cytoplasm and nucleus of eukaryotic cells.[56] The 26S proteasome is involved in ubiquitin-mediated protein degradation pathway. Specifically, although the X-ray crystallography of the entire 26S proteasome is still not available, its three-dimensional image has been generated by the cryo-electron microscopy.[57] As shown in Figure 1-10, the 26S proteasome consists of a barrel-shaped 20S protease core particle (720 kDa) and two 19S caps as regulatory particles (890 kDa).[58]

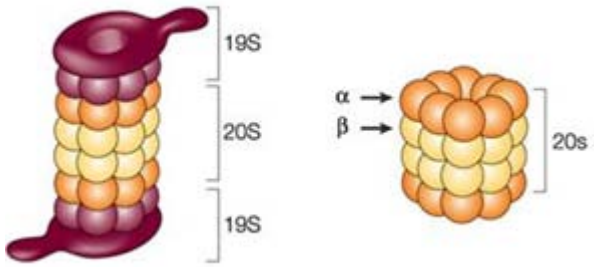

Figure 1-10 The proteasome multi-enzyme complex. (Reproduced from Adams *et al.*) [58]

The hollow cylindrical shape of the 20S core particle is comprised of four stacked heptameric rings, two inner rings of β1-7 subunits and two outer rings of α1-7 subunits. The two 19S regulatory particles contain two different subunits, the lid and the base. The lid firstly controls the access of substrates to the 20S core by recognising and cleaving of the polyubiquitin chains. The base then is responsible

for unfolding the substrate and opening the tunnel of the α-ring. This then allows the substrates to access into the proteolytic pocket of 20S core.[59]

1.2.3 Important proteasome-targeted proteins

The ubiquitin-proteasome system was first described in 1989[60] and cyclins were the substrates of the proteasome.[61] Since then, extensive studies have shown that the UP pathway is responsible for degrading intracellular proteins involved in various cellular functions such as cell cycle progression, oncogenesis, apoptosis, regulation of gene expressions, inflammation and DNA repair (see Table 1-1). The ubiquitin-proteasome system therefore maintains the hoemeostasis of protein levels for molecular signalling and cellular survival.

Table 1-1 Selected substrates of ubiquitin-proteasome pathway

Function	Substrate
Cell cycle progression	$p27^{Kip1}$, p21, cyclins
Oncogenesis	p53, $p27^{Kip1}$, bax, IκB
Apoptosis	Bcl-2, cIAP, XIAP
Regulation of gene expression	c-Jun, E2F1, IκB, β-catenin
Inflammation	IκB, p105 precursor of NF-κB

(1) Cell cycle progression

The proteasome-mediated proteolysis of cell-cycle regulatory proteins functions as a major regulatory mechanism for the cell cycle progression. Cyclins A, B, D and E,[62] cyclin-dependent kinase inhibitor p27 (as described in Chapter 1.1.4) and p21, transcription factor E2F, Rb and the tumour suppressor p53 have all been shown as the substrates for the UP pathway.[63] Inhibiting their degradation processes can sensitise the cell to apoptosis.[64]

(2) IκB

The nuclear factor κB inhibitor (IκB) is also a substrate for the UP pathway.[65] Its substrate, the nuclear factor κB (NF-κB), is a transcription factor that regulates the

expression of numerous genes involved in immune response, cellular proliferation, apoptosis and cell migration.[66]

Specifically, NF-κB is inactivated and sequestered in the cytoplasm by IκB during the resting state. The presence of stimuli such as reactive oxygen species (ROS) and tumour necrosis factor alpha (TNFα), can activate NF-κB through the phosphorylation, ubiquitylation and subsequent proteasomal degradation of IκB. The activated NF-κB is then transported into the nucleus to bind to the specific sequences in the promoter regions of the target genes. This results in an increased expression of the genes including the anti-apoptotic genes (Bcl-2, IAP), cell-proliferated genes (interleukins) and angiogenesis genes.[67]

The growth-promoting and anti-apoptotic property of NF-κB makes it a target for cancer chemotherapy. Since the UP pathway is responsible for the IκB degradation, perturbing the proteasomal activity may help stabilise the levels of IκB and consequently inhibits the transcriptional activity of NF-κB.

1.2.4 **The ubiquitin proteasome pathway in cancer**

The proteasomal degradation of tumour suppressor and pro-apoptotic proteins are found to be deregulated in many human malignancies.[68, 69] Table 1-2 shows the examples of the UP pathway dysregulation for some important proteins.

Table 1-2 The UP pathway in cancer

Substrate	Proteolysis degradation	Functional effect	Biological effect	Tumour type
p27	increased	p27 inactivation	tumour progression	lung, colon, prostate, ovary, colorectal carcinomas,[70] breast cancer[71]
p53	increased	p53 inactivation	transformation	ovarian,[72] gastric cancer[68]
Cyclin D, B1 and E	decreased	Cyclin D, B and E over-expression	tumour progression	many common tumours[73, 74]
IκB	increased	increasing the NF-κB activation	resistance to TNF-α killing	lung cancer[75]

As mentioned before, the deregulation of p27 is believed to occur at the post-tranlational stage. It has been found that the oncogenic signals can accelerate the activation of several protein kinases that ubiquitinate p27, resulting in the p27 proteolysis.[76, 77] It is worth noting that although p21 belongs to the same family of CKI, it is mostly regulated at the transcriptional level.

Another tumour suppressor, p53, regulates the surveillance of DNA damage, cellular stress and deregulated oncogenic expression. In tumour cells, p53 tends to be excessively ubiquitinated, because it is targeted by an over-expressed oncogenic E3 ligase, murine double minute 2 (Mdm2). This results in the proteasomal degradation of p53.[78] Cyclin B1, D1 and E are frequently over-expressed in many common tumours. Study have shown that this results from the reduced proteasomal degradation.[79]

Finally, cancer cells require high levels of the NF-κB to suppress apoptosis and express the genes involved in tumour metastasis and angiogenesis. The increased levels is attributed to an increased phosphorylation and degradation of IκB.[80]

1.2.5 **Targeting the proteasome for cancer therapy**

As a promising cancer therapy, the UP pathway is difficult to target due to a lack of specificity. Nevertheless, recent experiments have demonstrated that many types of proliferating malignant cells are more susceptible to the UP pathway inhibition than the normal cells.[81-83] Most malignant cells exploit the UP pathway to promote proliferation and to suppress the apoptotic pathway. The excessive demand for protein synthesis makes those highly proliferative cells vulnerable to the UP pathway inhibition.

Targeting specific enzymes involved in the UP pathway makes it possible to control specific proteins turnover and the resulting cellular responses. Those target enzymes can be categorised into three groups, based on the sequential steps of the UP pathway: (1) kinases activity, (2) ubiquitination system and (3) proteasome activities.

It has been known that many proteins need to be phosphorylated before they enter the ubiquitin proteasome pathway. These phosphorylations at the serine or threonine residues of the substrates form the binding sites for the ubiquitin ligases of which the F-box domains can promote the ubiquitination.[84] Accordingly, targeting those kinases involved in the phosphorylation could modulate the degradation of specific proteins, such as p27, p53 and IκB and leave others unaltered. However, studies have also shown that disrupting this kinase activity can also stimulate their degradations by ER stress.[85]

Developing inhibitors of ubiquitination enzymes can be another way for pharmacological interventions since the ubiquitin proteasome pathway is initiated by ubiquitination. The ubiqutin ligation enzymes E2 and E3 and deubiquitylation enzymes (DUBs) are of particular focus.[86] The specificity of E3s to their downstream substrates enables their corresponding inhibitors to selectively perturb ubiquitination and hence degradation process. These inhibitors can be selectively designed to target their phosphorylation recognition sites, the protein-protein interaction site, E2-E3 interaction site and the ligation active site. Figure 1-11 (a) lists some small-molecule inhibitors of ubiquitin ligases.

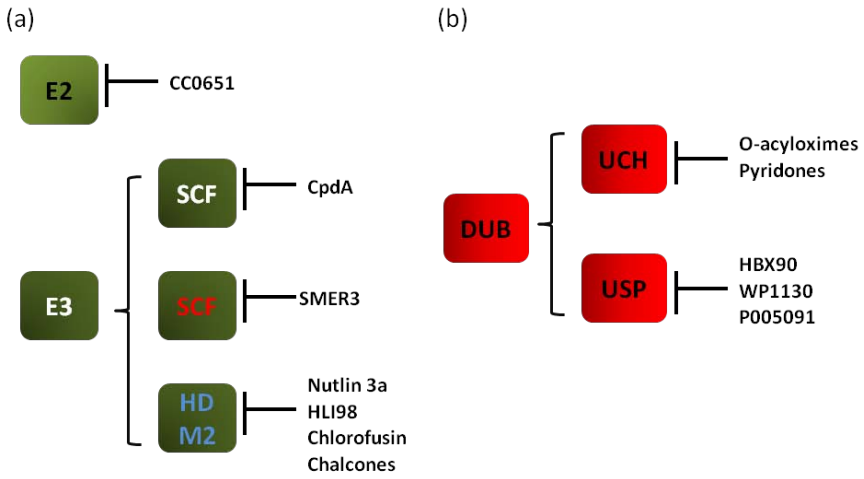

Figure 1-11 Small-molecule inhibitors of UP pathway. (a) Ubiquitin ligases, E2 and E3. (b) DUBs. (Adapted from Edelmann *et al.*)[86]

On the other hand, DUBs that are ubiquitin-specific can trim the corresponding ubiquitin from the tagged substrates. Accordingly, their inhibitors are developed to promote degradations of tumourigenic proteins such as cyclins from deubiquitylation.[87] The two best-characterised DUBs are ubiquitin-specific

proteases (USPs) and ubiquitin C-terminal hydroylases (UCHs). The design of these inhibitors have been challenging because of the structural similarities of DUBs and the complexity of protein-protein interactions.[88] In addition, depleting the ubiquitin pool is another side effect.[86] Therefore, clinical use of DUB inhibitors requires further investigations. Figure 1-11 (b) lists some small-molecule inhibitors of DUBs.

The last step of the UP pathway is the proteolytic degradation by 26S proteasome. The 26S proteasome is currently the most promising target in the drug development and its protein degradation function has been extensively studied in the past 15 years.

1.2.6 Active sites of 20S proteasome

As mentioned in Section 1.2.2, the 20S proteasome subunit is responsible for proteolytic activities. The 20S core consists of four heptameric rings. The outer rings are composed of seven different α subunits, α_1-α_7, while the inner rings are composed of seven different β subunits, β_1-β_7.[89] These four rings form three continuous proteolytic active sites in the middle (Figure 1-12).[90] The one near the β_5 subunits, called the "chymotrypsin-like" (CT-L) pocket, cleaves after the *C*-terminal of hydrophobic residues. The one near the β_2 subunits is called the "trypsin-like" (T-L) pocket that cleaves after basic residues. The active site near the β_1 subunits cleaves after acidic residues is called the "caspase-like" (C-L) pocket.

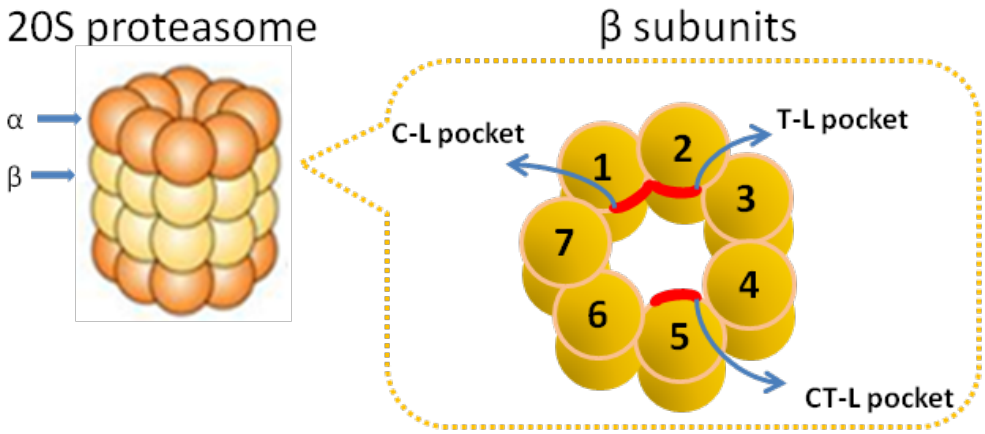

Figure 1-12 Active sites of eukaryotic 20S proteasome.

The three pockets jointly exhibit the overall proteolytic activity of 20S proteasome. Unlike other cellular proteases that utilise an internal residue to cleave amide bonds, studies have revealed that the proteasome utilises the side chain of the amino-terminal threonine of the β-subunits as the catalytic nucleophile.[91, 92]

The proteolytic mechanism of proteasome was initially understood by utilising protease inhibitors. Peptide aldehydes are well-characterised inhibitors on the hydroxyl groups of serine for proteases. By applying them to the proteasome, the X-ray diffraction studies showed similar inhibiting functions. The hemiacetal bond formed with the *N*-terminal threonine of β-subunits of the proteasome resembles its transition state of the proteolytic reaction.[98] Furthermore, the three *N*-terminal threonines of each of the subunits were proven as the active sites of the proteasome.[93] Thus, development of proteasome inhibitors that can impede activity of proteasome makes them feasible candidates for therapeutic intervention.

1.3 **Proteasome inhibitors**

Initially, proteasome inhibitors were used only as biological research tools due to their high toxicity.[94] Later, several studies showed that proliferating malignant cells are more susceptible to proteasome blockade than normal cells when treated with proteasome inhibitors PSI (**4**), LLnV[81] and lactacystin (**20**).[95] Other studies targeting the proteasome by using small molecule inhibitors resulted in positive therapeutic outcomes in 60 different cancer cell lines.[96] Moreover, no mutations of proteasomes in malignancies have been found as cancer cells are shown to utilise this system.[97] In 2003, bortezomib, the first proteasome inhibitor drug was approved by FDA for treatment of multiple myeloma. This opens a new window for cancer therapeutics and a series of proteasome inhibitors are being developed.

In general, developing proteasome inhibitors is aimed to stabilise several dysreguated proteins, triggering further signal pathway to suppress cell proliferation.[98, 99] Many types of synthetic as well as naturally occurring proteasome inhibitors have been developed for clinical and preclinical use.

1.3.1 Cell death mechanisms induced by proteasome inhibitors

Several pathways have been proposed to explain the antitumor activity of proteasome inhibitors for different types of cancers. Most of them serve to stabilise proapoptoic regulatory proteins.[100] Figure 1-13 illustrates some known mechanisms.

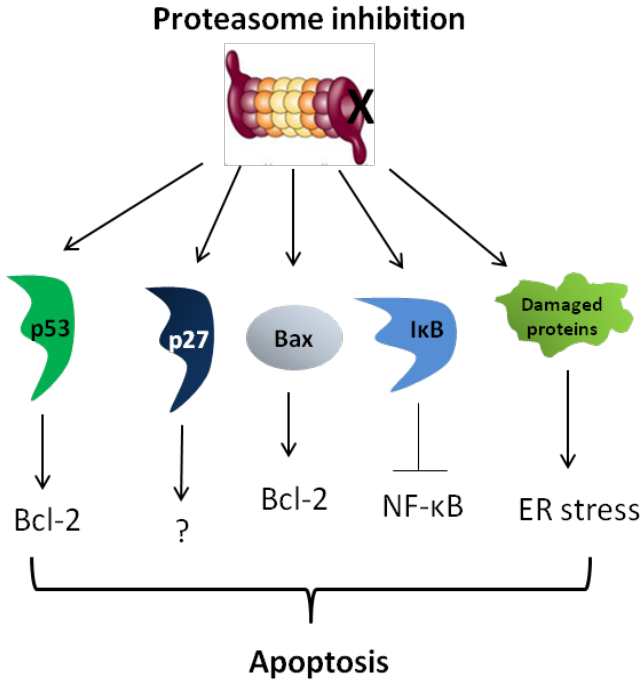

Figure 1-13 Mechanisms of induction of apoptosis by proteasome inhibitors

There are two most prevailent pathways for the proteasome inhibition induced apoptosis: (1) The accumulation of both tumour suppressor proteins (p27, p53), and cell death signal proteins (Bcl-2), and (2) the inhibition of survival signals (NF-κB).

As discussed in Section 1.1.5, the tumour suppressor proteins are over-degraded in many cancer cells. When proteasome inhibitors are used and hence the UP pathway is perturbed, the cancer cells are observed to undergo apoptosis predominately in the G1 phase.[99] Proteasome inhibitions are found helpful to stabilise and accumulate p53 and p27.[100] The stabilisation of p53 enabled cell cycle arrest in the G1-phase and promotes the cell apoptosis by inducting the pro-apoptotic protein called Bcl-2 gene family bax. The stabilisation of p27 has also been shown to result in cell apoptosis, though this mechanism is still unclear. Moreover, as a substrate of the proteasome, the pro-apoptosis factors, like Bax and Noxa, can also be

accumulated by proteasome inhibition. This also increases their relative level to anti-apoptotic Bcl-2 proteins, which help cell apoptosis. To sum up, proteasome inhibitors cause the stabilisation of p27, p53 and Bax levels, which leads to the cell cycle arrest and eventually the cancer cell apoptosis.

Another important pathway is to inhibit the transcriptional activity of NF-κB by stabilising the level of IκB (see Section 1.2.3). Both *in vitro* and *in vivo* studies of proteasome inhibitors have shown that the growth arrest and apoptosis of pancreatic and colorectal cancer cell lines are NF-κB dependent.[101, 102] Tumour metastasis and angiogenesis are suppressed because of the reduced gene expressions for the growth factors, adhesion molecules, anti-apoptosis and angiogenesis signals

Clearly, several apoptotic pathways are induced by proteasome inhibitors. However, having wide range of effects on cells also makes it difficult to identify one specific pathway responsible for their antitumor activities. Hence, the specificity and exact mechanism of action of each proteasome inhibitors are still open for further exploration.

1.3.2 **Design of proteasome inhibitors**

As shown in Figure 1-10, proteasome consists of a 20S core particle and two 19S regulatory caps. Based on X-ray crystallography, the crystal structure of the eukaryotic 20S subunit has been elucidated. Most proteasome inhibitors are designed to reversibly or irreversibly block the 20S active sites.[103] On the contrary, the mechanism of recognition, unfolding and translocation of substrates by the 19S are still poorly understood.

To measure the potency of 20S proteasome inhibitors, specific fluorogenic peptide substrates can be designed and introduced to target on particular active sites of the proteasome.[104] These engineered substrates penetrate cell membranes and are rapidly hydrolysed by the corresponding active sites. Specifically, these substrates are short peptides incorporating a fluorogenic group at the *C*-terminal, which can be selectively cleaved in the active pockets of the proteasome and release a highly

fluorogenic product. Thus, measuring the intensity of the resulting fluorescence enables quantitative evaluation of the proteasomal activity.

Studies found that the chymotrypsin-like (CT-L) pockets of the 20S proteasome are more sensitive to most inhibitors than the other two.[105, 106] In the following sections, eight major classes of proteasome inhibitors and their inhibitory mechanism are discussed.

1.3.3 **Major classes of proteasome inhibitors**

Based on the chemical structure of the pharmacophores, eight major classes of proteasome inhibitors have been identified: peptide aldehyde, peptide vinyl sulfones, peptide epoxyketones, β-lactones, macrocyclic vinyl ketones, flavonoids, peptide boronates and cyclic peptides. The former six classes are covalent inhibitors, and the later two classes are non-covalent inhibitors. In general, the reversible non-covalent inhibitors are pharmacological preferred due to their greater specificity and stability.

Table 1-3 summarises the inhibitory activities of various proteasome inhibitors. Activities are reported for the three proteolytic sites of proteasome, the CT-L, T-L and C-L pockets. Lower values of *Ki*, IC_{50} or higher $K_{obs}/[I]$ indicate higher effectiveness of a compound in inhibiting proteolytic functions. It is worth noting that inter-study comparison of inhibitor potency may not be appropriate since each study may differ in cell lines, assays, protocols or experimental conditions. The detailed inhibitory properties and their mechanisms are discussed in the following sections.

Table 1-3 Difference classes of proteasome inhibitors and their selective representatives[107]

Class	Compounds	Origin	Inhibition of 20S active sites [a] *Ki* (μM) or IC_{50} (μM) or $K_{obs}/[I]$ (M^{-1} s^{-1})			20S source
			CT-L	T-L	C-L	
Peptide aldehyde	Leupetin (**1**)	Natural product	-	*Ki* = 1.2	-	Bovine pituitary
	Calpain inhibitor I (**2**)	Synthetic	*Ki* = 5.7	*Ki* = 50	IC_{50} = 205	Bovine pituitary
			IC_{50} = 6.6	IC_{50} = 6	IC_{50} = 21	Human leukemia
	Calpain inhibitor II (**3**)	Synthetic	*Ki* = 33	*Ki* = 186	IC_{50} = 280	Bovine pituitary
	PSI (**4**)	Synthetic	IC_{50} = 0.25	-	-	Bovine pituitary
	MG132 (**5**)	Synthetic	IC_{50} = 0.024	IC_{50} = 9.215	IC_{50} = 2.288	Human red blood
	Tyropeptin	Natural product	IC_{50} = 0.14	IC_{50} = 5	IC_{50} = 68	Human HL60
	TP-110 (**7**)	Synthetic	IC_{50} = 0.027	IC_{50} > 100	IC_{50} > 100	Human HL60
	Fellutamide B (**6**)	Natural product	IC_{50} = 0.0094	IC_{50} = 2	IC_{50} = 1.2	mammalian
Peptide vinyl sulfones	ZLVS (**11**)	Synthetic	$K_{obs}/[I]$ = 29	$K_{obs}/[I]$ = 8	$K_{obs}/[I]$ = 5	Human U373MG
	NLVS (**10**)	Synthetic	$K_{obs}/[I]$ = 6790	$K_{obs}/[I]$ = 5.3	$K_{obs}/[I]$ = 6.4	Bovine red blood
			$K_{obs}/[I]$ = 5000	$K_{obs}/[I]$ = 3.4	$K_{obs}/[I]$ = 4	Bovine reticulocyte
Peptide boronates	MG262 (**12**)	Synthetic	*Ki* = 0.00003	-	-	Rabbit muscle
	P341	Synthetic	*Ki* = 0.62	-	-	Rabbit muscle
	(Bortezomib) (**13**)		IC_{50} = 0.0038	-	-	Human red blood
	MLN9708 (**14**)	Synthetic	IC_{50} = 0.0034	IC_{50} = 3.5	IC_{50} = 0.031	
	CEP-18770 (**15**)	Synthetic	IC_{50} = 0.0038	-	-	Human red blood
Peptide epoxyketones	Epoxomicin (**16**)	Natural product	$K_{obs}/[I]$ = 10000	$K_{obs}/[I]$ = 80	$K_{obs}/[I]$ = 21	Rabbit muscle
			Ki = 0.007	*Ki* = 0.35	*Ki* = 2.6	Bovine red blood
	Carfilzomib (**18**)	Synthetic	Ki_{nact}/Ki = 33000 [b]	Ki_{nact}/Ki < 100	Ki_{nact}/Ki < 100	Human red blood
β-lactones	Latacystin (**20**)	Natural product	$K_{obs}/[I]$ = 1500	$K_{obs}/[I]$ = 110	$K_{obs}/[I]$ = 17	Rabbit muscle
			IC_{50} = 0.259	-	-	Human red blood
	Omuralide (**21**)	Natural product	$K_{obs}/[I]$ = 8530	$K_{obs}/[I]$ = 253	$K_{obs}/[I]$ = 37	Bovine red blood
	Salinosporamide A (**22**)	Natural product	IC_{50} = 0.0035	IC_{50} = 0.028	IC_{50} = 0.43	Human red blood
	Antiprotealide (**24**)	Natural product	IC_{50} = 0.038	-	-	yeast
	Cinnabaramide A (**25**)	Natural product	IC_{50} = 0.001	-	-	Human red blood
	Belactosin A (**23**)	Natural product	IC_{50} = 0.21	-	-	Rabbit
			IC_{50} = 0.82	IC_{50} = 4.9	IC_{50} =2	Human red blood

Table 1-3 Continued

Claass	Compounds	Origin	Inhibition of 20S active sites [a] *Ki* (μM) or IC_{50} (μM) or K_{obs}/[I] (M^{-1} s^{-1})			20S source
			CT-L	T-L	C-L	
Syrbactins	Syringolin A (**26**)	Natural product	K_{obs}/[I] = 863	K_{obs}/[I] = 94	K_{obs}/[I] = 6	Human red blood
	Glidobactin A (**27**)	Natural product	K_{obs}/[I] = 3377	K_{obs}/[I] = 141	-	Human red blood
Flavonoids	EGCG (**28**)	Natural product	IC_{50} = 0.68	-	-	Rabbit
	Genistein (**29**)	Natural product	IC_{50} = 26	-	-	Rabbit
Cyclic Peptides	TMC-95A (**30**)	Natural product	IC_{50} = 0.0054	IC_{50} = 0.2	IC_{50} = 0.06	Human leukemia
			Ki = 0.0011	*Ki* = 0.043	*Ki* = 0.65	yeast
	Linear TMC-95A (**31**)	Synthetic	*Ki* = 0.85	*Ki* >> 100	*Ki* = 0.98	Rabbit reticulocyte
	Argyrin A (**32**)	Natural product	*Ki* = 0.076	*Ki* = 0.112	*Ki* = 0.081	Human red blood

[a] K*i* (Inhibition constant) is the binding affinity of the proteasome inhibitors, IC_{50} value is the 50 % inhibitory concentration of the proteasome inhibitors, K_{obs} (Observed rate of proteasome inhibition) /[I] (Inhibitor concentration) is the second-order rate constant. [b] Ki_{nact} (the rate constant of proteasome inactivation)/*Ki* (Inhibition constant between proteasome and inhibitors) is equivalent to the second-order rate constant K_{obs}/[I].

1.3.3.1 **Peptide aldehydes**

Peptide aldehydes are the earliest developed proteasome inhibitors, inspired by the observation that the natural compound leupetin (**1**) has inhibitory effects on the T-L activity of the proteasome.[108] Calpain inhibitor I (**2**) and calpain inhibitor II (**3**) were first synthesised and shown to inhibit the CT-L pocket.[109] Since then, many aldehyde-based molecules with higher potency and selectivity, such as PSI (**4**) and MG132 (**5**) have been developed. Two naturally occurring molecules, fellutamide B (**6**) and tyropetin A analogy (TP110) (**7**) that were recently identified in this class have been shown to potently inhibit the CT-L activity with IC_{50} values below 100 nM.[110, 111]

The inhibitory mechanism of peptide aldehydes relies on the formation of a reversible hemiacetal adduct. Specifically, the aldehyde covalently binds to the hydroxyl group of the Thr1 in the β subunits of the 20S proteasome (Figure 1-14), resulting in the proteasome inhibition. However, due to the instability of its functional group and its insufficient specificity to the proteasome, peptide aldehyde is less considered as a potential therapeutic.

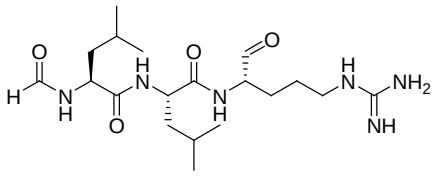

Leupeptin **(1)**

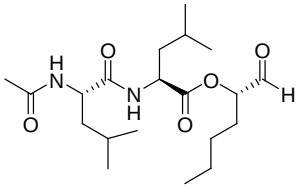

Calpain Inhibitor I **(2)**

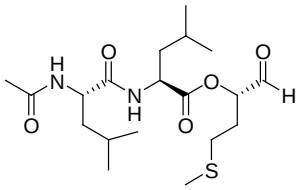

Calpain Inhibitor II **(3)**

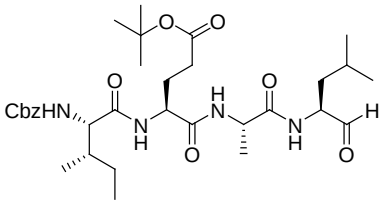

PSI **(4)**

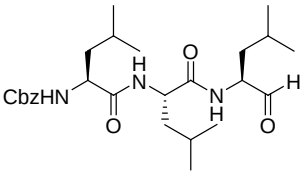

MG-132 **(5)**

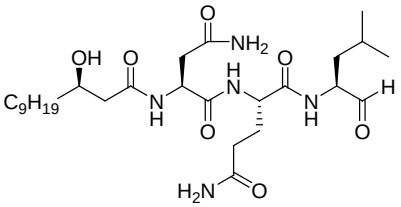

Fellutamide B **(6)**

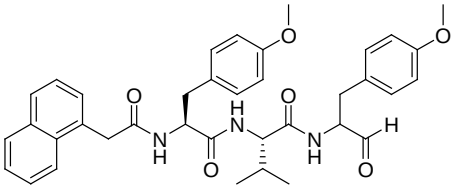

TP-110 **(7)**

Inhibitor

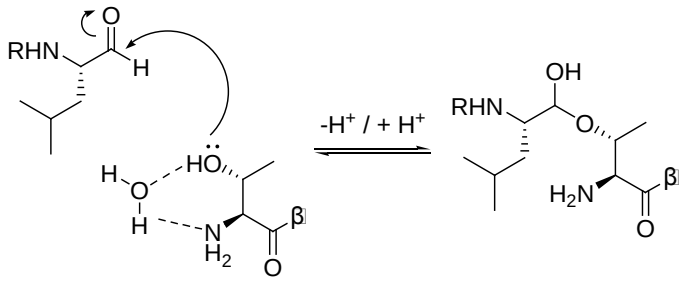

Thr1 of Proteasome

Figure 1-14 Mechanism of proteasome inhibition by peptide aldehyde.

1.3.3.2 **Peptide vinyl sulfones**

To address the limitations of the peptide aldehydes, non-aldehyde peptide proteasome inhibitors were synthesised. Examples include peptide benzamide (**8**),[112] peptide α-ketoamide (**9**)[113] and peptide vinyl sulfones. ZLVS (Z-Leu3-VS) (**11**), a vinyl sulfone analogue of MG132 (**5**), is a synthetic irreversible proteasome inhibitor firstly reported in 1997.[114] Its inhibition mechanism is *via* the formation of

an irreversible ether bond, *i.e.* the hydroxyl group of the Thr1 covalently adds to the vinyl group *via* a Michael addition pathway (Figure 1-15).

Several radioiodine-coordinated vinyl sulfones have been described to label proteasome since this class of inhibitors are relatively easy to synthesise.[115] Their irreversible binding specificity to the β-subunits of proteasome makes them ideal proteasome probes. Specifically, the incubation of radio-iodinated inhibitors with cellular extracts leads to their covalent binding with β-subunits of proteasomes. The resulting radio-labelled proteasome can be isolated and visualised in two-dimensional isoelectric focusing SDS/PAGE.[114] For example, NLVS (**10**) which is modified from ZLVS (**11**) is widely used as a proteasome probe. However, the low potency of these inhibitors is a major limitation to be considered as potential therapeutic drug.

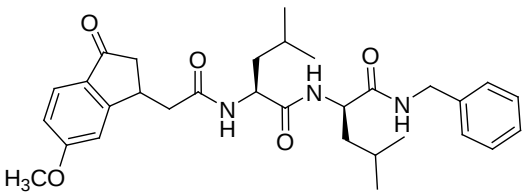

peptide benzamide **(8)**

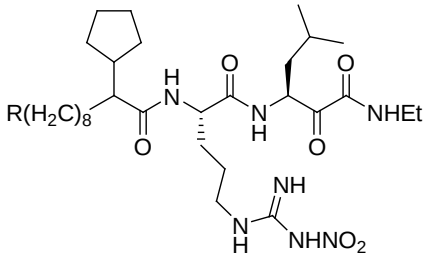

peptide α-ketoamide **(9)**

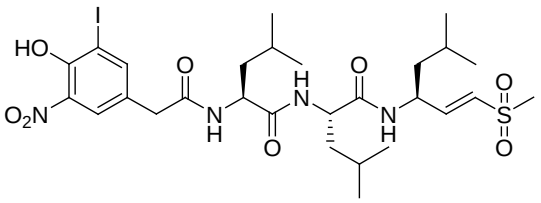

NLVS **(10)**

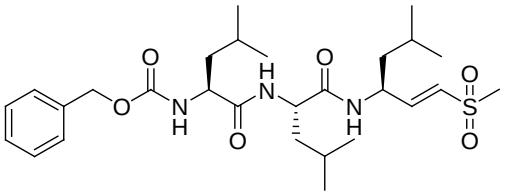

ZLVS **(11)**

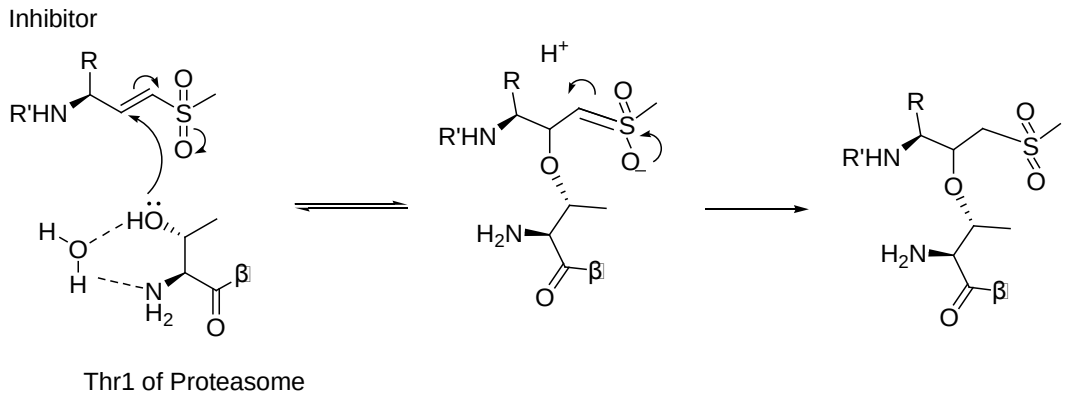

Figure 1-15 Mechanism of proteasome inhibition by peptide vinyl sulfones.

1.3.3.3 **Peptide boronates**

Various aldehyde replacements were examined in attempt to enhance the inhibitory activity. The breakthrough was achieved by the replacement of an aldehyde with a boronic acid, forming the peptide boronates.[116] It had been well documented that peptidyl boronic acid is a potent serine protease inhibitor before it was applied to proteasome.[117] The availability of an empty *p*-orbital on a boron atom is appropriate to accept the lone pair from the oxygen in serine. Accordingly, the formation of the stable tetrahedral borane complex with the Thr1 of proteasome was anticipated to increase the binding affinity. With a boron-derived modification, MG262 (**12**) was proved to be more than a 100-fold more potent than its parent compound MG132 (**5**).[116] Further structure simplifications of MG262 (**12**) gave rise to the nanomolar dipeptide boronic acid proteasome inhibitor PS341 (**13**).

PS341 (Bortezomib or Velcade®) is the first and has been so far the only proteasome inhibitor in clinical use. Its mechanism relies on the property that a peptide boronate is able to form a reversible non-covalent tetrahedral complex. Specifically, an X-ray diffraction study showed that the boronate group forms a tetrahedral adduct with the hydroxyl group of the Thr1 in the β subunits (Figure 1-16). The stable tetrahedral borane complex effectively slows the dissociation rate of the boronate-proteasome adduct and yields a low *Ki* value.[118] Studies on the mode of action also showed that the peptide boronate exhibits a very high selectivity to proteasome over many common serine proteases. Moreover,

bortezomib, at therapeutic concentrations, was demonstrated to bind exclusively to β5 and β1 of the S20 subunit, *i.e.* it mainly inhibits the CT-L and C-L activities.[119]

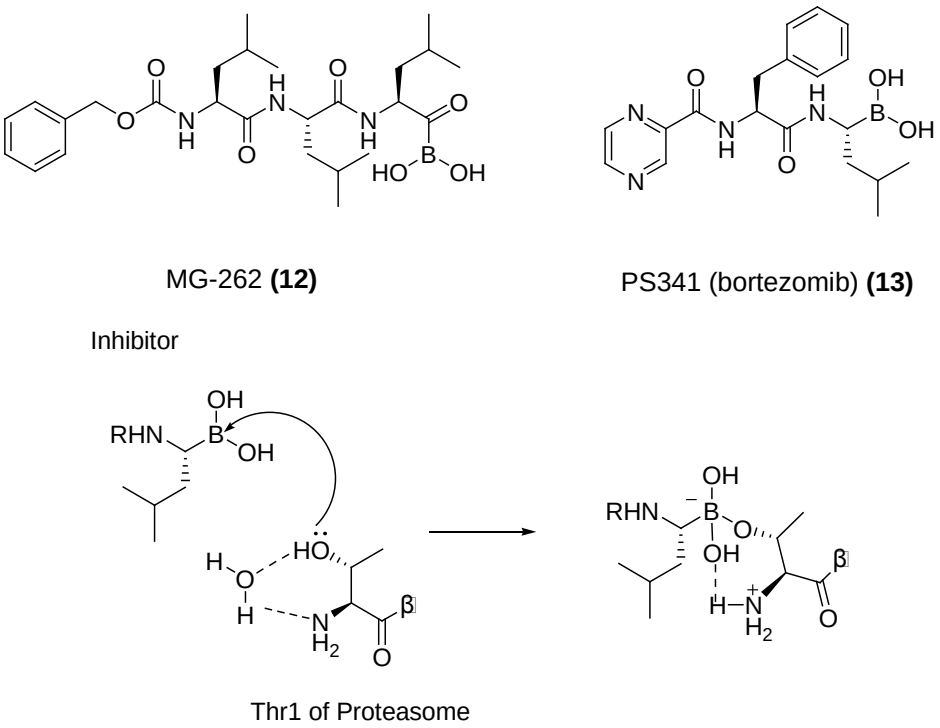

Figure 1-16 Mechanism of proteasome inhibition by peptide boronates.

Bortezomib initially was approved for the treatment of multiple myeloma (MM) and mantle lymphoma. Later, studies showed that it also has significant antitumour activities against various other malignancies, such as breast, brain, colorectal, lung, ovarian and pancreatic cancers.[58] Several preclinical studies on bortezomib showed that it can induce apoptosis in tumour cells *via* the NF-κB pathway[58] and the endoplasmic reticulum (ER) stress response pathway.[120]As described in Section 1.2.3, inhibiting the former pathway by stabilising the IκB reduces the expressions of growth-promoting and anti-apoptotic genes. On the other hand, the protein aggregation raised by proteasome inhibition can disrupt protein folding in the ER, triggering a stress signal pathway known as unfolded protein response pathway (UPR). The activation of UPR induces the cell cycle arrest and eventually apoptosis.[121] Since proteasome inhibition by bortezomib can trigger various cell death mechanisms, the effective pathways on different types of cancers still need further clarification.

The adverse-effects[122] and the emergence of drug resistance[123] motivated the development of second-generation peptide boronates. MLN2238 (**14**)[124] and CEP-18770 (**15**)[125] are the two successful examples under clinical trials for the treatment of MM. Similarly to bortezomib (**13**), MLN2238 and CEP18870 interact with the CT-L and C-L active sites. Although the two new generation boronates exhibit less potency than bortezomib, they have significantly lower toxicities. Moreover, MLN2238 and CEP18870 are orally bio-available when they are formulated as a boronic ester pro-drug.[126]

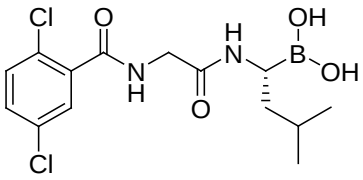

MLN2238 **(14)**

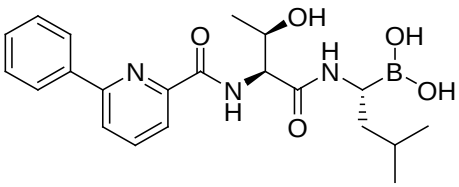

CEP-18770 **(15)**

1.3.3.4 **Peptide epoxyketones**

The class of peptide epoxyketones as proteasome inhibitors were identified from microbial antitumour activity screens in the late 1990s.[127] Two natural products, epoxomycin (**16**) and eponemycin (**17**) were found to irreversibly bind the CT-L active site of the proteasome. Apart from the high selectivity, this specificity is the unique feature of peptide epoxyketone inhibitors due to its distinctive inhibition mechanism.[128]

As revealed by the epoxomycin co-crystallisation with the yeast 20S proteasome, the epoxomycin forms a six-membered morpholino ring (**19**) with the Thr1 of the 20S proteasome (Figure 1-17). This is achieved by a two-step reaction. Firstly, the carbonyl group of the epoxyketone is nucleophilically attacked by the hydroxyl group of the Thr1, forming a hemiacetal, similarly to the mechanism for peptide aldehyde. Then, the free amine of the Thr1 *N*-terminal attacks the epoxide ring to afford the morpholino adduct (Figure 1-17). Consequently, the participation of both the β-hydroxyl and α-amino groups of the Thr1 residue results in high binding affinity.

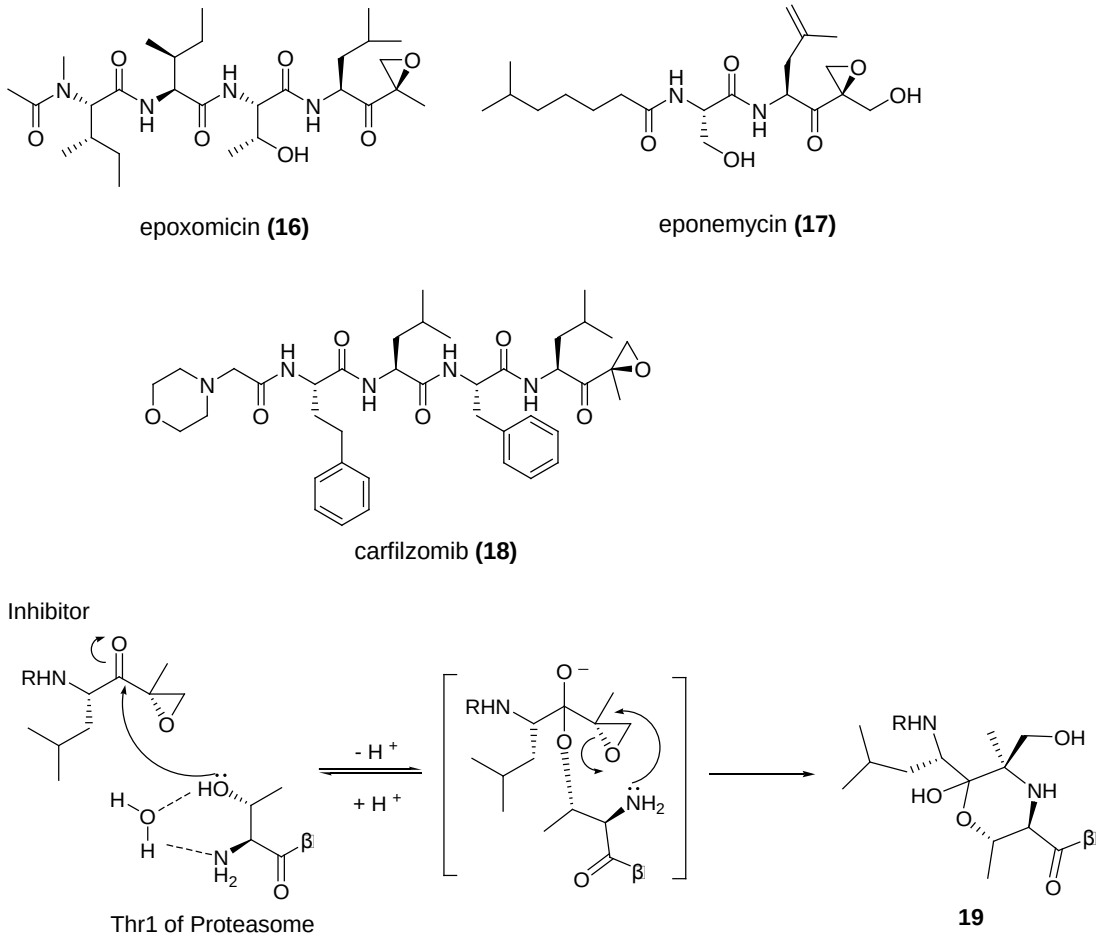

Figure 1-17 Mechanism of proteasome inhibition by peptide epoxyketones.

By utilising the specificity of the epoxyketones, hundreds of peptide epoxyketone analogues have been synthesised. A large proportion of them are developed as site-selective proteasome probes.[129] In comparison with the clinically-used bortezomib, carfilzomib (**18**) exhibited higher potency of inhibiting the CT-L proteolytic activity in phase I trials in patients with the chronic hematologic malignancies.[130] In phase II trials, carfilzomib has achieved an extraordinary 24 % partial response rate in heavily pre-treated MM patients. Their phase III trial for MM is being undertaken.

1.3.3.5 **β-Lactones**

Unlike the previous classes, β-lactones are non-peptide, small size nature products. For example, lactacystin (**20**), originally isolated from a microbial metabolite in 1991, was found to induce neurite growth in a mouse neuroblastoma cell line.[131]

Corey *et al*. achieved the total synthesis and found that it irreversibly blocks the β5 subunit of mammalian proteasome.[132] Thus, lactacystin is regarded as a proteasome inhibitor targeting the CT-L pocket.

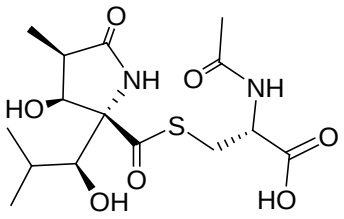

Lactacystin **(20)**

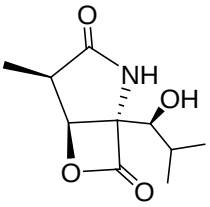

Omuralide **(21)**

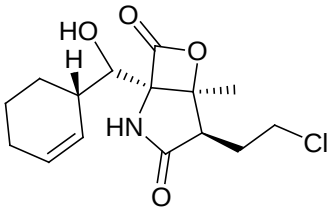

Salinosporamide A **(22)**

The inhibition mechanism of lactacystin can be divided into two consecutive steps (Figure 1-18 (a)).[93] Firstly, in the aqueous solution lactacystin is spontaneously hydrolysed into *clasto*-lactacystin-β-lactone (**21**) termed omuralide and *N*-acetylcysteine. Secondly, the carbonyl group in this β-lactone ring is opened by the β-hydroxyl group of Thr1 to form a ester bond. However, this ester bond can be slowly hydrolysed, hence reducing the inhibition potency. To overcome this problem, several alternative β-lactone proteasome inhibitors have been discovered.

Salinosporamide A (**22**), also known as NPI0052 or marizomib, is a secondary metabolite of marine actinomycete *Salinispora tropica*.[133] It is currently undergoing clinical trials for MM. Sharing similar chemical structure to omuralide (**21**), salinosporamide A possesses a unique chlorine moiety that enhances the potency. In addition to forming a ester bond to the Thr1 of proteasome, the carbon near chloride is further nucleophilic attacked by the neighbouring hydroxyl group, forming a tetrahydrofuran ring (Figure 1-18 (b)).[134] This tetrahydrofuran ring blocks the access site of Thr1 from deacylation, and hence increases inhibition stability. Other β-lactone analogues, such as belactosins (**23**), anti-protealide (**24**) and cinnabaramide (**25**) also show high potency with IC_{50} in nanomolar ranges.[107]

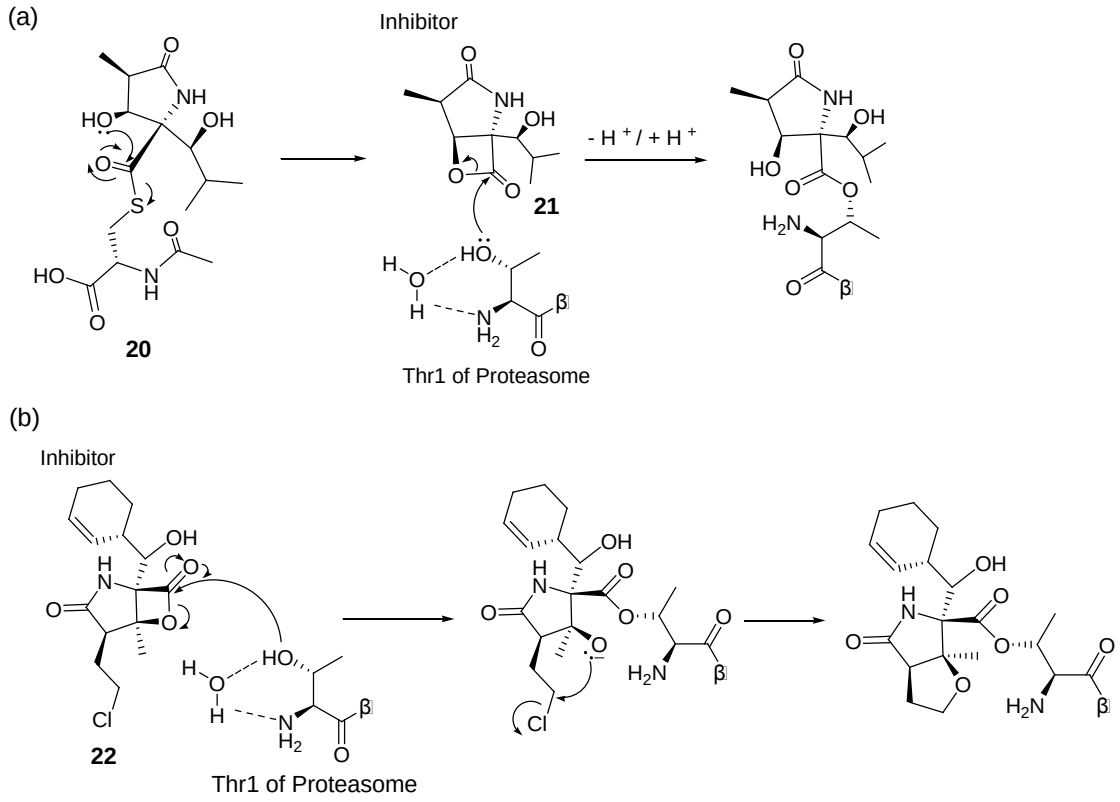

Figure 1-18 Mechanism of proteasome inhibition by (a) lactacystin, (b) Salinosoporamide A.

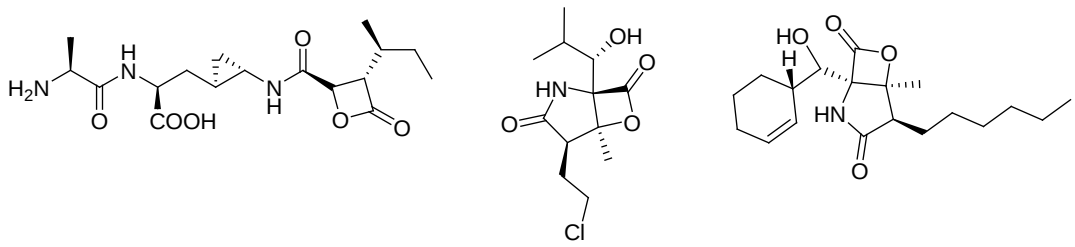

Belactosin A **(23)** Antiprotealide **(24)** Cinnabaramide A **(25)**

Several reports have demonstrated that lactacystin is around five-fold less potent than epoxomycin (**16**) and it also inhibits other cellular proteases.[135] Moreover, their complex structures tend to hamper the development of β-lactone-based therapeutic agents.[133]

1.3.3.6 **Macrocyclic vinyl ketones (syrbactins)**

Syrbactins are 12–membered lactam natural products containing an α,β-unsaturated amide moiety and recently have been shown to be useful proteasome inhibitors. Syringolin A (**26**) and glidobactin A (**27**), are two examples isolated respectively

from *Pseudomonas synringae pv Syringae*[136] and *Polyangium brachyspomm.*[137] Studies have shown that these two compounds and their analogues can inhibit proliferation and induce apoptosis in neuroblastoma and ovarian cells.[138] The crystal structure of the syrbactins in complex with the yeast proteasome showed that syrbactins covalently bind to the β5 subunit of the proteasome, with the mechanism similar to the peptide vinyl sulfones (Section 1.3.3.2).[138] Specifically, the hydroxyl group of Thr1 undergoes 1,4-addition to the double bond of the syrbactins and forms an irreversible ether bond (Figure 1-19).[135] Although syrbactins exhibit proteasome inhibition and apoptotic properties, few studies apply it as a research tool or a therapeutic agent.

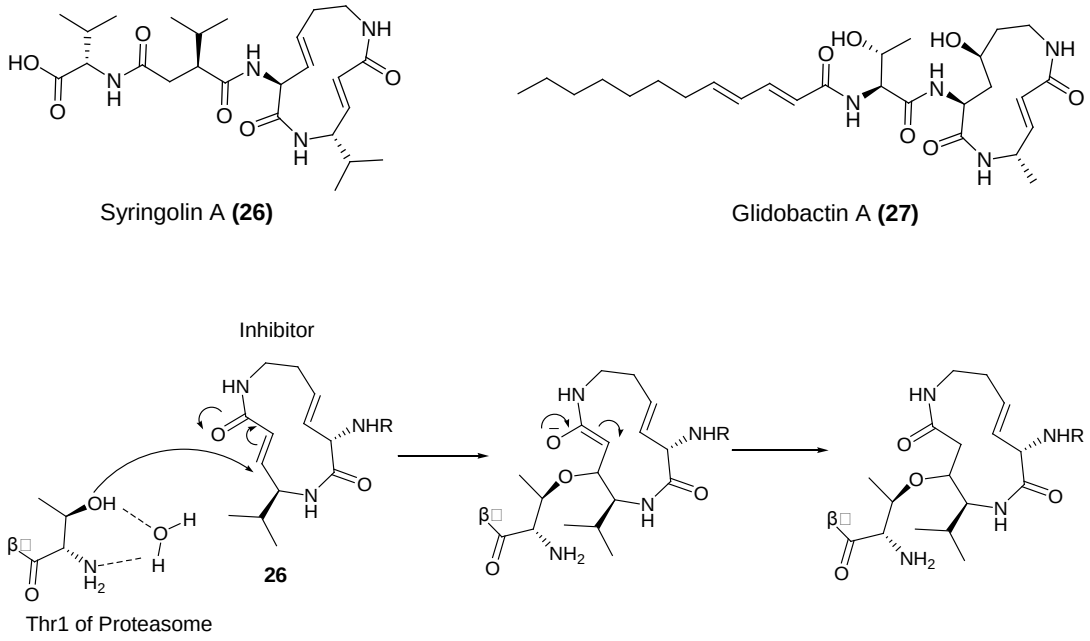

Figure 1-19 Mechanism of proteasome inhibition by syrbactins.

1.3.3.7 **Flavonoids**

The origins of this class are mainly from food. Epidemiological studies suggest that polyphenols in green tea are associated with anticancer effects.[139] In particular, epigallocatechin-gallate (EGCG) (**28**), representing the largest proportion of the polyphenols, has been shown for proteasome inhibition.[140] *In vitro* and *in vivo* studies showed that EGCG mainly inhibits the CT-L active site of the proteasome. Based on computational docking studies, the inhibition undergoes *via* the acylation

of the hydroxyl group of Thr1 by the ester group of EGCG.[141] EGCG is unstable under physiological conditions, thus further developments aims to a pro-drug form.

Epidemiological studies also showed that high soy consumption is associated with less occurrence of cancers including breast, colon and prostate cancers.[142] Genistein (**29**), one of the bioactive isoflavones found in soybean, has been shown mainly to inhibit the proteasomal CT-L activity, though the binding mode to the CT-L active site has not yet been elucidated. Moreover, *in vitro* and *in vivo* studies suggested that genistein is a weaker proteasome inhibitor than EGCG from green tea.[143]

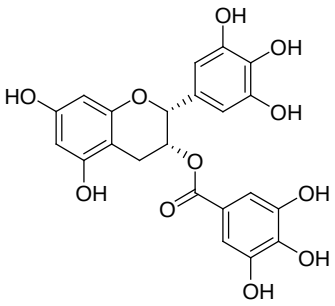

EGCG **(28)**

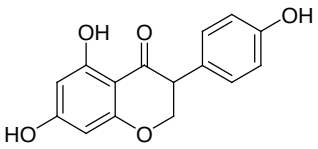

Genistein **(29)**

1.3.3.8 **Cyclic peptides**

Apart from the covalent inhibitors mentioned above, some inhibitors utilise hydrogen bonds, van der Walls forces and hydrophilic/hydrophobic interactions and hence can target on very specific positions of the proteasome. From a clinical perspective, non-covalent inhibitors are anticipated to have less side-effect due to this higher selectivity.

Cyclic peptides are one of the non-covalent proteasome inhibitors. TMC-95A (**30**) and its diastereoisomeric derivatives, originally isolated from *Apiospora montagnei Sacc* TC1093, were proven to be potent proteasome inhibitors with IC_{50} values in the nanomolar range.[144] Their macrocyclic structure are characterised by (1) the cyclic tripeptide array containing a tyrosine, and an asparagine and an unusual oxidised tryptophan residue, (2) a (*Z*)-1-propenylamide subunit and (3) a 3-methyl-2-oxopentanoic acid subunit. The total synthesis and X–ray co-crystal study have been reported respectively by Williams *et al.* and Groll *et al.*[145, 146] Both works

have shown that TMC-95A interacts with the yeast 20S proteasome by forming five hydrogen bonds (Figure 1-20). These non-covalent interactions result in inhibition of CT-L, T-L, C-L proteolytic activities respectively with IC_{50} of 1.1 nM, 43 nM and 650 nM. Further tests on the linear conformation of TMC-95A (**31**) suggest that the linear tripeptide only retains 1/100 inhibitory activities, indicating the necessary structure of constrained ring.[147] Therefore, more SAR studies are needed to simplify the macrostructure of TMC-95A.

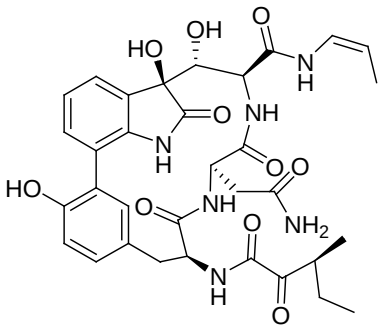

TMC-95A **(30)**

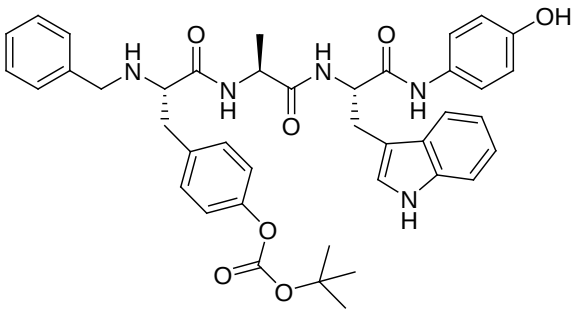

TMC-95A linear analog **(31)**

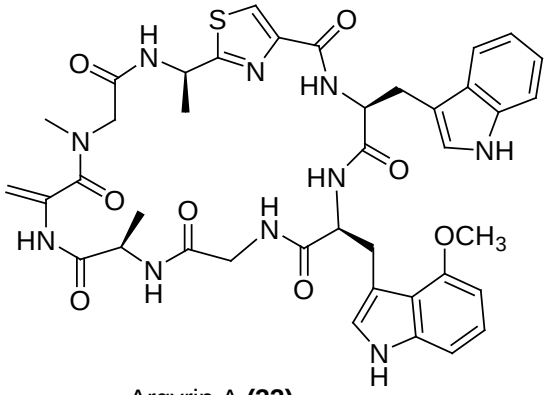

Argyrin A **(32)**

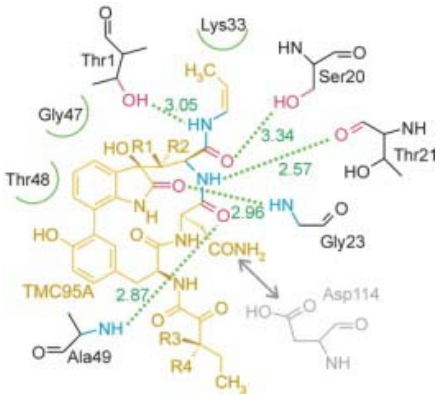

Figure 1-20 Interaction of TMC-95A to the active site of proteasome β2 subunit. (Taken from Groll *et al.*)[146]

Since the recent discovery of proteasome inhibition activities for another cyclic peptide, argyrin A (**32**),[148] an increasing number of researches have emerged focusing on its structural interaction with the proteasome three pockets.[3]

1.4 **Argyrins**

Argyrins were first isolated by Sasse *et al.* in 2002 from a myxobacterium strain *Archamgium gephyra*.[148] The two major products isolated from the fermentation broth were named argyrin A (**32**) (fermentation yield 6 mg L^{-1}) and argyrin B (**33**) (13 mg L^{-1}). Another six derivatives were also found as minor products, named argyrin C-H. The structures of these eight argyrin analogues were further elucidated by NMR spectroscopy, chemical degradation and X-ray analysis.[149]

Argyrin A, a cyclic octapeptide, was identified as a proteasome inhibitor by Nickeleit *et al.* in 2008.[3] The study concluded two advantages. Firstly, argyrin A exhibits antitumour activity in many cancers by inducing apoptosis mainly *via* p27-dependent mechanism. Secondly, argyrin A is capable of targeting the pre-existing tumour vessels directly by inhibiting angiogenesis.[3]

The exploitation of the chemotherapeutic potential of argyrins and their derivatives is difficult because it requires laborious efforts to isolate sufficient amounts of the compounds from the microorganism. To overcome this difficulty, Ley *et al.* firstly described a total synthesis of argyrins in 2002,[150] followed by Bülow *et al.* in 2010[151] and Wu *et al.* in 2011.[152]

1.4.1 **Bioactivity of argyrin A**

All argyrins exhibit antibacterial activities and are able to inhibit the growth of mammalian cell cultures.[148] More recently, high-throughput screening of p27 expression in human cancer cells found that argyrin A stabilises the p27 levels in many human cancer cells, including human colon cancer cells (HCT116), human colon adenocarcinoma cells (SW480) and cervical cancer cells (HeLa).[3] Since p27 turnover mechanism are mediated by the 20S proteasome, further functional studies using purified human S20 proteasome established that argyrin A mediate dose-

dependent inhibition of CT-L, T-L and C-L proteolytic activities (Figure 1-21).[3] Furthermore, the apoptosis potency across the cancer cell lines are comparable with clinically-used bortezomib (**13**). The accumulation of other proteasome substrates such as p53, Bax and IκB were also observed following argyrin A treatment.[3]

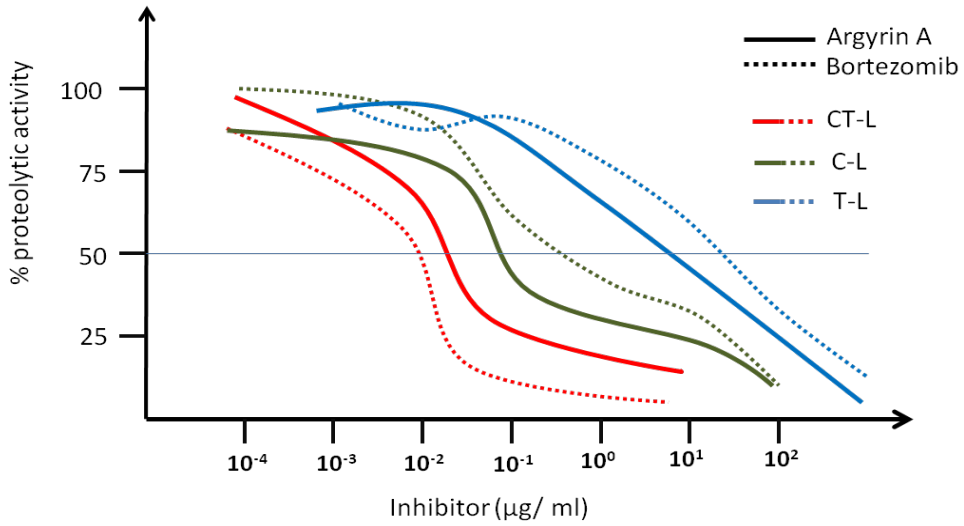

Figure 1-21 argyrin A and bortezomib dose-dependent inhibition of CT-L, C-L and T-L pockets. (Adapted from Nickeleit *et al.*)[3]

In addition to apoptosis, stablisation of p27 level is also shown to suppress tumour blood vessel formation.[3] Nickeleit and his co-workers observed that following treatment with argyrin A, tumour tissues exhibit a lower rate of endothelial cell focal adhesion *in vitro*. This can be explained by the p27 inhibition of RhoA, a GTPase promoting focal adhesion and stress fibre formation.[153]

The antitumour activity of argyrin A has also been tested *in vivo* in mice with human colon-cancer-derived xenografts.[3] The intraperitoneal injection of argyrin A can inhibit 20S proteasome activity, leading to a significant reduction in tumour size. More importantly, comparing with bortezomib, argyrin A treatment is better tolerated on animals. There were no discomforts and weight loss being reported in treatment with argyrin A.[3]

1.4.2 Structure analysis of argyrins

From the biosynthetic perspective, argyrins are non-ribosomally derived cyclic octapeptides containing unusual thiazole and tryptophan residues. Firstly, the 2-(1-

amino)-thiazole-4-carboxylic acid in all argyrins can be formed by the cyclisation and dehydrogenation of an alanyl-cysteine depeptide. These thiazole-contained peptides can be widely found in microbial and marine natural products.[154] Secondly, 4-methoxytryptophan in argyrin A, B, F, G, H can be derived from a tryptophan by hydroxylation and *O*-methylation.[149]

Figure 1-22 (a) illustrates the structural analysis of argyrin A (**32**). It can be seen that argyrin A is a cyclic octapeptide containing a sarcosine (Sar[8]), a exocyclic double bond dehydroalanine (Dha[7]), a (*R*)-alanine ((*R*)-Ala[6]), a glycine (Gly[5]), a tryptophan derivative with a methoxy substituent at *C*-4 of the indole (4-MeO-Trp[4]), a tryptophan (Trp[3]) and a dipeptide thiazole derivative of (*R*)-alanine ((*R*)-Ala[1]-Thz[2]).

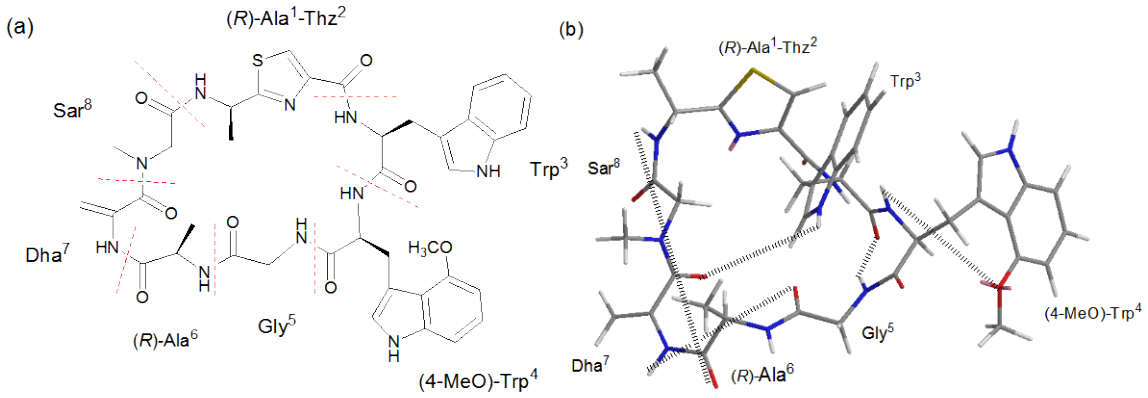

Figure 1-22 Structure and configuration of the argyrin A. (a) Structure and configuration of the argyrin A. (b) Intramolecular hydrogen bonds of argyrin A.

The backbone of argyrin A adopts a compact conformation with a dimension of 10 × 6 × 5 Å^3, and two constraints dominate the dynamics of this macrocycle.[155] One is that the thiazole ring is coplanar with the adjacent peptide bonds. This arrangement results in a planar constraint. The other constraint is created from the alkene group in the exocyclic alkene (Dha[7]).[155] The overall conformation is further stabilised by five intramolecular hydrogen bonds (Figure 1-22 (b)), of which three are within the macrocyclic ring and two are between the ring and the (4-MeO)-Trp[4] and Trp[3] side chains respectively.[155]

1.4.3 **SAR studies of argyrins as a potent proteasome inhibitor**

Stauch *et al.* proposed an argyrin A/proteasome model by molecular modelling.[155] The docking mode of argyrin A generated by the program GOLD is based on the three assumptions: (a) argyrin binds to the canonical catalytically active sites on the proteasome's β subunits, motivated by the observations from MG-132 and bortezomib, (b) the bioactive conformation of argyrin remains similar after its interaction with the proteasome, and (c) the three binding pockets are inspired by a yeast proteasome and bortezomib, with the side chains replaced by human equilents.

Three interactions can be found for all the pockets when argyrin A blocks the proteasome (Figure 1-23). Specifically, Thr21 in proteasome forms two hydrogen bonds between the NH and the carbonyl groups with their respective carbonyl and NH of Trp^3 of the argyrin A. Another group of hydrogen bonds can be formed between the NH group in proteasome's Gly47 and the carbonyl in (*R*)-Ala^6 of argyrin. Moreover, the hydroxyl group and the positive-charged *N*-terminus of Thr1 can form hydrogen bond and polar interaction with the carbonyl groups of Gly^5 and Dha^7 respectively.

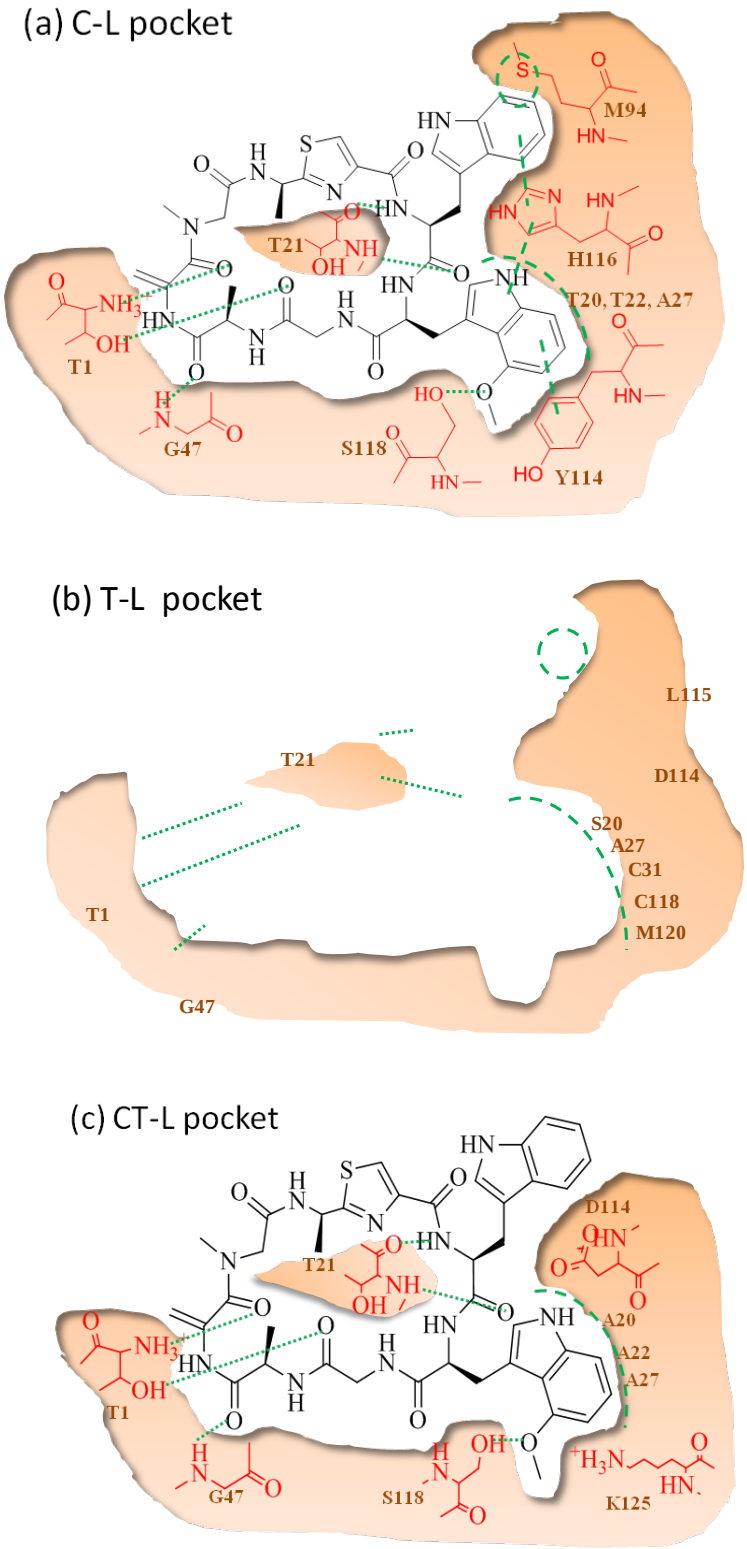

Figure 1-23 Binding poses of argyrin A with three active sites of proteasome. (a) A caspase-like binding pocket. (b) A trypsin-like binding pocket. (c) A chymotrypsin-like binding pocket. (Reproduced from Stauch *et al.*)[155]

In addition to those common patterns, distinct interactions can be found for each pocket. At the C-L pocket (Figure 1-23 (a)), argyrin Trp^3 and Trp^4 are respectively sandwiched between His116 Met94, and between His116 and Tyr114. The hydroxyl group of S118 also forms a hydrogen bond to the methoxy group of Trp^4.

At the T-L binding pocket (Figure 1-23 (b)), Trp^4 and Trp^3 are both located inside the hydrophobic side pocket containing Leu115, Ser20, Ala27, Cys31, Cys118 and Met120. It is worthy to note that there is no hydrogen bond between the pocket and the methoxy group of Trp^4, which is different from the other two pockets.

At the CT-L pocket (Figure 1-23 (c)), Trp^4 is surrounded by the side pocket containing Asp114, Ala22, Ala27, Lys125 and Ser118. The hydroxyl group of Ser118 form a hydrogen bond to the methoxy group of Trp^4, similarly to the C-L pocket.

To provide argyrin derivatives for SAR study, Stauch *et al.* synthesised a series of argyrin derivatives and measured their activities using purified human proteasomes.[155] The argyrin B, C, D and H were obtained by fermentation, and other derivatives shown in Table 1-4 were synthesised. Note that argyrin 6 has no exocyclic alkene, and Dha^7 was replaced by Gly. The remaining 20S proteasome activities after inhibition were determined using CT-L, T-L and C-L fluorogenic substrates. Moreover, the cytotoxic IC_{50} values were obtained after incubation of colon carcinoma cells (SW480) with argyrin derivatives.

Table 1-4 SAR data of argyrins and synthetic derivatives.[155]

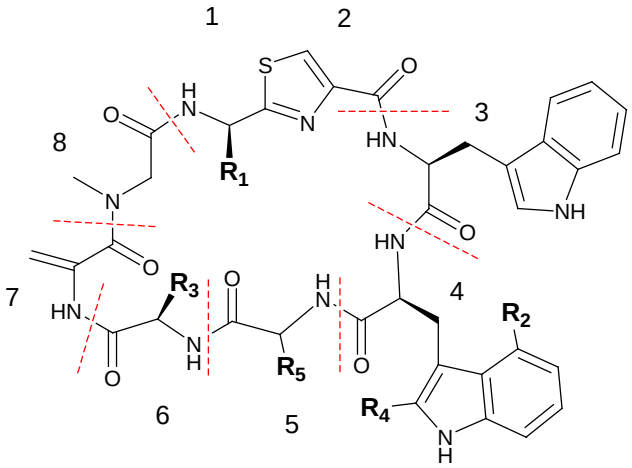

Argyrins [a]	R_1	R_2	R_3	R_4	R_5	Proteasome remaining activity (%) [b]			IC_{50} (nM) [c] SW-480
						C-L	T-L	CT-L	
Argyrin A (**32**)	CH_3	OCH_3	CH_3	H	H	29 ± 5.2	45 ± 4.5	30 ± 6.0	3.8 ± 0.3
Argyrin B (**33**)	CH_3	OCH_3	CH_2CH_3	H	H	52 ± 3.0	55 ± 8.5	58 ± 6.5	4.6 ± 0.6
Argyrin C (**34**)	CH_3	OCH_3	CH_3	CH_3	H	38 ± 8.3	40 ± 7.0	43 ± 5.5	1.5 ± 1.1
Argyrin D (**35**)	CH_3	OCH_3	CH_2CH_3	CH_3	H	50 ± 6.0	62 ± 8.0	64 ± 5.2	3.6 ± 2.0
Argyrin E (**36**)	CH_3	H	CH_3	H	H	65 ± 4.0	70 ± 3.0	70 ± 5.5	520 ± 270
Argyrin F (**37**)	CH_2OH	OCH_3	CH_3	H	H	35 ± 7.0	38 ± 6.5	28 ± 2.5	4.2 ± 0.4
Argyrin G (**38**)	CH_2OH	OCH_3	CH_2CH_3	H	H	60 ± 6.5	75 ± 3.0	65 ± 4.5	63 ± 55
Argyrin H (**39**)	H	OCH_3	CH_3	H	H	52 ± 5.5	60 ± 7.0	51 ± 8.0	30 ± 2
Argyrin 1	CH_2OH	H	CH_2CH_3	H	(*R*)-CH_2OH	65 ± 7.0	70 ± 7.5	55 ± 3.5	1050 ± 180
Argyrin 2	CH_2OH	H	CH_2CH_3	H	H	68 ± 4.6	75 ± 2.7	62 ± 19	3800 ± 43
Argyrin 3	CH_3	H	CH_2CH_3	H	H	72 ± 13.3	74 ± 2.9	92 ± 3.0	>4000
Argyrin 4	CH_2OH	OCH_3	CH_3	H	(*R*)-CH_3	54 ± 2.5	72 ± 4.5	50 ± 3.0	90 ± 0.2
Argyrin 5	CH_2OH	OCH_3	CH_3	H	(*S*)-CH_3	65 ± 3.0	89 ± 2.5	87 ± 2.5	2300 ± 180
Argyrin 6	CH_3	OCH_3	CH_3	H	H	100 ± 6.5	85 ± 6.5	87 ± 6.5	3600 ± 400

[a.] Argryin A-H are naturally occurring analogues, and Argyrin 1-6 are synthetic analogues.
[b.] Proteasome activity assays were carried out in a 100 µL reaction volume containing 1.2 µM Argyrin, 2 µg human erythrocyte-derived 20S proteasomes, Tris/EDTA: 20mM Tris/HCL; 1mM EDTA ; pH 7.8 and 50 µM fluorogenic substrate at 37 °C.
[c.] The cytotoxicity of argyrins was measured by MTT assay after 5 days of incubation at 37 °C and 10 % CO_2.

Based on the SAR study, argyrin A and F are apparently the most potent derivatives. By comparing them with argyrin E, 1, 2 and 3, it can be seen that the methoxy group at R_2 in Trp^4 is essential for activity. This can be explained by the hydrogen bonds of the methoxy group to the hydroxyl group of S118 in the C-L and CT-L pockets. Moreover, the comparison with argyrin 6 shows that the absence of the *exo*-alkene group of Dha^7 residue in argyrin also significantly reduce the activity. This suggests that the removal of structural constraint increases the flexibility of the macrocycle, which eventually reduces argyrin interaction capability with the three pockets. These two essential elements are consistent with the docking model.

The activity of argyrin F is slightly higher than that of argyrin A, which can be explained by an enhanced stability of the complex. Specifically, the hydroxyl group of serine in argyrin F can form an additional hydrogen bond to the carbonyl group of the conserved residue Gly23.

By comparing argyrin B with argyrin A, elongating the methyl side chain of (*R*)-Ala^6 by one carbon atom is well tolerated. For argyrin C and D, the additional methyl group at the C^2 position of indole side chain of Trp^4 is also tolerable, probably because this additional group can be readily accommodated without changing the conformation of Trp^4.

By comparing argyrin 4 and 5 with argyrin F, R_5 is substituted by (*R*)-Ala and (*S*)-Ala respectively. The former structure (pro-*R*) is tolerable while the later (pro-*S*) is detrimental. One possible explanation is that the steric hindrance between the methyl group of (*S*)-Ala and the carbonyl group of Trp^4 would distort the conformation of the macrocycle, and this methyl group would also clash with the protein backbone at Thr 20 near the T-L and CT-L pockets.

Based on an existing small library of argyrin analogues, it is unrealistic to draw any definitive SAR conclusion, apart from the apparent crucial requirement of MeO-Trp^4. To fully identify the optimal binding and proteasomal inhibition, unique analogues of argyrins are required. Thus, establishing a robust synthetic access to argyrins would allow for the construction of a wide range of analogues for detailed biological investigations.

1.5 **Aims and objectives**

While argyrins have been proven to inhibit proteasome function, its inhibition mechanism is still poorly understood.[3] In order to further explore argyrin biological function, chemical syntheses are necessary for obtaining diverse analogues.

The aim of the project is the total synthesis of argyrin A and analogues thereof, particularly with regards to the substituted tryptophan ($Trp^4(X)$). A new methodology by adopting Fmoc solid-phase chemistry and macrocyclisation strategies is introduced. A new synthetic route providing access to a wide range of tryptophan derivatives is also established.

The overall synthetic plan is outlined in Scheme 1-1. Among those seven amino acid building blocks, Fmoc-tryptophan derivatives (**43**), *N*-Boc-(*R*)-Ala-Thz-OH (**44**) and Fmoc-phenylselenocysteine (**42**) are not commercially available and hence synthesised.

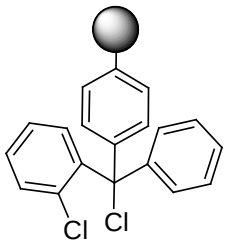

2-Chlorotrityl chloride resin

(40)

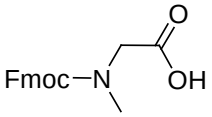

Fmoc-Sar[8]-OH

(41)

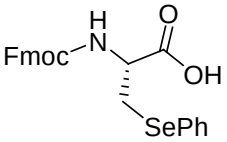

Fmoc-Ph(Se)[7]-OH

(42)

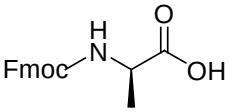

Fmoc-(*R*)-Ala[6]-OH

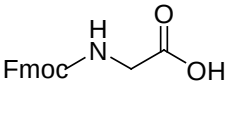

Fmoc-Gly[5]-OH

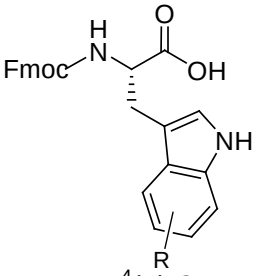

Fmoc-Trp[4](X)-OH

(43)

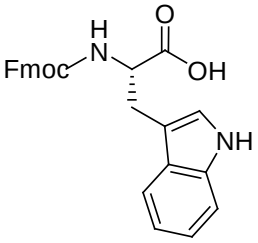

Fmoc-Trp[3]-OH

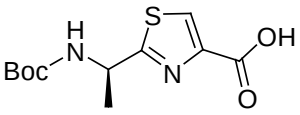

Boc-(*R*)-Ala[1]-Thz[2]-OH

(44)

Fmoc solid phase peptide synthesis

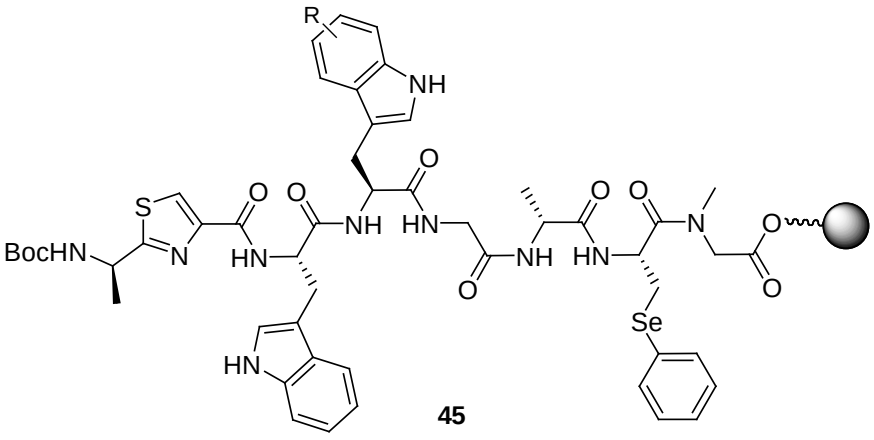

45

50 %(*v/v*) TFA/DCM, 1~2 h

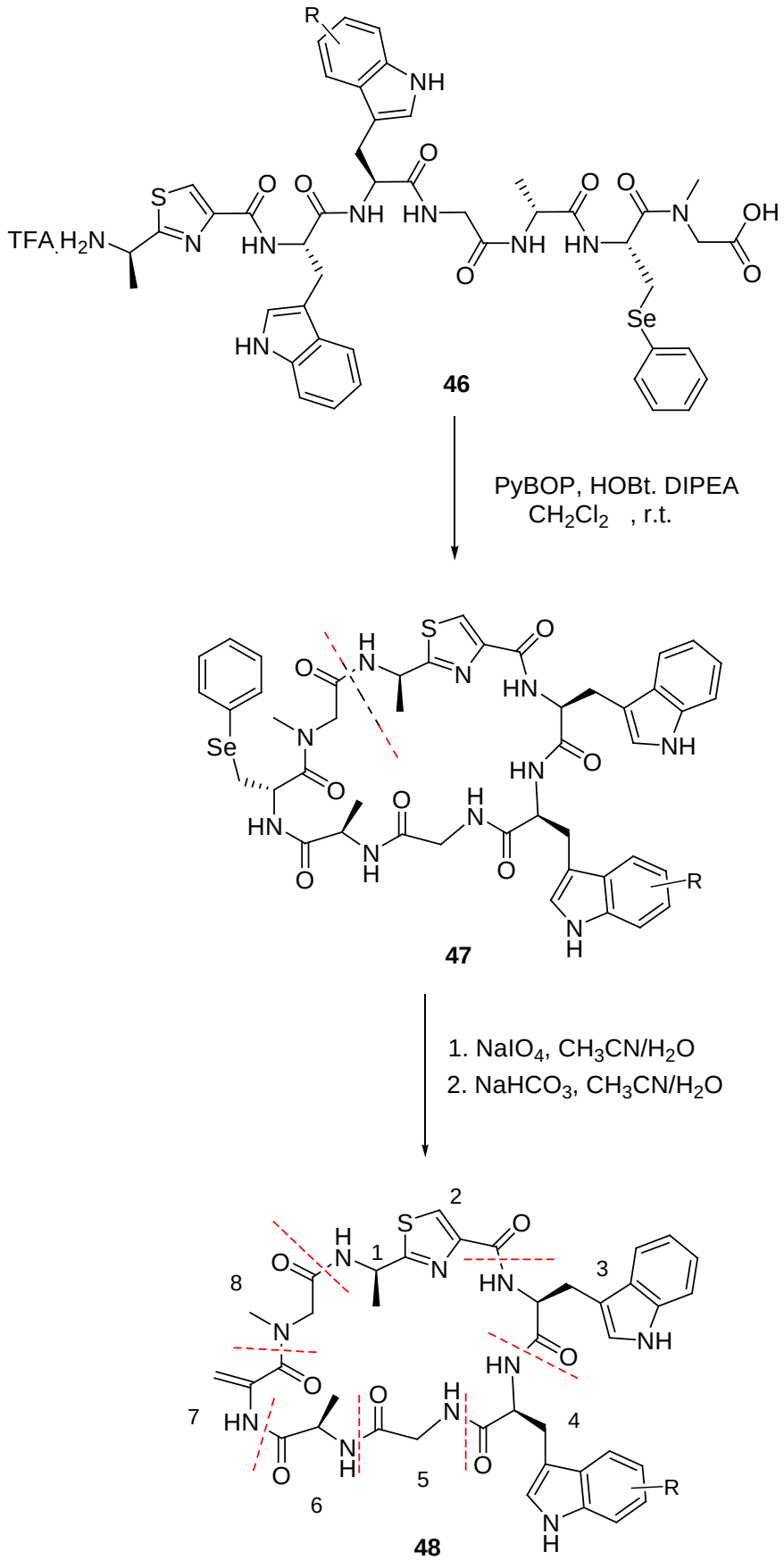

Scheme 1-1 Retrosynthetic analysis of argyrin A and analogues thereof

Initially, attention is focused on synthesis of optically pure Fmoc-tryptophan derivatives (**43**). There are numerous reports on the synthesis of optically pure tryptophan derivatives. However, they are either restricted to substitution at specific positions or requiring reagents that are not affordable. Therefore, the retrosynthetic strategy for Fmoc-protected tryptophan derivatives (**43**) is illustrated in Scheme 1-2. The key step (step c) utilising diastereoselective Strecker synthesis is developed in this thesis. The detail of this new approach is discussed in Chapter 2.

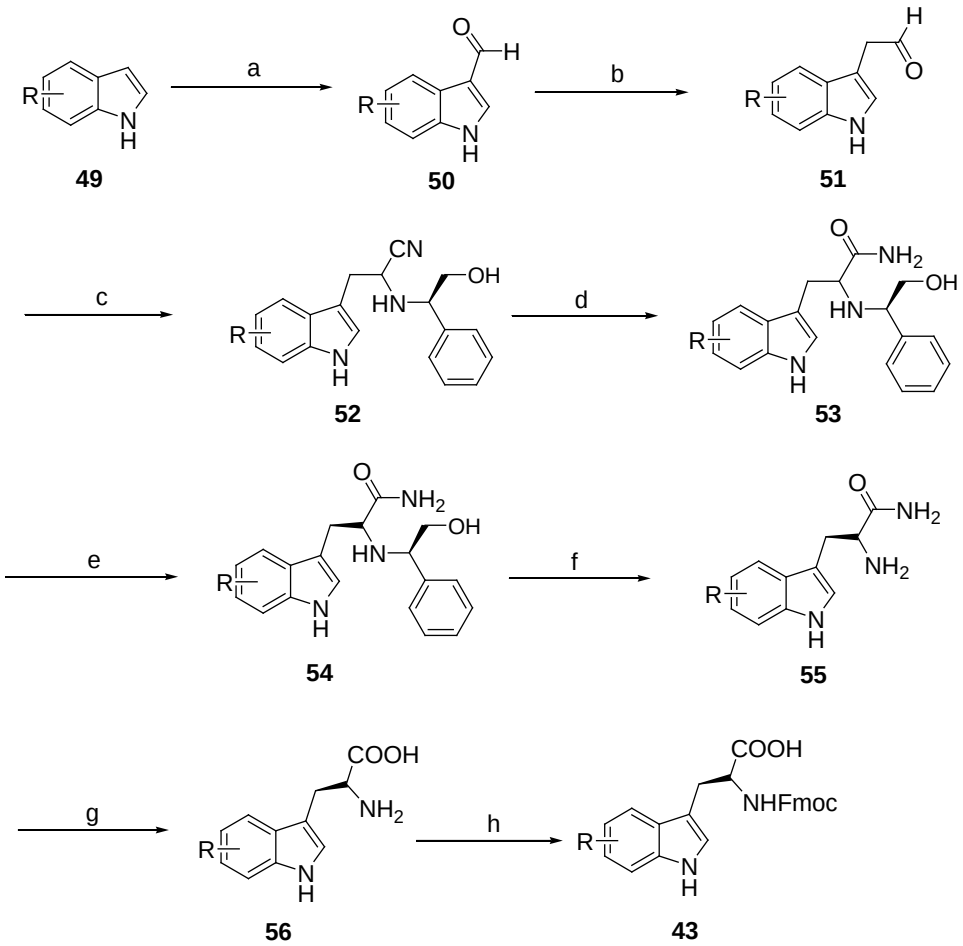

Scheme 1-2 Synthesis of Fmoc-tryptophan derivatives (43); Reagents and conditions: (a) $POCl_3$, DMF, 0 °C then 45 °C; (b) i. $Ph_3PCH_2OCH_3$, n-BuLi; ii. HCl, THF, reflux; (c) (*R*)-2-Phenylglycinol, NaCN, AcOH, MeOH; (d) H_2O_2, Na_2CO_3, DMSO; (e) Recrystallisation or RP-HPLC; (f) Pd/ C, NH_4HCO_2, MeOH, reflux; (g) 1 M HCl, reflux; (h) Fmoc-OSu, $NaHCO_3$, THF/H_2O.

The second unusual building blocks (*R*)-Ala^1-Thz^2-OH (**44**) is prepared by four-step synthesis, outlined in scheme 1-3. The crucial step (step c) involves two-step modified Hantzsch thiazole formation. In addition, another analogy of the thiazole-

containg dipeptide, the oxazole dipeptide (**63**), is also synthesised. The synthetic scheme is shown in Scheme 1-4.

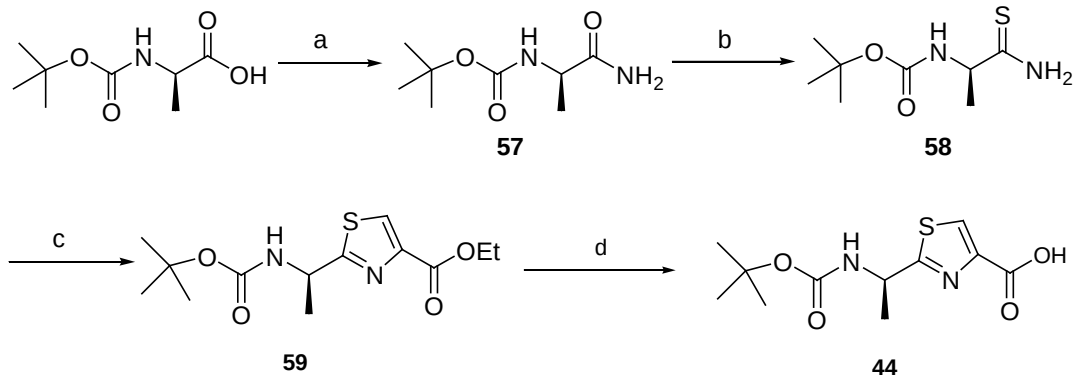

Scheme 1-3 Synthesis of Boc-(*R*)-Ala-thiazole (44); Reagents and conditions: (a) DCC, HOBt, NH_3, CH_2Cl_2, 0 °C; (b) Lawesson's reagent, THF, 0 °C; (c) i. $BrCH_2COCO_2Et$, $KHCO_3$, DME, -15 °C; ii. TFAA, 2,6-lutidine, DME, -15 °C; (d) LiOH, THF/H_2O, room temp.

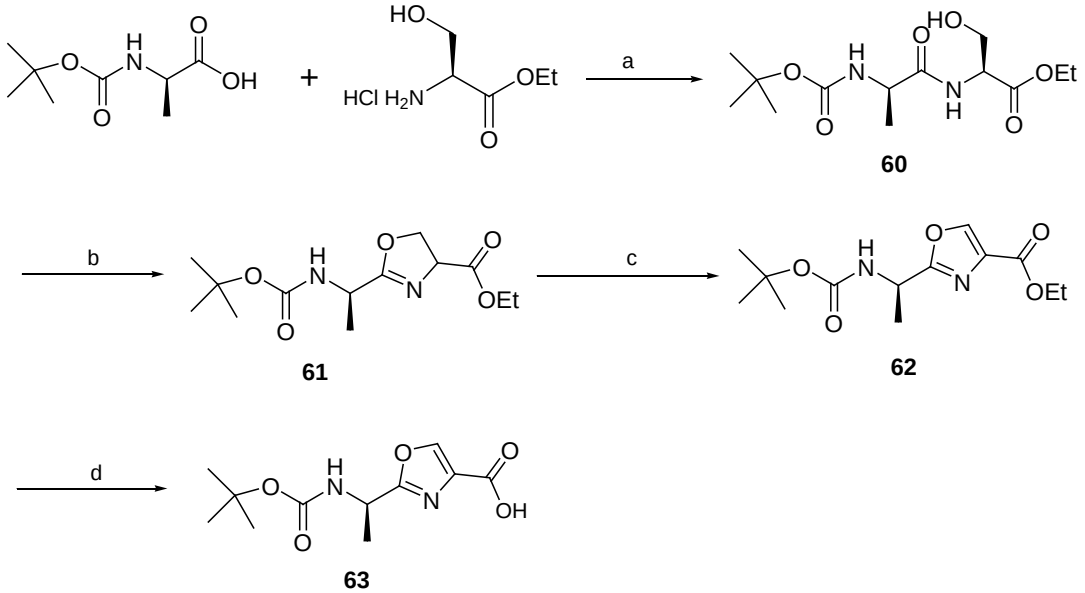

Scheme 1-4 Synthesis of Boc-(*R*)-Ala-oxazole (63); Reagents and conditions: (a) DCC, HOBt, DIPEA, CH_2Cl_2, 0 °C; (b) Burgess reagent, microwave, 70 °C; (c) CuBr, PhCOOO-*t*-Bu, benzene, reflux; (d) LiOH, THF/MeOH/ H_2O, room temp.

As the third unusual building block dehydroalanine is unstable, the synthesis strategy involved the utilisation of a masked precursor, phenylselenocysteine, which is eventually converted at the final step to the desired dehydroalanine residue. To obtain the phenylselenocysteine, a four-step synthetic scheme based on a previous report is utilised, shown in Scheme 1-5. The detail of the thiazole- and

oxazole-containing dipeptide and the Fmoc-phenylselenocysteine (**42**) is discussed in Chapter 3.

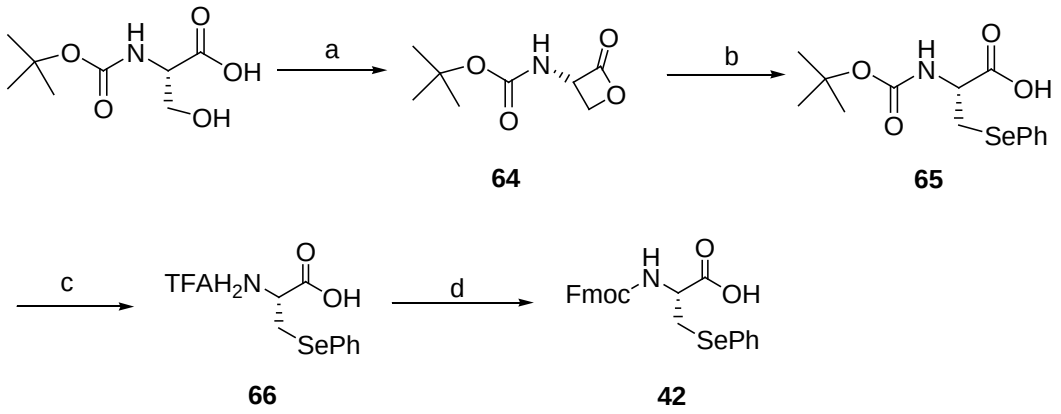

Scheme 1-5 Synthesis of Fmoc-phenylselenocysteine (42); Reagents and conditions: (a) DEAD, PPh_3, THF, -78 °C to room temp.; (b) PhSeSePh, $NaBH(OMe)_3$, EtOH, room temp.; (c) THF/CH_2Cl_2, room temp.; (d) Fmoc-OSu, $NaHCO_3$, THF/H_2O, room temp.

The prevailing method for chemical assembly of argyrin is solution-phase peptide synthesis. It was envisaged that Fmoc SPPS approach provides a much easier methodology for assembling the linear peptide. The macrocycle ring is installed using solution phase head-to-tail intramolecular cyclisation of the linear peptide. The oxidative removal of the phenylselenocysteine eventually completes the argyrin synthesis. The Fmoc solid phase peptide synthesis, macrocyclisation strategy and biological evaluation of synthesised argyrin analogues are discussed in Chapter 4.

Chapter 2

Synthesis of Fmoc-(*S*)-tryptophan derivatives

As outlined in Section 1.5, an unusual amino acid building block of argyrin A is the (*S*)-tryptophan derivative (**43**). In fact, tryptophan is one of the essential amino acid with less than 1% abundance in nature. Although both stereo-isomers of tryptophan can be found in naturally occurring peptides, only the (*S*)-stereoisomer of tryptophan is utilised as the source of ribosomally-encoded proteins. A structural feature of tryptophan is the indole moiety, which largely affects the physicochemical properties of tryptophan. In general, the indole ring provides the molecule with amphipathicity, *i.e.* its N-H group can form hydrogen bonds and its aromaticity enables non-polar interactions.[156] Moreover, biological activities of many tryptophan-contained natural products, particularly second metabolites, are related to specific substituents in the indole moiety. For example, rhopaladin

alkaloids containing 5-bromo- and 6-hydroxy-tryptophan are shown to be inhibitory to CDK4,[157] mitragynine alkaloids containing 4-methoxy-tryptophan derivatives have antinociceptive activity,[158] iotrochamides B containing 5-bromo-tryptophan displayed antitrypanosomal activity[159] and rebeccamycin having 7-chloro-tryptophan derivatives have anticancer activity.[160] Hence, tryptophan derivatives can be considered to be an active moiety for these natural products.

A multitude of synthetic methods has been described in literatures in order to provide these building blocks. In this chapter, seven existing methods toward the synthesis of enanatiomerically pure tryptophan are reviewed, followed by developing of a novel route to access to a wide range of tryptophan derivatives.

2.1 **Existing methods**

Current methods for synthesising enantiomerically pure (*S*)-tryptophan derivatives rely on either enzymatic or chemical approaches. There are two types of enzymes being employed in the former approach. One approach adopts *N*-acylase and generally involved a final-step resolution of the racemates. The acylase resolution releases the desired (*S*)-tryptophan in a mixture containing the unprocessed *N*-acetyl-(*R*)-tryptophan.[150] Two examples are presented in Section 2.1.1 and 2.1.2. The other approach adopts purified tryptophan synthase that can directly alkylate serine with indole derivatives, which is reviewed in Section 2.1.3. In contrast, studies based on chemical synthesis required multi-step processes and are low yielding. However, these multi-step synthetic schemes allowed access to a wider range of indole-substituted tryptophan. The key challenges are the stability of intermediates and stereoselectivity of reactions. Therefore, specialised procedures and chiral auxiliaries are usually employed, as in those studies outlined in Section 2.1.4 and 2.1.5.

2.1.1 **Ley's approach to the synthesis 4-methoxy-(*S*)-tryptophan**

In order to prepare the desired 4-methoxy-tryptophan for total synthesis of argyrin B, Ley *et al*. in 2002 developed a six-step synthetic route to *N*-Cbz-4-MeO-(*S*)-tryptophan.[150]

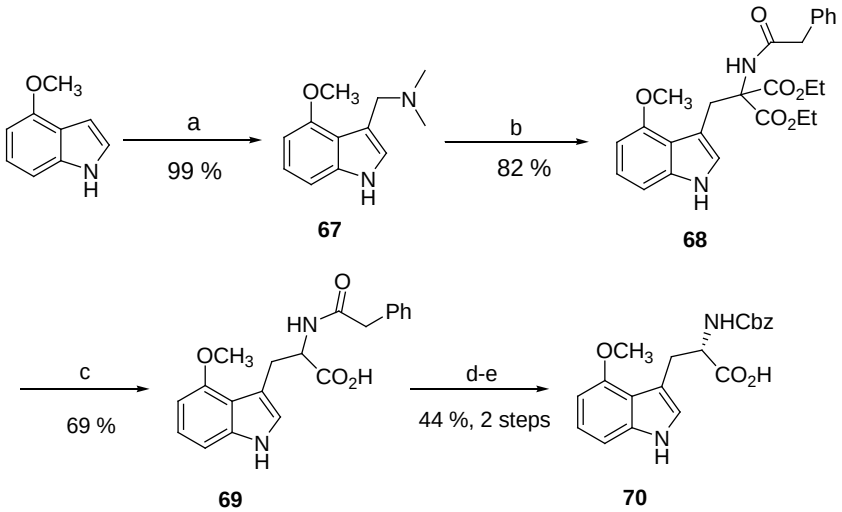

Scheme 2-1 Synthesis of *N*-Cbz-4-MeO-(*S*)-tryptophan (70) by Ley's group; Reagents and conditions: (a) $CH_2NMe_2^+I^-$, CH_3CN, room temp.; (b) $(C_2H_5O_2C)_2CHNHCOCH_2Ph$, EtONa Then **68** and Me_2SO_4, EtOH, room temp.; (c) i. NaOH, MeOH/dioxane, 50 °C; ii. Dioxane, 100 °C; iii. NaOH, MeOH/dioxane, 50 °C; (d) Immobilised penicillin G acylase, $MeOH/H_2O$, room temp.; (e) Cbz-Cl, $NaHCO_3$, THF/H_2O, room temp.

As shown in Scheme 2-1, the starting material 4-methoxyindole was subjected to aminoalkylation reaction, *i.e.* Mannich reaction, by treatment of Eschenmoser's salt. The gramine derivative **67** underwent alkylation using the enolate of malonic ester to give **68**. Saponification of the diester followed by further acid- or base-mediated decarboxylation of the carboxylic acid gave racemic 4-methoxytryptophan derivatives **69**. Finally, chiral resolution was performed by treatment with immobilised penicillin G acylase. This route utilised enzymatic kinetic resolution of the racemic precursors. In fact, the enzymatic optical resolution using acylase was based on the method used by Wade *et.al* for the synthesis of 5-bromo-(*S*)-tryptophan in 1980.[161]

The unreacted substrate was removed and the desired amino acid was *N*-protected with Cbz to provide optically pure *N*-Cbz-4-MeO-(*S*)-tryptophan **70** in 44% yield. Unfortunately, the penicillin G acylase used in the chiral resolution was no longer

commercially available. Another group reported that using other immobilised acylases resulted in poor conversion.[151]

2.1.2 Konda-Yamada's approach for the synthesis of 7- and 6-bromo-(*S*)-tryptophans

Another route that involved enzymatic hydrolysis of *N*-acyltryptophan was reported by Konda-Yamada in 2002 (Scheme 2-2).[162] This synthetic route took advantage of the elegant construction of racemic tryptophan put forward by the Yokoyama's group.[163] Tryptophan was synthesised directly from indole and serine. This one-step bio-mimetic synthesis is not only efficient (> 80 % yield), but also avoids the use of protection and deprotection steps in the synthetic route. Although this method is relatively straightforward, the two resulting isomers (**71**) require an additional chiral separation step. The enantiomeric specific separation was conveniently performed with (*S*)-aminoacylase and (*R*)-aminoacylase to give optically pure (*S*)-tryptophan and (*R*)-tryptophan, respectively. Further investigation by Sanderson *et al.* in 2008 successfully applied this route to a range of 5- and 6-substituted tryptophan derivatives.[164] However, a number of factors affect the yields, including the substituents, aminoacylase sources, pH and temperature.[164] Furthermore, applying this method to the indole system with bulky substituents, such as iodo or nitro, was found to be less efficient. It was envisaged that the poor efficiency was due to the limited accessibility to enzyme active site.

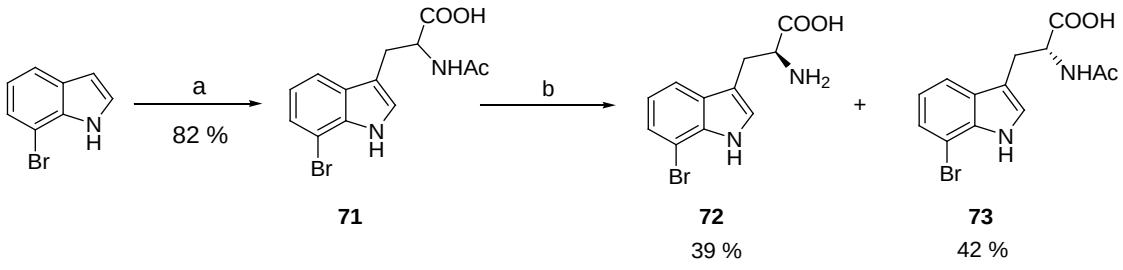

Scheme 2-2 Synthesis of 7-Br-(*S*)-tryptophan (72) by Konda-Yamada's group; Reagents and conditions: (a) (*S*)-Serine, $AcOH/Ac_2O$, 75 °C; (b) (*S*)-Aminoacylase, phosphate buffer pH = 7, $CoCl_2 \cdot 6H_2O$.

2.1.3 Goss approach for the synthesis of (*S*)-halotryptophans

Since tryptophan synthase was firstly used to synthesise 5-fluoro-tryptophan, several groups have utilised this strategy towards different tryptophan derivatives from 1974-2006.[165] However, this biotransformation method was hampered by time-consuming purification of enzymes and the limited solubility of substrates. In 2006, Goss's group reported a scalable procedure to synthesise (*S*)-halotryptophans.[166] The procedure utilised the tryptophan synthase from the lysate of a commercially available microorganism, *Salmonella enterica* (Scheme 2-3(a)). In fact, this biotransformation was achieved by three sequential reactions (Scheme 2-3(b)).

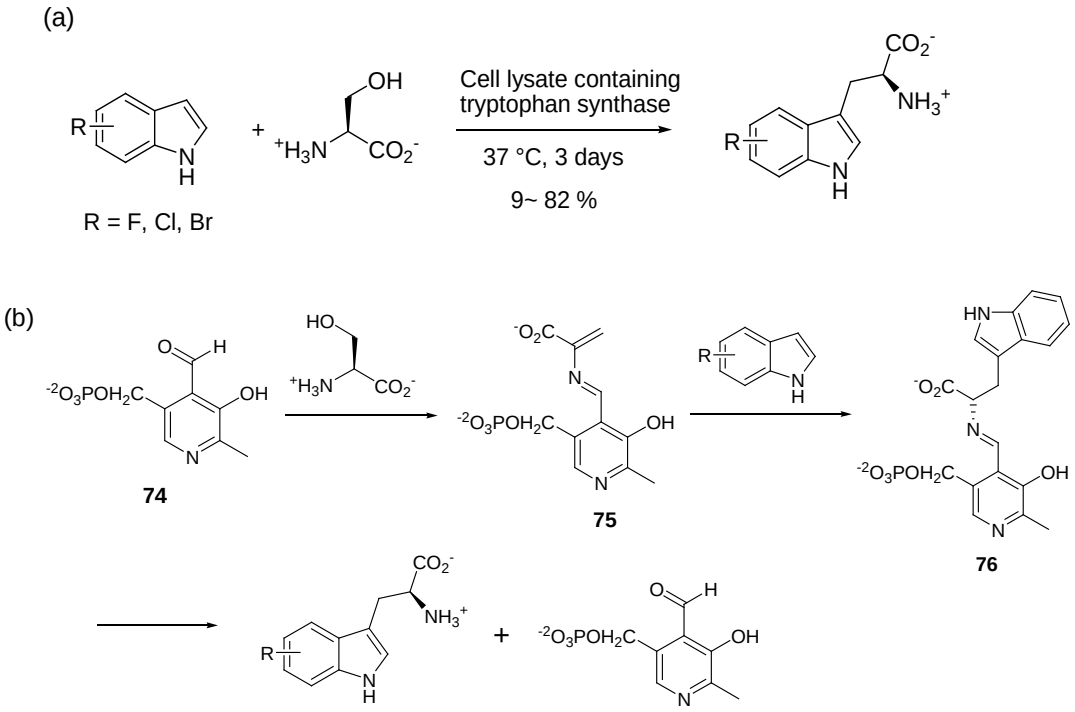

Scheme 2-3 Synthesis of (*S*)-halotryptophans by Goss' group. (a) Overall enzymatic synthesis of (*S*)-halotryptophans. (b) Tryptophan synthase mediated conversion of serine and haloindoles to tryptophans with PLP.

In the first step, serine was reacted with pyridoxal 5'-phosphate cofactor (PLP) (**74**) to form a Schiff's base, followed by dehydration to give **75**. In the second step, the indole derivative undergoes Michael addition with **75** to afford **76**. Finally, hydrolysis of **76** releases PLP and the tryptophan derivatives. The yield of

transformation after one cycle was nearly 50%. Although this enzymatic synthesis was readily accessible and environmentally friendly, applying this procedure to the indole ring system with various substitutions at 4-, 5-, 6- and 7-positions was not successful, especially with substitutions at the 4- or 7-positions. The specificity of the enzyme resulted in poor tolerance for bulky substituents and for substitutions at the 4- or 7-positions.

2.1.4 **Hengartner's approach to synthesis of 6-methyl-(*R*)-tryptophan**

As illustrated in Scheme 2-4, to prepare the sweetening agent 6-methy-(*R*)-tryptophan **83**, Hengartner's group successfully introduced asymmetric catalytic hydrogenation of **79** to afford 6-methyl-(*R*)-tryptophan **83** in high enantiomeric excess (ee).[167] The hydrogenation substrate **79** was prepared from 6-methyindole **77** in three steps. The starting material **77** was subjected to Vilsmeier formylation to give aldehyde **78**, which condensated with ethyl malonate to give a 5:1 mixture of two isomeric acetamidoacrylic esters **79** and **80**. Saponification of the ester **79** forms **81** which is a better substrate for enantioselective catalytic hydrogenation. Various catalysts have been extensively studied, and the results showed that the phosphine ligand **84** in combination with [Rh (cod) $Cl]_2$ gave the best yield (100 %) and ee (83 %). The hydrogenation product was identified as pure *R* configuration. Finally, *N*-acetyl group is carefully removed under mild conditions to afford enantiomerically pure **83**.

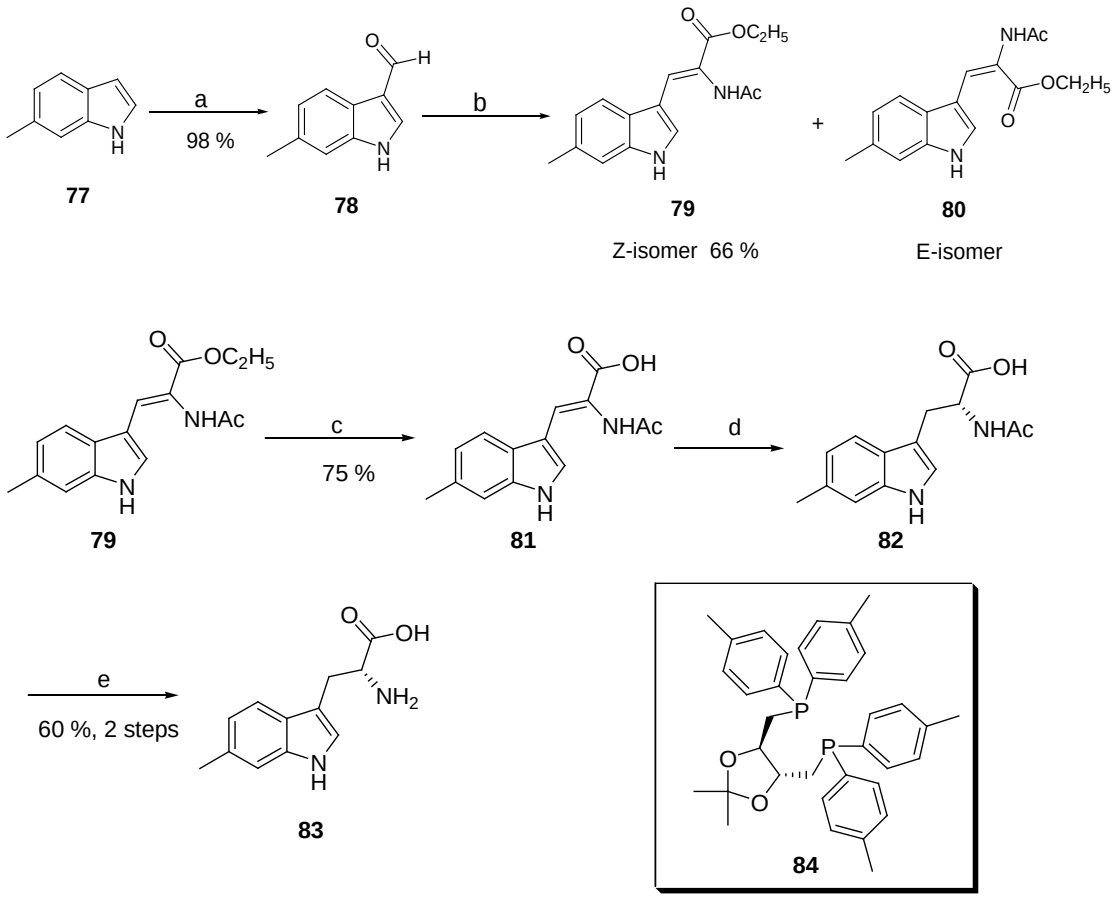

Scheme 2-4 Synthesis of 6-methyl-(*R*)-tryptophan (83) by Hengartner's group; Reagents and conditions: (a) $POCl_3$, DMF, room temp.; (b) Ethyl acetamidomalonate, Ac_2O, pyridine, room temp.; (c) NaOH, 70 °C; (d) H_2, **84**, $[Rh(cod)Cl]_2$, MeOH, room temp.; (e) 2.5 M HCl, reflux.

2.1.5 Synthetic approaches to 4-methoxy-tryptophan

2.1.5.1 Nickeleit's approach for the synthesis of 4-methoxy-(*S*)-tryptophan

A similar route using catalytic hydrogenation was recently developed by Nickeleit's group in 2010.[151] In order to prepare 4-methoxy-(*S*)-tryptophan, required for the total synthesis of argyrin F, a new catalyst was introduced to provide 4-methoxy-(*S*)-tryptophan **89** in excellent yield (99 %) and high ee (99 %). The seven-step synthesis is illustrated in Scheme 2-5. The initial three-step reaction gave the hydrogenation substrate **87**. Thus, the starting material 4-methyoxyindole was subjected to Vilsmeier formylation to give aldehyde **85**, followed by *N*-Boc protection of indole. Next, using phosphonoglycine and DBU, the Horner-

Wadsworth-Emmons reaction was applied to convert indole-3-carboxaldehyde **86** to (*Z*)-dehydrotryptophan **87** as a single isomer. It is worth noting that the (*Z*) geometric selectivity of this method is superior to Hengartner's method outlined in Section 2.1.4.

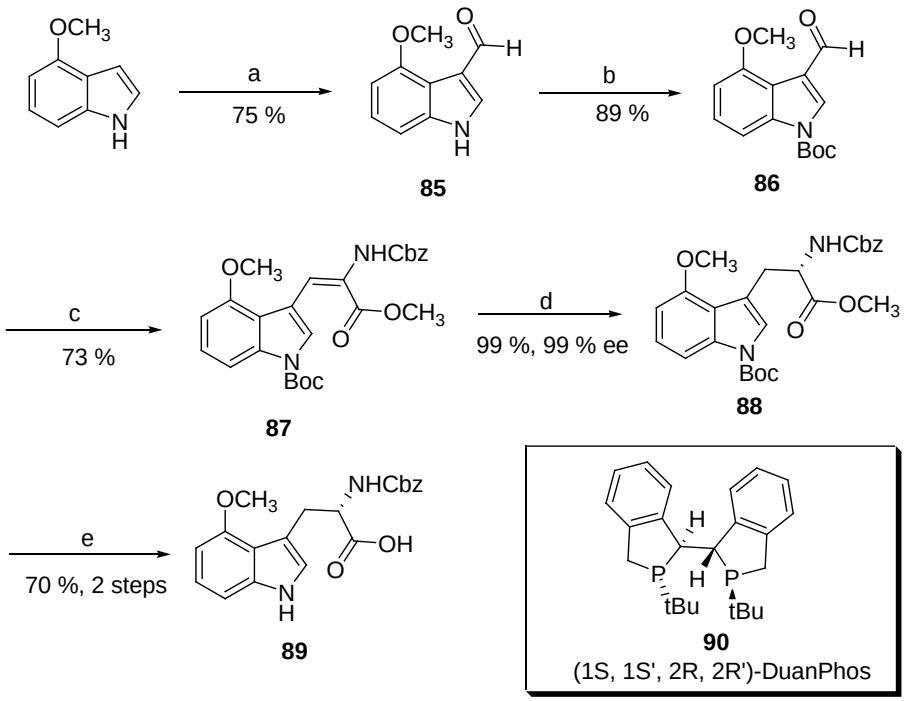

Scheme 2-5 Synthesis of *N*-CBz-4-methoxy-(*S*)-tryptophan (89) by Nickeleit's group; Reagents and conditions: (a) $POCl_3$, DMF, 45 °C; (b) $(Boc)_2O$, DMAP, DCM, room temp.; (c) **(***Z***)-***α*-Phosphonoglycine trimethyl ester, DBU, DCM, room temp.; (d) H_2, $Rh(cod)_2BF_4$, **90**, MeOH, room temp.; (e) i. TFA, DCM, room temp.; ii. LiOH, THF/ MeOH/ H_2O, room temp.

The synthesised substrate **87** was then subjected to asymmetric hydrogenation. In fact, this specific strategy was first described by Moody *et al*. in 2004.[168] Using the catalyst $Rh(cod)_2BF_4$, in combination with DuanPhos ligand **90** under 10 bar of hydrogen gave an enantiomerically pure tryptophan **88**. Finally, the desired product **89** was obtained by TFA-mediated acidolysis of the Boc group followed by saponification of the methyl ester.

2.1.5.2 **Cook's approach for the synthesis of 4-methoxy-(*R*)-tryptophan**

In the course of a total synthesis of the indole alkaloids mitragynine, Cook and colleagues reported a new route for the synthesis of 4-methoxy-(*R*)-tryptophan in 2009 (Scheme 2-6(b)).[169] Unlike other methods which use indole derivatives as

starting materials, Cook employed Larock heteroannulation of iodide-substituted alanine **94** with the internal alkyne **93a** directly to build the stereogenic centre of the tryptophan. The propargyl-substituted Schöllkopf chiral auxiliary **93a** was prepared from the reagent **91**, which can be obtained from (*R*)-valine and (*S*)-glycine using standard four-step procedures.[170] Thus, reaction of **91** with diphenyl (trimethylsilyl)propargyl phosphate **92** gave diastereoselective products **93a** and **93b** in 46 : 1 ratio (Scheme 2-6 (a)). It is worth mentioning that the leaving group in **92** other than phosphate, such as bromo or *O*-tosyl, gave poorer diastereoselectivities.[171]

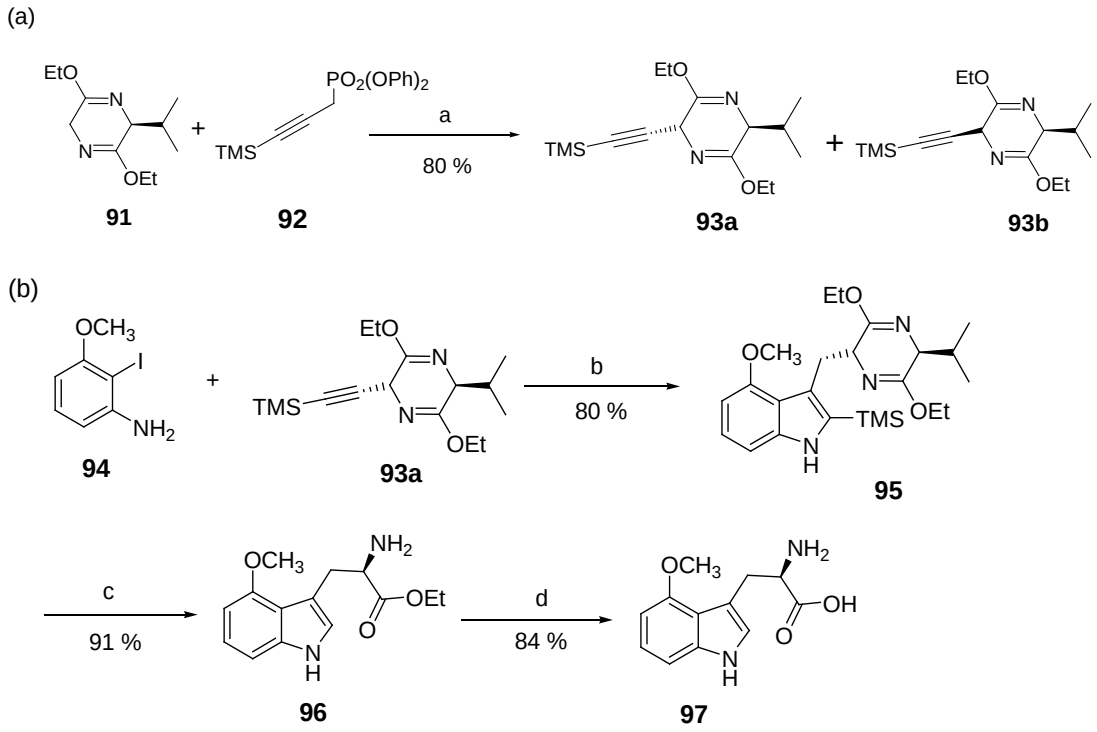

Scheme 2-6 Synthesis of 4-methoxy-(*R*)-tryptophan (97) by Cook's group; Reagents and conditions: (a) *n*-BuLi, THF, -78 °C; (b) $Pd(OAc)_2$, K_2CO_3, LiCl, DMF, 100 °C; (c) 2 M HCl, THF, room temp.; (d) NaOH, EtOH, room temp.

Internal alkyne **93a** was then used for the Larock heteroannulation (Scheme 2-6 (b), step b). Good regio- and stereo-selectivity were reported when TMS propargyl-substituted Schöllkopf chiral auxiliary **93a** was used. As shown in Figure 2-1, this selectivity was attributed to the steric interactions between the methoxy substituent and the TMS on the alkyne. The less sterically hindered intermediate **98** is more favoured than the intermediate **99**. Thus, the corresponding product **95** was formed.

Next, the Schöllkopf chiral auxiliary and indole-2-silyl group in **95** were hydrolysed in 2 M aqueous HCl to afford 4-methoxy-(*R*)-tryptophan ethyl ester **96**. Finally, saponification of the ethyl ester afforded 4-methoxy-(*R*)-tryptophan **97**. In general, this method is a short synthetic process and gives good yield, but the general application is restricted by the regio-selectivity of annulation which relies on the presence of steric group at the aromatic ring.

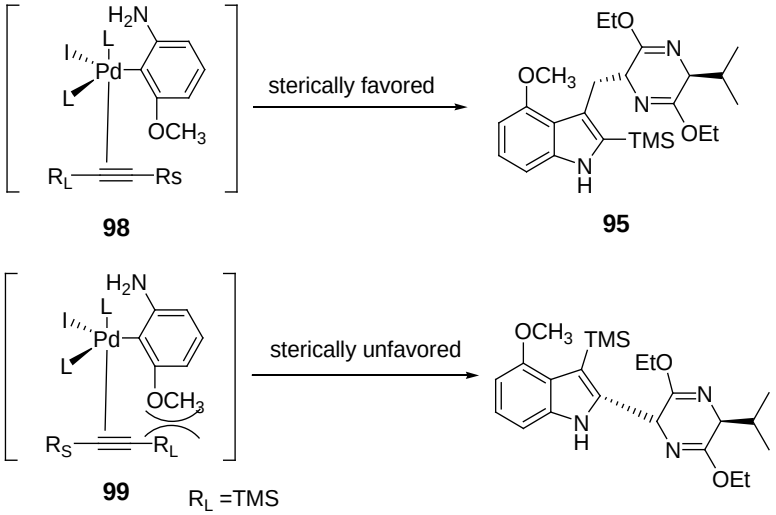

Figure 2-1 Proposed steric effect for the Larock heteroannulation.

2.1.5.3 **Jiang's approach for the synthesis of 4-methoxy-(*S*)-tryptophan**

In the course of a total synthesis of argyrin A, Jiang *et al*. successfully adopted a ligand-less palladium-catalysed one-pot annulation reaction previously established by Zhu in 2006.[152, 172] The five-step synthesis is outlined in Scheme 2-7(a). Similar to Cook's strategy (Section 2.1.6), the tryptophan derivatives were directly constructed from a heteroannulation reaction between an aldehyde **100** prepared from glutamic acid in three steps (Scheme 2-7(b)) and the aryl iodide **94**.[173] The glutamic acid was firstly converted to diester **103**, followed by Boc protection of the amine. Then dimethyl *N*,*N*-di-Boc-glutamate **104** was then reduced with diisobutylaluminium hydride (DIBAL) under mild conditions to form the aldehyde **100** in good yield. With the aldehyde **100** in hand, it was annulated to aryl iodide **94** using Zhu's conditions [$Pd(OAc)_2$, DMF, DABCO, 85 °C] to afford the desired tryptophan derivative **101**. Finally, selective deprotection of *N*-Boc and hydrolysis of the methyl ester **102** gave *N*-Boc-4-methoxy-(*S*)-tryptophan. So far, among these

established synthetic routes to prepare tryptophan derivatives, Jiang's approach not only tolerates a wide range of substituent in the indole ring, but also afforded good yields. However, it is envisaged that the application of this strategy for the synthesis of halotryptophans would be drastically limited since aryl halides could interfere with the annulation reaction.

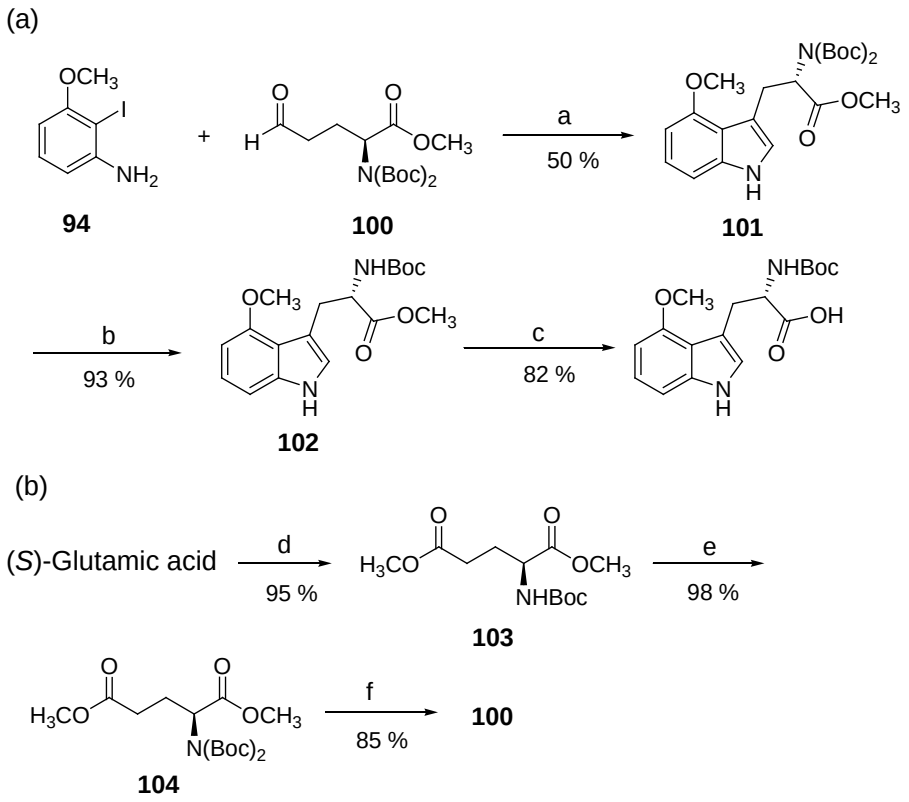

Scheme 2-7 Synthesis of 4-methoxy-(*S*)-tryptophan by Jiang's group; Reagents and conditions: (a) $Pd(OAc)_2$, DABCO, DMF, 85 °C; (b) $BiBr_3$ (10 mol %), MeCN, room temp.; (c) LiOH, THF/ MeOH/ H_2O, room temp.; (d) i. TMSCl, MeOH; ii. Boc_2O, Et_3N, MeOH; (e) Boc_2O, DMAP, MeCN; (f) DIBAL, Et_2O, -78 °C.

2.2 **Preparation of tryptophan analogues using new method exploiting Strecker condensation with (*R*)-2-phenylglycinol**

The literature methods in Section 2.1 provide several possible methodologies for the preparation of tryptophan derivatives. However, most of these methods suffer from some limitations. For example, they might require reagents which are not economically viable or lack of generality. Therefore, an alternative route of accessing to a wide range of tryptophan derivatives was established as shown in Scheme 2-8. All desired Fmoc-tryptophan derivatives were synthesised from

corresponding indoles in seven steps. Briefly, inspired by the method established by Bayston *et al.* that cyclopropanecarboxaldehyde reacts with an α-alkylbenzylamine to give a mixture of two diastereomeric aminonitriles in 3.2 to 1 ratio, the key step of the synthesis is the use of chiral auxiliary (*R*)-2-phenylglycinol and mild conditions for hydrolysis of α-amino nitriles to α-amino acids (Scheme 2-8, steps c and d).[174]

A detailed consideration of each step is disclosed in the following sections.

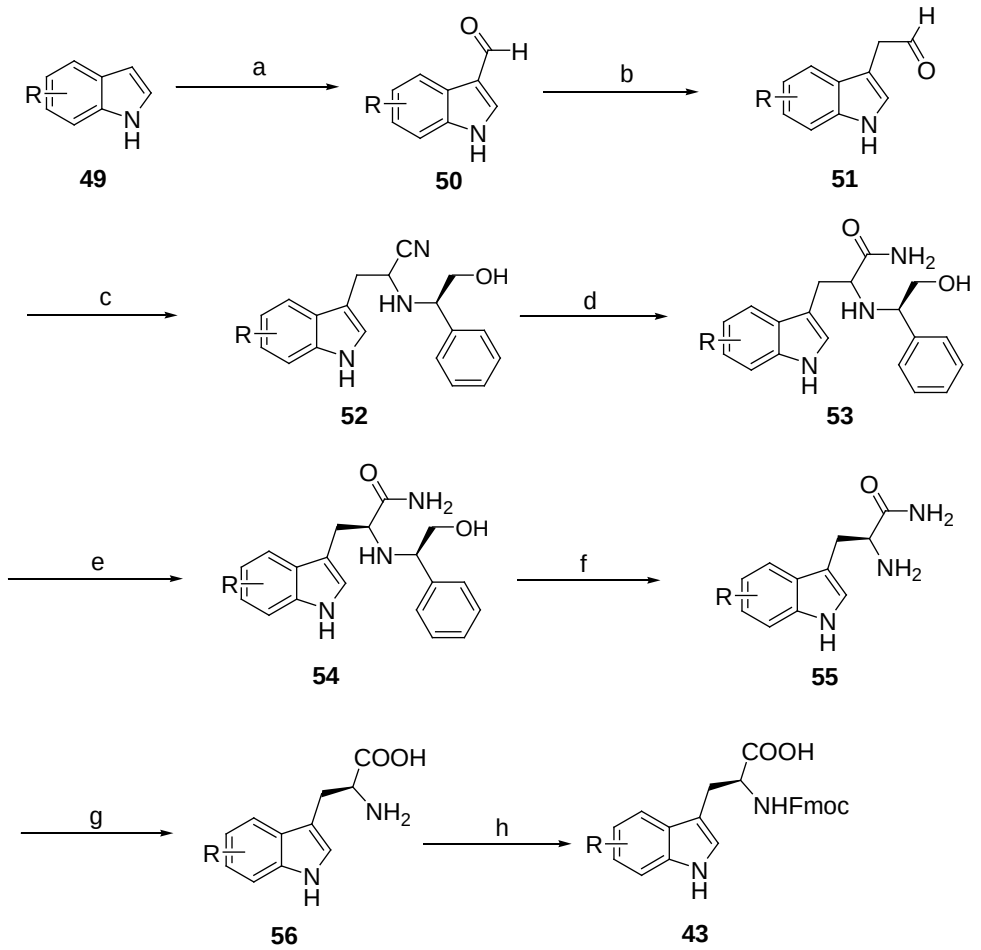

Scheme 2-8 Summary of a new method exploiting Strecker amino acid synthesis of (*S*)-tryptophan analogues (43); Reagents and conditions: (a) $POCl_3$, DMF, 0 °C then 45 °C; (b) i. $Ph_3PCH_2OCH_3$, n-BuLi; ii. HCl, THF, reflux; (c) (*R*)-2-Phenylglycinol, NaCN, AcOH, MeOH; (d) H_2O_2, Na_2CO_3, DMSO; (e) Recrystallisation or RP-HPLC; (f) Pd/ C, NH_4HCO_2, MeOH, reflux; (g) 1 M HCl, reflux; (h) Fmoc-OSu, $NaHCO_3$, THF,/H_2O.

2.2.1 **Vilsmeier-Haack formylation**

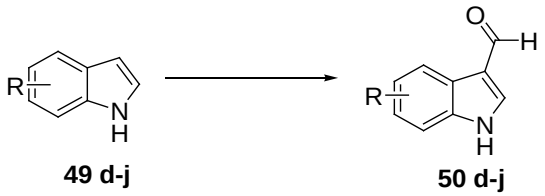

49 d-j **50 d-j**

	d	**e**	**f**	**g**	**h**	**i**	**j**
R =	6-F	7-Et	5-Me	5-MeO	4-MeO	1-Me	2-Me

As shown in Scheme 2-8, the initial step in this synthesis is to install an aldehyde at the 3-position of the indole ring. Vilsmeier-Haack reaction is one of the most commonly used for formylation of electron-rich aromatic compounds to yield aromatic aldehydes.[175] The Vilsmeier reagent is normally prepared *in situ* by the addition of a *N,N*-disubsituted formamide, such as DMF or *N*-methylformanilide to phosphorus oxychloride or phosgene. The heteroaromatic compounds, such as indole derivatives, undergo formlyations when treated with Vilsmeier reagents. Good regioselectivity at *C*-3 indole carbon can be achieved, as electron-rich *C*-3 of the indole system gives the lowest resonance transition state. The mechanism of the Vilsmeier formylation of indole derivatives is shown in Figure 2-2.

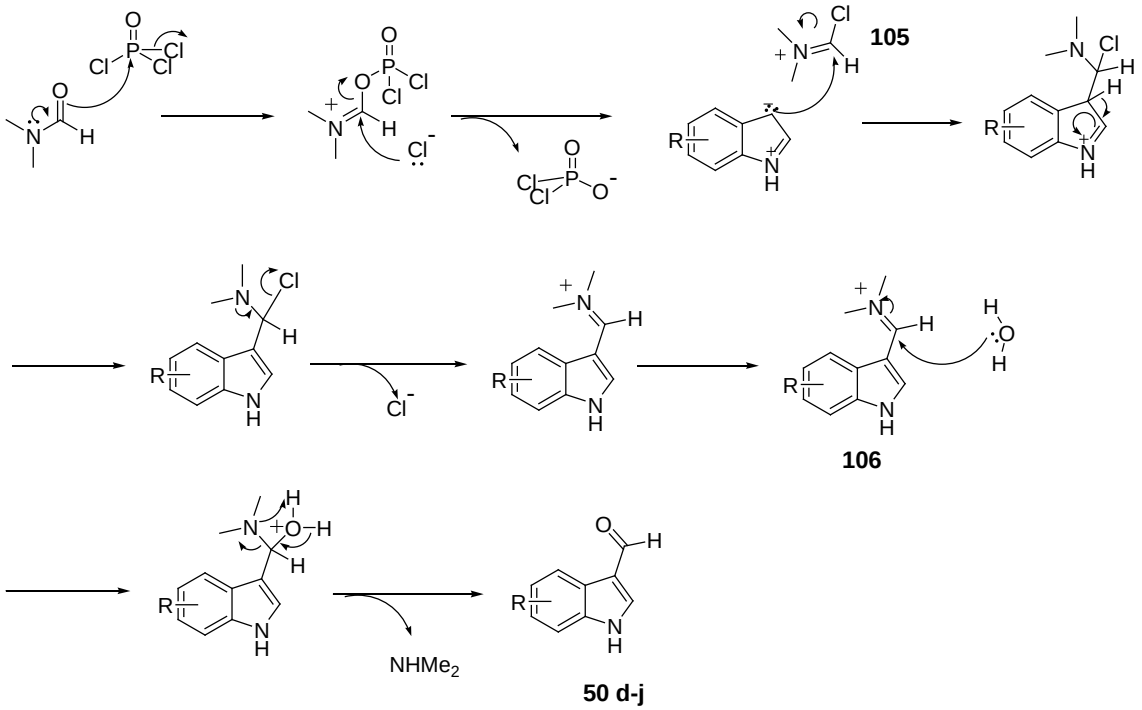

Figure 2-2 Proposed mechanism of Vilsmeier formylation.

The first step is formation of the electrophilic iminium **105** which is prepared from DMF and $POCl_3$. In practice, DMF was used as a reagent and as a solvent. The iminium intermediate **105** then underwent electrophilic substitution to the electron rich position of indole ring. The intermediates **106** are unstable and can be easily hydrolysed. Therefore, the next step is to hydrolyse **106** using $Na_2CO_{3(aq)}$ to give indole-3-carboxaldehyde derivatives (**50d-j)**.

In theory, regardless of the R group in the indole ring, the formlyation takes place exclusively at *C*-3 position under controlled temperature. Initially, 3 equivalents of Vilsmeier reagent were used, following the literature conditions at 45 °C for 2 h.[151] The production of aldehydes **50d-j** were confirmed by ^{1}H NMR analysis, which revealed the appearance of a distinctive aldehyde singlet at δ 10.02 ppm. Thus, most of the indole derivatives were successfully converted to the corresponding indole-3-carboxaldehydes in good yields. However, lower yields (50-60 %) were obtained for the methoxyindoles (**49g** and **49h**), even though the starting material methoxyindoles had been completely consumed. Consequently, a number of reaction conditions were evaluated; including changes in the reaction temperature and duration. Surprisingly, increasing the reaction temperature from 45 to 100 °C resulted in formation of both 3-formylated and *N*-formylated products. Presumably,

the thermodynamic stable product, *N*-acylated indole, could be formed at the high temperature. Moreover, low yields were observed due to poor solubility of the methoxy-substituted product during the work-up procedure.

2.2.2 **Homologation of aldehyde *via* Wittig reaction**

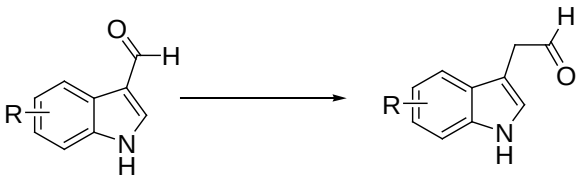

50a-j **51a-j**

	a	**b**	**c**	**d**	**e**	**f**	**g**	**h**	**i**	**j**
R =	H	5-Br	5-Cl	6-F	7-Et	5-Me	5-MeO	4-MeO	1-Me	2-Me

In order to apply the Strecker amino acid synthesis strategy (Section 2.2.3) for the synthesis of tryptophan derivatives, the resultant aldehydes must be extended by one-carbon unit. This transformation is commonly known as a homologation reaction. Homologation of aldehydes has been extensively studied.[176-178] However, conventional methods involving the reaction of the diazoalkane with aldehydes to produce ketones or alcohols is not applicable for Strecker amino acid synthesis.[176, 177] Other than diazoalkane derived homologation, Wittig reagents are also employed in aldehyde homologations which produce a homologous aldehyde.

Here, Wittig reaction was applied using (methoxymethyl)triphenylphosphonium chloride **107** to yield enol ethers which easily undergo acid-catalysed hydrolysis to the corresponding aldehydes.[178] The mechanism of this two-step homologation is shown in Figure 2-3.

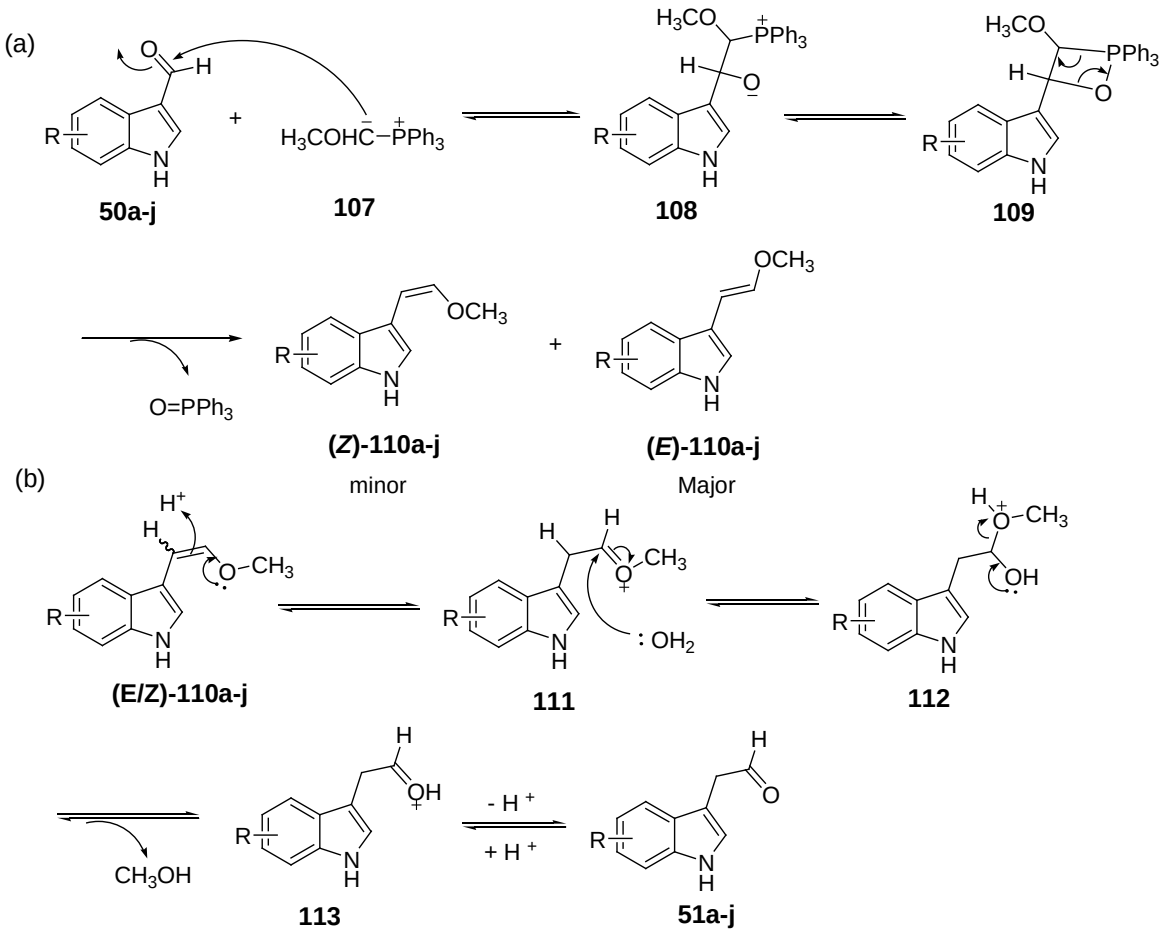

Figure 2-3 Mechanism of two-step aldehyde homologation (a) Wittig reaction. (b) Acid-catalyst hydrolysis of enol ether.

The reaction was initiated by the ylide formation (Figure 2-3(a)). Phosphonium ylide **107** was prepared *in situ* as a dark red solution in dry THF by stirring the phosphonium salt with a strong base, *n*-butyllithium. Next, **50d-j** and commercially available aldehydes **50a-c** were added dropwise to the mixture under a nitrogen atmosphere, and ylide **107** then readily underwent nucleophilic substitution at the carbonyl groups of the aldehydes to give the diionic betaines **108**. The betaine intermediates were then converted to the lower energy state form, which is known as an oxaphosphetane **109**. Finally, the formation of stable triphenylphosphine oxide drives the elimination to give the *E*- and *Z*-alkenes. As expected, a major spot and a minor spot were observed by TLC after work-up. Although other factors could affect the *E/Z* ratio, stabilised ylide was established to give the *E*-configuration **110a-j** as the major product, as the less crowded of trans-oxaphosphetane was formed under thermodynamic control. Indeed, desired *E/Z*

enol ether formation was confirmed by ^{1}H NMR analysis, which revealed the disappearance of the aldehyde proton (δ = 10.5 ppm, s, C*H*O) in the starting material **50b** and the appearance of the two pairs of alkene protons (δ = 5.58, 6.19 ppm, d, for *E*-isomer and δ = 5.94, 7.03 ppm, d, for *Z*-isomer) in the enol ether **110b** (Figure 2-4). In addition, although the stereoselectivity outcome is an important concern for the Wittig reaction, it should not have an effect on the subsequent enol ether hydrolysis. Therefore, a mixture of two isomers was used directly in the next step of the reaction.

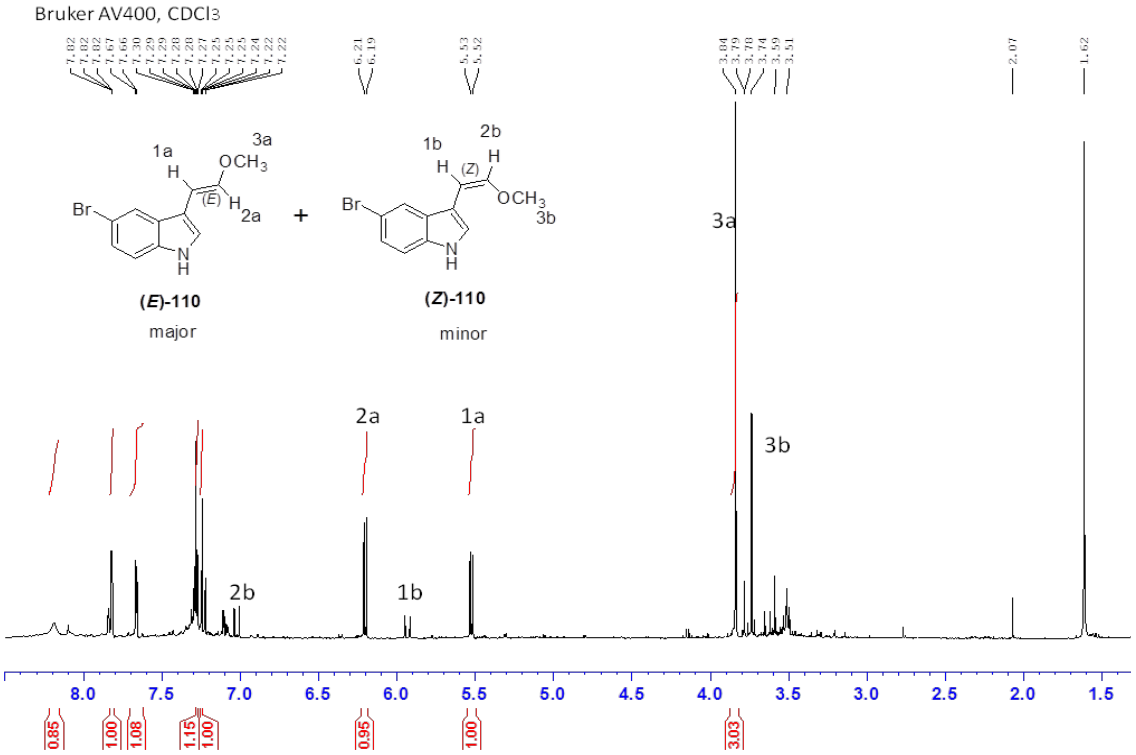

Figure 2-4 ^{1}H NMR spectrum of 5-bromo-3-(2-methoxyvinyl)-1*H*-indole (110b).

The enol ethers **110a-j** are relatively unstable compounds. Consequently, **110a-j** following a rapid silica gel chromatography to avoid decomposition were immediately subjected to acid-catalysed hydrolysis to the aldehydes. The mechanism of acid-catalysed hydrolysis of enol ether is shown in Figure 2-3(b). The delocalisation of the oxygen long pair led to the protonation of the alkenic carbon to produce oxonium intermediates **111**. The unstable oxonium ions **111**

were nucleophilically attacked by water to form hemiacetal intermediates **112**, which subsequently yielded the desired aldehydes **51a-j**.

Initially, the acid hydrolysis of all enol ether derivatives was examined by refluxing in a mixture of 1 M aqueous HCl (12 mL) and THF (18 mL). This condition gave the homologated aldehydes in moderate yields when R = H (**110a**), halogens (**110b, 110c, 110d**) and ethyl (**110e**) but less than 10 % yields when R = Me (**110f**) and MeO (**110g** and **110h**). Under the standard acid-catalysed hydrolysis conditions, these indoles with an electron-donating substituent (**110f, 110g, 110h**) resulted in decomposition.

Table 2-1 Optimisation of enol ether hydrolysis for 5-methoxy-(*E/Z*)-3-(2-methoxyvinyl)-1*H*-indole (110g).

	Temperature	Solvent	Acid	Conc.	Time (h)	Observation
1	Reflux	THF/ H_2O	HCl	0.1 M	2	product (47 % crude yield) and decomposition
2	Reflux	Acetone/H_2O	HCl	0.1 M	2	product (43 % crude yield) and decomposition
3	Reflux	THF/ H_2O	HCl	0.4 M	2	product (9 % crude yield) and decomposition
4	Room temp.	THF/ H_2O	HCl	0.1 M	48	no reaction for 3 h, decomposition over 48 h
5	Room temp.	THF/ H_2O	acetic acid	3 eq.	5	starting material and trace amount of product
6	Reflux	THF/ H_2O	acetic acid	3 eq.	2	decomposition
7	Room temp.	THF/ H_2O	formic acid	3 eq.	5	starting material and trace amount of product
8	Reflux	THF/ H_2O	TsOH	3 eq.	3	decomposition
9	Room temp.	THF/ H_2O	$Hg(OAc)_2$	1 eq.	3	decomposition

To avoid decomposition of methoxy substituted analogues (**110g, 110h**), the hydrolysis of **110g** was studied under various conditions. A systematic evaluation of a series of acids and at various concentrations took place. The result of this study, summarised in Table 2-1, indicates that heating is required since no hydrolysis occurred when the reaction was carried out at room temperature (entry 4). No improvement was obtained using acetone/H_2O as the reaction solvent (entry 2). Moreover, replacing HCl with milder acids, such as acetic acid (entry 6), formic acid (entry 7) and toluenesulfonic acid (entry 8)[179] also failed to give the product. Another attempt by treatment with $Hg(OAc)_2$ followed by KI-induced elimination

also failed in this study (entry 9).[180] These disappointing results led to the consideration of fine balance between the acid concentration and reaction temperature. Improved yield (47 %) was obtained by decreasing the HCl concentration (entry 1). Although decomposition of **110g** cannot be avoided, the yield was nevertheless considered acceptable.

The results of eight analogues are summarised in Table 2-2. To sum up, the efficiency of acid hydrolysis of the enol ethers **110a-j** is dependent on the aryl substitution of the indole ring. Regardless of the substitution positions, indoles with an electron-donating substitution **110e-h** are more labile to acid-mediated decomposition than their counterparts with electron-withdrawing groups **110b-d**. Hence, the two-step homologation reaction was monitored carefully by TLC to avoid the decomposition of the indole subunit.

Table 2-2 Hydrolysis of (*E*/*Z*)-3-(2-methoxyvinyl)-1*H*-indole (110a-j)

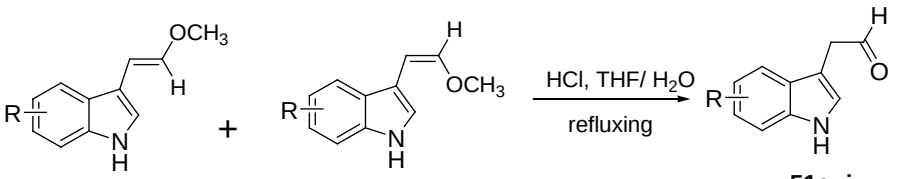

(*E*)-110a- j **(*Z*)-110a- j** **51a- j**

Starting material **(*E*/*Z*)-110a-j**	R	Acid conc. (M)	Reaction time (h)	Crude yield of **51a-j** (%)
110a	H	0.4	2.5	69
110b	5-Br	0.4	2	74
110c	5-Cl	0.4	2	74
110d	6-F	0.4	2	73
110e	7-Et	0.4	2	65
110f	5-Me	0.4	1.5	60
110g	5-MeO	0.1	1.5	55
110h	4-MeO	0.1	1.5	47
110i	1-Me	0.4	2	76
110j	2-Me	0.4	2	70

It is also worth noting that **51a-j** are unstable. In fact, the crude homologated aldehydes were initially yellow in EtOAc / hexane solution, but on removal of solvent the reaction mixtures were gradually decomposed to dark oils which were

no longer soluble in EtOAc. Consequently, the crude aldehydes **51a-j** were directly subjected to Strecker amino acid synthesis.

2.2.3 **Strecker amino acid synthesis**

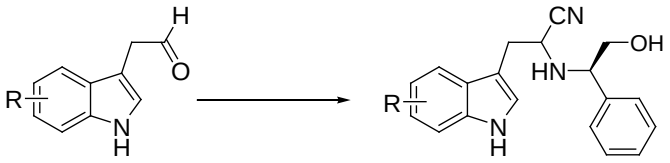

51a- j **52a- j**

	a	**b**	**c**	**d**	**e**	**f**	**g**	**h**	**i**	**j**
R =	H	5-Br	5-Cl	6-F	7-Et	5-Me	5-MeO	4-MeO	1-Me	2-Me

The classical Strecker amino acid synthesis was developed over 160 years ago by Adolph Strecker.[181] This α-amino acid synthesis can be divided into two successive steps. The first step is condensation of an aldehyde with an amine in the presence of a cyanide salt to form an α-amino nitrile. The second step is hydrolysis of α-amino nitrile to carboxylic acid. In the classical Strecker synthesis, racemic α-amino acid was obtained. Hence, several asymmetric synthesis methods have been developed.

In general, chiral auxiliary reagents for asymmetric Strecker synthesis can be divided into two classes. The first uses a chiral catalyst to facilitate an enantioselective product. A number of metal-coordinated catalysts which consist of chiral ligands attached to metals such as Al, Ti and Zr have been described to provide enantioselective products in good yields.[182-184] In addition to metal catalysts, several organo-catalysts which comprise a chiral diketopiperazine, guanidine or Schiff base have also been developed.[185]

The second class uses a chiral inducing agent, such as β-amino alcohol,[186, 187] amino diols, α-arylethylamines[188-190] and their derivatives to give a diastereoselective α-amino nitrile at different level of chiral purity. The major advantages of this class of chiral auxiliaries are (1) most of them are inexpensive and easily accessible, (2) their removal can be achieved under mild conditions and (3) they tolerate broad range of substrates. Therefore, a chiral inducing auxiliary was chosen for the tryptophan derivative synthesis.

Initially, the simplest chiral inducing agent (*S*)-methylbenzylamine **115** was introduced in the asymmetric Strecker synthesis of α-amino nitriles **117a-j**. The mechanism of the first step condensation is shown in Figure 2-5. The reaction is initiated by protonation of the carbonyl oxygen of the aldehyde. The intermediate **114** is then nucleophilically attacked by the amine **115** to form an imine **116**. Next, cyanide ion attacks to the iminium carbon to afford aminonitriles **117a-j**. In the process of nucleophilic addition, the cyano nucleophile is more favourable to attack from the less shielded diastereotopic face (re-face) therefore preferentially affording (*S*,*S*) isomer **117 a-j** in excess.

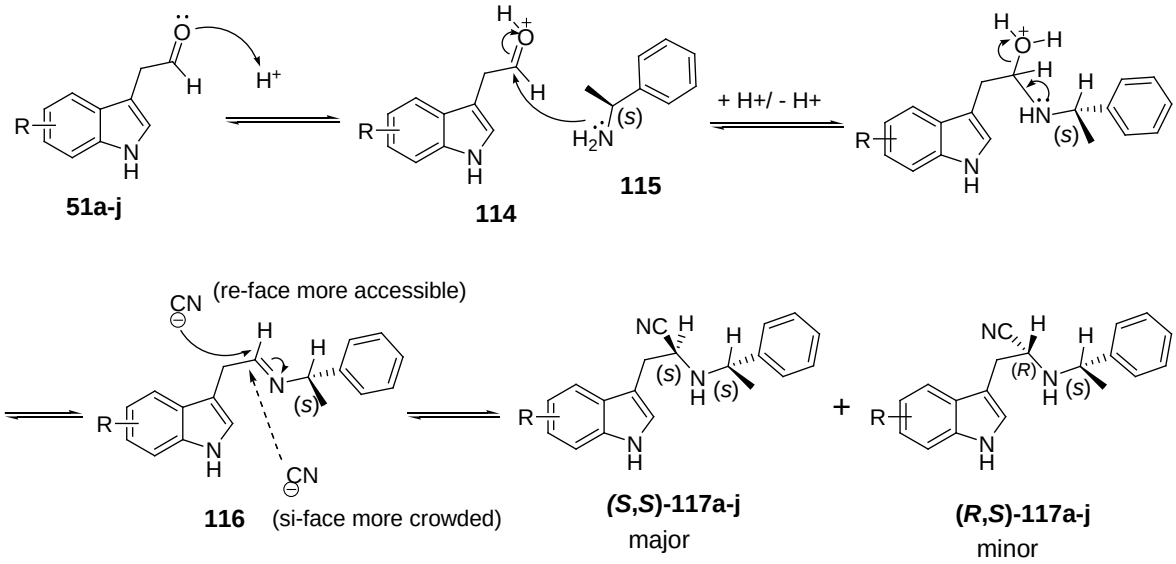

Figure 2-5 Mechanism of amino nitrile formation.

In practice, an one-pot Strecker synthesis of the α-amino nitriles was used. Thus, one equivalent of amine **115** was added to a mixture of the aldehydes **51a-j**, sodium cyanide and acetic acid in methanol at 0 °C. The reaction mixtures were allowed to warm to room temperature and were stirred for 16 h. However, monitoring the progress of the reaction by TLC was found to be difficult since starting materials (**51a-j**) and products (**117a-j**) showed similar R_f values in many solvent pairs. The mixtures were stirred for 16 h, followed by an aqueous work-up. The desired products (*S*,*S*)-**117a-j** and (*R*,*S*)-**117a-j** were obtained in 30-70 % yield in a ratio of 3 : 1. The diastereomeric ratio of (*S*,*S*) and (*R*,*S*) was established by ^{1}H NMR on the basis of the relative integration between two isomers. Figure 2-6 illustrates the ^{1}H NMR of crude amino nitrile **117a**. The three to one ratio of the

two diastereomers was obtained by comparing the integration of the methyl signal at δ = 1.35 ppm for (*S*,*S*)-**117a** and δ = 1.39 ppm for (*R*,*S*)-**117a**. In addition, this diastereoselectivity was further confirmed by RP-HPLC analysis which is shown in Figure 2-7.

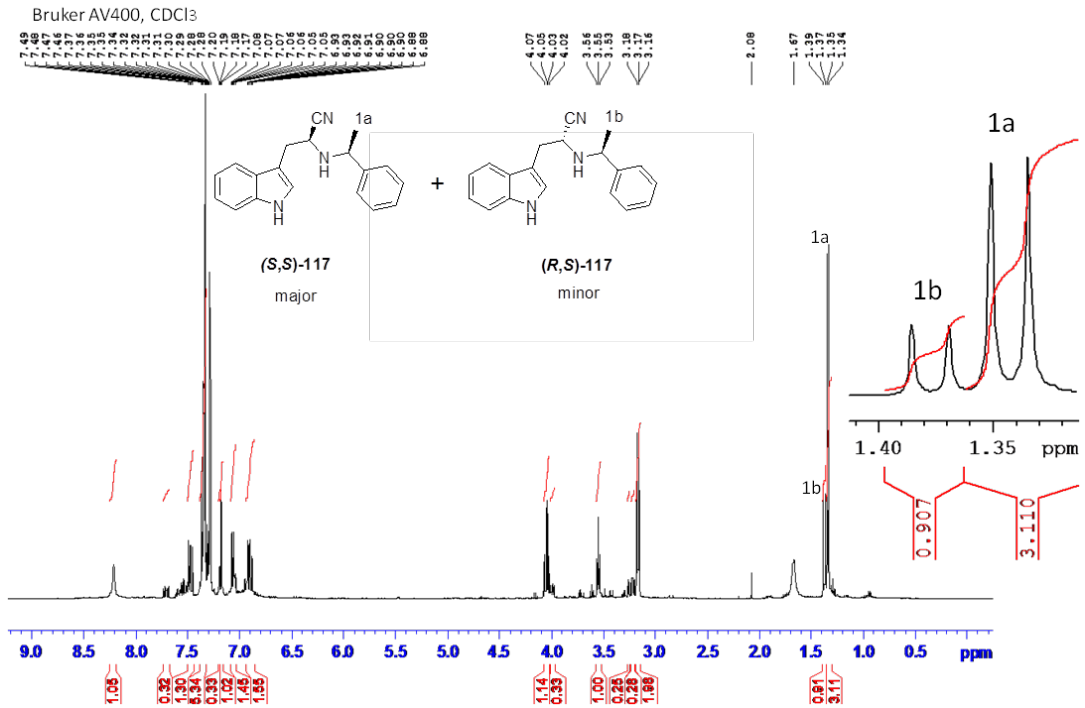

Figure 2-6 **^{1}H NMR spectrum of a mixture of amino nitriles (*S*,*S*)-117a and (*R*,*S*)-117a.**

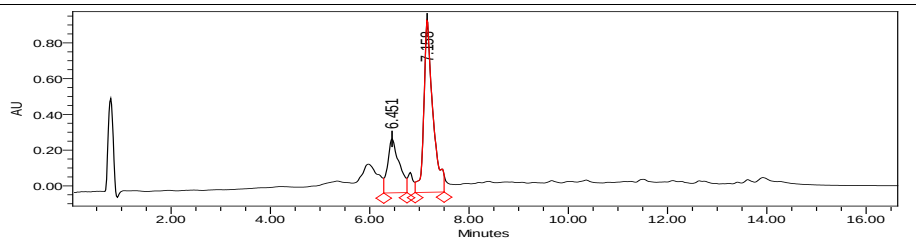

	Name	Retention time	Area	% Area	Height
1	(*R*,*S*)-**117a**	6.041	7961803	23.41	575107
2	(*S*,*S*)-**117a**	7.177	26041955	76.59	2019790

Figure 2-7 RP-HPLC trace of a mixture of the amino nitriles (*S*,*S*)-117a and (*R*,*S*)-117a. Peaks were identified using MS. The method used was 3-30 % B over 10 min at 3 mL/min (Onyx Monolithic C_{18}, 100 x 4.6mm). Eluent detection was monitored by UV absorbance at 216 nm.

In view of other chiral auxiliaries reported in the literature, which gave higher diastereomeric excess, another chiral auxiliary (*R*)-2-phenylglycinol **118** was applied to the asymmetric synthesis (Figure 2-8 (a)). According to the literature,

(*R*)-2-phenylglycinol **118** gave high diastereomeric excess in a broad range of substrates and the two diastereoisomers can be separated by column chromatography.[187, 191, 192] In principle, the hydroxyl group in (*R*)-2-phenylglycinol not only stabilises the predominant reactive conformer **119** by forming a hydrogen bond to the imine (Figure 2-8(b)),[187] but also facilitates interaction to silica gel leading to better chromatographic separation. However, in practice, no differences were observed between two chiral auxiliaries. The products were obtained as a 3:1 mixture of two diastereomers.

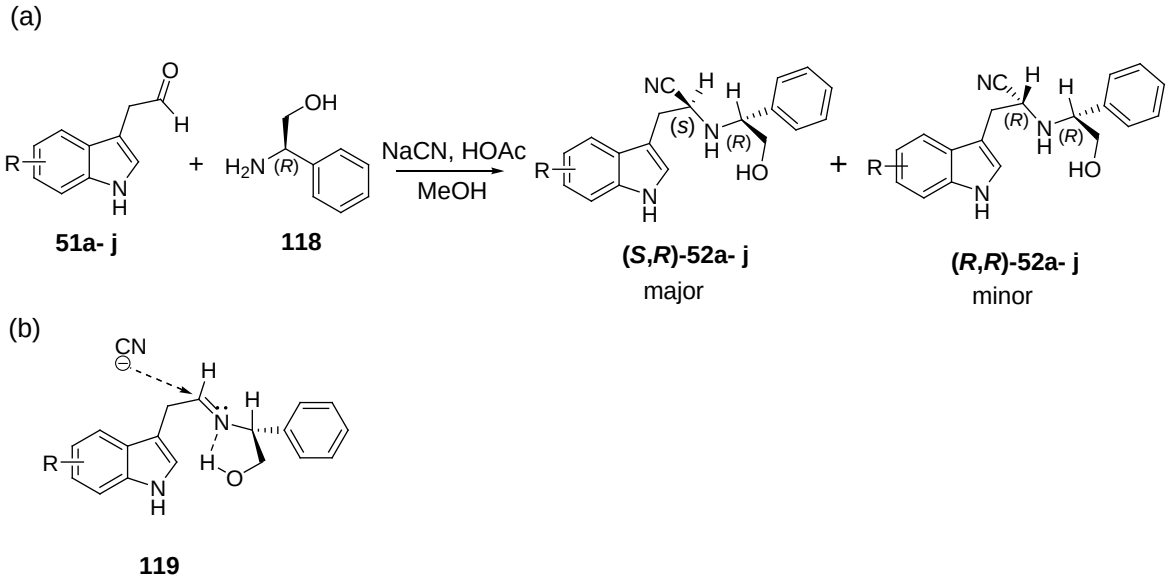

Figure 2-8 (a) Strecker synthesis using 118 as a chiral auxiliary. (b) Proposed intermediate of (*R*)-2-phenylglycinol induced chiral selectivity.

Unfortunately, confirmation of the absolute configuration by X-ray crystallographic analysis was not achieved since single crystals of neither amino nitriles **117a-j** nor **52a-j** could not be obtained. The major (*S*,*R*) configuration assigned was based on the literature precedents with simpler substrates.[174, 193] Several attempts also have been made to separate the two diastereisomers by fractional crystallisation. However, it was observed that only bromo-substituted analogy **52b** barely gave crystals. Moreover, these two isomers only showed one spot in TLC analysis which suggested column chromatography separation would be difficult. Therefore, it was decided that the two diastereisomers would be separated at a later stage.

The second step of Strecker amino acid synthesis is to hydrolyse α-aminonitriles to their corresponding α-amino acids. Initial attempts to hydrolyse aminonitriles **117a-j** and **52a-j** directly to amino acids **120a-j** and **121a-j**, respectively, were found to be difficult (Figure 2-9).

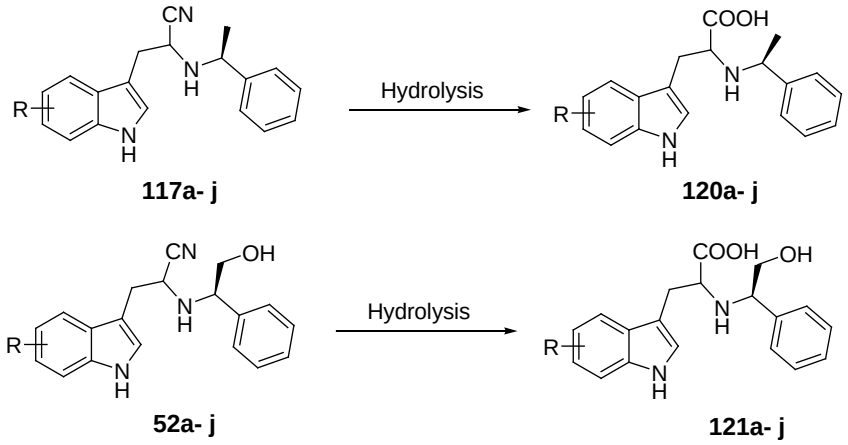

Figure 2-9 Hydrolysis of amino nitriles to amino acids.

Specifically, initial experiments were focused on acid- or base-catalysed hydrolysis methods.[194-196] The conversion of the aromatic nitrile to the corresponding carboxylic acid is a well-established procedure, but for the aliphatic nitrile it was not always straightforward. Typical acid- or base-catalysed hydrolysis methods require concentrated acid or strong alkali base at high temperatures. As was expected, these severe acidic conditions led to the decomposition of the α-aminonitriles, and only trace amount of α-amino acid was detected (Table 2-3, entries 1-9).

On the other hand, it was anticipated that base-catalysed hydrolysis could alleviate this problem. Unfortunately, no desired product was detected (entries 10 and 11). Moreover, alternative milder condition utilising sonochemistry in the presence of low concentration of aqueous HCl was employed (entry 12).[197] Again, no satisfactory result was obtained from the ultrasound-assisted hydrolysis. It can be concluded from these observations that the harsh acidic or basic conditions were detrimental to the indolyl subunit. Hence, alternative approaches were explored.

Table 2-3 Acid- and base-catalysed hydrolysis of the α-aminonitriles to the amino acids

	Acid/ Base	Solvent	Temp.	Time	Observation
1	3 M HCl	H_2O/THF	69 °C	2 days	trace amount of amino acid
2	3 M HCl	H_2O/MeOH	70 °C	1 day	decomposition, recovery tiny amount of starting materials
3	4 M HCl	H_2O/THF 2:1	78 °C	1 day	trace amount of amino acid
4	6 M HCl	H_2O/MeOH	r.t.	3.5 days	decomposition, recovery tiny amount of starting materials
5	6 M HCl	H_2O only	80 °C	2 days	trace amount of amino acid
6	6 M HCl	MeOH	70 °C	1 day	decomposition, recovery most of starting materials
7	10 M HCl	Dioxane	90 °C	17 h	decomposition
8	12 M HCl	H_2O	50 °C	3.5 days	decomposition
9	50 % H_2SO_4	H_2O /DCM	r.t.	3.5 days	decomposition
10	NaOH	MeOH/ H_2O	60 °C	20 h	decomposition
11	$Ba(OH)_2$ 0.6eq	THF/H_2O	70 °C	2 days	decomposition
12	2 M HCl	THF/H_2O	70 °C)))) [a]	8 h	trace amount of amino acid

[a.] An ultrasonic horn operating at a frequency of 30 kHz was used.

Another feasible method to convert aminonitriles to amino acids is enzyme-catalysed hydrolysis. The major advantage of enzyme catalysing the conversion of nitrile substrates to its corresponding carboxylic acids is that the decomposition of labile functional groups in the substrates could be avoided. Enzyme catalysis can be accomplished *via* single-step reaction by nitrilase or *via* two-step reaction by nitrile hydratases and amidases.[198] There are several nitrilase-contained microorganisms which have been introduced to transform nitrile to its corresponding acid.[198] However, there are few reports on producing amino acid by using nitrilase, and neither even mentioning the usage of indole analogy as substrate of nitrilase, nitrile hydratases and amidases. The reactivity of these enzymes depends on factors including the chemical structure of substrate, pH and temperature. Therefore, to identify a microorganism or a nitrilase which are capable of hydrolysing aminonitriles **117a-j** or **52a-j**, large scale screening of possible strains and appropriate conditions would be anticipated.

Kinetic studies of acid- and base-catalysed hydrolysis of nitrile showed that the key obstacle of conversion of nitrile to carboxylic acid is hydrolysis of nitrile to amide.[199] Thus, alternative chemical transformation conditions were investigated for the preparation of amino acids **121a-j** *via* amino amides **53a-j** (Figure 2-10).

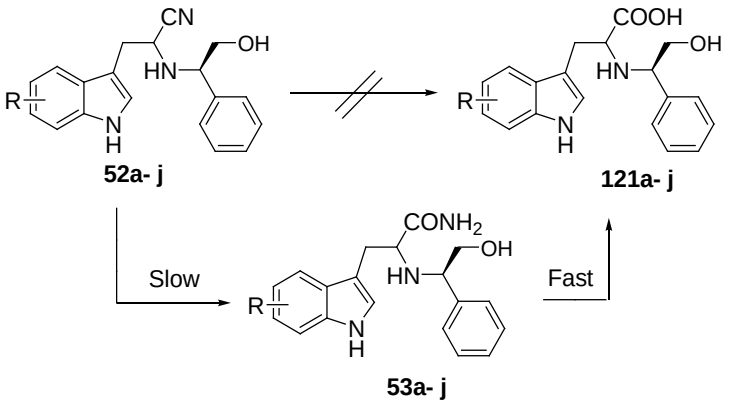

Figure 2-10 Hydrolysis of aminonitriles to acids *via* amino amides.

2.2.4 **Peroxide hydrolysis of α-aminonitriles**

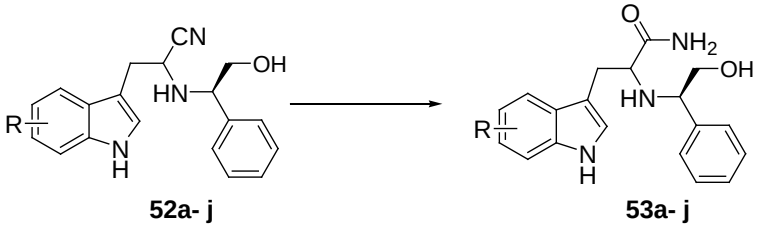

	a	**b**	**c**	**d**	**e**	**f**	**g**	**h**	**i**	**j**
R =	H	5-Br	5-Cl	6-F	7-Et	5-Me	5-MeO	4-MeO	1-Me	2-Me

Thus, a peroxide-mediated method reported by Katritzky was employed.[200] Aminonitriles **52a-j** were smoothly transformed into their corresponding amides **53a-j** by reacting with sodium peroxide in the presence of a mild base in dimethyl sulfoxide at room temperature. This method not only uses mild reaction conditions, but also possesses several advantages, including a short reaction time and ease of purification of the desired products.

The mechanism and kinetics of the reaction was studied by Wiberg *et al.*.[201] Although the stoichiometry of the reaction is normally written as an oxidation-reduction of hydrogen peroxide with the nitrile, the mechanism of the reaction is

not so simple (Figure 2-11(a)). Its specific mechanism can be understood in four-step sequence which is shown in Figure 2-11(b). The hydrogen peroxide first reacts with hydroxide anion to generate HOO^-. The nucleophile HOO^- is added to the nitrile to form a peroxycarboximidic acid intermediate **122**, which is believed to be the rate-determining step of the reaction. After a proton transfer, the peroxycarboximidic acid **123** undergoes oxidation-reduction with dimethyl sulfoxide (DMSO) to afford the amide and dimethyl sulfone ($DMSO_2$). It is worth noting that in this reaction, adding DMSO as a solvent or as an additive significantly increases the reaction rate by several hundred times.[201]

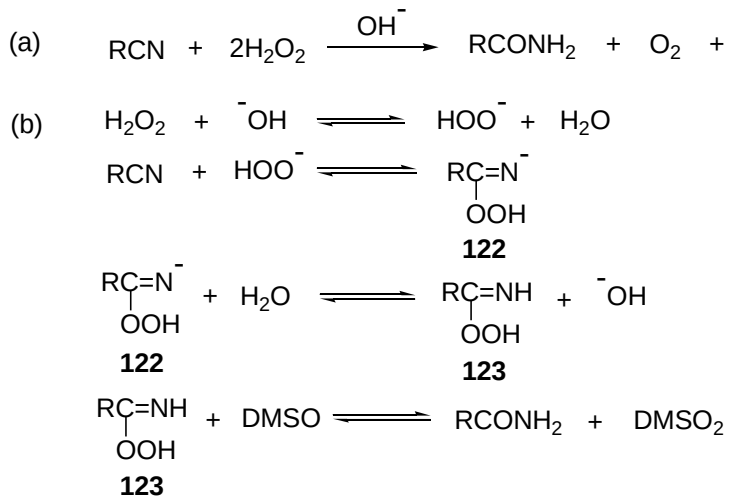

Figure 2-11 (a) Reaction of nitriles with alkaline hydrogen peroxide. (b) Proposed mechanism of peroxide hydrolysis of nitriles.

In practice, the aminonitriles **52a-j** were dissolved in a small amount of dimethyl sulfoxide (DMSO) in the presence of a catalytic amount of potassium carbonate. The reaction conditions employed an excess of 30 % aqueous hydrogen peroxide at room temperature for 2 h. A further quantity of hydrogen peroxide solution was added to allow the completion of the reaction. The use of DMSO as the reaction solvent was found to be useful as it dissolves aminonitriles very well and is miscible with hydrogen peroxide solution. The reaction conversions were clean and fast. All aminonitriles **52a-j** were converted to the corresponding amides **53a-j** in 50 - 80 % yields. The hydrolysis itself was highly selective, yielding the amide with no detectable further hydrolysis to acid. In addition, the 2-position of indole system was not oxidised during this treatment. Further optimisation of the yield

was achieved by modification of the work-up procedure. DMSO and by-product dimethyl sulfone were removed using a simple aqueous extraction without further purification. This hydrolysis procedure was subsequently carried out with a mixture of two diastereomers (*R,R*)-**52a-j** and (*S,R*)-**52a-j** to afford corresponding amides (*R,R*)-**53 a-j** and (*S,R*)-**54a-j**. It should be noted that all aminonitriles **52a-j** and amino amides **53a-j** are stable to store at room temperature without noticeable decomposition over at least several months.

2.2.5 **Separation of the two diastereoisomers**

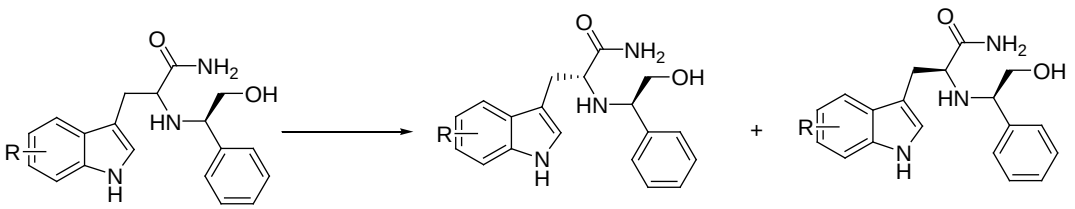

53a- j (*R,R*)-**53a- j** (*S,R*)-**54a- j**

	a	**b**	**c**	**d**	**e**	**f**	**g**	**h**	**i**	**j**
R =	H	5-Br	5-Cl	6-F	7-Et	5-Me	5-MeO	4-MeO	1-Me	2-Me

Having a mixture of two diastereomeric amides in hand, separation of (*R,R*)-**53a-j** and (*S,R*)-**54a-j** was attempted at this stage. Initially, the diastereomeric amides were separated using classical recrystallisation methods. The recrystallisation was carried out in many different solvents and their combinations. However, very few crystals were obtained for most analogues. Again, it was observed that only bromo-substituted (*S,R*)-**53b** gave crystals.

However, it was found that two distinct spots were observed when analysed by TLC using $CHCl_3$/MeOH = 6:1 was used as the mobile phase. This observation suggested that the two diastereoisomers could be separated by silica gel column chromatography. Indeed, the minor isomer (*R,R*)-**53a-j** eluted first, followed by the major isomer (*S,R*)-**54a-j** from a silica gel column using a chloroform-methanol (10:1) mixture as the eluent. The major (*S,R*) amino amides **54a-j** were obtained as white foams, whereas the minor (*R,R*) amino amides **53a-j** were obtained as yellow oils. The ratio of two separated amino amides was approximately 3:1. In addition, amino amides which were derived from chiral auxiliary **118** gave better separation than amino amides that were derivated form chiral auxiliary **115**. This observation

could be explained by the fact that the hydroxyl group of (*R*,*R*)-**53a-j** and (*S*,*R*)-**54a-j** makes important interactions with silica gel.

The ^{1}H NMR of two purified amino amides (*R*,*R*)-**53h** and (*S*,*R*)-**54h** are shown in Figures 2-12 and 2-13, respectively. It has been observed in the two ^{1}H NMR spectra that the two isomers gave distinct chemical shifts. However, confirmation of the absolute configuration by X-ray crystallographic analysis was unsuccessful since none of the amino amides could be obtained in a single crystal form. Hence, the absolute configuration would be confirmed at the last stage by conversion to (*S*)-tryptophan which can be used to compare with an authentic sample.

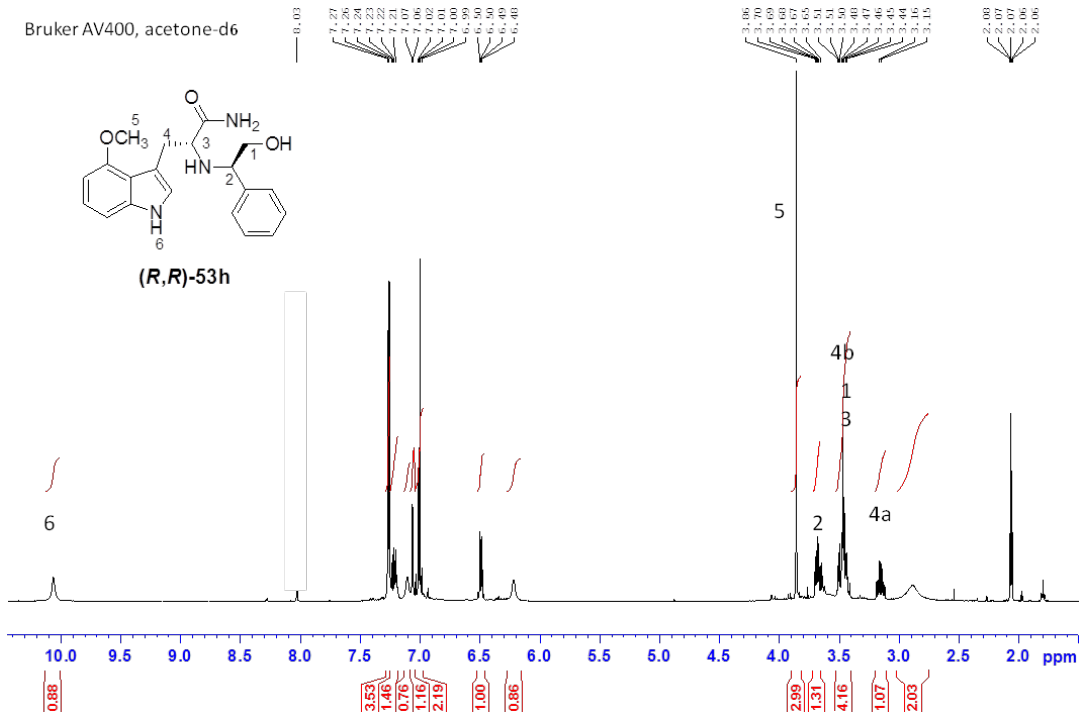

Figure 2-12 ^{1}H NMR spectrum of (*R*,*R*)-53h.

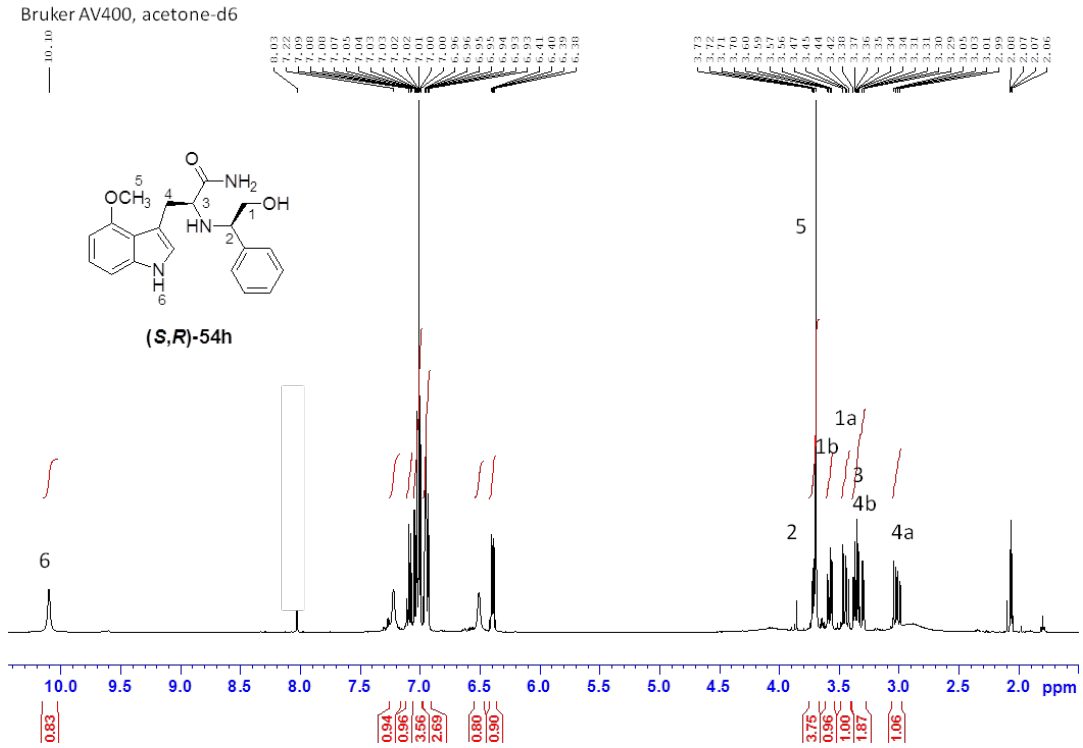

Figure 2-13 ^{1}H NMR spectrum of (*S,R*)-54h.

With the diastereomeric pure amino amides (*S,R*)-**54a-j** in hand, attention was turned towards hydrolysis of the amides to corresponding amino acids **121** (Figure 2-14). Several conditions were attempted to hydrolyse **54a-j** to the corresponding carboxylic acids **121**. Besides typical acidic and basic conditions,[202] nitrogen peroxide has also been examined.[203] Although all conditions gave the desired amino acids, the yields were very unsatisfactory (< 10 %). In most cases, the reaction led to inevitable decomposition products. Again, these results were attributed to the high susceptibility of the indole moiety to the acid treatment. Thus, in an attempt to avoid the decomposition problem, instead of converting amino amides **54a-j** to amino acids **121**, the chiral auxiliary of **54a-j** was first debenzylated by hydrogenolysis to free amines **55a-j** (Figure 2-14).

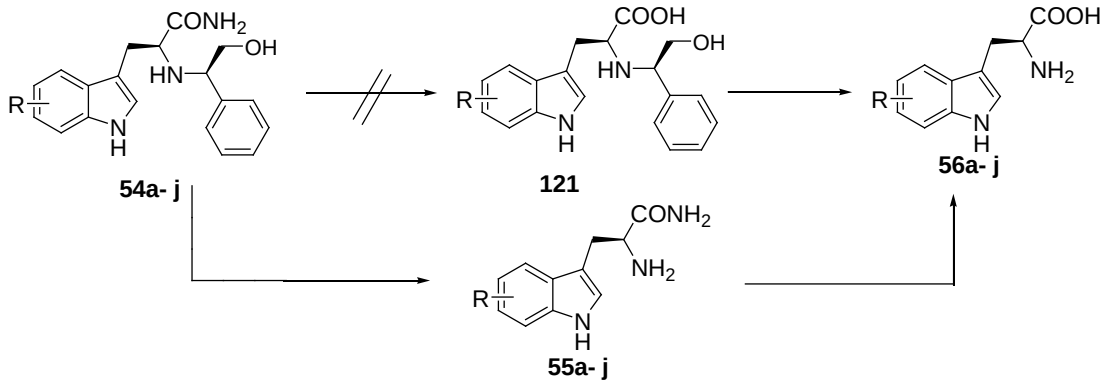

Figure 2-14 Hydrolysis of amino amides 54a-j to amino acids 56a-j *via* removal of the chiral auxiliary.

2.2.6 **Removal of the chiral auxiliary**

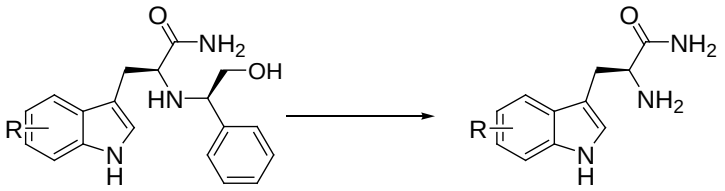

	a	**b**	**c**	**d**	**e**	**f**	**g**	**h**	**i**	**j**
R =	H	5-Br	5-Cl	6-F	7-Et	5-Me	5-MeO	4-MeO	1-Me	2-Me

It is well known that *N*-benzyl protecting group can be readily cleaved by catalytic hydrogenolysis.[204] The debenzylation is generally achieved in the presence of a catalytic amount of transition metal catalysts, such as palladium, platinum or rhodium on activated carbon under a hydrogen atmosphere. Among these catalysts, 5-10 % palladium on charcoal (Pd/C) is the most common catalyst to remove benzyl protecting groups.[204] In some difficult debenzylation, a more reactive Pearlman catalyst $Pd(OH)_2/C$ can be used.[205] The proposed mechanism of hydrogenolysis is illustrated in Figure 2-15. With the presence of Pd/C, hydrogen gas cleaves into two hydrogen radicals which are absorbed on the catalyst surface. The catalyst surface also coordinates the benzyl amine *via* electron-rich benzyl ring. Hydrogen radicals then transfer to the C-N bond of benzyl amine to form a free amine and a phenylethyl alcohol.

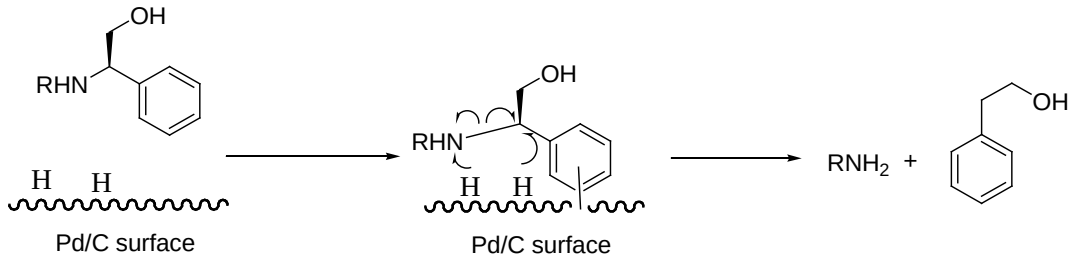

Figure 2-15 Mechanism of hydrogenolysis of modified benzyl amine.

In practice, a series of hydrogenolytic conditions were examined, and the results of which are summarised in Table 2-4. Initial attempt using a catalytic amount of 10 % Pd on activated carbon (20 % w/w) in MeOH under a balloon of hydrogen (1 atm, 72 h) did not give the desired amine (entry 1). Pd(OH) has been recommended as a more reactive catalyst in the hydrogenolysis of *N*-benzyl group.[205] However, even using more reactive and larger amount of catalysts failed to give desired amine (entries 2-4). Indeed, it has been reported in the literatures that α-substitution in the benzyl group prevented debenzylation under standard conditions.[206] Therefore, more vigorous conditions, such as more active catalysts or higher pressure of hydrogen gas is required.

Table 2-4 Catalytic hydrogenation removal of the chiral auxiliary

	Catalyst	Solvent	H_2 source	Time (h)	Result
1	10 % Pd/ C, 20 % w/w	EtOH	Balloon of H_2	72	Recovery of starting material
2	20 % Pd(OH)/C, 20 % w/w	EtOH/ AcOH = 1:1	Balloon of H_2	16	Recovery of starting material
3	20 % Pd(OH)/C, 100 % w/w	EtOH	Balloon of H_2	18	Recovery of starting material
4	20 % Pd(OH)/C, 50 % w/w	EtOH/ AcOH = 1:1	Balloon of H_2	17	Recovery of starting material
5	10 % Pd/ C, 100 % w/w	MeOH	HCO_2NH_4 5 eq. x 2	16	65 % yield
6	10 % Pd/ C, 100 % w/w	MeOH	HCO_2NH_4 2 eq. x 2	16	Reaction not complete
7	10 % Pd/ C, 100 % w/w	MeOH	HCO_2NH_4 large excess	16	60 % yield
8	10 % Pd/ C, 45 % w/w	MeOH	HCO_2NH_4 5 eq. x 2	20	65 % yield
9	10 % Pd/ C, 10 % w/w	MeOH	HCO_2NH_4 5 eq. x 2	20	Reaction not complete

Several alternative metal catalysts were then considered. However, it has been reported that in the presence of certain catalysts, such as platinum, nickel, copper and palladium hydroxide-barium sulfate, the 2,3-double bond of the indole ring might also be reduced.[207] Alternatively, catalytic transfer hydrogenation has been reported to promote *N*-debenzylation, in particular to the α-substituted benzylamine (entry 5).[208]

Catalytic transfer hydrogenation is typically carried out with a hydrogen source in the presence of a Pd/C. A large number of hydrogen donors have been used for catalytic transfer hydrogenation, including formic acid,[209] cyclohexene, cyclohexadiene[210] and ammonium formate.[211] Among these hydrogen sources, ammonium formate is the most convenient and efficient.[211] Thus, five equivalents of ammonium formate and catalytic amount of 10 % Pd/C were added to a solution of the *N*-benzyl amino amides **54a-j** in MeOH. The reaction mixtures were stirred at refluxing solvent for 4 h. Monitoring the reactions by TLC after 4 h usually revealed the presence of some starting materials. Additional equivalents of ammonium formate were added and the reaction mixture were stirred under reflux for a further 16 h, after which time TLC analysis showed the absence of starting materials. The reaction mixtures were filtered through a pad of Celite, and the filtrates were acidified with a small amount of 1 M aqueous HCl. The phenylethyl alcohol by-product was removed by liquid-liquid extractions. All non-halogen-substituted indole derivatives **54a**, **54d**, **54e**, **54f**, **54g**, **54h**, **54i**, **54j** were converted to the corresponding amines **55a**, **55d**, **55e**, **55f**, **55g**, **55h**, **55i**, **55j** in 50-80 % yields. The identity of the products was confirmed by mass spectrometry, ^{1}H and ^{13}C NMR analysis.

Studies were also carried out to determine the amount of catalysts and hydrogen donor required for optimum *N*-debenzylation. The results show that adding 5 eq. of ammonium formate twice in the presence of 45 % *w/w* catalyst was ideal (Table 2-4, entries 5-7). The rate of the reaction decreases substantially when only 2 eq. of ammonium formate was added. On the other hand, a large excess of ammonium formate does not increase the reaction rate, but made the removal of excess ammonium formate rather cumbersome. Similarly, 30 - 50 % *w/w* of Pd/C is ideal for the reaction (entries 8 and 9).

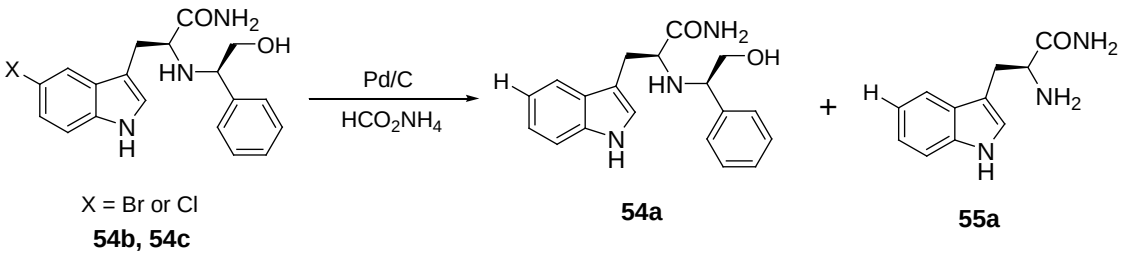

X = Br or Cl
54b, 54c

54a

55a

Figure 2-16 Competitive dehalogenation by hydrogenolysis.

However, limitations were encountered in the hydrogenolytic *N*-debenzylation of halogen-substituted indoles **54b** and **54c.** Hydrogenolysis of **54b** and **54c** led to concomitant dehalogenation, resulting in **54a** as a major product (Figure 2-16).[212] Only fluoro-substituted analogy **54d** gave desired product **55d** without causing dehalogenation. In addition, an interesting observation was obtained during monitoring the reaction. As shown by ^{1}H NMR and mass analysis, the mixture of a dehalogenated starting material **54a** and a dehalogenated product **55a** were formed during the reaction. This observation suggested that dehalogenation occurred prior to debenzylation. Although hydrogenolysis over a heterogeneous palladium catalyst for the *N*-α-substituted benzyl group are well established, selective removal of the *N*-α-substituted benzyl group in the presence of bromo- and chloro-substitution remains unexplored in literatures.

Consequently, several attempts on the selective removal of *N*-benzyl group in the presence of aryl halide were outlined in Table 2-5. A similar problem has been reported for the selective hydrogenolysis of *O*-benzyl groups in the presence of an aryl chloride. Li *et al.* found that the use of chloride salt provided the desired selectivity.[212] The reported conditions were evaluated; unfortunately, no desired products were observed by adding ammonium bromide and ammonium chloride for the debenzylation of **54b** and **54c**, respectively (entries 2 and 3). This result was attributed to the higher stability of benzyl amine. Moreover, an alternative approach utilising microwave irradiation in the presence of 1,4-cyclohexadiene with Pd/C was employed.[213] Again, no satisfactory conversion was obtained (entry 4). Another method reported by Srinivasa *et al.* to the hydrogenolysis of benzyl group tolerating halogen substituents was applied (entry 5).[214] No conversion occurred during the process. Lastly, replacing the protic solvent MeOH by an

aprotic solvent EtOAc to suppress the dehalogenation was also unsuccessful (entry 6). It was concluded that the reductive removal of *N*-α-substituted benzyl group in the presence of aryl halides (Br and Cl) was not feasible. Therefore, alternative methods for removal of *N*-α-substituted benzyl group need to be investigated.

Table 2-5 Catalytic transfer hydrogenation of *N*-α-substituted benzyl group

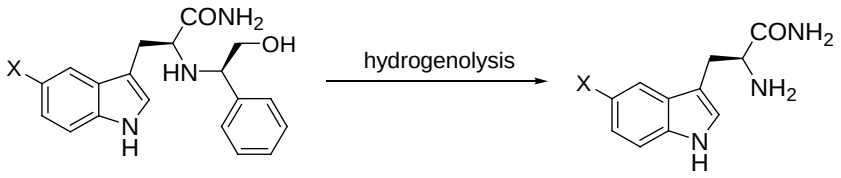

54b, 54c **55b, 55c**

	X	Catalyst	Solvent	H_2 source	Conditions	Observation
1	Cl	Pd/ C (40 % w/w)	MeOH	$HCOONH_4$	reflux, 26 h	Dechlorinated product
2	Cl	Pd/ C (40 % w/w), NH_4Cl	MeOH	$HCOONH_4$	reflux, 20 h	Dechlorinated product
	Br	Pd/ C (40 % w/w), NH_4Br	MeOH	$HCOONH_4$	reflux, 20 h	Debrominated product
3	Cl	Pd/C (10 % w/w), NH_4Cl	MeOH	$HCOONH_4$	M.W. (100W), 30 min, 100 °C	Dechlorinated product
4	Cl	Pd/C (10 % w/w)	MeOH	1,4-cyclohexadiene	M.W. (100W), 30 min, 100 °C	Major spot is starting material
5	Br	Zn dust 1 eq.	MeOH	$HCOONH_4$	reflux, 17 h	No reaction
6	Cl	Pd/ C (40 % w/w)	EtOAc	$HCOONH_4$	reflux, 26 h	Major spot is starting material

Because of the competing dehalogenation associated with the removal of the chiral auxiliary **118**, an alternative chiral auxiliary (*S*)-4-methoxy-α-methylbenzylamine (**124**) was employed. This chiral auxiliary provides advantages over the benzyl counterpart, since the *N*-4-methoxy-α-methylbenzyl (*N*-PMB) group can be readily removed by reductive, oxidative, acidolytic and other methods.[215]

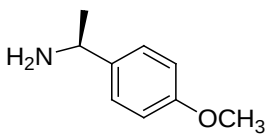

124

Initially, it was anticipated that the higher electronic density of the aromatic ring would accelerate the reaction rate of debenzylation by hydrogenolysis (Table 2-6,

entry 1). However, the result showed that dehalogenation problem remained the same. Hence, an oxidative approach using ceric ammonium nitrate (CAN) or 2,3-dichloro-5,6-dicyano-1,4-benzoquinone (DDQ) would be useful as an alternative method (entries 2 and 3).[216] Unfortunately, the reaction was not as straightforward as suggested by the literatures,[216, 217] since unreacted starting material and unidentified by-products were obtained.

Table 2-6 Removal of the *N*-4-methoxy-*α*-methylbenzyl group

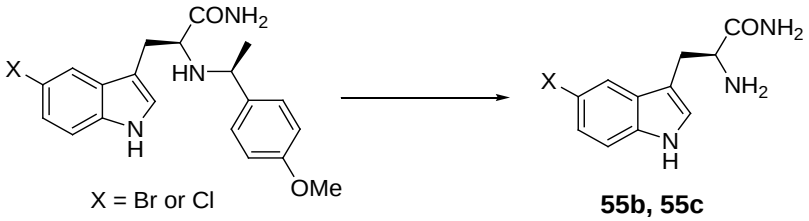

		Catalyst	H_2 source	Temp./ Time (h)	Observations
Reductive	1	Pd/C 20% w/w	$HCOONH_4$	reflux/ 23	Dehalogened starting material + dehalogened product
		Oxidative reagent	Solvent	Temp./ Time (h)	Result
Oxidative	2	DDQ	DCM/H_2O 5:1	r.t./ 16	Starting material
	3	CAN	MeCN/ H_2O 5:1	r.t./ 16	Starting material
		Acid	Scavenger	Temp./ Time (h)	Observations
	4	Neat TFA	-	r.t. / 17	No reaction, but no decomposition
	5	Neat TFA	-	70 °C/ 24	Starting material and tiny product
Acidolysis	6	Formic acid	Et_3SiH	90 °C/ 1	Starting material and product
	7	Neat TFA	iPr_3SiH	r.t. / 24	Starting material and tiny product
	8	Neat TFA	iPr_3SiH	60 °C/ 24	Product + tiny amount of starting material
	9	Neat TFA	iPr_3SiH	60 °C/ 41	Product

Since both the reductive and oxidative approaches were unsuccessful, the acidolysis approach was investigated.[218] Initially, no product was detected by treatment of **125b** with trifluoroacetic acid at ambient temperature (entry 4). Hence, the reaction mixture was heated to 70 °C for 24 h. Gratifyingly, the mass spectrum of crude mixture showed formation of the desired product. Several reaction

conditions including the acid reagents, reaction time and the use of scavengers were evaluated (entries 6 - 9).[219] It was clear that the best result was obtained by heating **125b** with TFA at 60 °C in the presence of triisopropylsilane (TIPS) for 41 h. Notably, the addition of TIPS, which is capable of irreversibly scanverging the reactive 4-methoxy-α-methylbenzyl cation is required. After TFA was removed *in vacuo,* the by-product was removed by trituration to afford amino amide as a trifluoroacetate salt in more than 90 % crude yield. Having established suitable reaction conditions, the other halogen analogue **125c** was also acidolysed to **55c**. ES-MS and ^{1}H NMR revealed the presence of the desired free amines **55b** and **55c**.

In summary, catalytic transfer hydrogenation has been demonstrated to be an effective method for the removal of *N*-α-substituted benzyl group. Selective removal of *N*-benzyl groups in the presence of an aryl halide required introducing 4-methoxy-α-methylbenzylamine as a chiral auxiliary. By employing a TFA-mediate acidolysis procedure, it was established that PMB group could be efficiently deprotected to give the free amines in good yields.

2.2.7 **Hydrolysis of α-amino amides to α-amino acids**

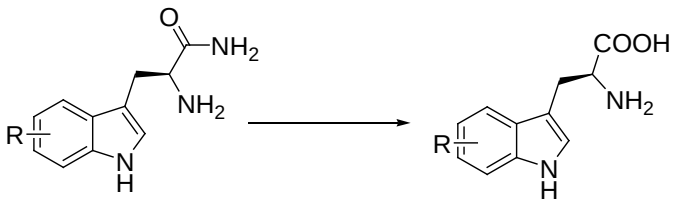

55a- j **56a- j**

	a	**b**	**c**	**d**	**e**	**f**	**g**	**h**	**i**	**j**
R =	H	5-Br	5-Cl	6-F	7-Et	5-Me	5-MeO	4-MeO	1-Me	2-Me

In order to find the appropriate reaction conditions for the hydrolysis of α-amino amides **55a-j** without causing decomposition, the first attempt was to use a very mild condition in aqueous solution of sodium peroxide.[220] MS analysis after 3 h reaction time revealed the presence of desired amino acids **56a-j**. However, the reaction only gave the desired products in low yields. In addition, large amount of salts produced from neutralising the basic reaction mixtures was found to be difficult to separate from the products. Hence, the focus of the studies was returned

to the classical acid-catalysed hydrolysis. The reaction mechanism was illustrated in Figure 2-17. Strong acid and heating are required for the efficient transformation.

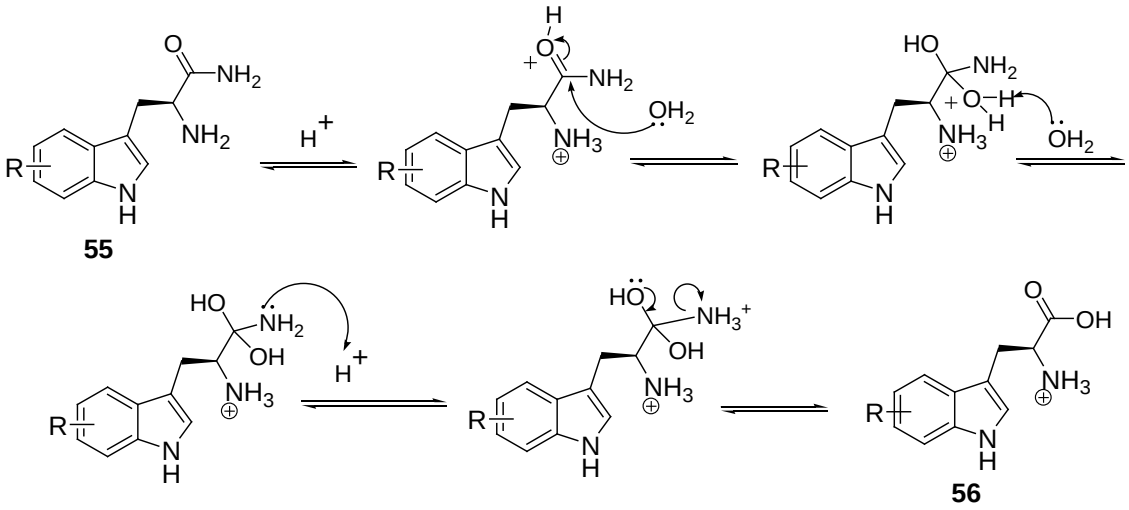

Figure 2-17 Mechanism of acid-catalysed hydrolysis of amides.

Initially, **55a-j** were treated with 5 M aqueous HCl under reflux. It was anticipated that high concentration of acid could result in decomposition of the starting materials. Surprisingly, TLC analysis after 2 h revealed the absence of starting materials (R_f = 0.7) and the presence of the products (R_f = 0.5), and some impurities. It is noteworthy to mention that the reactions were monitored by both silica TLC and neutral alumina TLC. The plates were eluted with a mixture of *n*-butanol: acetic acid: water, 3: 1: 1 *v*/*v* followed by ninhydrin stain; the amino amides **55a-j** appeared yellow colour whereas the resulting amino acids **56a-j** appeared purple colour on TLC plates. Further optimising the conditions gratifyingly established that the hydrolysis of **55a-j** were accomplished in good yields (> 95 %) by heating with 1 M hydrochloric acid for 5 h. The reaction conversions were clean and no decomposition of **55a-j** were observed.

^{1}H and ^{13}C NMR (D_2O) analyses of **55a-j** revealed that no differences were observed between the amides and carboxylic acids. Since the starting materials and the products displayed almost identical chemical shifts in NMR spectroscopy, the identity of the desired products was confirmed by mass spectrometry. Moreover, MS analysis of the products needs to be careful, as the *m/z* of the acids are only 1 mass less than the amide counterparts. For example, the successful conversion of

55e to **56e** was confirmed by disappearance of the amide (*m/z* = 232.1390) and the presence of a molecular ion at *m/z* = 233.1174 accounting for the acid **56e**.

2.2.8 **Fmoc-protection of tryptophan derivatives**

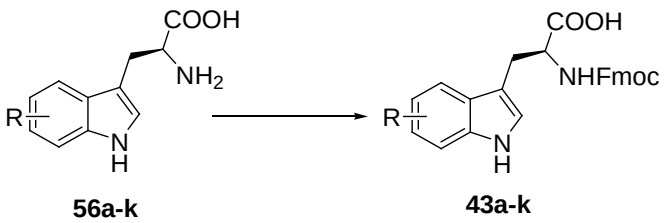

56a-k **43a-k**

	a	**b**	**c**	**d**	**e**	**f**	**g**	**h**	**i**	**j**	**k**
R =	H	5-Br	5-Cl	6-F	7-Et	5-Me	5-MeO	4-MeO	1-Me	2-Me	5-F

The final step in the synthesis of tryptophan-based building blocks is the protection of the α-amino group with Fmoc. The Fmoc (fluorenylmethoxy carbonyl) protection group is required for the solid-phase peptide synthesis of argyrin and analogues thereof. Typically, Fmoc-protection is carried out by reaction with a stoichiometric amount of Fmoc-OSu or Fmoc-Cl under basic conditions. The reaction mechanism is illustrated in Figure 2-18.[221]

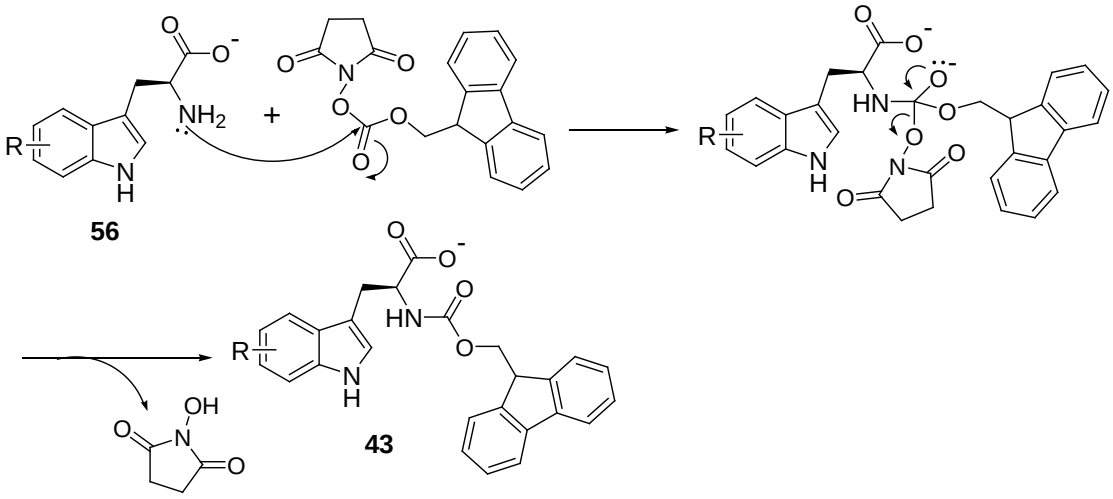

Figure 2-18 Mechanism of *N*-Fmoc protection using Fmoc-OSu.

One major advantage of the Fmoc group is its stability towards acidic conditions, allowing selective removal of acid-labile protection groups like Boc and *t*-butyl groups.[222] The advantage of using Fmoc-OSu rather than Fmoc-Cl is that Fmoc-

OSu eliminates the possibility of the formation of undesired anhydride side-product during the acylation reaction. [221]

Hence, tryptophan hydrochloric salts **56a-k** were dissolved in THF or acetone depending on their solubility. Two equivalents of aqueous sodium carbonate solution and one equivalent of Fmoc-OSu in THF were added. The solution was then stirred vigorously at room temperature for 2 -16 h. Subsequently, the reaction mixtures were subjected to an aqueous work-up followed by acidification to afford the final product **43a-k**. The yields of eleven analogues **43a-k** are listed in Table 2-7.

Table 2-7 *N*-Fmoc protection of tryptophan derivatives 43a-k.

Starting material		Product		Yield (%)	Melting point (°C)	$[\alpha]_D^{24}$ (*c* 1.0,MeOH)
56a	Trp	**43a**	Fmoc-Trp-OH	64	182-185	- 29
56b	5-Br-Trp	**43b**	Fmoc-5-Br-Trp-OH	20	130-132	- 23
56c	5-Cl-Trp	**43c**	Fmoc-5-Cl-Trp-OH	20	98-99	- 16
56d	6-F-Trp	**43d**	Fmoc-6-F-Trp-OH	50	102-104	- 19
56e	7-Et-Trp	**43e**	Fmoc-7-Et-Trp-OH	50	146-148	- 26
56f	5-Me-trp	**43f**	Fmoc-5-Me-trp-OH	66	178-179	- 15
56g	5-MeO-Trp	**43g**	Fmoc-5-MeO-Trp-OH	82	198-200	- 23
56h	4-MeO-Trp	**43h**	Fmoc-4-MeO-Trp-OH	62	168-171	- 27
56i	1-Me-Trp	**43i**	Fmoc-1-Me-Trp-OH	74	92-94	- 24
56j	2-Me-Trp	**43j**	Fmoc-2-Me-Trp-OH	40	182-185	- 15
56k	5-F-(*S*/*R*)-Trp	**43k**	Fmoc-5-F-(*S*/*R*)-Trp-OH	50	196-197	not applicable

The purity of the final products was established using analytical RP-HPLC. For example, a one major peak observed at t_R = 10.0 min by analytical RP-HPLC confirmed the purity of Fmoc-5-Cl-Trp-OH **43c** (Figure 2-19). Additionally, the identity of the products was confirmed by mass spectrometry and ^{1}H and ^{13}C NMR analysis. The stereochemical-identity was confirmed by determination of specific optical rotation $[\alpha]_D$ (Table 2-7). All Fmoc-tryptophan analogues showed levorotations which corresponds to the (*S*)-configuration in the literature.[164]

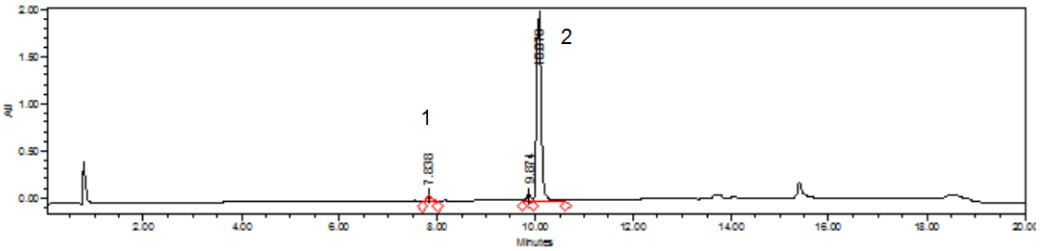

	Retention time	Area	% Area	Height
1	7.838	546350	4.31	67652
2	10.078	12137618	95.69	1950883

Figure 2-19 Analytical HPLC of Fmoc-tryptophan derivative 43c. Analysed using 10-60 % B over 10 min at 3 mL/ min on an Onyx Monolithic C_{18} column (100 x 4.6 mm). Eluent detection was monitored by UV absorbance at 216 nm.

The optical purity of **43a-j** was established by their specific optical rotations. The observed specific optical rotations $[\alpha]^{24}_{D}$ -29°, -23° and -19° (*c* = 1.0 in methanol) for *N*-Fmoc-(*S*)-tryptophan (**43a**), *N*-Fmoc-5-methoxy-(*S*)-tryptophan (**43g**) and *N*-Fmoc-6-fouro-(*S*)-tryptophan (**43d**), respectively, are comparable to the values reported in the literature $[\alpha]^{25}_{D}$ -28°, -24.5° and -16.8° (*c* = 1.0 in methanol).[164] The closely matched optical rotations suggest that the obtain Fmoc-tryptophan derivatives are of good enantiomeric purity. Moreover, this finding is in agreement with the hypothesis of the chiral induction described in Section 2.2.3 could install *S* configuration as the major product. The obtained Fmoc-protected tryptophan building blocks were used for the Fmoc solid phase peptide synthesis which will be discussed in Chapter 4.

2.3 **Conclusion**

A novel eight-step synthetic route has been developed for the construction of tryptophan analogues with high enantiomeric purity. This synthetic route enabled the synthesis of *N*-Fmoc-(*S*)-tryptophan derivatives from the corresponding indoles. As a result, the synthesis of tryptophan derivatives with a wide range of functional groups at various positions of the indole moiety was achieved.

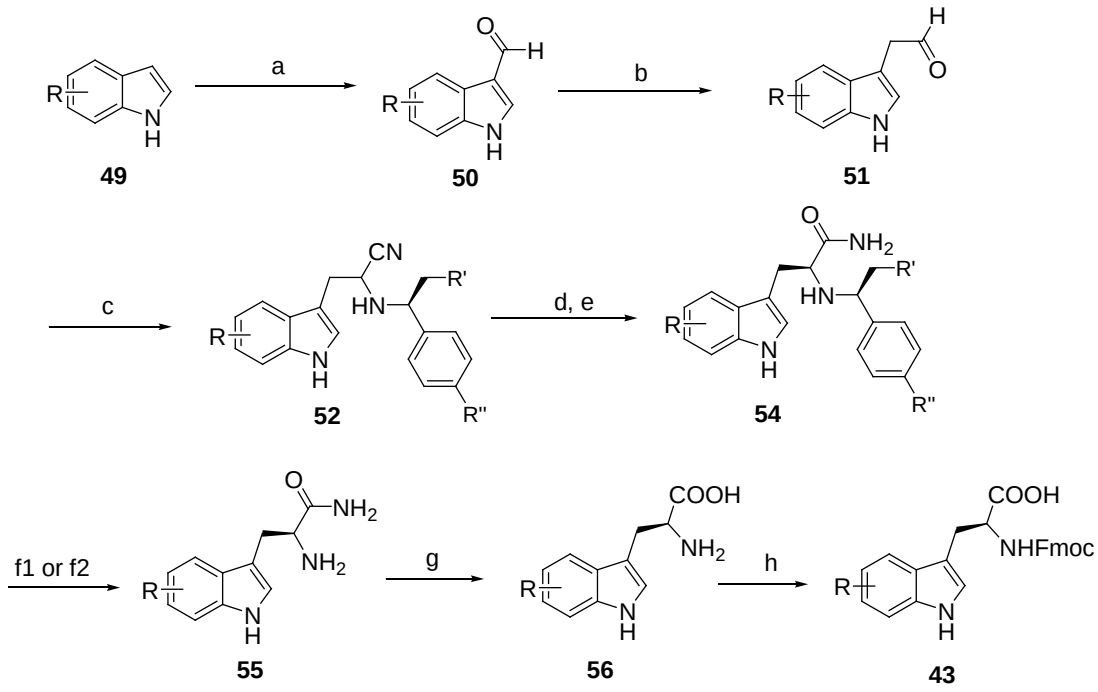

	a	**b**	**c**	**d**	**e**	**f**	**g**	**h**
R =	H	5-Br	5-Cl	6-F	7-Et	5-Me	5-MeO	4-MeO
R' =	OH	H	H	OH	OH	OH	OH	OH
R'' =	H	OCH_3	OCH_3	H	H	H	H	H

Figure 2-20 Synthesis Fmoc-tryptophan derivatives (43); Reagents and conditions: (a) $POCl_3$, DMF, 0 °C then 45 °C; (b) i. $Ph_3PCH_2OCH_3$, n-BuLi; ii. HCl, THF, reflux; (c) Chiral auxiliary, NaCN, AcOH, MeOH; (d) H_2O_2, Na_2CO_3, DMSO; (e) Recrystallisation or HPLC; (f 1) Pd/ C, NH_4HCO_2, MeOH, reflux; (f 2) TFA, TIPS, 60 °C; (g) 1 M HCl, reflux; (h) Fmoc-OSu, $NaHCO_3$, THF,/H_2O.

As summerised in Figure 2-20, commercially available indoles were subjected to Vilsmeier formylation to give aldehydes **50a-j** which were then homologated *via* Wittig reaction followed by acid hydrolysis of enol ether intermediates to afford aldehydes **51a-j**. The diastereoselective Strecker amino acid synthesis was achieved by using (*R*)-2-phenylglycinol as chiral auxiliary to give a diastereoisomeric mixture of (*S,R*)- and (*R,R*)-α-aminonitriles **52a,d-j** in 3 : 1 ratio. The mild peroxide hydrolysis condition was employed for the conversion of acid labile α-aminonitriles **52a,d-j** to corresponding α-amino amides **53a,d-j**. Subsequent separation of the major (*S,R*) α-aminoamides **54a,d-j** were readily obtained by silica gel column chromatography. The removal of chiral auxiliary was carried out using the catalytic transfer hydrogenation to afford (*S*)-tryptophan amide derivatives **55a,d-j**. In the case of the two halogen indole derivatives, **54b** and **54c**, *N*-debenzylation was accompanied by dehydrogenation. This problem was

overcome by introducing PMB as a chiral auxiliary (Figure 2-20, R' = H, R'' = OCH_3). The removal of *N*-PMB was then carried out using TFA-mediated acidolysis. Subsequent hydrolysis of all (*S*)-tryptophan amide derivatives **55a-j** to the corresponding (*S*)-tryptophan derivatives **56a-j** was accomplished by refluxing in 1 M aqueous hydrochloric acid for 5 h without causing decomposition. Finally, the *N*-terminus of amino acids was protected with Fmoc to afford **43a-j** which are suitable for the Fmoc solid phase peptide synthesis. All the intermediates reported are of good or reasonable purity and are fully characterised. The spectral data of all intermediates are in good agreement with the proposed structures.

The characteristic data of the synthetic Fmoc-(*S*)-tryptophan and Fmoc-5-bromo-(*S*)-tryptophan are consistent with the data reported in the literatures. The cumulative yields over this eight-step synthesis ranged from 2 to 5 %, due to the sensitivity of indole moiety, especially indoles with electron-donating groups. In comparison to literature synthesis, this route can be accessed with inexpensive commercially available reagents, and avoids using expensive chiral auxiliaries or resolving reagents.

Chapter 3

Synthesis of two key building blocks of argyrin A

As outlined in Section 1.5, the other two unusual amino acid building block of argyrin A are the dipeptide (*R*)-2(1-*tert*-butoxycarbonylamino)ethyl)thiazole-4-carboxylic acid and α,β-dehydroalanine. The aim of the research presented in this chapter is to synthesis thiazole- and oxazole-containing dipeptides and the precursor of the α,β-dehydroalanine analogues using existing procedures.

3.1 Synthesis of (*R*)-2(1-*tert*-butoxycarbonylamino)ethyl)thiazole-4-carboxylic acid

(*R*)-2(1-*tert*-butoxycarbonylamino)ethyl)thiazole-4-carboxylic acid, or abbreviate as *N*-Boc-(*R*)-Ala-Thz-OH (**44**), is a thiazole-containing dipeptide. The thiazole ring, which is a member of the azole heterocycles, has great aromaticity due to the conjugated π electron and a planar ring system. The thiazole moiety is abundantly found in secondary metabolic products of algae, fungi and marine organisms. In particular, a large number of these thiazole-containing secondary metabolites are peptide derivatives, many of which possess significant biological activities.[223] For example, hectochlorin isolated from a marine organism showed cytotoxic activities and is able to promote actin polymerisation.[224] The cyclic hexapeptide bistratamide

C and dolastatin 1 also exhibit cytotoxic activities.[225] However, the biological mode-of-action of these thiazole-containing compounds are poorly understood.

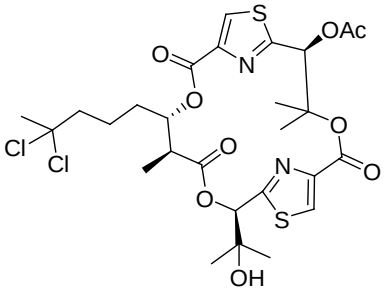

hectochlorin

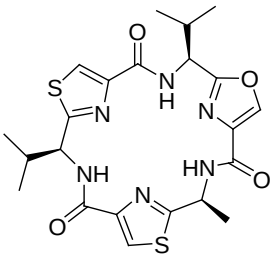

bistratamide C

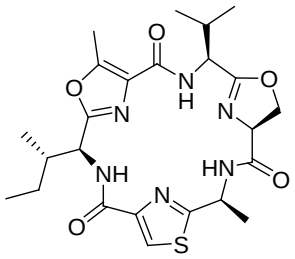

dolastatin 1

The biosynthetic pathway of these thiazole-containing amino acids was believed to be derived from the condensation of peptide precursors with cysteine, followed by cyclisation and oxidation.[226] Figure 3-1 shows biosynthetic pathway of the thiazole-containing amino acids derived from cysteine-containing peptidyl moiety. Cysteine side chain was reacted with preceding carbonyl group to generate 5-membered heterocycle ring, followed by dehydration to give thiazoline. Oxidation of thiazoline resulted in the heteroaromatic thiazole system. In contrast to the biosynthesis, two chemical synthetic routes have been established and these are discussed in Sections 3.1.1 and 3.1.2.

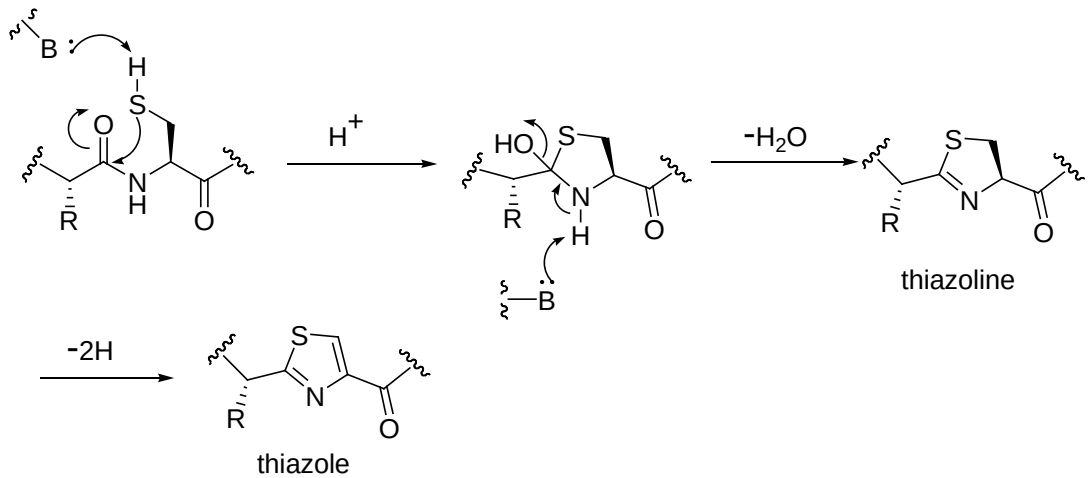

Figure 3-1 Proposed biosynthetic pathway of thiazole-containing amino acids

3.1.1 **Shioiri's approach**

In the course of synthesis of cytotoxic cyclic peptides, Shioiri and colleagues in 1987 reported a synthetic route towards optically pure thiazole amino acids.[227] The five-step synthesis is outlined in Scheme 3-1. The synthesis is similar to the biosynthetic route, which uses cysteine and (*R*)-alanine as building blocks. The key feature of Shioiri's approach is condensation of *N*-protected α-(*R*)-amino aldehyde **128** with cysteine methyl ester forming thiazolidine derivative **129** (step d, Scheme 3-1), followed by oxidative dehydrogenation of thiazolidine with manganese dioxide.

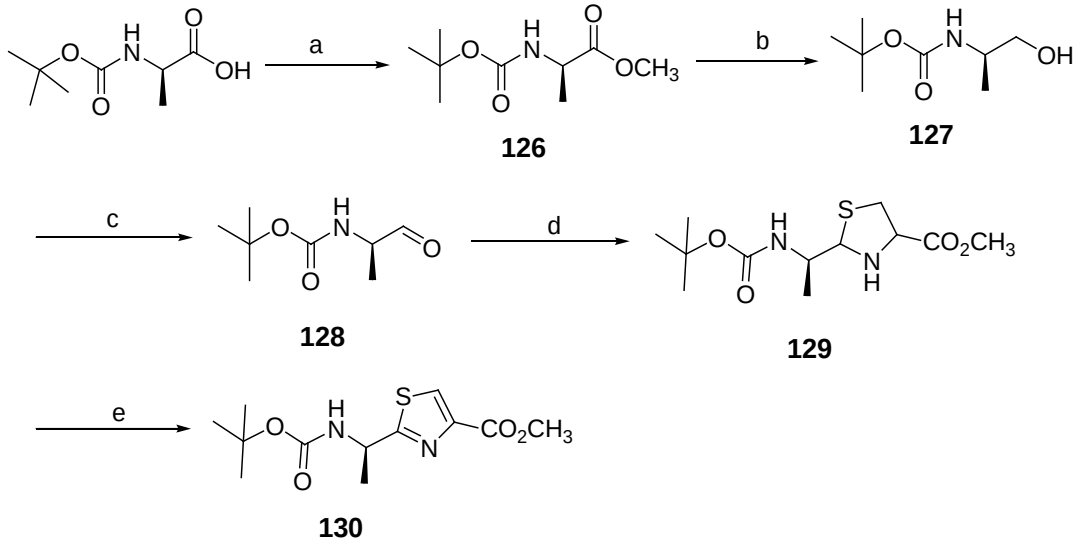

Scheme 3-1 Synthesis of *N*-Boc-(*R*)-Ala-Thz-OEt (130) by Shioiri's s group; Reagents and conditions: (a) CH_3I, $KHCO_3$, DMF; (b) $NaBH_4$, LiCl, THF/EtOH; (c) DMSO, pyridine-SO_3, Et_3N; (d) (*S*)-Cys-OMe, benzene; (e) MnO_2, benzene.

Firstly, in order to prepare the *N*-protected α-(*R*)-amino aldehyde **128**, commercially available Boc-(*R*)-Ala-OH was converted to the corresponding methyl ester **126**, which in turn was selectively reduced to the corresponding α-(*R*)-amino alcohol **127** under standard conditions. The transformation of (*R*)-amino alcohol **127** to *N*-protected α-(*R*)-amino aldehyde **128** was then achieved by Parikh-Doering oxidation. The subsequent condensation of aldehyde **128** with cysteine methyl ester afforded the thiazolidine derivative **129** as a mixture of *C*-4 epimers. Finally, oxidation of thiazolidine derivative **129** to the *N*-Boc-(*R*)-Ala-Thz-OEt **130** was accomplished by treatment with manganese dioxide. The cumulative yield of

this approach was around 50 % in high enantiomeric excess (> 99 %). In general, although this method gave products in good yield, it was later established that the manganese dioxide oxidation step was rather ineffective.[228, 229]

3.1.2 **Modified Hantzsch thiazole synthesis**

Another route for the preparation of thiazole-containing amino acid involved a modified Hantzsch thiazole synthesis. The Hantzsh condensation was first reported in 1889. Since then, this reaction has been widely used for the synthesis of thiazole-containing amino acid derivatives.[230] However, this method only yields racemic thiazole amino acids, even when starting with chiral precursors. Later, Schmidt *et al.* successfully modified the Hantzsch synthesis to produce enantiomerically pure thiazole amino acids in satisfactory yield.[231]

The four-step modified Hantzsch synthesis has become one of the most reliable route to thiazoles.[230] The key feature of Hantzsch thiazole formation involved the treatment of thioamides with ethyl bromopyruvate, followed by aromatisation to afford thiazole amino acid derivatives (steps c and d, Scheme 3-2). The methodology of each step will be detailed in the following four sections.

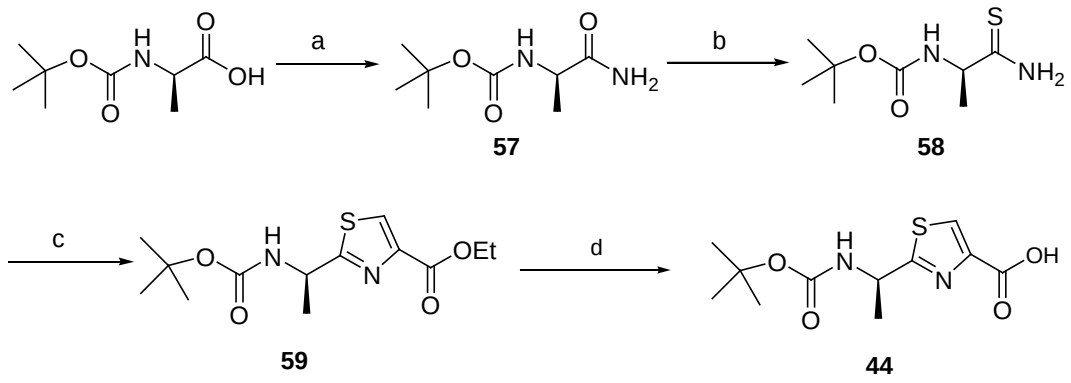

Scheme 3-2 Synthesis of *N*-Boc-(*R*)-Ala-Thz-OH (44); Reagents and conditions: (a) DCC, HOBt, NH_3, CH_2Cl_2, 0 °C; (b) Lawesson's reagent, THF, 0 °C; (c) i. $BrCH_2COCO_2Et$, $KHCO_3$, DME, -15 °C; ii. TFAA, 2, 6-lutidine, DME, -15 °C; (d) LiOH, THF/ MeOH/ H_2O, room temp.

3.1.2.1 **Preparation of *N*-Boc-(*R*)-Ala-NH$_2$**

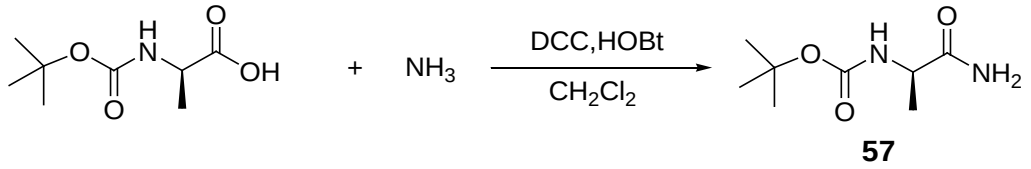

The initial step was the amidation of *N*-Boc-(*R*)-Ala-OH. α-Carbonyl was activated by using a mixture of *N,N'*-dicyclohexylcarbodiimide (DCC) (**131**) and 1-hydoxybenzotriazole (HOBt) (**132**), to yield the reactive acylating agent for a further nucleophilic acyl substitution with ammonia. The mechanism of amination is shown in Figure 3-2.

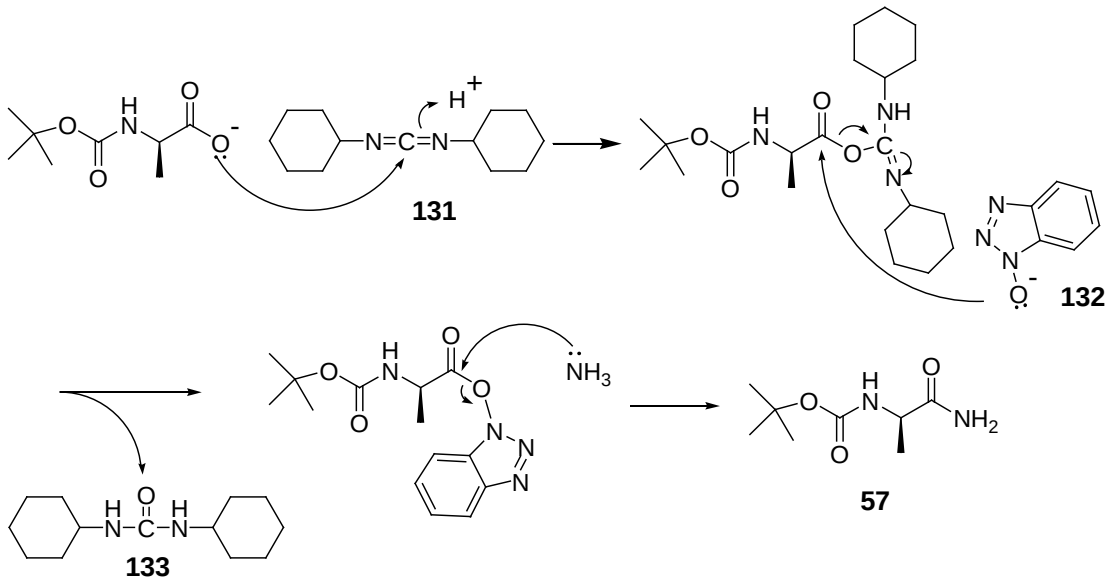

Figure 3-2 Mechanism of DCC and HOBt mediated amide formation

DCC (**131**) is one of the carbodiimide reagents that has been commonly used in peptide synthesis since 1955.[232] The auxiliary reagents, such as 1-hydroxy-7-azabenzotriazole (HOAt) and 1-hydroxybenzotriazole (HOBt) (**132**), not only suppress racemisation, but also enhance the reactivity.[233] The advantages of using DCC/HOBt coupling reagent are their relatively low prices and their by-product, urea (**133**) which is insoluble in most solvents and hence readily separable from the product.

Hence, DCC and HOBt were added to a solution of *N*-Boc-(*R*)-Ala-OH in DCM at 0 °C. The solution was warmed to room temperature and stirred for 1 h. The solution was cooled to 0 °C again and then was mixed with a solution of 0.5 M ammonia in dioxane or methanol. The reaction mixture was stirred vigorously for 1 h at room temperature. The suspension was filtered, and the filtrate was concentrated and purified to afford *N*-Boc-(*R*)-Ala-NH_2 (**57**) in quantitative yield. This transformation was confirmed by ^{1}H NMR analysis, which revealed the disappearance of the carboxylic acid proton (δ = 12.01 ppm) in the starting material and the appearance of the NH_2 protons (δ = 6.07 and 6.56 ppm) in **57**.

3.1.2.2 **Thionation of *N*-Boc-(*R*)-Ala-NH_2**

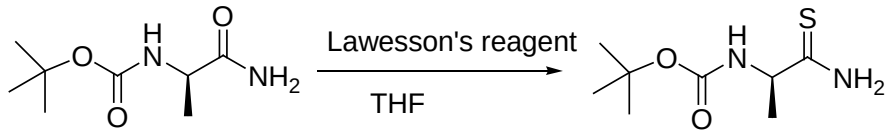

57 **58**

In the second step, a thionation reaction was carried out where the carbonyl (C=O) was converted to a thiocarbonyl (C=S) functionality. The thionation can be easily achieved by thionation reagent such as Belleau's reagent,[234] Lawesson's reagent[235] and phosphorus pentasulfide.[236] Among these thionation reagents, Lawesson's reagent **(134**) is one of the most convenient and cheap reagent for the conversion of ketones, esters, and amides to the corresponding thioketones, thioesters and thioamides.[235] Indeed, better yield was obtained by using Lawesson's reagent (86 %) than Belleau's reagent (36 %). The mechanism of thionation with Lawesson's reagent is shown in Figure 3-3.

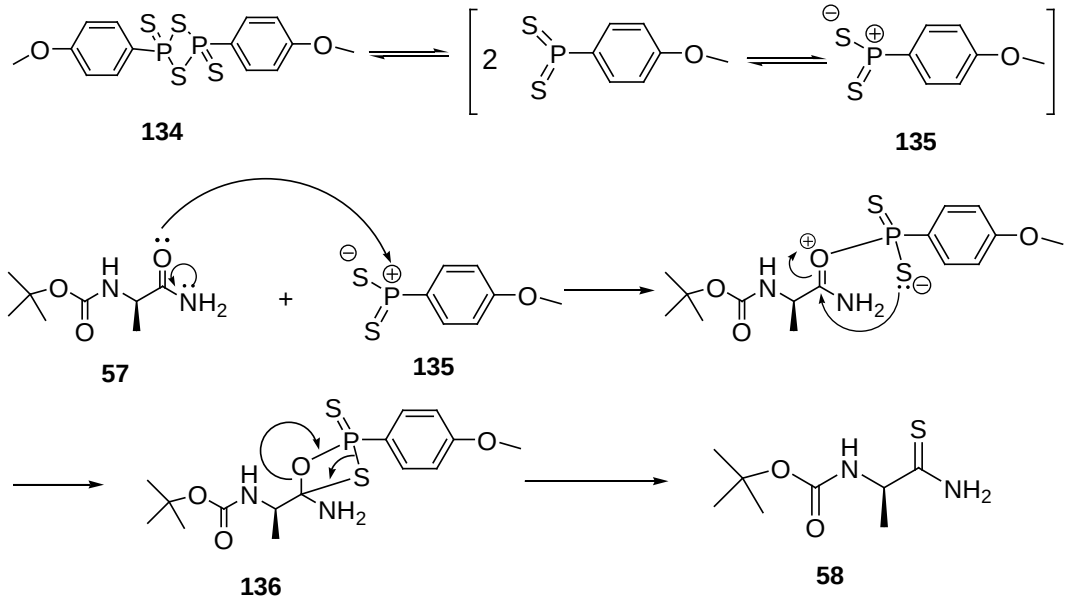

Figure 3-3 Mechanism of thionation with Lawesson's reagent

In solution, Lawesson's reagent (**134**) forms two reactive dithiophosphine ylides (**135**) which can react with electron rich carboxamide to give a thiaoxaphosphetane intermediate (**136**). The intermediate then undergoes spontaneous cycloreversion, resulting in the formation of the P=O bond and the thioamide **58**. It is noteworthy to mention that this cycloreversion step resembles the final step of Wittig reaction which was described in Section 2.2.2.

Hence, Lawesson's reagent (0.6 eq.) was added to a solution of *N*-Boc-(*R*)-Ala-NH_2 (**57**) in THF at 0 °C. The mixture was stirred at room temperature for 40 min. Having largely removed the excess Lawesson's reagent and by-product in an aqueous work-up, further purification afforded the desired thioamide **58** in 56-86 % yield (mp. 94-96 °C, literature 104-105 °C[150]). Successful thionation of **57** was further confirmed by FT-IR and ^{13}C NMR analysis. Specifically, FT-IR with an absorption at 1241 cm^{-1} accounted for the distinct C=S stretching. Additionally, ^{13}C NMR showed the disappearance of carbonyl group at δ = 176.03 ppm in the starting material **57** and the appearance of thiocarbonyl group at δ = 210.58 ppm in **58**.

3.1.2.3 **Modified Hantzsch thiazole formation**

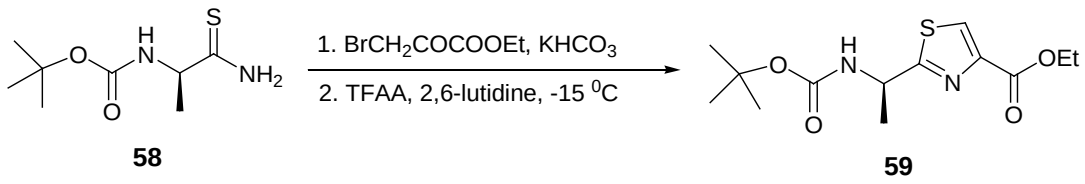

The modified Hantzsch reaction is the key step for the thiazole synthesis. A combination of the two-step reaction is required for the formation of the *N*-Boc-(*R*)-Ala-Thz ethyl ester **59** from the *N*-Boc-(*R*)-Ala-thioamide **58**. The mechanism of the two-step thiazole formation is shown in Figure 3-4. The reaction begins with condensation of thioamide **58** with ethyl bromopyruvate **137** in the presence of finely powdered $KHCO_3$ to give hydroxythiazoline derivative **138**. It has been shown that isolation or storage of hydroxythiazoline **138** leads to racemisation *via* an imine-enamine equilibration.[237] Without isolating the intermediate **138**, activation of the hydroxyl group of hydroxythiazoline with trifluoroacetic anhydride (TFAA) forms a good leaving group which could be eliminated to give the thiazole amino acid derivative **59**.

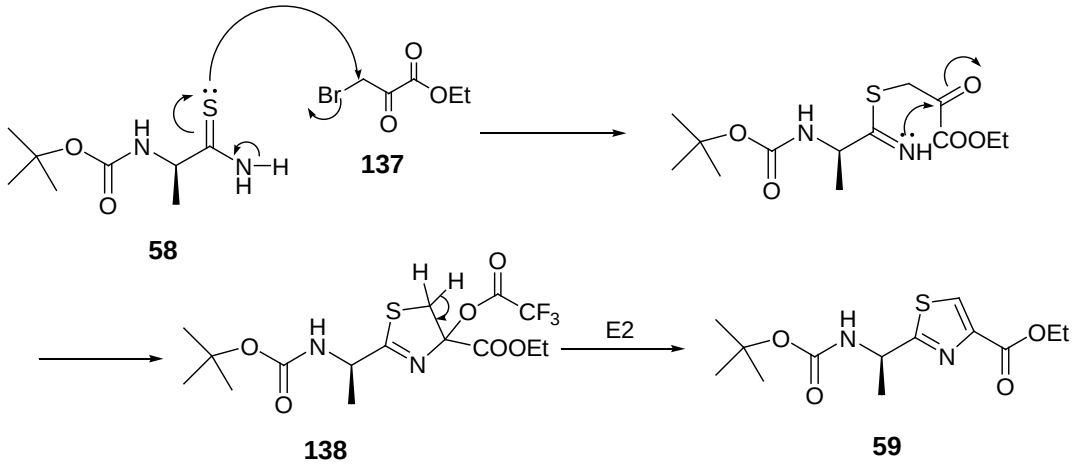

Figure 3-4 Mechanism of Hantzsch thiazole formation from thioamide

In order to prevent racemisation caused by the imine-enamine equilibration of thiazoline intermediate, various dehydration conditions were extensively investigated by other groups to suppress the tautomerisation. Mayers *et al.* established the best conditions which used a bulky base 2,6-lutidine and lowers the reaction temperature to -15 °C giving an ee > 99 %, in yield of 96 %.[238] Hence, the

solution of *N*-Boc-(*R*)-Ala-thioamide **58** in dry dimethoxyethane (DME) was cooled to -15 ° C and was treated with ethyl bromopyruvate in the presence of excess of finely powdered potassium bicarbonate. The mixture was stirred vigorously for 5 min, and the solution of 2,6-lutidine and trifluoroacetic anhydride in DME was added in one portion at -15 °C. After stirring at -15 °C for 1 h, TLC analysis revealed the absence of thiazoline intermediate **138**. The mixture was subjected to an aqueous work-up and subsequent column chromatography gave the (*R*)-Ala-Thz ethyl ester **59** in an overall yield of 49 %.

The identity of the product was confirmed by NMR analysis, mass spectrometry and melting point. Specifically, the distinctive singlet C5-H signal appearing at δ = 8.08 ppm in ^{1}H NMR revealed the formation of the thiazole ring. MS (ESI$^+$) detected a peak at *m/z* 323.1144 corresponding to the calculated value for the [M+Na]$^+$ species of **59**. However, the melting point obtained for **59** (mp = 80-82 °C) was five degree lower than the value found in the literature (mp = 85-86 °C [150]). The melting point depression can be attributed to amorphous solid or small impurities in the sample. The stereo-identity was confirmed by two independent methods: Determination of specific optical rotation $[\alpha]_D$ and using Mosher's chiral derivatising agent. The details will be discussed in Section 3.2.

3.1.2.4 **Saponification of ester to carboxylic acid**

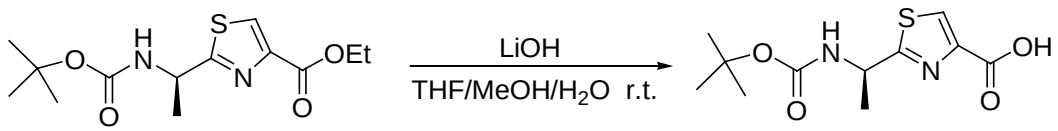

59 **44**

The final step for the preparation of the Boc-(*R*)-Ala-Thz-OH is the hydrolysis of the ethyl ester. The thiazole amino acid **44** is required as a building block in SPPS of argyrin. Esters can undergo hydrolysis in both acidic and basic conditions. However, acid-catalysed hydrolysis is of limited use because of the protected *N*-Boc would also be cleaved in acid conditions. Therefore, hydrolysis under basic conditions, also known as saponification, was chosen. Typically, saponification of ester is carried out in an aqueous alkali, such as sodium hydroxide or lithium

hydroxide, and is usually completed within few hours. The mechanism of base-catalysed hydrolysis of the ester is illustrated in Figure 3-5.

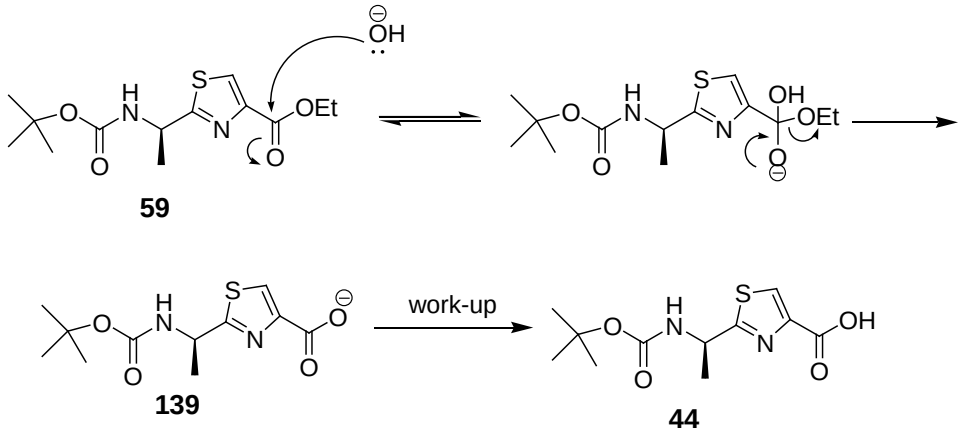

Figure 3-5 Base-catalysed hydrolysis of ester

Hence, (*R*)-Ala-Thz ethyl ester (**59**) and lithium hydroxide were dissolved in MeOH / H_2O (1:1) mixture. As the thiazole ester **59** was poorly soluble in water, addition of MeOH was required. The solution was stirred for 18 h. TLC analysis revealed the absence of starting material and the presence of product at the baseline. Unexpectedly, an additional spot was observed in TLC, which was assumed to be the solvent-facilitated transesterfication by-product. This hypothesis was further confirmed by ES-MS and ^{1}H NMR analysis. In order to avoid transesterfication during the hydrolysis, the MeOH / H_2O mixture was replaced by THF / H_2O. However, changing the solvent mixture resulted in lower reaction rates. By carefully adjusted solvent ratio of THF/H_2O/MeOH to 15:13:10, the desired product **44** was obtained in 88 % yield.

The purity of the final product was established using analytical RP-HPLC. The single peak observed in analytical HPLC confirmed the purity of the (*R*)-Ala-Thz-OEt building block. MS (ESI$^+$) detected a peak at *m/z* 295.0562 that corresponded to the calculated value for the [M+Na]$^+$ species of **44**. Furthermore, ^{1}H and ^{13}C NMR analysis confirmed the absence of ethyl ester signals and no methyl ester peak was detected. Therefore, the obtained dipeptide building block **44** was ready for the Fmoc solid phase peptide synthesis which will be discussed in Chapter 4.

3.2 **Determination of chiral purity by Mosher's reagent**

Determination of chiral purity can be achieved by numerous methods. Before 1960, the chiral purity of molecules relied on the measurement of optical rotation of the sample.[239] The value which was measured by a polarimeter under defined solvent, concentration and temperature can be compared to the optical rotation of the known enantiomerically pure sample. Today, measurement of optical rotation remains one of the most convenient methods for the indication of optical purity. However, there are two major limitations of this method. Firstly, the optical rotation is not perfect linear function of the enantiomeric composition. As a result, no accurate enantiomeric composition can be observed by this method. Secondly, the use of optical rotation for determination of chiral purity is subject to the some variability, including temperature, concentration and contamination. Given these two limitations, other independent methods have been developed to accurately determine the chiral purity.

The two major independent methods have been widely used to determine the optical purity. One method is employing analytical chiral HPLC or GC containing the single enantiomer of a chiral compound in the stationary phase.[240] The other method involves NMR analysis following derivatisation with a chiral reagent.[241] The principle of both methods is based on the formation of transient or permanent diastereoisomers. However, the former method is more expensive as the type of column used for separating a class of enantiomer is often specific and costly. On the contrary, the latter method is very convenient to determine both the optical purity and elucidate the absolute configuration of the chiral compounds. Hence, the derivatisation-NMR methodology was chosen to determine the optical purity of (*R*)-Ala-Thz-OEt (**59**).

3.2.1 **Mosher's derivatising agents**

The determination of optical purity by derivatisation of enantiomer with an enantiomerically pure reagent, followed by NMR spectroscopy analysis was introduced by Raban and Mislow in 1965.[241] Since then, a wide range of chiral derivatising agents have been reported, such as Pirkle's reagent **140**,[242]

chlorodioxaphospholane **141** [243] and Mosher's reagent **142** (Figure 3-6).[244] Among these chiral derivatising agents, α-methoxy-α-(trifluoromethyl)phenylacetic acid **142** (MTPA), also known as Mosher's reagent, is most commonly used.[244]

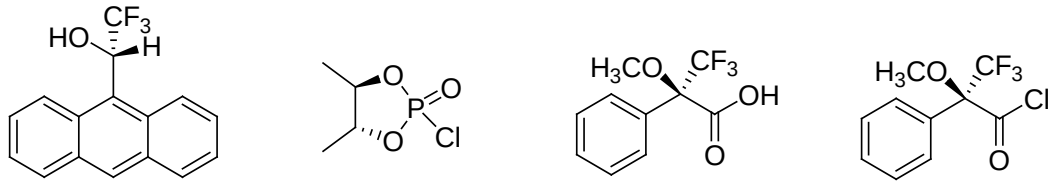

140 **141** **142** **143**

Figure 3-6 Chiral derivatising reagents

The enantiomerically pure (*R*)-MTPA-Cl (**143**) or (*S*)-MTPA-Cl reacts readily with primary and secondary alcohols or amines to afford diastereomeric esters or amides, which can be analysed by ^{1}H and ^{19}F NMR. The chiral purity can be determined by the differences in chemical shift of the non-equivalent proton or fluorine. Additionally, the ratio of enantiomeric composition can be established by the integration of those signals. Hence, to determine the chiral purity of *N*-Boc-(*R*)-Ala-Thz-OEt (**59**), (*R*)-MTPA-Cl was used as a derivatising reagent.

3.2.2 NMR determination of enantiomeric purity of dipeptide Boc-(*R*)-Ala-Thz-OEt

In order to forming diastereomeric (*R*)-MTPA-amide **145**, the *N*-Boc of Boc-(*R*)-Ala-Thz-OEt **59** was firstly removed by TFA-mediated acidolysis. The free (*R*)-Ala-Thz-OEt **144** was subsequently used for the condensation with (*R*)-MTPA-Cl (**143**) to afford the diastereomeric (*R*)-MTPA-amide **145** (Figure 3-7).

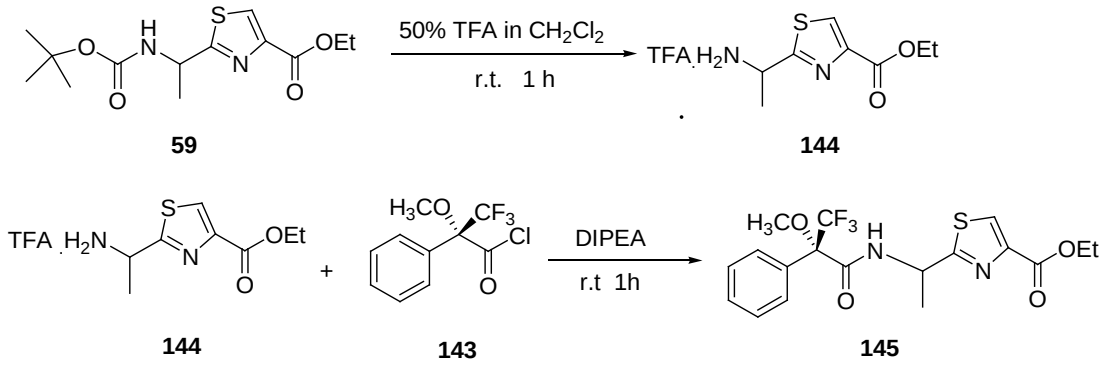

Figure 3-7 Synthesis of diastereomeric (*R*)-MTPA-amide (145).

Specifically, different batches of synthesised Boc-(*R*)-Ala-Thz-OEt were treated with 50 % *v/v* TFA in DCM at room temperature for 1 h to release the amine trifluoroacetate salt **144**. The (*R*)-Ala-Thz-OEt **144** was then treated with a stoichiometric amount of (*R*)-MTPA-Cl (**143**) in the presence of DIPEA in dry DCM. The reaction mixture was vigorously stirred under a nitrogen atmosphere for 1 h, after which the solvent was removed *in vacuo* and the residual material was subjected to an aqueous work-up to afford the diastereomeric (*R*)-MTPA-amides **145**.

The ^{1}H and ^{19}F NMR assignments for the (*R*)-MTPA-amides **145** are listed in Table 3-1. Three different batches using modified Hantzsch thiazole formation without isolation of the hydroxythiazoline intermediate were examined (entries 1-3). As expected, the results showed only single set of signals in both ^{1}H and ^{19}F NMR analysis (Figures 3-8 and 3-9). The evidence suggested that no racemisation occurred in these modified Hantzsch thiazole conditions and the obtained products were of high optical purity. The optical rotation obtained for *N*-Boc-(*R*)-Ala-Thz-OEt **59** ($[\alpha]^{21}_{D}$ = + 32 (*c* = 1.0 $CHCl_3$)) was slightly lower than the value reported in the literature ($[\alpha]^{25}_{D}$ = + 40.8 (*c* = 1.0 $CHCl_3$)[150]); the variation is postulated to be due to the effect of temperature on the measurements.

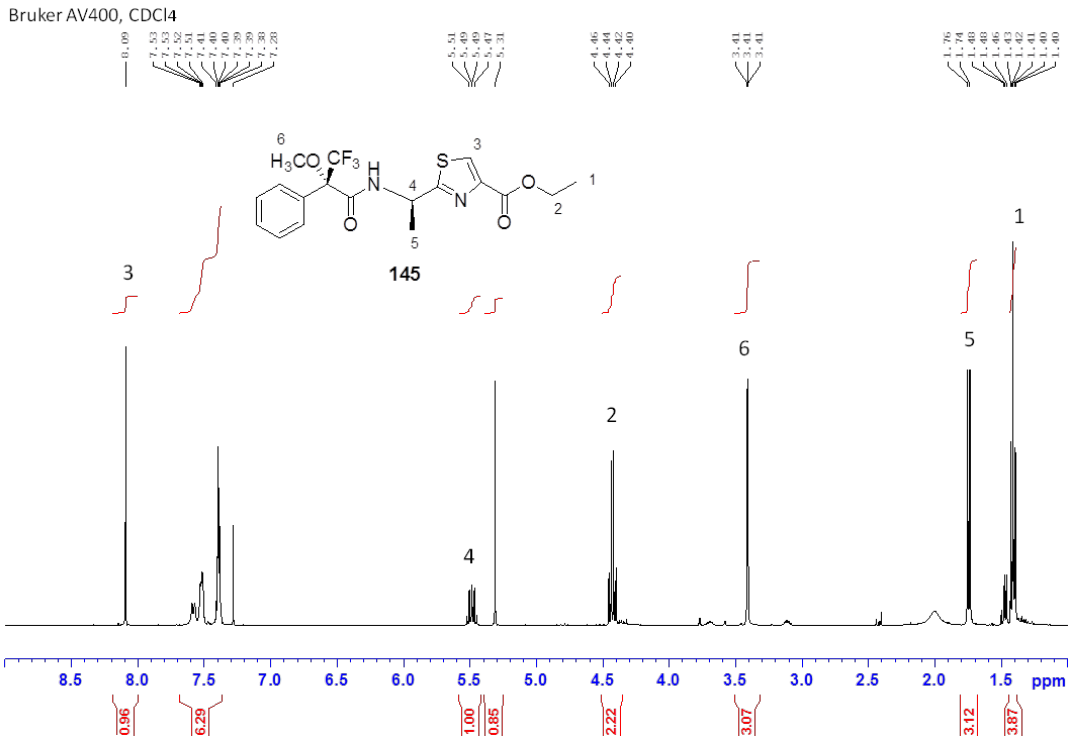

Figure 3-8 **^{1}H NMR analysis of (*R*)-MTPA-amide 145.**

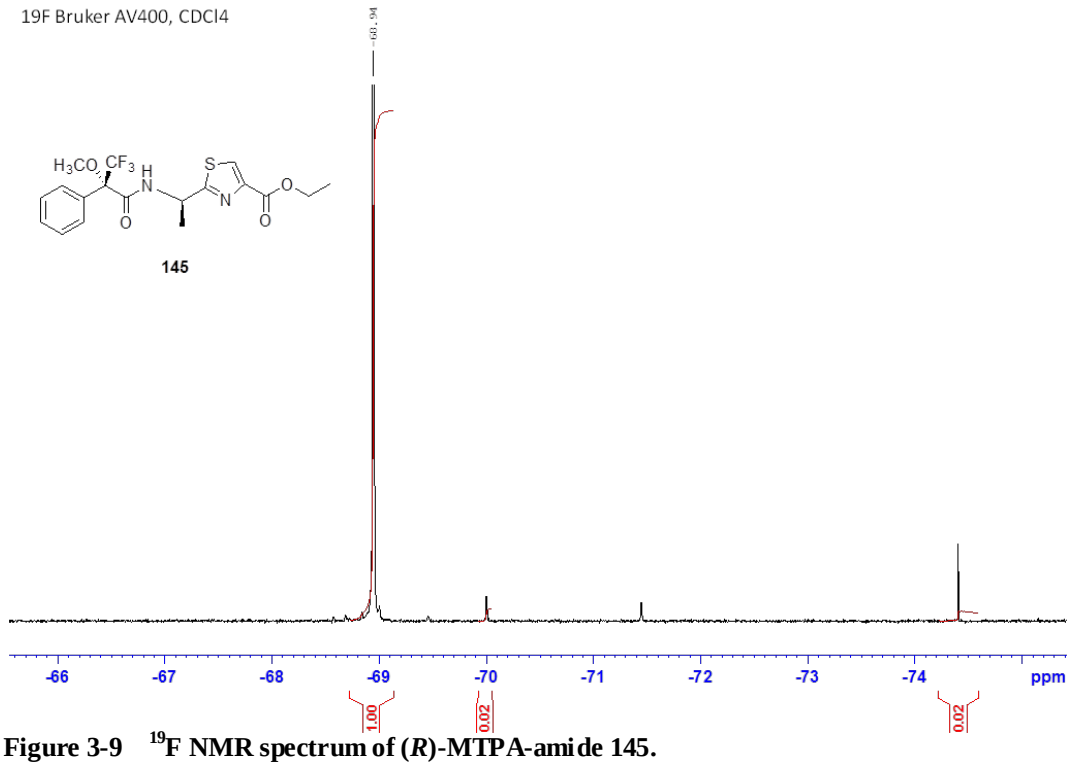

Figure 3-9 **^{19}F NMR spectrum of (*R*)-MTPA-amide 145.**

In contrast, two well-resolved sets of the chemical shifts in the ^{1}H NMR spectrum were observed ($\Delta\delta_{H}$ = 0.06 Hz) when the hydroxythiazoline intermediate was isolated in modified Hantzsch thiazole formation (Table 3-1, entry 4). In addition,

^{19}F NMR spectrum also showed two distinguished signals at δ_F = - 68.94 ppm and δ_F = - 68.57 ppm. Moreover, the optical rotation observed ($[\alpha]^{21}_D$ = + 4 (*c* = 1.0 $CHCl_3$)) is much lower than the value reported in the literature.[150] These results indicate that a racemic mixture was obtained, and are in agreement with the finding of the Meyers group.[238]

Table 3-1 NMR analysis of diastereoisomeric (*R*)-MTPA-amide 145 and optical rotations of *N*-Boc-(*R*)-Ala-Thz-OEt.

	Modified Hantzsch thiazole formation	1H NMR (*R*,*R*) : (*S*,*R*)	^{19}F NMR δ (-68.94:-68.57)	Diastereoisomeric ratio (*R*:*S*)	$[\alpha]^{21}_D$ (*c* =1.0 $CHCl_3$)
1	Step 1 for 2 min	> 99:1	> 99:1	> 99:1	+ 32.0
2	Step 1 for 5 min	> 99:1	> 99:1	> 99:1	+ 32.3
3	Step 1 for 10 min	> 99:1	> 99:1	> 99:1	+ 30.3
4	Isolation of intermediate	50.3 : 49.7	50.7: 49.3	51:49	+ 4.3

In conclusion, Hantzsch thiazole formation without isolation of the intermediate resulted in desired product with high enantiomeric purity. Therefore, modified Hantzsch thiazole reaction is generally applicable for the synthesis of optically pure thiazole amino acids. On the basis of the spectroscopic features and optical rotation data, the quality of the synthesised *N*-Boc-(*R*)-Ala-Thz-OH **44** is suitable for the Fmoc solid phase peptide synthesis which is discussed in Chapter 4.

3.3 **Synthesis of Boc-(*R*)-Ala-oxazole-OH**

Having synthesised the required dipeptide Boc-(*R*)-Ala-Thz-OH building block, attention was then focused on the synthesis of Boc-(*R*)-Ala-oxazole-OH. Like thiazole ring, oxazole is also a member of azoles and abundantly found in marine organisms, many of which possess significant biological activities. For example, taxaline, a simple oxazole-containing alkaloid exhibited antituberculosis activity.[245] Bengazole A, isolated from a marine sponge, showed anti-proliferation of many human cell lines.[246] Almazole D, a metabolite isolated from a red seaweed displayed anti-bacterial activities.[247]

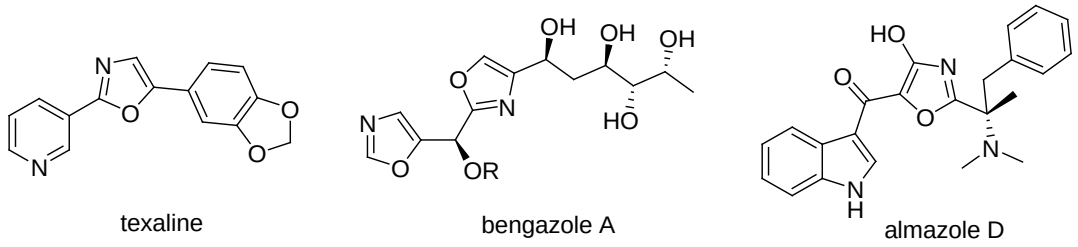

Similar to the thiazole-containing peptide, the biosynthetic pathway of the oxazole-containing amino acid was derived from the condensation of peptide precursors with threonine, followed by cyclisation and oxidation.[248] Due to the interest of many active oxazole-containing natural products, new oxazole formation methodologies have been established. The three literature approaches were utilised and discussed in the following sections.

3.3.1 **Classical Hantzsch oxazole approach**

The initial strategy was carried out using the classical Hantzsch oxazole synthesis. Following the literature procedure outlined in Scheme 3-3, *N*-Boc-(*R*)-Ala-OH was first coupling with ammonia under standard conditions to give the amide **57**.[249] Subsequent reaction with ethyl bromopyruvate in the presence of 3,4-epoxycyclopentene afforded corresponding 4-hydroxyoxazoline, followed by dehydration to give the desired (*R*)-Ala-oxazole-OEt **146**. It is worthwhile to note that the addition of a large excess of 3,4-epoxycyclopentene as an acid scavenger prevents acid-catalysed imine-enamine tautomerisation and hence suppresses the epimerisation of 4-hydroxyoxazoline. [249]

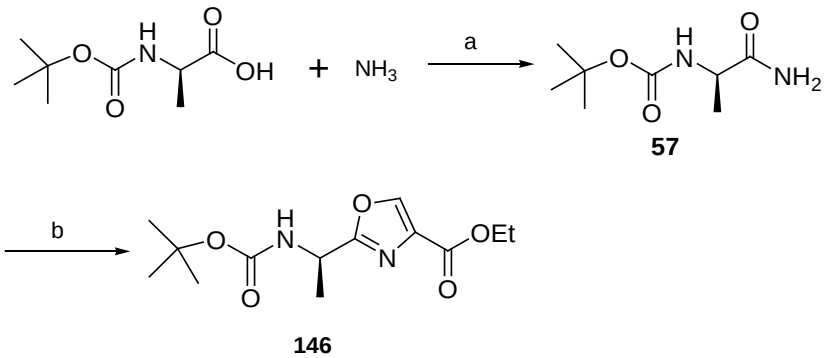

Scheme 3-3 Classical Hantzsch synthesis of (*R*)-Ala-oxazole-OEt (146); Reagents and conditions: (a) DCC, HOBt, DIPEA, DCM; (b) i. $BrCH_2COCO_2Et$, 3,4-epoxycyclopentene, DME. ii.TFAA, 2,6-lutidine, DME, -15 °C.

Specifically, *N*-Boc-(*R*)-Ala-OH and ammonia in dioxane were reacted with DCC and HOBt in the presence of a slight excess of DIPEA. The urea by-product was removed by filtration and the filtrate was subjected to column chromatography to give the amide **57** in quantitative yield. The synthesised amide **57** was then employed for the Hantzsch oxazole synthesis. Similar to the thiazole synthesis described in Section 3.1.2.3, the solution of amide **57** in dry DME was cooled to -15 ° C and was treated with ethyl bromopyruvate in the presence of finely powdered potassium bicarbonate and 3,4-epoxycyclopentene. The mixture was stirred vigorously for 5 min. The solution of 2,6-lutidine and trifluoroacetic anhydride in DME was added in one portion at -15 ° C. The reaction was left to stir at -15 °C for 1 h. Unexpectedly, TLC analysis indicated that no product was formed. After an aqueous work-up, MS and ^{1}H NMR analysis showed only the starting material. It should be noted that no 4-hydroxyoxazoline intermediate **147** was detected by TLC or in ^{1}H NMR analysis. It was hypothesised that the lower electron density of oxygen may result in inefficiency of nucleophilic attack of the ethyl bromopyruvate **137** (Figure 3-10). Therefore, an alternative oxazole synthesis strategy was then investigated.

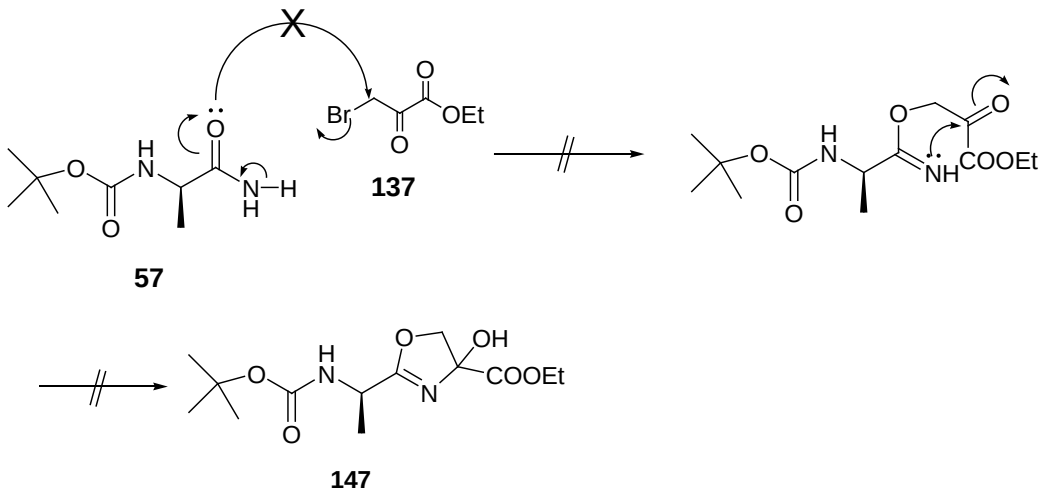

Figure 3-10 Proposed mechanism of Hantzsch oxazoline formation.

3.3.2 **Mitsunobu approach to synthesis of oxazole**

Another strategy for the construction of the oxazole ring was introduced by Wipf *et al*. in 1992, exploiting the intramolecular Mitsunobu reaction of serine-containing diepeptides.[250] This method was further adopted by Yamada *et al*. for the synthesis

of Boc-(*R*)-Ala-oxazole building block.[251] As shown in Scheme 3-4, the synthesis started with the coupling reaction of *N*-Boc-(*R*)-Ala-OH and serine ethyl ester using standard peptide coupling reagents. The dipeptide **148** was then cyclised to oxazoline **149** under Mitsunobu condition, followed by peroxide oxidation to provide the desired *N*-BOC-(*R*)-Ala-oxazole-OEt **146**. The detail of Mitsunobu reaction will be discussed in Section 3.4.2.1.

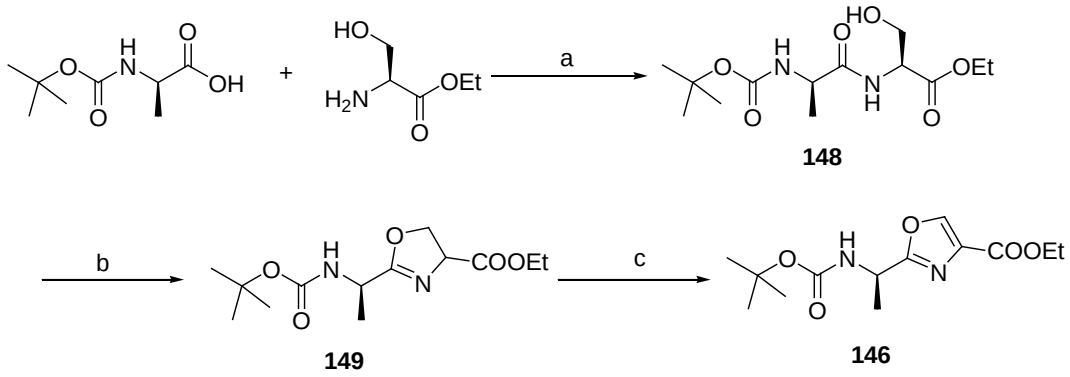

Scheme 3-4 Synthesis of *N*-Boc-(*R*)-Ala-oxazole-OEt (146) *via* Mitsunobu reaction. Reagents and conditions: (a) DCC, HOBt, DIPEA, DCM; (b) Diisopropyl azodicarboxylate, Ph_3P, THF, 0 °C. (c) i. $KN(TMS)_2$, THF-toluene, then PhSeCl, -78 °C. ii 30 % H_2O_2, DCM, 0 °C.

Thus, *N*-Boc-(*R*)-Ala-OH and serine ethyl ester were reacted with DCC and HOBt in the presence of a slight excess of DIPEA. The urea by-product was removed by filtration and the filtrate was subjected to column chromatography to afford the dipeptide **148** in quantitative yield. The resulting dipeptide **148** in dry THF was treated dropwise with 1.5 eq. of diisopropyl azodicarboxylate (DIAD) and triphenylphosphine over 5 min at 0 °C under a nitrogen atmosphere. After complete addition, the reaction mixture was warmed to room temperature and left to stir for 4 h. Unfortunately, TLC analysis revealed that no product was formed. Subsequent work-up and purification of the crude reaction mixture gave the by-product triphenylphosphine oxide and the starting material, recovered in 40 % yield. The reaction was found to be unsuccessful with more vigorous stirring and increasing reaction time.

3.3.3 **Burgess approach to synthesis of oxazole**

The key step of oxazole synthesis is the formation of oxazoline intermediate **149**. In addition to intramolecular Mitsunobu cyclisation, one alternative method is utilising Burgess reagent. Wipf *et al*. later introduced methyl *N*-(triethylammoniumsulphonyl)carbamate **150**, also known as Burgess reagent, in the preparation of oxazole-containing natural products.[252] As shown in Scheme 3-5, the dipeptide **148** was cyclised with Burgess reagent **150** to give the oxazoline **149**, followed by peroxide oxidation to afford oxazole dipeptide **146**. The reaction details will be discussed in the following sections.

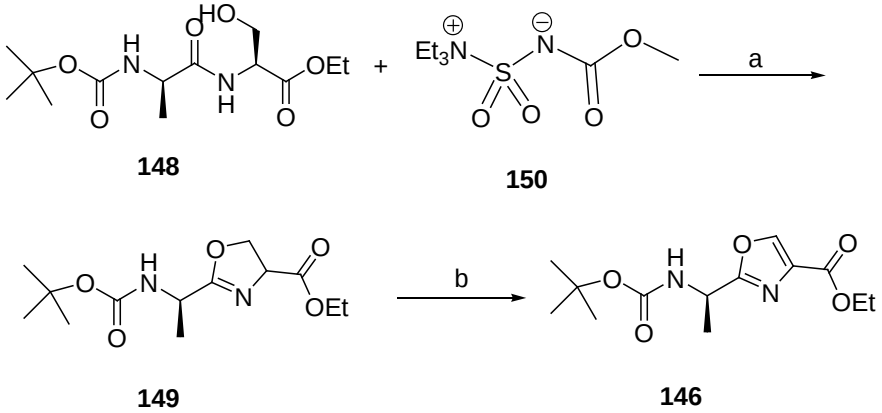

Scheme 3-5 Synthesis of Boc-(*R*)-Ala-oxazole-OEt (146) using Burgess reagent. Reagents and conditions: (a) THF, 70 °C; (b) PhCOOO-*t*-Bu, CuBr, benzene, reflux.

3.3.3.1 **Cyclisation of hydroxyl amino acids with Burgess reagent**

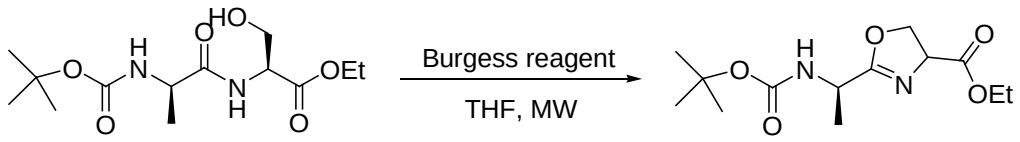

148 149

Burgess reagent **150** is a mild and selective dehydrating agent which has been widely used for the cyclodehydration of hydroxyl amides or thioamides to afford the corresponding heterocycles.[253] The mechanism of this type of oxazoline formation is outlined in Figure 3-11. The hydroxyl group of serine attacks the sulfonyl group of Burgess reagent to give the intermediate **151**, followed by intramolecular cyclisation to afford the oxazoline **149**. According to the literature,

epimerisation in α-carbon can be suppressed compared with other cyclisation methods.[253]

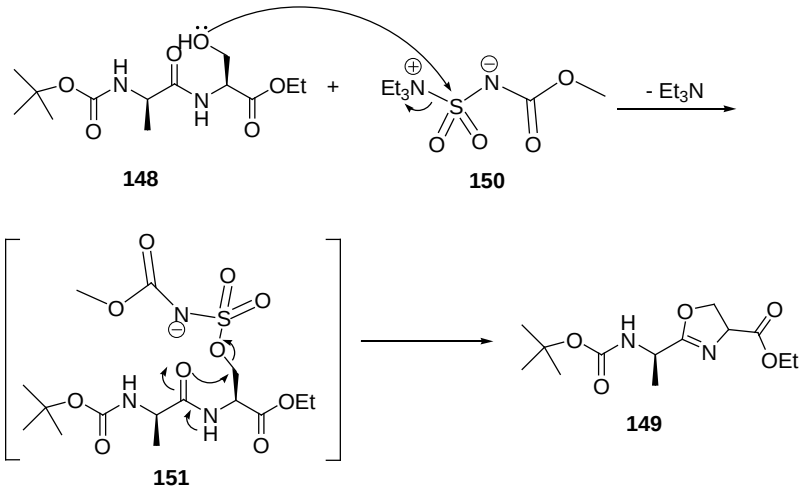

Figure 3-11 Mechanism of oxazoline formation by reaction of *N*-Boc-(*R*)-Ala-Ser-OEt with Burgess reagent.

Initial attempts focused on using the condition as described in the literature.[254] To a solution of the dipeptide **148** in THF was added 1.1 equivalents of Burgress reagent. The reaction mixture was then refluxed for 5 h, after which TLC analysis showed only starting material and decomposition of Burgress reagent. Several alternative conditions were also investigated. Table 3-2 outlines the conditions used for the synthesis of Boc-(*R*)-Ala-oxazoline **149**. The first attempt was to increase the reaction temperature by the use of dioxane as a solvent (entry 2). However, no improvement was obtained and 40 % starting material was recovered. Another attempt to use dry THF gave the desired product but in a very low conversion (entry 3). It appeared that no satisfactory yield could be obtained in routine thermal conditions. Therefore, the reaction was conducted under microwave irradiation, as reported by Brain *et al.* (entry 4).[255] Surprisingly, the yield was drastically improved to 64 - 81 %. No elimination by-product was detected under these conditions.

Table 3-2 Optimisation of oxazoline formation

	Equivalent of Burgess reagent	Solvent	Temperature (°C)	Time	Result
1	1.1	THF	66	5 h	no reaction
2	1.1	Dioxane	100	5 h	no reaction
3	1.1	dry THF	66	5 h	2 % yield
4	1.1	THF	M.W., 70	30 min	64 - 81% yield

Thus, 1.1 eq. of Burgess reagent was added to a solution of dipeptide **148** in dry THF under a nitrogen atmosphere. The reaction mixture was irradiated for 30 min with a microwave power of 100 W. TLC analysis revealed the absence of dipeptide **148** and the presence of the two new products. The mixture was subjected to an aqueous work-up and subsequent column chromatography gave the (*R*)-Ala-oxazoline ethyl ester **149** in an overall yield of 64 - 81 %. It was ascertained that the product **149** was composed of two distinct spots by TLC analysis and it was proposed that these corresponded to diastereoisomers of the oxazoline. ^{1}H NMR also showed two sets of doublet signals, assigned to the C-4H of the oxazoline ring. Although there is no stereoselectivity in this oxazoline formation, two diastereomeric oxazolines should oxidise to a single oxazole product in the next step. Therefore, a mixture of two isomers was used directly in the next step of the reaction.

3.3.3.2 **Peroxide oxidation of oxazoline to oxazole**

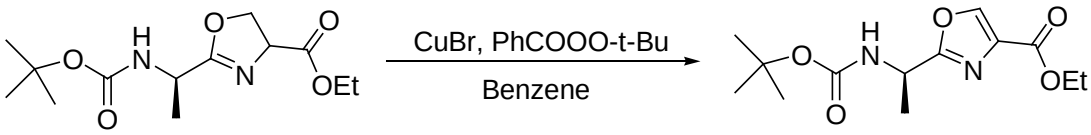

149 **146**

Three methods have been reported for the oxidation of oxazolines to oxazoles: (1) NBS with either benzoyl peroxide or light, (2) $BrCCl_3$/DBU reagent and (3) Kharasch-Sosnovsky reaction.[256-259] The disadvantage of the first method is that a concomitant α-bromination side product could be formed using NBS, with either benzoyl peroxide or light as the radical initiator.[256] Both of the two remaining methods have been investigated for the synthesis of 2,4-disubstituted oxazoles and

thiazoles.[257-259] Hence, Kharasch-Sosnovsky oxidation was firstly chosen in order to establish suitable reaction conditions.[258] The proposed copper ion-catalysed radical mechanism is shown in Figure 3-12.

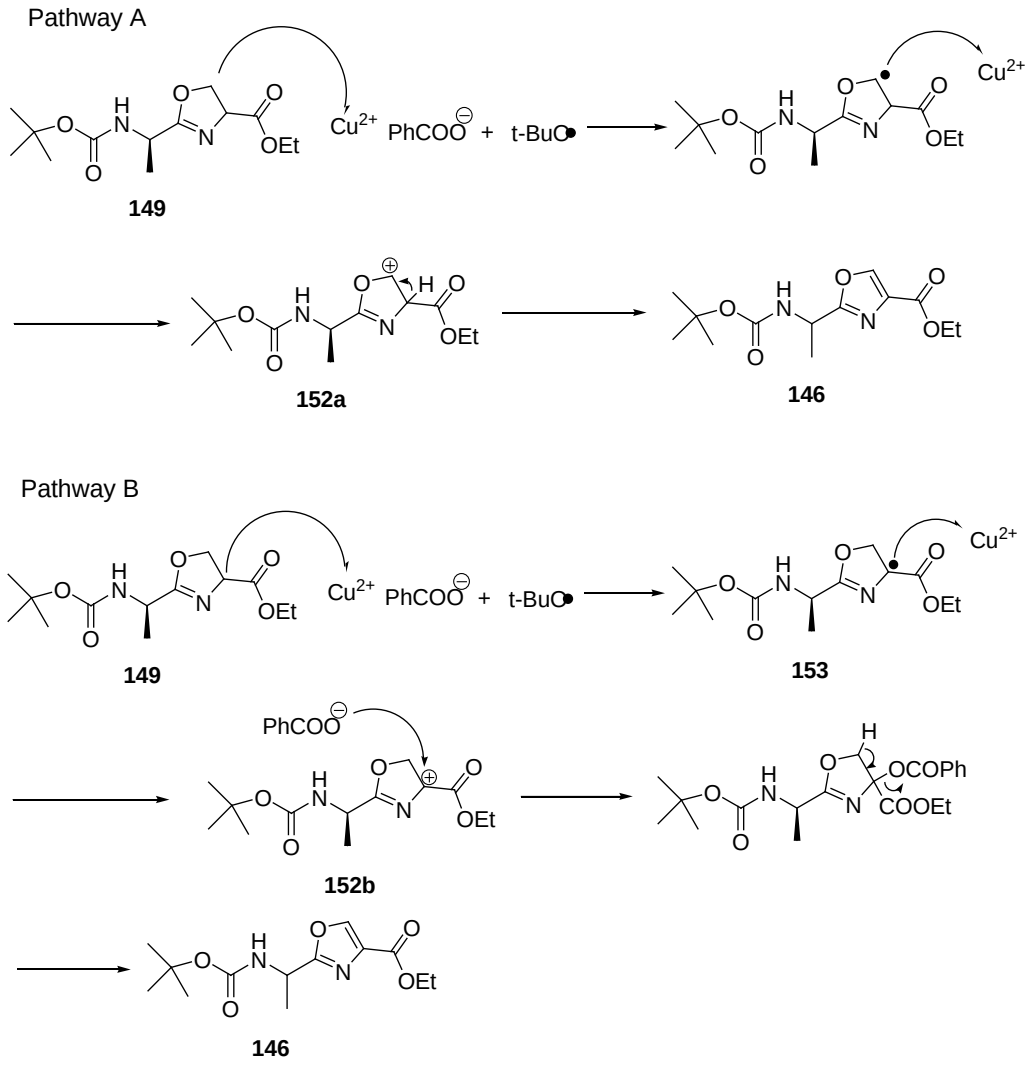

Figure 3-12 Oxidation of oxazoline (149) to oxazole (146) by two possible copper ion-catalysed mechanisms.

The process begins with decomposition of peroxyester catalysed by Cu^{+}, and the resulting oxidised Cu^{2+} then reacts with oxazoline **149** to generate a carbon radical, which could be either at 4- or 5-position of the oxazoline ring. In mechanistic pathway A, the intermediate α-oxa radical is further oxidised by Cu^{2+} to form oxonium intermediate **152a**, which rapidly loses a proton to give the oxazole **146**. In path B, the more favourable captodative radical **153** is oxidised by Cu^{2+} to form oxonium intermediate **152b**.[260] **152b** is further attacked by benzoic acid anions, followed by *syn*-elimination to give the oxazole **146**.[256]

Hence, 1.5 eq. of *tert*-butyl perbenzoate was added to a boiling solution of the oxazoline **149** and CuBr in benzene over 1 h. The reaction mixture was further refluxed for 1 h. TLC analysis revealed the absence of oxazoline **149** and the presence of the product along with some impurities. The mixture was subjected to an aqueous work-up and subsequent column chromatography afforded the (*R*)-Ala-oxazole ethyl ester **146** in an overall yield of 60-72 %.

Similar to the thiazole analogue describing in Section 3.1.2.3, the distinct singlet signal appearing at δ = 8.18 ppm in the ^{1}H NMR spectrum revealed the formation of the oxazole ring. Additionally, stereochemical-identity was confirmed by using Mosher's chiral derivatising agent (Figure 3-13).

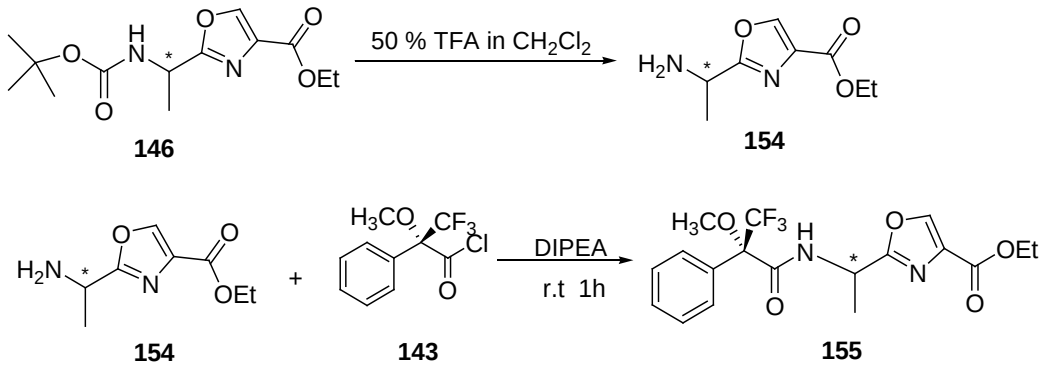

Figure 3-13 Synthesis of diastereomeric (*R*)-MTPA-amide 155.

To determine the chiral purity of the oxazole derivative **146**, *N*-Boc was firstly removed by TFA-mediated acidolysis. The free (*R*)-Ala-oxazole-OEt **154** was subsequently used for the condensation with (*R*)-MTPA-Cl (**143**) to afford the diastereomeric (*R*)-MTPA-amide **155**. ^{1}H and ^{19}F NMR spectra of (*R*)-MTPA-amide **155** are shown in Figures 3-14 and 3-15, respectively. Surprisingly, two well-resolved sets of the chemical shifts in ^{1}H and ^{19}F NMR were observed. The results indicated that a mixture of (*R*,*R*)-**155** and (*R*,*S*)-**155** was obtained. These results are in disagreement with the literature reported by Khapli *et al.* and Brain *et al.*[253,255] The evidence from ^{1}H and ^{19}F NMR spectra strongly suggests that epimerisation had occurred.

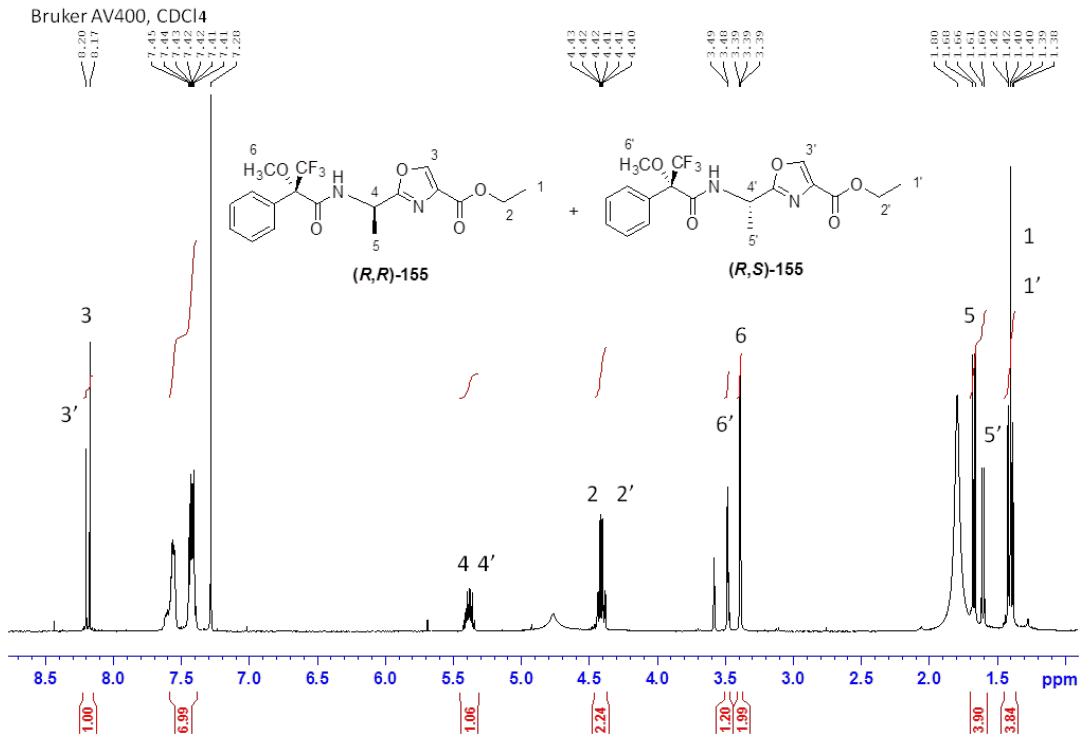

Figure 3-14 ^{1}H NMR spectrum of the diastereomeric (*R*)-MTPA-amide 155.

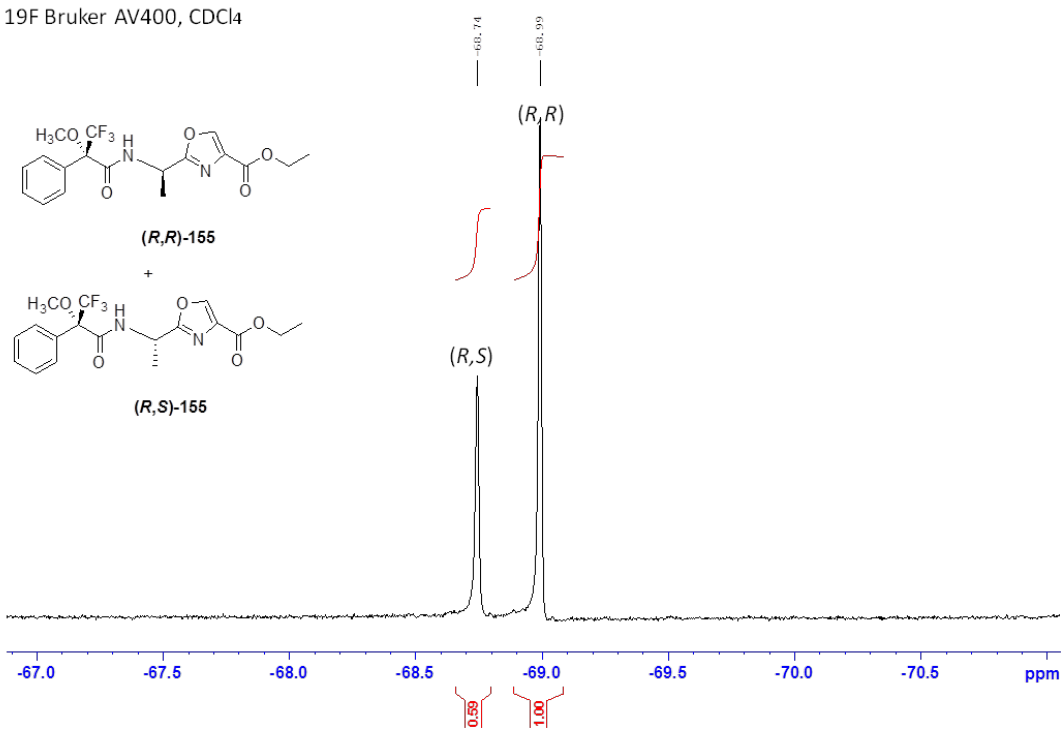

Figure 3-15 ^{19}F NMR spectrum of the diastereomeric (*R*)-MTPA-amide 155.

The epimerisation was postulated to be due to the isolation of the oxazoline intermediate. The isolated oxazoline intermediate **149** can undergo an imine-enamine tautomerization resulting in epimerisation as shown in Figure 3-16.

Therefore, the synthesised racemic *N*-Boc-(*R*)-Ala-oxazole **146** was not suitable for the Fmoc solid phase peptide synthesis.

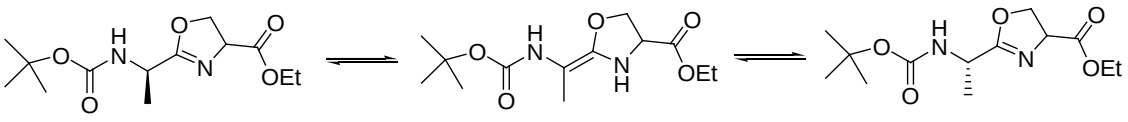

149

Figure 3-16 Racemisation *via* an imine-enamine type equilibration.

3.4 **Synthesis of a dehydroalanine precursor**

Dehydroamino acids including dehydroalanine and dehydrobutyrine are important constituents of numerous naturally occurring peptides, many of which possess biological activities. For example, a cyclic peptide microcystin is a potent hepatotoxin.[261] Another cyclic peptide thiostrepton shows antibiotic activity by inhibiting several biochemical pathways at the ribosomal GTPase centre.[262]

The incorporation of dehydroamino acids into these cyclic peptides exert a conformational constrain, leading to an increase in the rigidity of structure, which

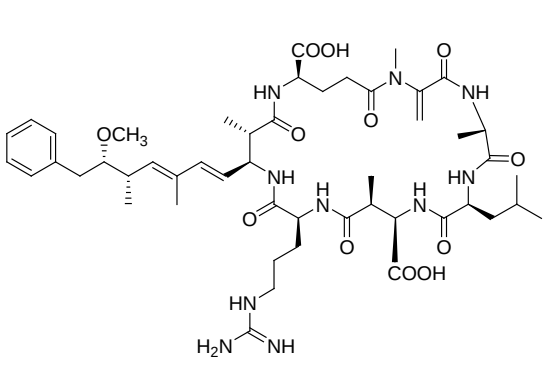

microcystin

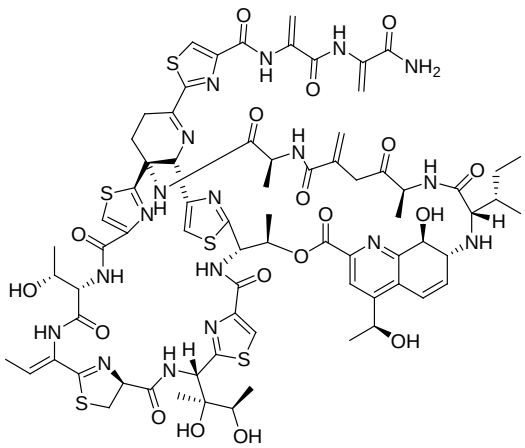

thiostrepton

is likely to be essential for the biological activities.[263] Moreover, owing to the electrophilicity of dehydroamino acids, it has been shown that dehydroalanine allows access to a wide variety of unusual amino acids *via* nucleophilic Michael addition[264] or acid-catalysed cross-coupling processes.[265]

On the other hand, as a Michael acceptor, dehydroalanine readily react with a wide range of nucleophiles, including amines, nitrogen heterocycles and thiols, making it

incompatible with conventional methods of peptide synthesis.[266, 267] Hence, the most common approach for the installing of dehydroalanine in peptides involves incorporation of a masked residue, which can be subsequently unmasked to the dehydroalanine at the final stage. In the following sections, three major methods for installing this functional residue into polypeptides are investigated.

3.4.1 **Previous reports for installing dehydroalanine in peptides**

The biosynthetic pathway of dehydroalanine and dehydrobutyrine are believed to be predominantly derived from the dehydration of serine and threonine residues, respectively. In contrast to the biosynthesis, several chemical synthetic routes have been described to install dehydroamino acid residues into polypeptides. However, due to the reactivity of α,β-unsaturated alkenes, most reported methodologies relied on the incorporation of a masked precursor at an early stage in peptide synthesis, followed by conversion to the α,β-unsaturated amino acid after the completion of peptide synthesis.

A review of literature led to the identification of three strategies for the preparation of dehydroalanine precursor. These strategies include the activation and elimination of serine derivatives,[268] oxidative elimination of *S*-alkyl or *S*-aryl protected cysteine derivatives[269] and oxidative elimination of phenylselenocysteine derivatives.[270] The latter two methodologies were applied, one of which resulted in the successful preparation of dehydroalanine precursor. The detail of the three strategies is discussed in the following sections.

3.4.1.1 **Serine approach**

The preparation of dehydroalanine residues was first achieved by Koshland *et al*. in 1963. Koshland successfully converted the serine residue in chymotrypsin to dehydroalanine in the course of investigating the catalytic role of Ser195.[271] As illustrated in Figure 3-17 (A), the hydroxyl group of a serine residue reacts readily with *p*-toluenesulfonyl chloride to form the *O*-tosylated serine derivative **156**, and subsequent *β*-elimination of *O*-tosylserine **156** under alkaline conditions provides dehydroalanine **157**. However, Sakai *et al*. reported that the elimination of *O*-

tosylated serine derivatives does not always produce the desired dehydroalanine; instead, aziridine derivatives **158** were obtained in high yield.[272] Ranganathan *et al*. improved this method by reacting serine with oxalyl chloride in the presence of triethylamine (Figure 3-17(B)). However, the yield was strongly affected by the peptide length and the position of the dehydroalanine residue in the peptide chain.[268] Therefore, a new approach utilising cysteine as a dehydroalanine precursor was studied.

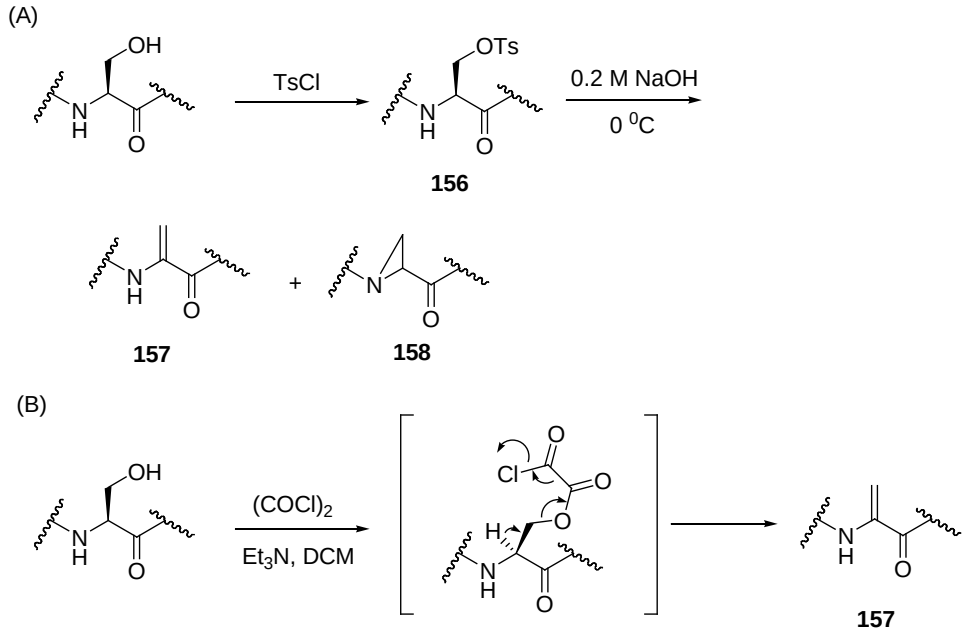

Figure 3-17 Synthesis of dehydroalanine from serine. (A) Koshland's approach. (B) Ranganathan's approach.

3.4.1.2 Attempted preparation of dehydroalanine precursor *via* cysteine

An alternative method to prepare dehydroalanine is using *S*-alkyl or *S*-aryl protected cysteine derivative as a precursor. After completion of peptide synthesis, subsequent oxidative elimination reactions led to desired dehydroalanine residue.[273] As shown in Figure 3-18, commercially available *N*-Boc protected *S*-methyl cysteine **159** was incorporated during peptide synthesis. After completion of peptide synthesis, peptide **160** was allowed to convert to the dehydroalanine **162** by oxidation and elimination. This conversion involved formation of sulfoxide **161** using sodium metaperiodate, followed by DBU-facilitated elimination under reflux

condition. This method was reported to be compatible with both Boc and Fmoc strategies.

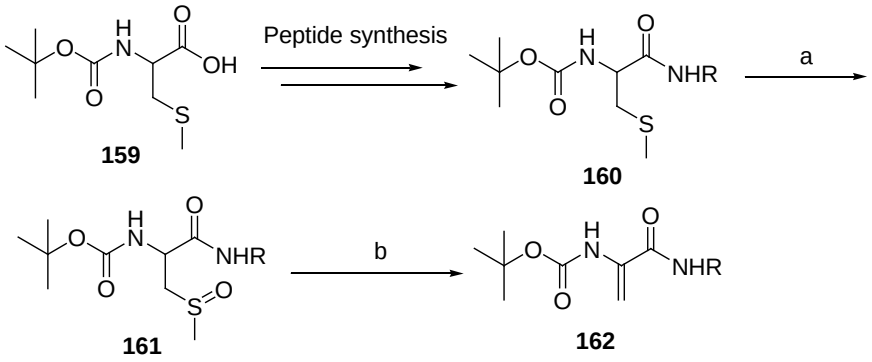

Figure 3-18 Synthesis of dehydroalanine from S-methyl cysteine; Reagents and conditions: (a) $NaIO_4$, H_2O, dioxane; (b) DBU, MeOH or dioxane, reflux.

However, the temperature required to effect elimination of β-methylsulfinyl derivatives was found to vary over a wide range (25-140 °C). In addition, the high temperature appeared to be too harsh for the synthesis of larger peptides, which typically denature at high temperatures. Furthermore, the synthesised dehydroalanine can readily undergo polymerisation at this high temperature.[274] Therefore, a lower temperature, solid-phase procedure was investigated by Yamada's group. [275]

As shown in Figure 3-19, Yamada's strategy involved a side-chain unprotected cysteine linking to the Merrifield resin (**163**), a commonly used chloromethylated polystyrene solid support for SPPS. After completion of peptide synthesis, desired peptides were released from the solid support *via* an *S*-oxidative eliminated to dehydroalanine, which is mediated by *m*-chloroperbenzoic acid (*m*-CPBA) and 1,8-diazabicycloundec-7-ene (DBU). The resulting dehydroalanine-containing peptides could be obtained in good yields (75- 86 %) and purity (95- 98 %).

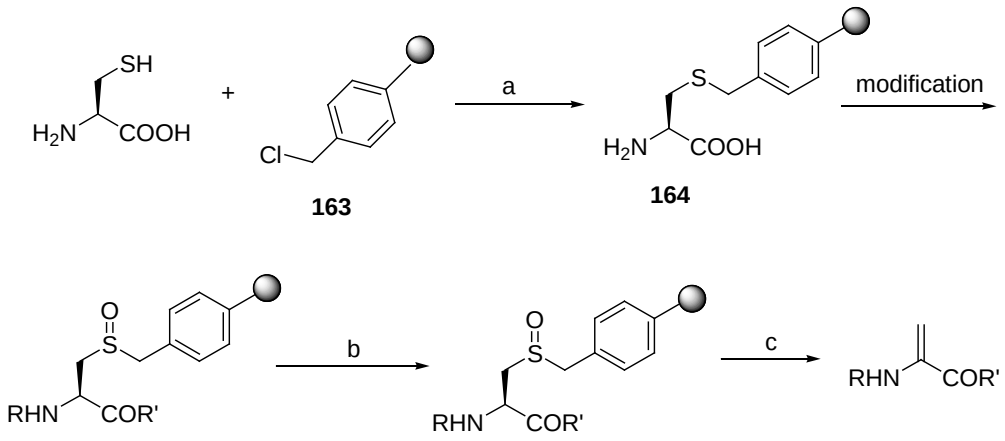

Figure 3-19 Solid-phase synthesis of dehydroalanine derivatives; Reagents and conditions: (a) DBU, DMF; (b) *m*-CPBA, DCM; (c) DBU, DCM.

Thus, in order to establish suitable conditions, initial attempt was carried out using Yamada's approach. Following the literature procedure, the first step in this synthesis requires attachment of cysteine to Merrifield resin (**163**) through nucleophilic substitution by the thiol side-chain functionality to produce **164**. Hence, two equivalents of DBU was added to a solution of unprotected cysteine in DMF under a nitrogen atmosphere,[276] and was left to stir overnight. Determination of the loading efficiency was achieved through measuring UV absorbance of Fmoc attachment to the free *N*-terminal of cysteine. However, the best obtained loading was only 0.03 mmol g^{-1}, which was substantially lower than what was reported in the literature (0.38 mmol g^{-1}).[276] The observed low loading was postulated to be due to the potential competing reaction of the *N*-terminal attachment to resin. Therefore, *N*-Boc-cysteine was used to enhance the loading efficiency. Unfortunately, the highest loading obtained from this study was 0.052 mmol g^{-1}, even though the reaction was performed at high temperature (60 °C).

Since monitoring the reaction was not practicable and the observed efficiency of the reaction was too low, an alternative approach for the synthesis of dehydroalanine peptides was sought.

3.4.2 Preparation of the dehydroalanine precursor, phenylselenocysteine

Walter and co-worker found in 1971 that selenocysteine derivatives could be easily converted to dehydroalanine derivatives under mild oxidative elimination conditions.[277] They observed that treatment with sodium metaperiodate or hydrogen peroxide, diphenylmethylselenocysteine was oxidised to the corresponding selenoxide derivative, which spontaneously eliminates to dehydroalanine derivative at room temperature (Figure 3-20). Hence, such advantageous have been exploited for the synthesis of selenocysteine derivatives as a dehydroalanine precursor. In particular, phenylselenocysteine was successfully adopted by Shirahama *et al.* for the synthesis of dehydroamino acid-containing peptides.[278] This approach is compatible with solution-phase and the standard solid-phase peptide synthesis.

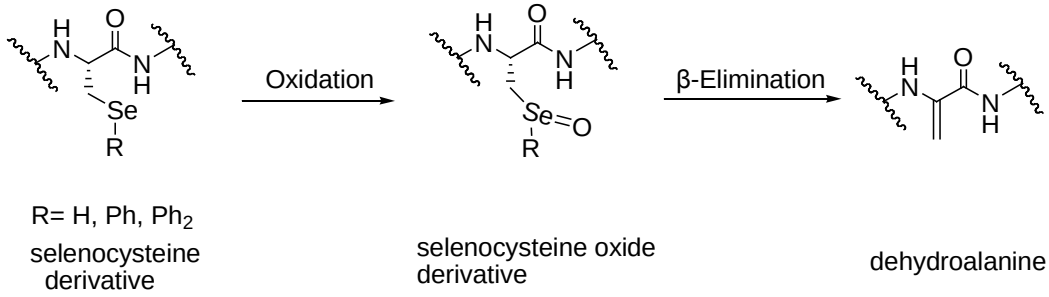

Figure 3-20 Phenylselenocysteine as a dehydroalanine precursor.

Thus, one of the earliest and most predominant methods for the preparation of optically pure phenylselenocysteine was developed by the same group.[279] Van der Donk *et al.* further modified this strategy by introducing this mild, chemoselective method to standard Fmoc-SPPS.[270] This approach for the synthesis of Fmoc-phenylselenocysteine was achieved and outlined in Figure 3-21; these transformations are discussed in the following sections.

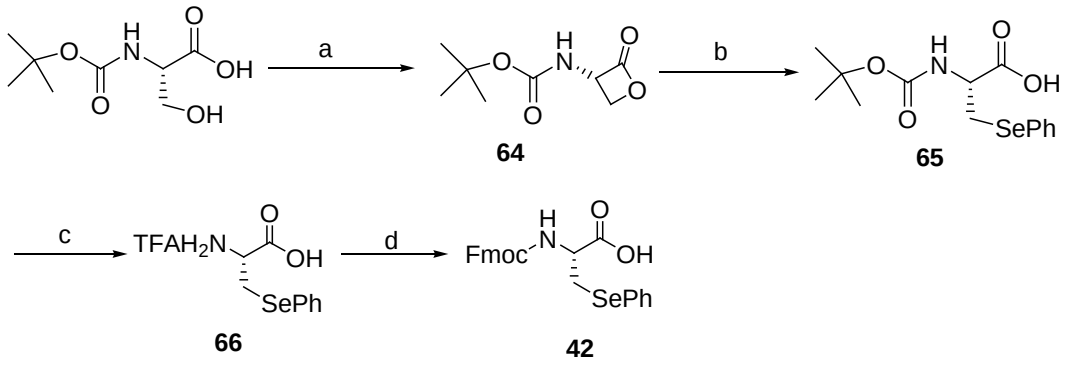

Figure 3-21 Synthesis of dehydroalanine precursor Fmoc-phenylselenocysteine (42). Reagents and conditions: (a) DEAD, PPh_3, THF, -78 °C to room temp.; (b) PhSeSePh, $NaBH(OMe)_3$, EtOH, room temp.; (c) TFA/DCM, room temp.; (d) Fmoc-OSu, $NaHCO_3$, THF/H_2O, room temp.

3.4.2.1 **Synthesis of β-lactone ring *via* Misunobu reaction**

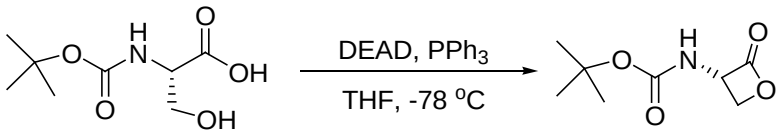

The first step is the formation of β-lactone ring *via* intramolecular Mitsunobu reaction. Mitsunobu *et al.* first reported this type of reaction which has become a useful tool in organic synthesis since its discovery in 1967.[280] In general, the reaction is a method for converting alcohols into various functional groups such as esters, aryl ethers and thioethers. The process involves activating an alcohol into a good leaving group, which then undergoes nucleophilic substitution (S_N2) by nucleophiles, including carboxylic acids, phenols and diols. The reaction mechanism is illustrated in Figure 3-22.

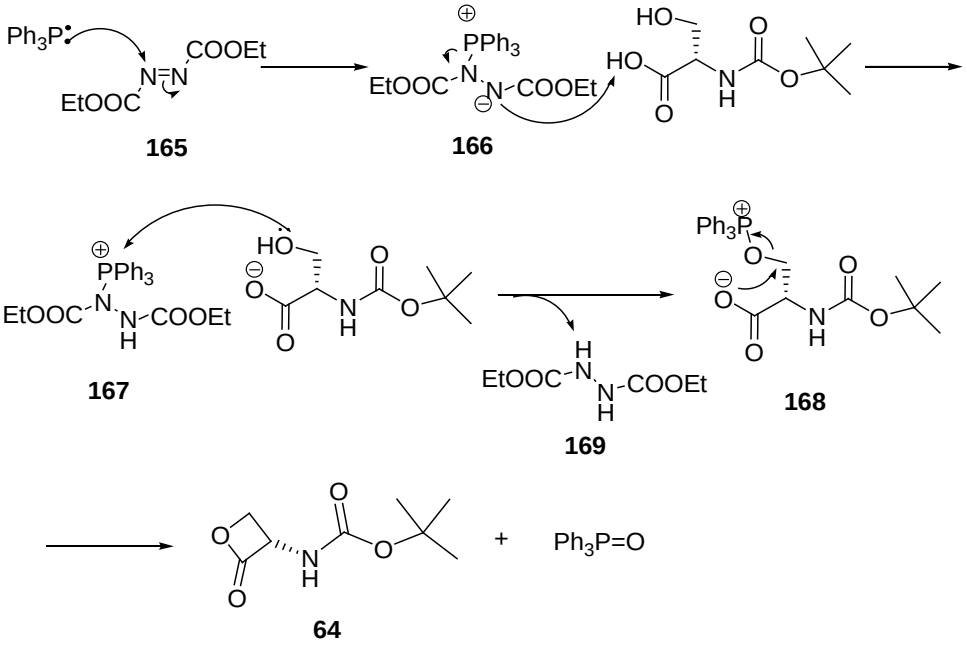

Figure 3-22 Mechanism of intramolecular Misunobu reaction to form β-lactone ring (64).

Initially, an oxidising azo reagent, diethyl azodicarboxylate (DEAD) (**165**) or diisopropyl azodicarboxylate (DIAD), reacts with triphenylphosphine to form betaine intermediate **166** which is then protonated by carboxylic acid of serine to form the phosphonium salt **167**. In the alcohol activation step, the resulting triphenylphosphine group of phosphonium salt **167** is transferred to the hydroxyl group of serine. Thus, alkoxyphosphonium salt **168** and hydrazine by-product **169** are generated. Finally, the carboxylate group of serine undergoes an intramolecular nucleophilic substitution to afford the desired lactone ring **64** and by-product triphenylphosphine oxide.

Thus, triphenylphosphine in dry THF under nitrogen atmosphere at -78 °C was treated with a stoichiometric amount of DEAD. A solution of Boc-(*S*)-serine in THF was then added dropwise to the mixture over 30 min. After completion of addition, the mixture was stirred at -78 °C for 20 min and the mixture was slowly warmed to room temperature over 2.5 h. After work-up and purification, the highly pure β-lactone product **64** was obtained in 38-45 % yield. Another commonly used oxidising azo reagent DIAD was also employed for this reaction. Unfortunately, no improvement in yields was observed.

It was anticipated that the ring strain of 4-membered β-lactone results in low reaction efficiency. Indeed, storage of the β-lactone results in decomposition.

Therefore, the β-lactone product **64** after purification was used immediately in the next step. The identity of the products was confirmed by mass spectrometry, NMR analysis and melting point. The observed data were in agreement with the values reported in the literature.[150]

3.4.2.2 Ring opening of the β-lactone

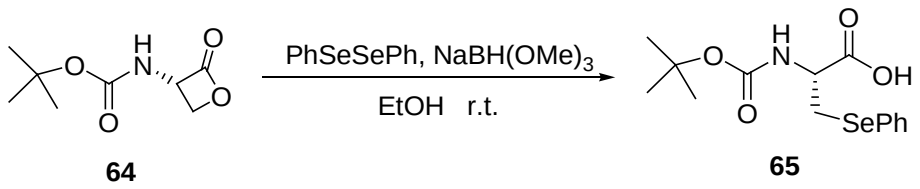

In the second step, the β-lactone **64** was reacted with phenyl selenide anion to form the phenylselenocysteine derivatives **65**. In general, the benzeneselenolate anion is generated *in situ via* reduction of diphenyl diselenide with two equivalents of sodium trimethoxyborohydride.[279] In order to avoid the reduction of the reactive lactone, reduction of diphenyl diselenide is conducted before a solution of the lactone is added. The reaction mechanism is illustrated in Figure 3-23. The reactivity of the β-lactone ring comes from the ring strain and the masked aldol functionality. Hence, substitution of β-lactone ring can proceed *via* either acyl C=O bond or alkyl C-O bond fission. Regioselective ring opening depends on the choice of nucleophile. In general, small or highly polarised hard nucleophiles favour a charge-directed interaction, resulting in acyl C=O cleavage. Soft nucleophiles, on the other hand, favour an orbital interaction over charge, resulting in alkyl C-O cleavage.[281] As a soft nucleophile, phenyl selenide anion mediated a nucleophilic substitution (S_N2) of the carboxylate residue to from the thermodynamically stable product.

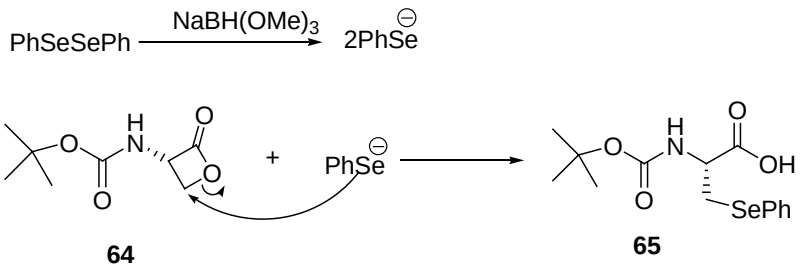

Figure 3-23 Mechanism of β-lactone ring opening by phenyl selenide anion.

Hence, sodium trimethoxyborohydride was added to a solution of diphenyl diselenide in dry ethanol under a nitrogen atmosphere. The yellow solution was stirred for 30 min. β-Lactone **64** in dry ethanol was then added to this solution and the reaction mixture was stirred at room temperature for 2 h. After an aqueous work-up, the product was obtained in quantitative yield. ^{1}H NMR spectrum of the product showed that only the desired product **65** was formed. MS analysis revealing the distinctive selenium isotope patterns centred at *m/z* 368.0377 (^{80}Se), which was assigned as the $[M+Na]^+$ species. The optical rotation of **65** was determined, and the obtained value ($[\alpha]_D^{23}$ = -34 (*c* = 1.0, MeOH)) is comparable to that reported in the literature ($[\alpha]_D^{25}$ = -36.8 (*c* = 1.0, MeOH)).[150]

3.4.2.3 **Deprotection of *N*-*tert*-Butyl carbamates group**

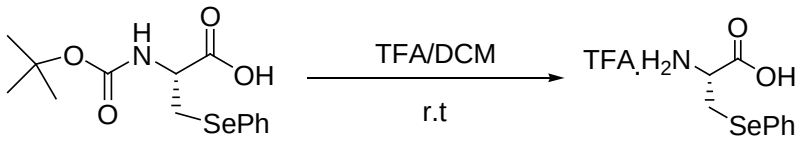

65 **66**

In order to install the *N*-Fmoc protecting group on phenylselenocysteine which can be used for the Fmoc solid phase peptide synthesis, the *N*-Boc protecting group must be removed. Several strategies for the selective removal of *N*-Boc protecting group in the presence of other function groups have been studied extensively in the past few years. In general, cleavage of *N*-Boc protecting group is achieved by using acidic conditions, such as HCl in EtOAc or dioxane,[282] TFA in DCM, H_2SO_4 in *t*-BuOAc and *p*-TsOH in *t*-BuOAc.[283] In some highly activated amines, such as aromatic heterocycles, cleavage of *N*-Boc protecting group can also be achieved under basic conditions.[284] Amongst these *N*-Boc deprotecting methods, acidolysis by TFA in DCM or HCl in dioxane are the most commonly used.[284] As shown in Figure 3-24, the key step of acidolysis of Boc group is the cleavage of *tert*-butyl carbamate under acidic conditions and the generation of *tert*-butyl cation. In some cases, a scavenger is required to remove the *tert*-butyl cation, preventing butylation of the target molecule.

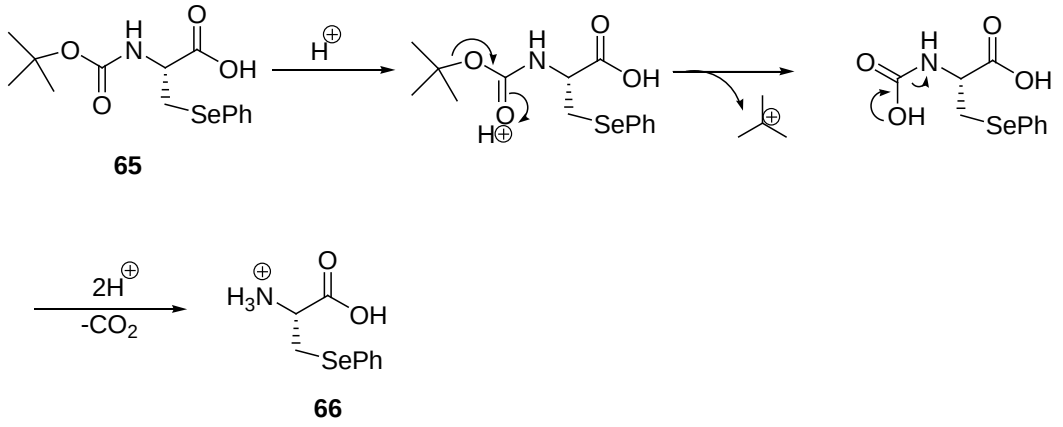

Figure 3-24 Mechanism of *N*-Boc deprotection *via* acidolysis.

Hence, the *N*-Boc-phenylselenocysteine **65** was treated with a solution of 50 % *v/v* TFA in DCM for 1 h. A successful conversion of **65** to **66** was confirmed by ^{1}H NMR analysis, with a loss of a singlet at δ = 1.43 ppm being observed which corresponded to the *t*-butyl of *N*-Boc. Further confirmation was provided by ES-MS revealing a peak at *m/z* 246.0019, which was assigned as the $[M+H]^+$ species.

3.4.2.4 **Fmoc-protection of phenylselenocysteine**

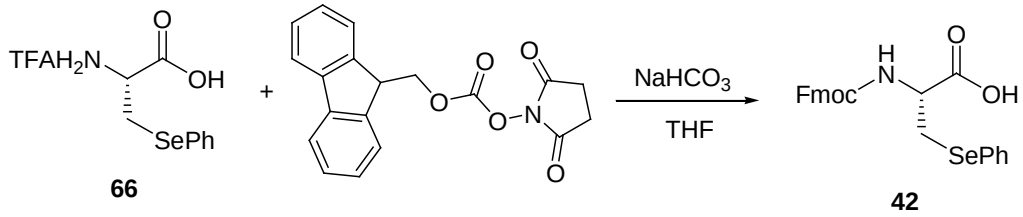

In the final step, phenylselenocysteine **66** was protected with Fmoc by reacting with a stoichiometric amount of Fmoc-OSu under basic conditions to afford *N*-Fmoc phenylselenocysteine **42** in a yield of 85-95 %. The obtained product was identified by MS and NMR analysis.[150] In addition, the purity of the final product was established using analytical RP-HPLC. The major peak (t_R = 10.91 min) observed in analytical RP-HPLC showed a purity greater than 98 % (Figure 3-25).

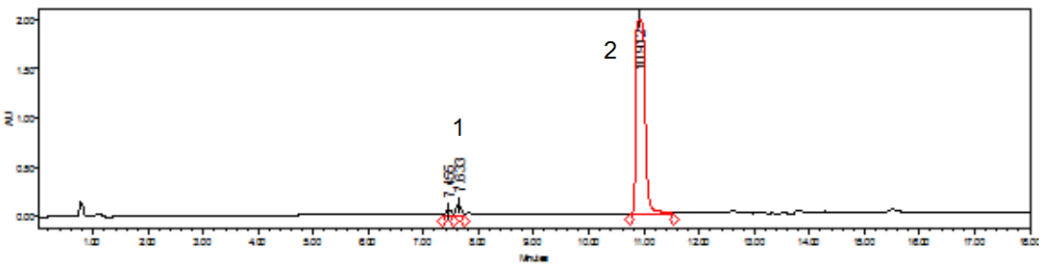

	Retention time	Area	% Area	Height
1	7.633	414945	1.75	53961
2	10.912	23342684	98.25	2006986

Figure 3-25 RP-HPLC analysis of *N*-Fmoc phenylselenocysteine (42). Analysed using 10-60 % B over 12 min at 3mL/ min method on an Onyx Monolithic C_{18} column (100 x 4.6 mm). Eluent detection was monitored by UV absorbance at 216 nm.

3.5 **Conclusion**

The synthetic route to the *N*-Boc-(*R*)-Ala-Thz-OH dipeptide building block (**44)** was achieved using literature procedures. This four-step reaction enabled a quick and efficient process to optically pure product in overall yields of 26–30 %. The spectroscopic data of the thiazole dipeptide was identical to those reported in the literature.[150] In addition, the optical purity of the dipeptide was confirmed by both optical rotation and the Mosher's method.

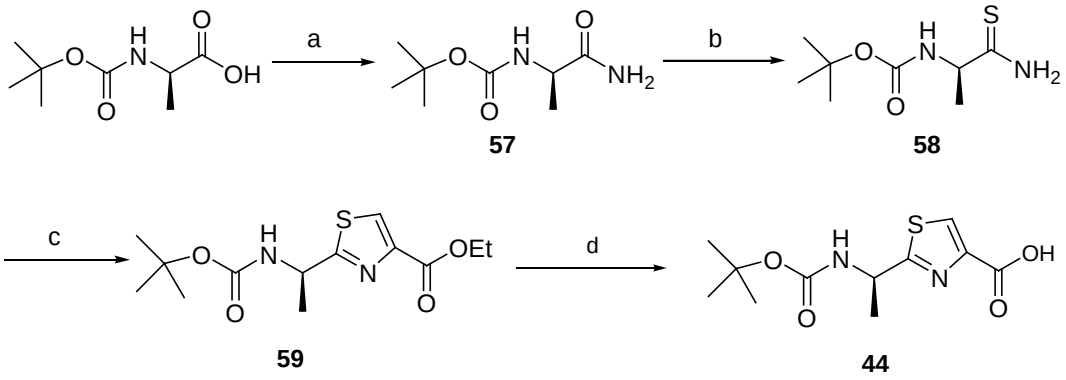

Figure 3-26 Synthesis of *N*-Boc-(*R*)-Ala-Thz-OH (44); Reagents and conditions: (a) DCC, HOBt, NH_3, CH_2Cl_2, 0 °C; (b) Lawesson's reagent, THF, 0°C; (c) i. $BrCH_2COCO_2Et$, $KHCO_3$, DME, -15 °C; ii.TFAA, 2, 6-lutidine, DME, -15 °C; (d) LiOH, THF/ MeOH/ H_2O, room temp.

As summarised in Figure 3-26, the key step in constructing the thiazole dipeptide **44** was using a modified Hantzsh-thiazole formation. This involved amination of the *N*-Boc protected (*R*)-Ala-OH to the corresponding amino amide **57** and thionation with Lawesson's reagent. The resulting thioamide **58** was then cyclised

using ethyl bromopyruvate to afford thiazoline intermediate, followed by treatment of TFAA and 2,6-lutidine to give the desired thiazole dipeptide **44**.

In addition, synthesis of *N*-Boc-(*R*)-Ala-oxazole dipeptide analogues also attempted by using reported methods. The key synthetic in constructing the oxazole dipeptide **146** was using Burgess reagent followed by radical oxidation. The synthesis involved coupling of *N*-Boc-(*R*)-Ala-OH with serine ethyl ester. The resulting dipeptide was then reacted with Burgess reagent under microwave irradiation to afford the oxazoline intermediate. Finally, treatment of *tert*-butyl perbenzoate and CuBr gave the desired oxazole dipeptide analogue in overall yields of 35–38 %. However, extensive epimerisation of the α-stereogenic centre had occurred during the chemical transformation of oxazoline to oxazole. These results indicated that both the thiazoline and oxazoline intermediates are liable to racemisation. Therefore, in order to provide the optically pure *N*-Boc-(*R*)-Ala-oxazole dipeptide analogue, a reinvestigation of the literature methods is required.

For the preparation of α,β-dehydroalanine, phenylselenocysteine was chosen as a reliable precursor of the α,β-dehydroalanine building block. As summerised in Figure 3-27, the four-step synthesis for the *N*-Fmoc-protected phenylselenocysteine **42** was achieved using literature procedures. The formation of the phenylselenocysteine was achieved by two chemical transformations. The first step involves intramolecular Misunobu reaction to convert *N*-Boc-serine into a β-lactone derivative **64**. The use of DEAD or DIAD as oxidising azo reagents did not influence the product yield. The second step is diphenyl diselenide-mediated ring opening to afford *N*-Boc-phenylselenocysteine **65**.

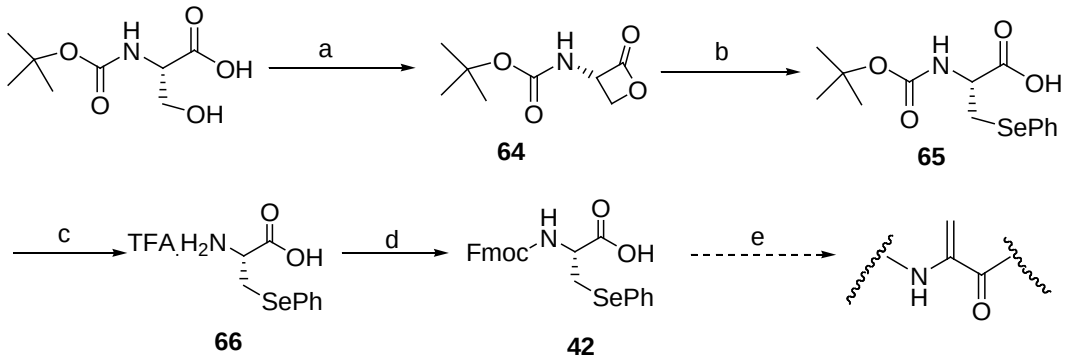

Figure 3-27 Synthesis of dehydroalanine precursor, Fmoc-phenylselenocysteine (42). Reagents and conditions: (a) DEAD, PPh_3, THF, -78 °C to room temp.; (b) PhSeSePh, $NaBH(OMe)_3$, EtOH, room temp.; (c) TFA/DCM, room temp.; (d) Fmoc-OSu, $NaHCO_3$, THF/H_2O, room temp. (e)) i. $NaIO_4$, CH_3CN/H_2O; ii. Na_2CO_3, CH_3CN/H_2O.

N-Boc-deprotection with 50 % *v/v* of TFA/DCM followed by *N*-Fmoc protection with Fmoc-OSu afforded the desired *N*-Fmoc-phenylselenocysteine (**42**) which is suitable for the Fmoc solid phase peptide synthesis. The overall yield over this four-step synthesis ranged from 35 to 40 % which was comparable to the yield reported in the literature.[150] In comparison to the *S*-aryl protected cysteine derivatives, the phenylselenocysteine methodology provided higher efficiency and chemoselectivity. Unmasking of the dehydroalanine by oxidative elimination in the ultimate step of the synthesis of argyrin is discussed in detail in Section 4.5.

Chapter 4

Fmoc solid-phase peptide synthesis and biological evaluation of argyrin A and analogues

In the previous three chapters, three unusual amino acid building blocks of argyrin A, namely Fmoc-methoxy-(*S*)-tryptophan (**43h**), Boc-(*R*)-Ala-Thz-OH (**44**) and Fmoc-phenylselenocysteine (**42**) have been prepared. As outlined in Chapter 1.5, the ultimate aim of this project is the synthesis of cyclic octapeptide argyrin A and analogues thereof. All previous studies into the total synthesis of argyrin analogues used traditional solution methods.[150-152] In order to enhance the synthesis efficiency and to avoid laborious purification procedures after each peptide coupling step, Fmoc solid-phase chemistry is exploited for the synthesis of argyrin A and analogues thereof.

In this chapter, the three existing solution-phase synthesis of argyrin A are summarised first, followed by brief introduction of Fmoc-SPPS. Next, attention is focused on establishing solid phase peptide synthesis of the title compound and analogues thereof. Thus, attachment of the first amino acid residue to the solid support is discussed, followed by coupling of subsequent amino acids in the peptide chain. Next, cleavage of peptide from the solid supports will be described, followed by solution phase head-to-tail cyclisation of linear peptide. Finally, unmasking the dehydroalanine precursor by oxidative elimination methods afforded the final cyclic peptide argyrin A and analogues.

In addition, as mentioned in Section 1.4.4, two independent groups have shown that argyrin A displays cytotoxic activity as a result of proteasome inhibition. At the end of this chapter, in order to further ascertain the importance of an amino acid residue in argyrin with regards to the antiproliferative effect and to gain more insight into structure-activity relationship, all synthesised argyrin analogues were evaluated in cytotoxicity assays.

4.1 Existing solution-phase approaches for the synthesis of argyrin A

The construction of the amide skeleton of argyrin A and analogues thereof has been achieved by traditional solution–phase peptide bond formations. Ley *et.al* in 2002 first reported the total synthesis of argyrin B using this strategy which required the preparation of two tripeptides (**170**, **172**) and the dipeptide (**59**) fragment as shown in Figure 4-1.[150] The tripeptides were assembled in four steps by sequential condensation of the three *N*-protected amino acids, and the dipeptide **59** was prepared using the method describing in Section 3.1.2. With the three fragments in place, removal of *N*-Cbz form **170** and coupling with the free acid from **59** afforded pentapeptide **171**. Similarly, removal of *N*-Boc protection from **172** and coupling with the free acid from **171** afforded the fully assembled octapeptide **46.** Macrocyclisation was achieved by deprotection of **46** at two termini, followed by intramolecular coupling. Finally, phenylselenocysteine was unmasked to reveal a dehydroalanine residue to yield argyrin **48**.

This approach was later adopted by Nickeleit's group in 2010[151] and Jiang's group in 2011[152] for the total synthesis of 10 argyrin analogues. However, the synthesis of more analogues was hampered by the limitation of this approach, including the time-consuming nature of the lengthy process and extensive purification necessary after each peptide coupling step. In this thesis, the Fmoc solid-phase peptide synthesis approach is introduced for the total synthesis of argyrin A and analogues thereof.

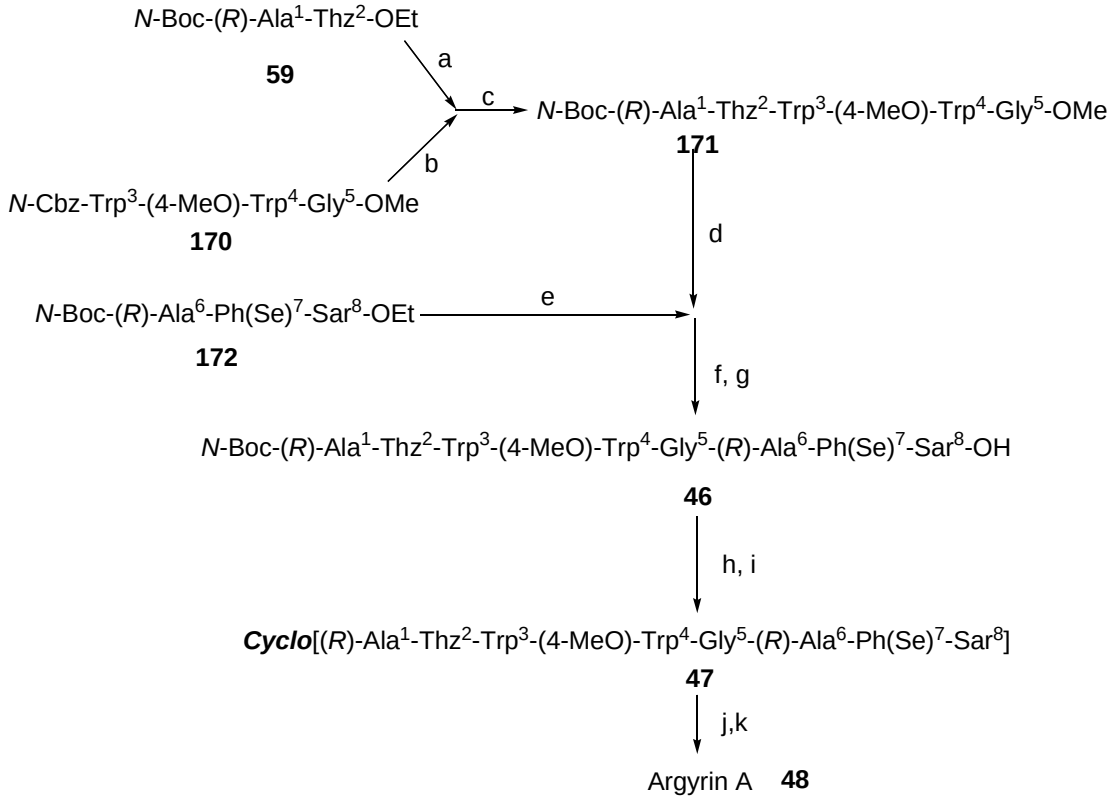

Figure 4-1 Solution-phase synthesis of argyrin by Ley *et al.*.[150] Reagents and conditions: (a) LiOH, THF/MeOH/H_2O, room temp.; (b) H_2, Pd/C, MeOH, room temp.; (c) EDC, HOBt, DCM, room temp.; (d) LiOH, THF/MeOH/H_2O, room temp.; (e) TFA/DCM, room temp.; (f) EDC, HOBt, DIPEA, DCM; (g) LiOH, THF/MeOH/H_2O, room temp.; (h) Anisole/TFA, room temp.; (i) TBTU, HOBt, DIPEA, DCM, room temp.; (j) $NaIO_3$, dioxane/H_2O, room temp.; (k) $NaHCO_3$, CH_3CN/H_2O, room temp.

4.2 **Principles of solid-phase peptide synthesis**

Solid phase peptide synthesis (SPPS), first reported by Bruce Merrifield,[285] is a technique for assembling a peptide chain on a polymeric support. The primary advantage of SPPS is high yield for each step of coupling compared with solution phase coupling, especially in longer sequences. In addition, excess reagents and by-products could be easily removed by wash and filtration, and intermediates are not purified.

Fmoc/t-Bu solid-phase peptide synthesis (SPPS) was first reported by Sheppard *et al.* in 1978.[286] Compared with original Merrifield SPPS approach, Sheppard's orthogonal approach allowed reactions to be carried out under milder conditions. This approach utilises the combinations of the base-labile Fmoc group for α-amino group protection and the acid-labile group for side-chain protection of amino acids. Scheme 4-1 illustrates the principles of Fmoc SPPS. The synthesis proceeds in a *C*-terminal to *N*-terminal fashion, which is opposite to ribosome protein synthesis.

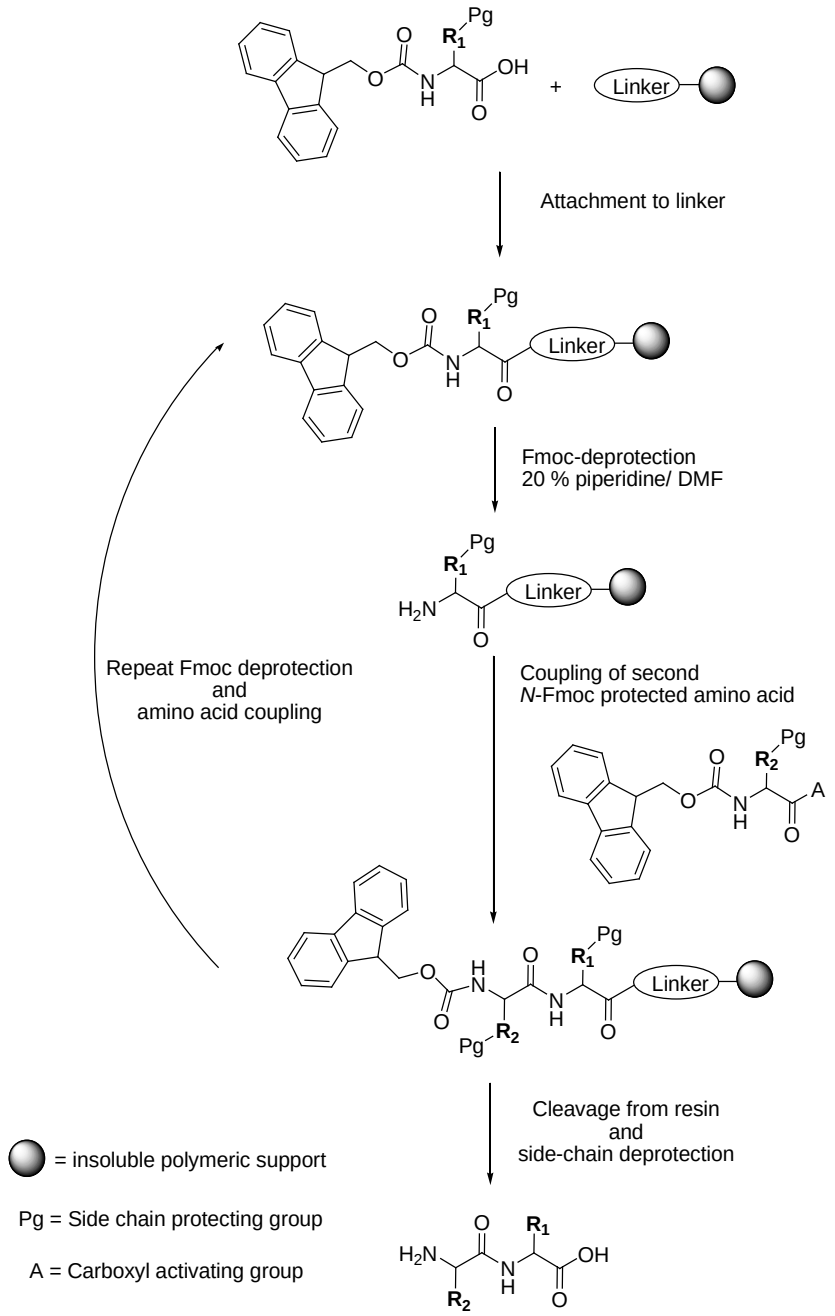

Scheme 4-1 The general principles of solid–phase peptide synthesis.

The initial step of Fmoc SPPS is the attachment of *C*-terminus amino acid residue to a solid support *via* a linker. The choice of the suitable linker is discussed in detail in Section 4.2.1. Typically, the *C*-terminal amino acid is attached to a linker by forming an ester or an amide bond which can be easily cleaved by acidolysis. The Fmoc protecting group is then removed with 20 % *v/v* piperidine in DMF prior to coupling with the next Fmoc-protected amino acid.[287] Amide bond formation is achieved by activation of the Fmoc-protected amino acid. The three major carboxyl activating reagents are discussed in Section 4.2.2. After coupling, excess reagents are removed by simple washing procedures. This deprotection-coupling cycle is repeated until the target peptide sequence is assembled. In the final step, the desired peptide is cleaved from solid support with the simultaneous removal of the side-chain protections.

4.2.1 **Linker resins used for the solid phase peptide synthesis**

Linker resins, generally refers to the insoluble solid support with a linker which enable the attachment of the *C*-terminal of a peptide chain. The peptide coupling reaction can be carried out on the surface or inside of the particles. The ideal properties of the resin for efficient SPPS include (1) chemical inertness and ability to swell in solvents used in peptide synthesis, such as DMF and DCM, and (2) readily functionalised to allow for the attachment of a linker.[288] To date, polystyrene (PS) is the most commonly used resin in SPPS.[288] Some of the newer resins, such as polyethylene glycol (PEG)[289] and PEG-PS[290], have been developed for the synthesis of difficult sequences by disruption of aggregation of the growing peptide chain.

Linkers are chemical functional groups to provide a reversible linkage between the peptide chain and the solid support, and to protect the *C*-terminal carboxyl group. Ideally, they are designed to be stable throughout the SPPS cycle and to be selectively cleaved at the end of the synthesis without damage to the product. A serious of linkers have been developed to yield peptide acids, peptides amides or sulphonamides upon cleavage. Figure 4-2 lists three linker resins which are considered for the Fmoc SPPS of argyrin A and analogues thereof.

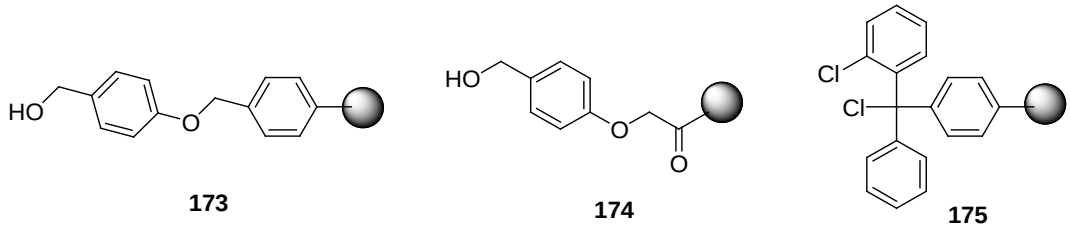

173 **174** **175**

Figure 4-2 Linker resins considered for the Fmoc SPPS of argyrin

In order to release peptide acid for the macrocyclisation of linear argyrin precursor, Wang resin (**173**), 4-hydroxymethylphenoxyacetyl (**174**) and 2-chlorotrityl chloride resin (**175**) were considered.[291] Among these three linkers, **173** and **174** using ester linkage to the peptide require 90-95 % TFA to release of the assembled peptide. In contrast, a hyperacid-labile linker **175**, permits the release of peptide acid under very mild conditions, typically 1-5 % TFA for 5 min, due to the high stability of the trityl cation.[292] Since the peptide-ester bond formed with 2-chlorotrityl resin has sufficient stability during the conventional coupling conditions, it was chosen as a suitable linker for the synthesis of linear argyrin precursor.

4.2.2 Carboxyl activating reagents

The carboxyl activation is usually achieved through increasing electrophilicity of the carbonyl group by replacement of the hydroxyl with electron withdrawing group. As mentioned in Section 3.1.2.1, DCC- and HOBt-mediated carboxyl activation is commonly used in solution amide bond formation. However, the insolubility of the dicyclohexylurea by-product causes problems during SPPS procedures. Therefore, the onium coupling reagents, including phosphonium and aminium (or guanidinium) salts are gradually replacing traditional carbodiimide reagents in SPPS.[293]

The choice of the carboxyl activating reagent is one of the factors that can contribute to the success of SPPS. The ideal carboxyl activating reagent requires the following properties: (1) good solubility in numerous organic solvents and can be used at high concentration, (2) suppress side reactions, such as racemisation caused by direct enolisation or *via* oxazolone formation (Figure 4-3 (a) and (b)) and terminates the peptide chain, caused by reacting with the *N*-terminal of the peptide

(Figure 4-3(c)),[291] (3) not toxic, corrosive and does not result in formation of toxic by-products, and (4) commercially available and chemically stable.

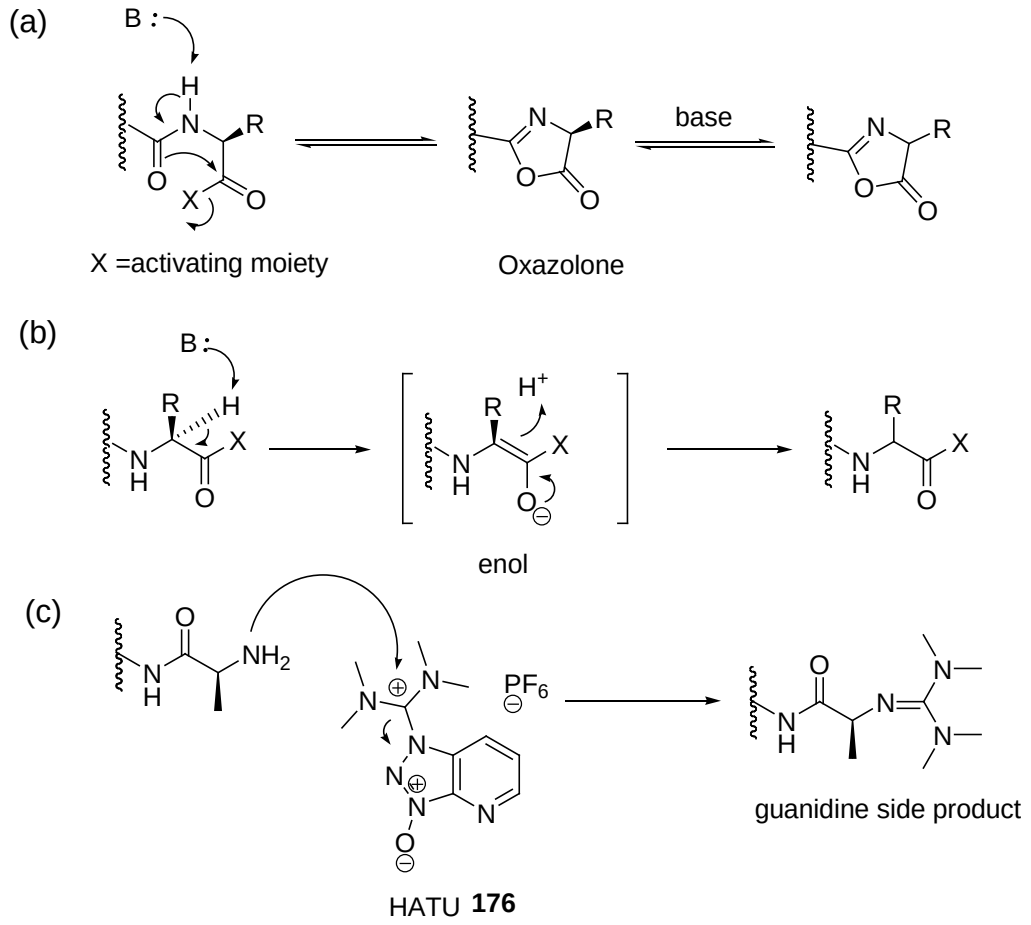

Figure 4-3 (a) Racemisation *via* oxazolone formation. (b) Racemisation *via* enolisation. (c) A guanidine side product is produced when the aminium coupling reagent is directly reacted to the *N*-terminal of the peptide.

Phosphonium coupling reagent was the first onium salt used in SPPS in 1975 by Castro *et al.*.[294] Based on HOAt and HOBt, he developed a new phosphonuam-based coupling reagent, namely benzotriazol-1-yloxy-tris(dimethylamino)-phosphonium hexafluorophosphate (BOP) **177**. More recently, benzotriazol-1-yl-oxytripyrrolidinophosphonium hexafluorophosphate (PyBOP) **178** and (ethyl cyano(hydroxyimino)acetato)-tri-(1-pyrrolidinyl)-phosphonium hexafluoro-phosphate (PyOxim) **179** were introduced, where the dimethylamine subunit was replaced by pyrrolidine. [295] This change could avoid the generation of highly toxic hexamethylphosphoramide (HMPA) by-product. The mechanism of carboxyl activation by the phosphonium reagent is shown in Figure 4-4 (b).

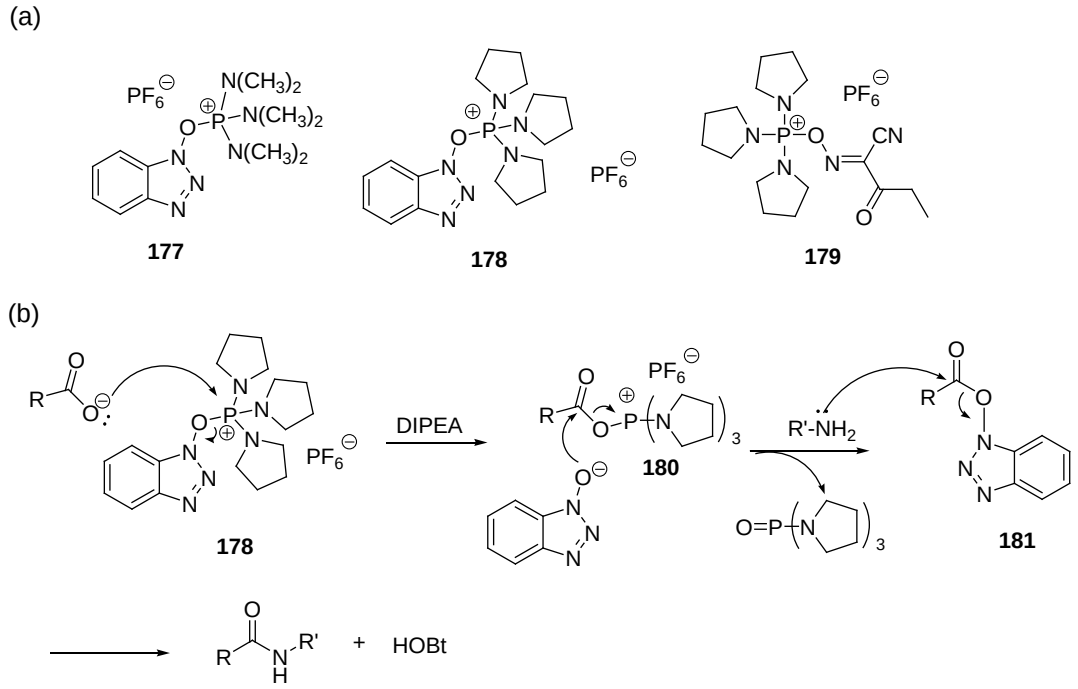

Figure 4-4 (a) Three phosphonium reagents for SPPS. (b) Mechanism of carboxyl activation by the phosphonium reagent PyBOP (178).

The carboxylate anion attacks the phosphonium cation generating a highly reactive acyloxyphosphonium intermediate **180**, which is nucleophilically attacked by the liberated hydroxybenzotriazole anion to afford the activated benzotriazolyl ester **181**. The peptide bond is formed by a further nucleophilic acyl substitution with an amine, in a same manner to the DCC/HOBt activation described in Section 3.1.2.1. The major advantage of phosphonium reagent to the aminum reagent is that the excess unreacted reagent does not guanidate with free amine (Figure 4-3 (c)), resulting in termination of peptide chain elongation. Other advantages, such as easy handling, storage, and high efficient in the coupling of sterically hindered amino acids have been reported in the literature. [296]

Aminium coupling reagents, also known as uronium reagents, are also derived from HOAt and HOBt. Gross *et al.* introduced HBTU (**182**) in 1978 as the first aminium reagent.[297] Since then, a variety of analogues such as HATU (**176**), TBTU (**183**) having higher coupling efficiency and lower racemisation rate were developed. It was established that the choice of counterion have no effect on the coupling efficiency. However, it has been shown that **183** having tetrafluorobortate is more soluble than **176**, allowing preparation of more concentrated solution. [296]

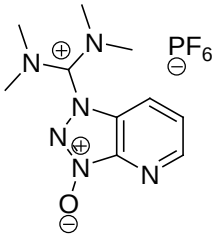

176

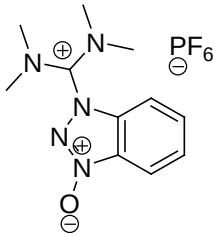

182

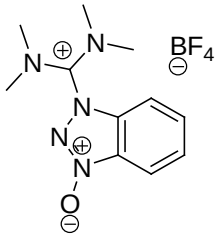

183

Thus, three commonly used carboxyl activation reagents have been chosen in this project. HATU (**176**), a well-known aminium based reagent, has been shown to have high efficiency in the coupling of sterically hindered amino acids. In addition, it is also effective in avoiding epimerisation under a various coupling conditions.[298] Aminium salts which would yield guanidinium by-products with peptidyl amines and hence results in termination of peptide elongation.[294]

PyBOP (**178**), a phosphonium based reagent, is easy to handle and store. It also shows high efficiency in the coupling of sterically hindered amino acids. PyOxim (**179**), a new PyBOP based reagent, shows superior solubility in solvents employed in SPPS, and achieves higher optical purity of peptide products and efficiency of reactions in the production of both linear and cyclic peptide sequences.[295]

4.3 **Synthetic strategies for linear argyrin A**

As shown in Scheme 4-2, Fmoc SPPS was used for the synthesis of the nine linear argyrin precursors. In the retrosynthetic analysis of argyrin A, disconnection site of the macrostructure is crucial as it could ultimately determine the success of the cyclisation. After carefully analysis of the peptide sequences, the sarcosine was chosen as the *C*-terminal end.[299] There are three major advantages in the choice of sarcosine as the *C*-terminal end. Firstly, epimerisation of *C*-terminus during backbone macrocyclisation could be avoided as sarcosine is an achiral amino acid. Secondly, sarcosine is a non-sterically hindered residue which gives synthetic advantage in macrocyclisation. Thirdly, acid-labile *N*-Boc of the last residue could be simultaneously removed while the fully assembled peptide was released from the solid support.

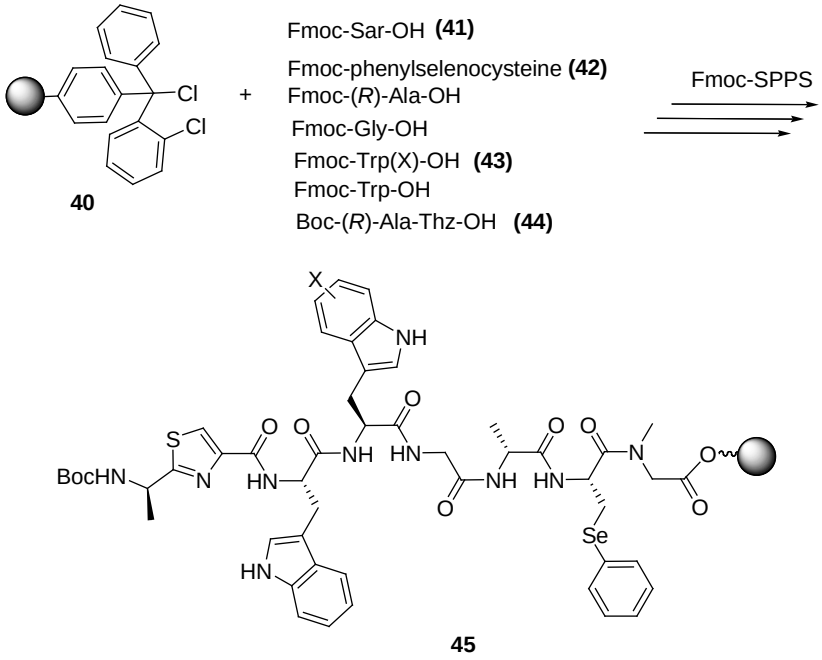

Scheme 4-2 Fmoc SPPS of linear argyrin precursors (45).

4.3.1 Condensation of Fmoc-sarcosine with 2-chlorotrityl chloride polystyrene

Assembly of the linear octapeptide precursors started with attachment to the solid support through the carboxylic group of a sarcosine residue. In order to release peptide acid for the cyclisation, 2-chlorotrityl chloride polystyrene linker resin (**40**) was chosen. The coupling of Fmoc-sarcosine (**41**) to 2-chlorotrityl chloride polystyrene (**40**) is illustrated in Figure 4-5.

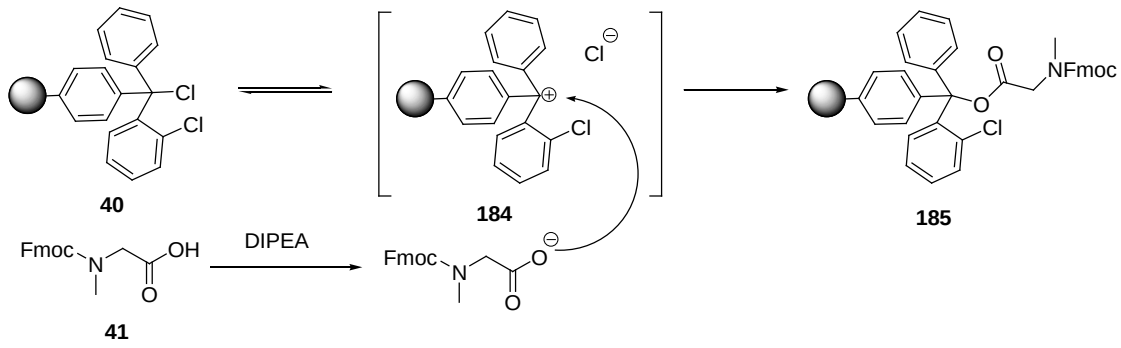

Figure 4-5 Esterfication of 2-chlorotrityl chloride resin (40).

The coupling proceeds *via* an S_N1 mechanism.[300] In DCM, 2-chlorotrityl chloride undergoes heterolysis to give an equilibrium mixture of the chloride anion and the

2-chlorotrityl cation **184**. The stabilised tertiary cabocation **184** undergoes nucleophilic attack by carboxylate of sarcosine to form an ester bond. Thus, 2-chlorotrityl chloride resin was swollen in DCM for 1 h, followed by condensation with a stoichiometric amount of Fmoc-Sar-OH in the presence of DIPEA (2 eq.) in DCM. The reaction mixture was gently stirred at room temperature for 2 h, after which the reaction was quenched using a small amount of methanol. The resin **185** was stored and re-swollen in a suitable solvent prior to use. The efficiency of loading was 70%, based on theoretical loading as described in Section 6.5.

4.3.2 **Carboxyl activation and peptide assembly**

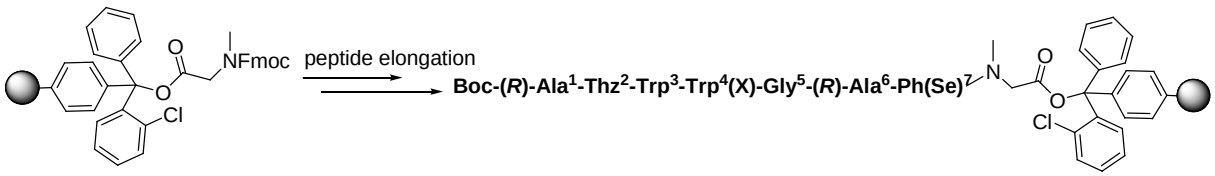

185 **45**

The second stage of Fmoc-SPPS involves repeated Fmoc deprotection and amino acid coupling. Firstly, removal of Fmoc group is achieved using 20 % *v/v* piperidine in DMF. Secondly, the carboxyl group of *N*-Fmoc protected amino acid is activated to promote nucleophilic attack by the amino group of the peptidyl resin to form peptide bond.

Thus, the resin **185** was pre-swollen in DMF/DCM for 16 h. The Fmoc group was then removed using 20 % piperidine in DMF. The resin was washed with DMF (10 min 2.6 mL min^{-1}) and the peptide sequence was assembled manually. For the commercially available *N*-Fmoc amino acids, *i.e.* Fmoc-(*R*)-Ala-OH, Fmoc-Gly-OH and Fmoc-Trp-OH, each coupling reaction was carried out using the mixture of *N*-Fmoc amino acid (2 eq.), activating reagent PyOxim (2 eq.) and DIPEA (4 eq.). For the synthesised unusual amino acids, specifically, Fmoc-Ph(Se)-OH (**42**), Fmoc-Trp(X)-OH (**43**) and Boc-(*R*)-Ala-Thz-OH (**44**), each coupling reaction was carried out using the mixture of *N*-Fmoc amino acid (1.5 eq.), activating reagent PyOxim (1.5 eq.) and DIPEA (3 eq.). The coupling efficiencies were monitored by the effluent of Fmoc deprotections at 290 nm. All acylation reactions were repeated twice prior to the coupling the next *N*-Fmoc amino acid. After repeating six

deprotection-coupling cycles, the target linear peptides were assembled. The resulting linear peptides then will be cleaved from the linker-support.

4.3.3 **Cleavage of linear peptides and purification**

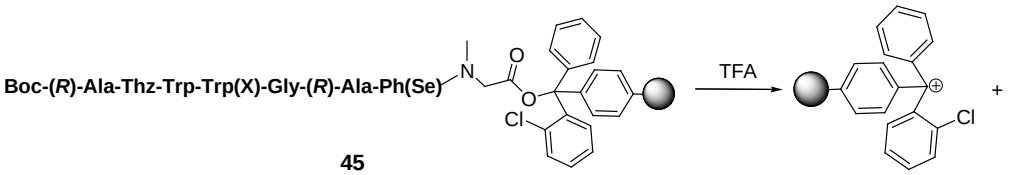

45

H-(*R*)-Ala-Thz-Trp-Trp(X)-Gly-(*R*)-Ala-Ph(Se)-Sar-OH **46a-g**

	a	**b**	**c**	**e**	**f**	**g**
X =	H	5-Br	5-Cl	7-Et	5-Me	5-MeO

Release of the linear peptide **46a-g** from the 2-chlorotrityl solid support can be accomplished by acidolysis using 1-5% trifluoroacetic acid. However, in order to simultaneously deprotect the *N*-terminus Boc protecting group, 50 % *v/v* TFA in DCM was used. During the acidolysis step, the generation of the *tert*-butyl carbocation could undergo undesired butylation of Trp residues. Therefore, scavengers were required to trap the reactive *tert*-butyl cation. The mixture of triisopropylsiliane (TIPS) and water are commonly used as scavengers in the cleavage cocktail.[291]

Thus, resin-bound linear peptides (**45**) were treated with TFA/DCM/TIPS/H_2O (49:49:1:1) for 1 h at room temperature. The crude linear peptides (**46**) were precipitated from ice-cold diethyl ether. The resulting materials were then suspended in water and lyophilised overnight to afford orange powders. All crude linear peptides were analysised by RP-HPLC and MS. For example, analysis of the crude peptide material **46e** by RP-HPLC showed one major peak of the desired linear peptide at t_R = 10.7 min (Figure 4-6 (a)). The elution profiles of all analogues are similar in terms of components and retention time. The identities of all analogues were confirmed by MS.

(a)

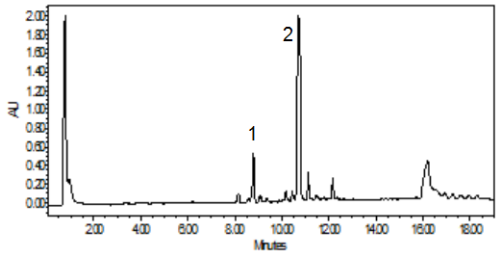

	Retention time	% Area	MS
1	8.86	14.5	841.3278
2	10.62	84.3	999.2575

(b)

H-(*R*)-Ala-Thz-Trp-Trp(X)-Gly-(*R*)-Ala-Dha-Sar-OH

186

Figure 4-6 (a) The crude HPLC analysis of the linear peptide 46e. (b) Major by-product at t_R = 9.00 min. Sample was analysised using the method; 1 – 35 % B over 10 min at 3 mL/min. The column used was an Onyx Monolithic analytical C_{18} column (100 x 4.6 mm).

In addition, the minor peak at t_R = 8.86 min was further analysed by MS. The observed molecular ion was 158 mass units less than the molecular ion of the desired product, which was assigned to the unmasked dehydroalanine-containing peptide **186** (Figure 4-6 (b)). Disappearances of the selenium isotopic patterns were also observed. It was postulated that during repeated Fmoc deprotection step in SPPS, the dissolved oxygen in piperidine/DMF mixture resulted in partial oxidative elimination of phenylselenocysteine.

Table 4-1 summarised the purity of crude peptides and yields. Fortunately, based on the observation, it seems dehydroalanine moiety is stable to 50 % TFA acidolysis and peptide coupling conditions. The crude linear peptides were used for the cyclisation step without further purification.

Table 4-1 Summary of the crude yield, purity and MS for the linear peptides 46a, 46b, 46c, 46e, 46f and 46g.

#	Sequence	Yield (%)	Purity [a] (%)	t_R (min) [b]	MS Calculated $[M+H]^+$	MS Measured
46a	H-(*R*)-Ala[1]-Thz[2]-Trp[3]-Trp[4]-Gly[5]-(*R*)-Ala[6]-Ph(Se)[7]-Sar[8]-OH	56	90	10.3	971.2777	971.2323
46b	H-(*R*)-Ala-Thz-Trp-(5-Br)-Trp-Gly-(*R*)-Ala-Ph(Se)-Sar-OH	60	69	10.5	1049.1882	1049.1888
46c	H-(*R*)-Ala-Thz-Trp-(5-Cl)-Trp-Gly-(*R*)-Ala-Ph(Se)-Sar-OH	56	86	12.1	1005.2388	1005.2287
46e	H-(*R*)-Ala-Thz-Trp-(7-Et)-Trp-Gly-(*R*)-Ala-Ph(Se)-Sar-OH	54	84	10.6	999.3090	999.2575
46f	H-(*R*)-Ala-Thz-Trp-(5-Me)-Trp-Gly-(*R*)-Ala-Ph(Se)-Sar-OH	59	79	11.5	985.2943	985.2867
46g	H-(*R*)-Ala-Thz-Trp-(5-MeO)-Trp-Gly-(*R*)-Ala-Ph(Se)-Sar-OH	64	78	10.4	1001.2883	1001.2643

[a.] Peptide purity determined from integration of RP-HPLC peak.
[b.] RP-HPLC was performed on Onyx Monolithic analytical C_{18} column (100 x 4.6 mm). Eluent was monitored by UV absorbance at 216 nm. Linear gradient was 1-35 % B over 10 min at 3mL /min.

Moreover, in order to confirm that the observed single peaks in the HPLC were optically pure, commercially available racemic *N*-Fmoc-(5-Br)-(*S/R*)-tryptophan was installed by SPPS to afford crude linear peptidic material as a mixture of two diastereoisomers. The resulting product was analysed by RP-HPLC and MS. Not surprisingly, as shown in Figure 4-7, the two major peaks at t_R = 10.2 min and 10.5 min in HPLC trace were well-resolved and afforded the same *m/z* 1049.18. This result provided the confidence that **46b** is exclusively a single component.

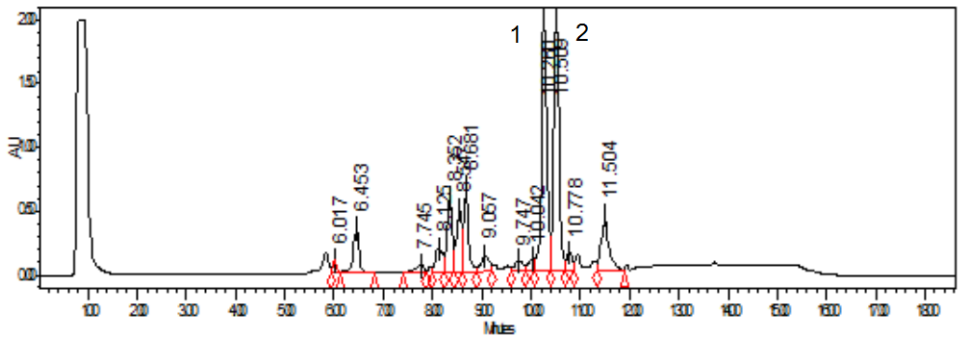

	Retention time	Area	% Area	MS
1	10.260	15530099	27.21	1049.1888
2	10.509	15346703	26.88	1049.1886

Figure 4-7 RP-HPLC analysis of diastereomeric linear peptides derived from the installation of (5-Br)-(*S/R*)-Trp-OH. Sample was analysed using the method; 1–35 % over 10 min at 3 mL /min. The column used was an Onyx Monolithic analytical C_{18} column (100 x 4.6 mm).

4.4 Macrocyclisation of argyrin A and analogues thereof

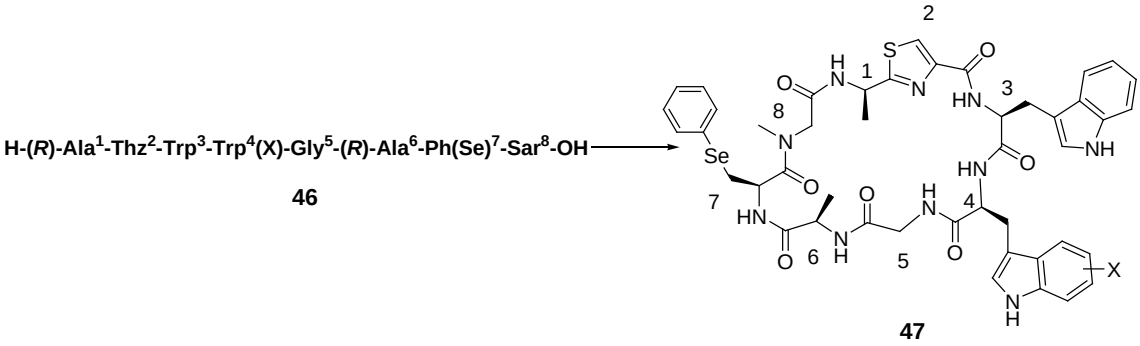

	a	b	c	e	f	g
X =	H	5-Br	5-Cl	7-Et	5-Me	5-MeO

One of the key steps in the synthesis of cyclic octapeptide argyrin A is the macrocyclisation. In general, there are two major macrocyclisation strategies: one is on-resin head-to-tail cyclisation, and the other is traditional solution-phase cyclisation under high dilution conditions. On-resin cyclisation requires linking the side chain of the trifunctional amino acid to the resin. Cyclisation thus can be performed while peptides remain anchored to the resin. The advantage of the on-resin cyclisation strategy is that intramolecular reaction is favoured which results in minimising the formation of cyclodimers and oligomers.[301] Although on-resin cyclisation strategy appears to be a good choice for the ring closure, the linear

argyrin A lacks trifunctional amino acids, such as aspartic acid, lysine or serine, which can be attached to the solid support. Therefore, a traditional solution-phase cyclisation was used.

To avoid cyclodimerisation or oligomerisation side reactions during the macrocyclisation, the reaction was performed in high dilution conditions (10^{-3}- 10^{-4} M). In addition, PyBOP (**178**) was chosen as the carboxyl-activating reagent to avoid the *N*-guanidylation of the amino terminus. The mechanism of PyBOP-mediated cyclisation is shown in Figure 4-8.

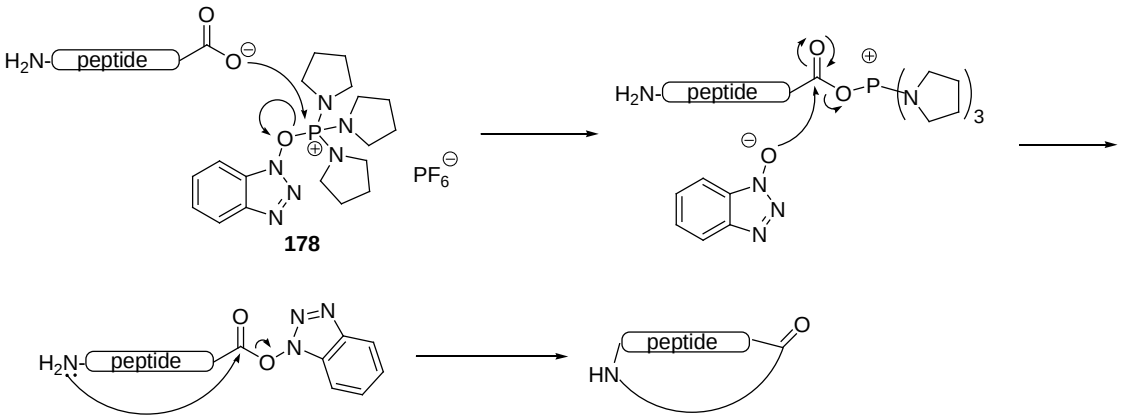

Figure 4-8 Mechanisum of PyBOP-mediated cyclisation.

Initially, cyclisation of **46** was performed in DCM at a concentration of 0.5 mM in the presence of PyBOP (2 eq.) and DIPEA (3 eq.). The reaction mixture was stirred at room temperature for 72 h, and the reaction was monitored by RP-HPLC. Subsequence MS analysis of the major peak observed by RP-HPLC confirmed the identity of the cyclised peptide. However, following work-up, the yield was rather unsatisfactory (< 10 %). The reaction condition was then further optimised. Optimum results were obtained with the mixture of PyBOP (3 eq.), HOBt (3 eq.) and DIPEA (9 eq.) at 0.5 mM peptide concentration. Under these conditions, HPLC and MS analysis revealed that reactions were almost complete after 48 h with no evidence of oligomeric side products. Figure 4-9 shows the crude analytical HPLC of cyclic peptide **47e**. The two peaks at t_R = 0.8 min and 1.4 min were DMSO and coupling reagents, respectively. The major peak at t_R = 9.9 min was the desired cyclic peptide, whereas the minor peak at t_R = 7.9 min was found to be the cyclisation of the unmasked dehydroalanine-containing peptide **186**.

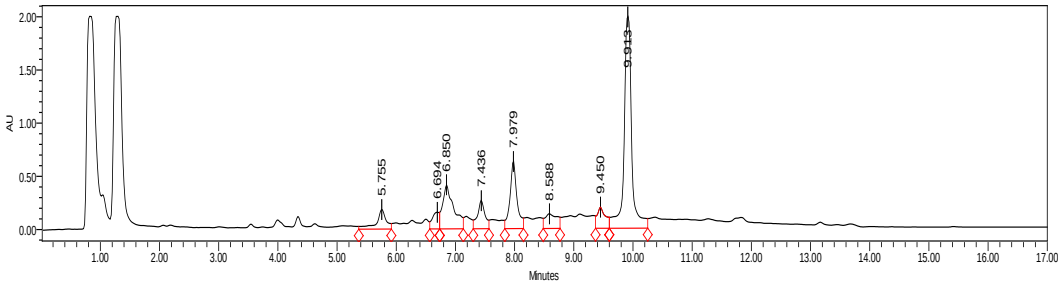

	Retention time	Area	% Area	MS
1	7.979	9323561	15.11	823.2346
2	9.913	35425646	56.86	981.2607

Figure 4-9 The crude HPLC trace of cyclic peptide 47e. Sample was analysed using the method; 10 –60 % B over 12 min at 3 mL /min. The column used was an Onyx Monolithic analytical C_{18} column (100 x 4.6 mm).

The major peaks of six analogues were purified by preparative RP-HPLC to afford cyclic peptides **47a**, **47b**, **47c**, **47e**, **47f** and **47g** in 11-28 % yield (Table 4-2). The impure linear peptide **46** is most likely attributable to the low yield of cyclisation step. Nevertheless, the purity and yields of the cyclic peptides after preparative HPLC were suitable for the final step of synthesis.

Table 4-2 Summary of the purified yield, RP-HPLC retention time and MS for the cyclic peptides 47a, 47b, 47c, 47e, 47f and 47g.

#	Sequence	Yield [a] (%)	t_R (min) [b]	ES-MS $[M+H]^+$ calcd	ES-MS $[M+H]^+$ measured
47a	***Cyclo*** [(*R*)-Ala^1-Thz^2-Trp^3-Trp^4-Gly^5-(*R*)-Ala^6-Ph(Se)^7-Sar^8]	30	8.5	953.2672	953.2571
47b	***Cyclo*** [(*R*)-Ala-Thz-Trp-(5-Br)-Trp-Gly-(*R*)-Ala-Ph(Se)-Sar]	17	9.9	1031.1777	1033.1757
47c	***Cyclo*** [(*R*)-Ala-Thz-Trp-(5-Cl)-Trp-Gly-(*R*)-Ala-Ph(Se)-Sar]	20	9.5	987.2282	987.2104
47e	***Cyclo*** [(*R*)-Ala-Thz-Trp-(7-Et)-Trp-Gly-(*R*)-Ala-Ph(Se)-Sar]	28	9.9	981.2985	981.2607
47f	***Cyclo*** [(*R*)-Ala-Thz-Trp-(5-Me)-Trp-Gly-(*R*)-Ala-Ph(Se)-Sar]	27	9.4	967.2828	967.2723
47g	***Cyclo*** [(*R*)-Ala-Thz-Trp-(5-MeO)-Trp-Gly-(*R*)-Ala-Ph(Se)-Sar]	11	8.5	983.2777	983.2693

[a] Yield refers to purified yields form preparative RP-HPLC.
[b] RP-HPLC was performed on Onyx Monolithic analytical C18 column (100 x 4.6 mm). Eluent was monitored by UV absorbance at 216 nm. Linear gradient was 10-60 % B over 12 min at 3 mL /min.

Analysis of the isolated products using MS revealed all *m/z* values corresponded to the $[M+H]^+$ species of cyclic peptides (Table 4-2). In addition, characterisation of **47a**, **47b**, **47c**, **47e**, **47f** and **47g** was confirmed by ^{1}H NMR and by 2D ^{1}H-^{1}H COSY NMR analysis. Figures 4-10 and 4-11 show the ^{1}H and COSY NMR of **47e**, respectively. Specifically, the presence of the characteristic NH signals at δ_H 7.44 (d, J = 3 Hz, 1H), 7.58 (d, J = 7 Hz, 1H), 8.11 (d, J = 9 Hz, 1H), 8.35 (s, 1H), 8.65 (d, J = 9 Hz, 1H) and 8.92 (t, J = 5 Hz, 1H) ppm indicated the six secondary amides. In addition, the observed correlation of these six amide signals with their adjacent α protons in the COSY spectrum confirmed the unambiguous cyclic skeleton. The remaining upfield proton resonances were assigned by detailed inspection of the COSY spectrum.

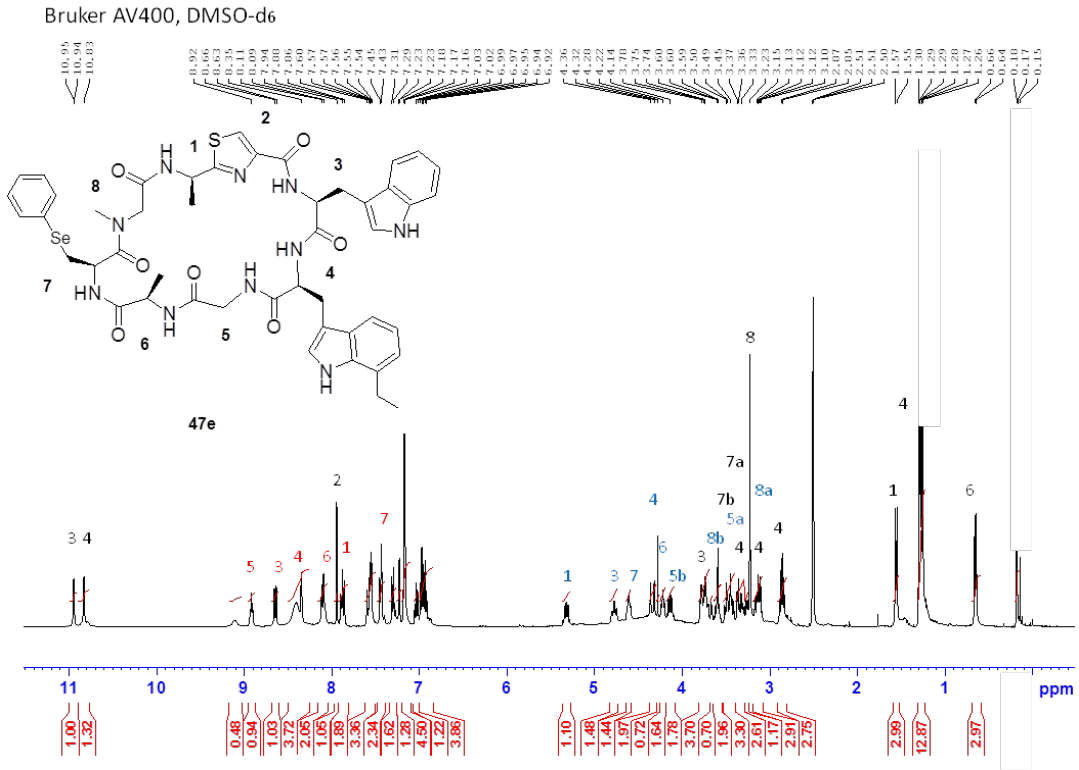

Figure 4-10 ^{1}H NMR spectrum of cyclic peptide 47e. Amide-NH are labelled red, α-protons are blue and others are black.

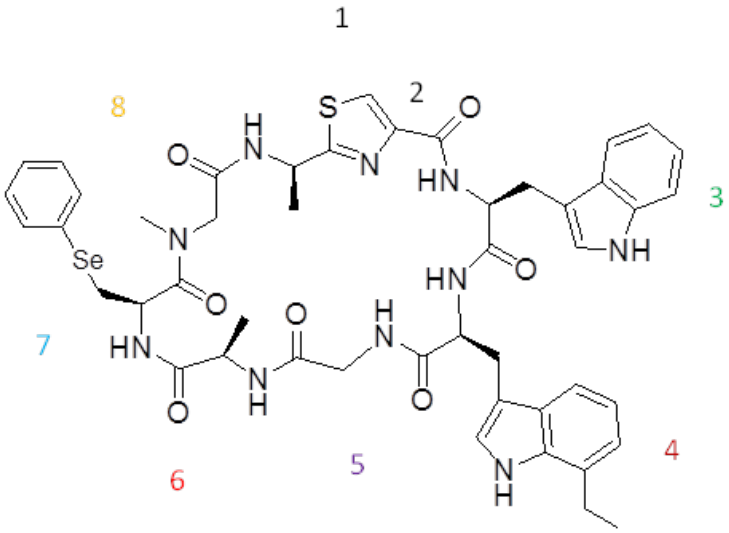

47e

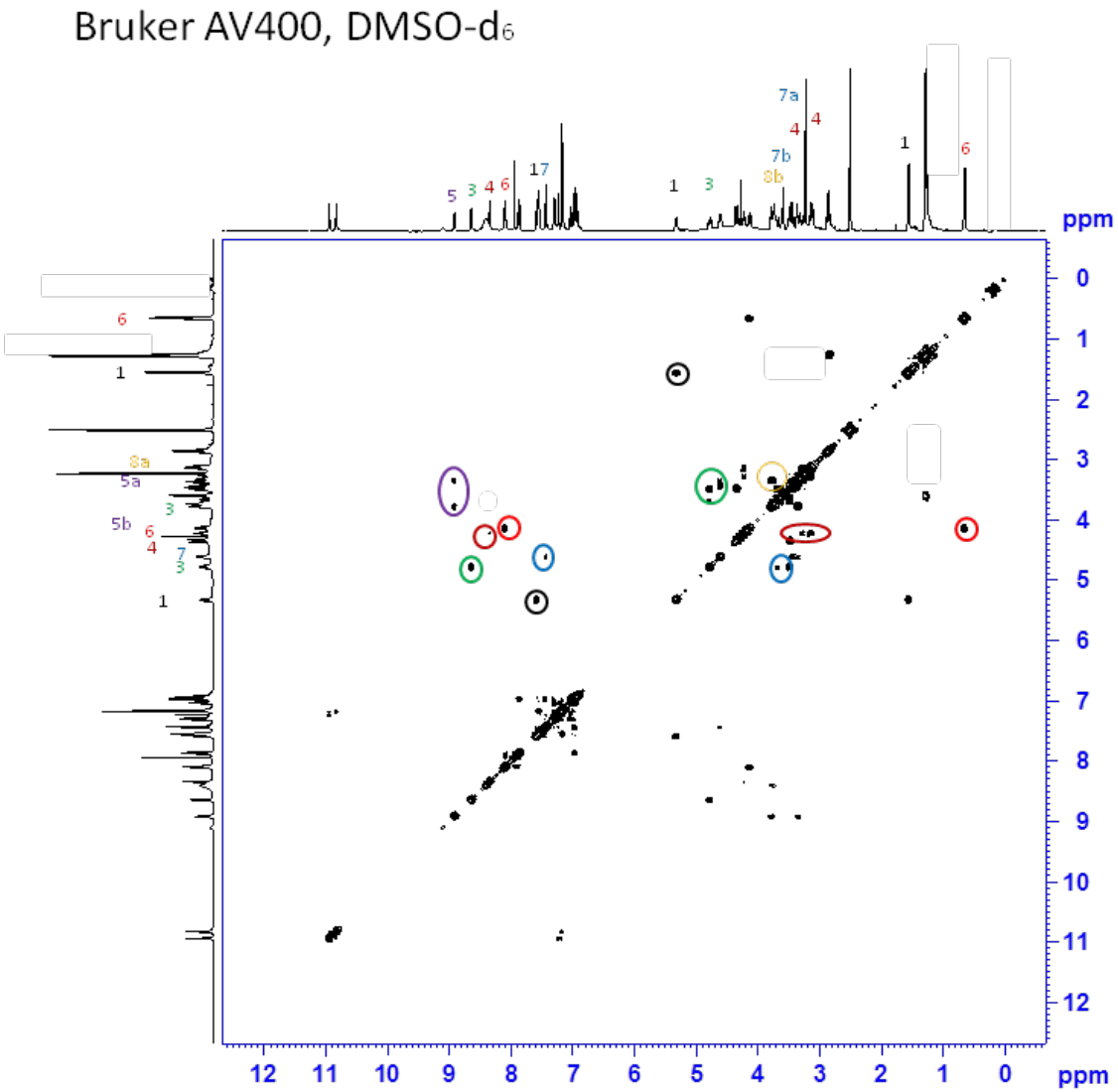

Figure 4-11 ^{1}H-^{1}H COSY spectrum of cyclic peptide 47e.

4.5 **Oxidative elimination of phenylselenocysteine**

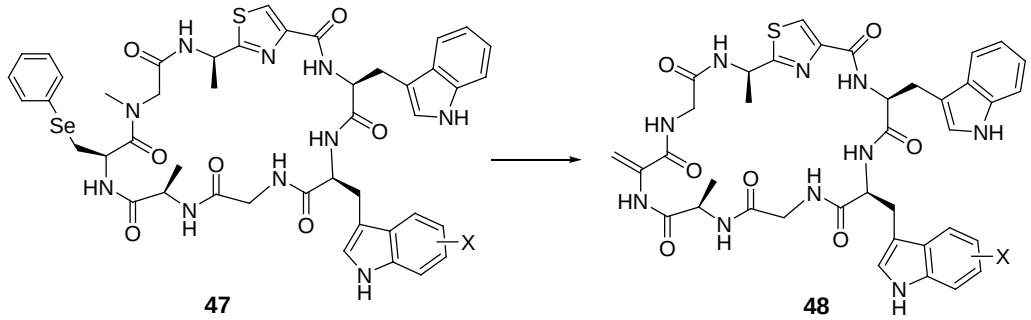

47 **48**

	a	**b**	**c**	**e**	**f**	**g**
X =	H	5-Br	5-Cl	7-Et	5-Me	5-MeO

The final step of argyrin synthesis was to unmask the α,β-unsaturated dehydroalanine residue. The conversion of the incorporated phenylselenocysteine residue to dehydroalanine was achieved through oxidative elimination.[270] As shown in Figure 4-12, the phenylseleno moiety was firstly oxidised to the phenylselenoxide (**187**) by treatment with a mild oxidising agent, such as hydrogen peroxide (H_2O_2) or sodium periodate ($NaIO_4$). Subsequent *syn*-elimination of phenylselenoxide (**187**) afforded the *exo*-methylene moiety (**188**).

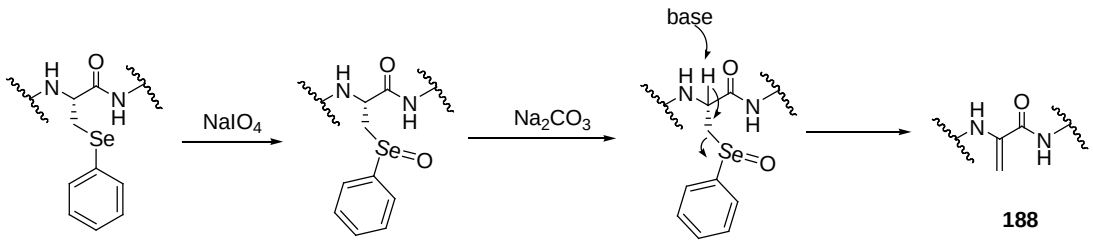

Figure 4-12 Oxidative elimination of phenylselenocysteine to dehydroalanine.

Hence, sodium periodate (4 eq.) was added dropwise to the cyclic peptide **47** in water/acetonitrile mixture at room temperature followed by stirring for 2 h. Formation of the phenylselenoxide-containing intermediate (**187**) was seen as a major component in RP-HPLC and MS analysis. The solvent was removed and the residual material was extracted with water and DCM/IPA. Isopropyl alcohol (IPA) was added due to the low solubility of phenylselenoxide-containing intermediate. Subsequently elimination reaction of **187** was initially carried out using saturated aqueous $NaHCO_3$ in acetonitrile as described in the literature.[150] However, RP-

HPLC analysis after three days revealed that the elimination was not completed (Figure 4-13(a)). In order to reduce the reaction time, the same reaction was carried out using saturated Na_2CO_3 aqueous solution. Gratifyingly, based on RP-HPLC analysis, the elimination was almost completed after 48 h (Figure 4-13(b)). The main peak at t_R = 10 min is the eliminated product and the leading shoulder of the main peak is the unreacted phenylselenoxide intermediate.

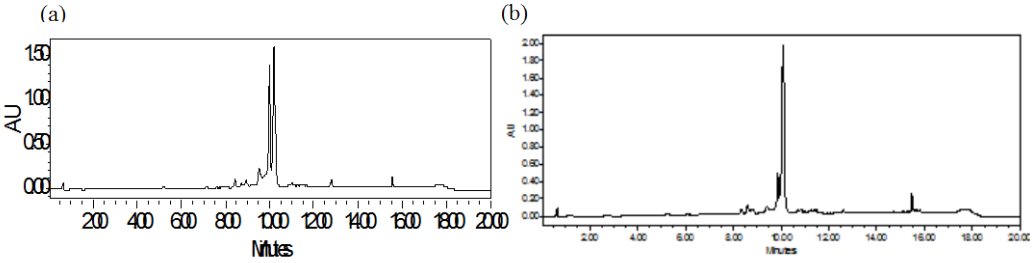

Figure 4-13 RP-HPLC analysis of β-elimination of phenylselenoxide 187. (a) Using aqueous $NaHCO_3$ for 3 days. (b) Using aqueous Na_2CO_3 for 24 h. Samples were analysed using the method; 10 – 60 % B over 12 min at 1 mL /min. The column used was an Onyx Monolithic analytical C_{18} column (100 x 3 mm).

Successful conversion was confirmed by MS with disappearance of the selenium isotopic patterns and molecular ion peak of the product being detected. The major peaks were purified by preparative RP-HPLC to afford argyrin A and analogues in 52-67 % yields (Table 4-3). Using **47e** as an example, the successful transformation of **47e** to **48e** was confirmed by ^{1}H NMR analysis, which revealed the disappearance of the aromatic protons (δ = 7.17 ppm), CH_2 (δ = 4.33 and 4.37 ppm) and α-proton (δ = 4.60 ppm) in the phenylseleno moiety (Figure 4-10) and the appearance of the two singlet protons (δ = 4.92 and 5.16 ppm) in the alkene moiety (Figure 4-14). A study of the literature for dehydroalanine-containing peptides confirmed that no spin-spin splitting was observed for these ^2J germinal protons.[270]

The assignment of proton resonances was established from 2D COSY spectrum. The backbone of cyclic peptide can be derived from cross signals between amide protons and their corresponding α-protons. For example, the amide proton (δ = 8.12 ppm) of the (*R*)-Ala^6 moiety which is labeled 6 in red colour in Figure 4-15, showed a cross signal to its α-proton (δ = 4.35 ppm). This α-proton also displays a correlation with the methyl group of (*R*)-Ala.

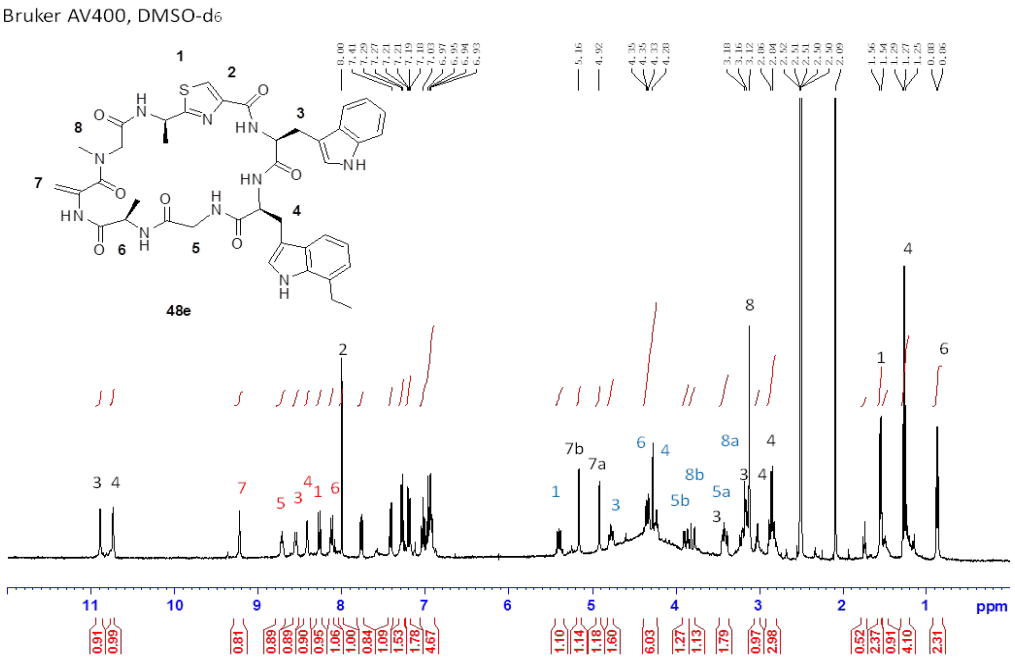

Figure 4-14 ^{1}H NMR spectrum of the argyrin A analogue 48e. Amide-NH are labelled red, α-protons are blue and others are black.

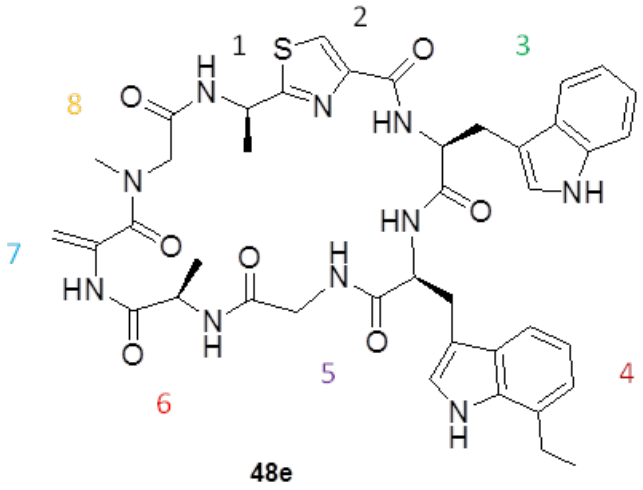

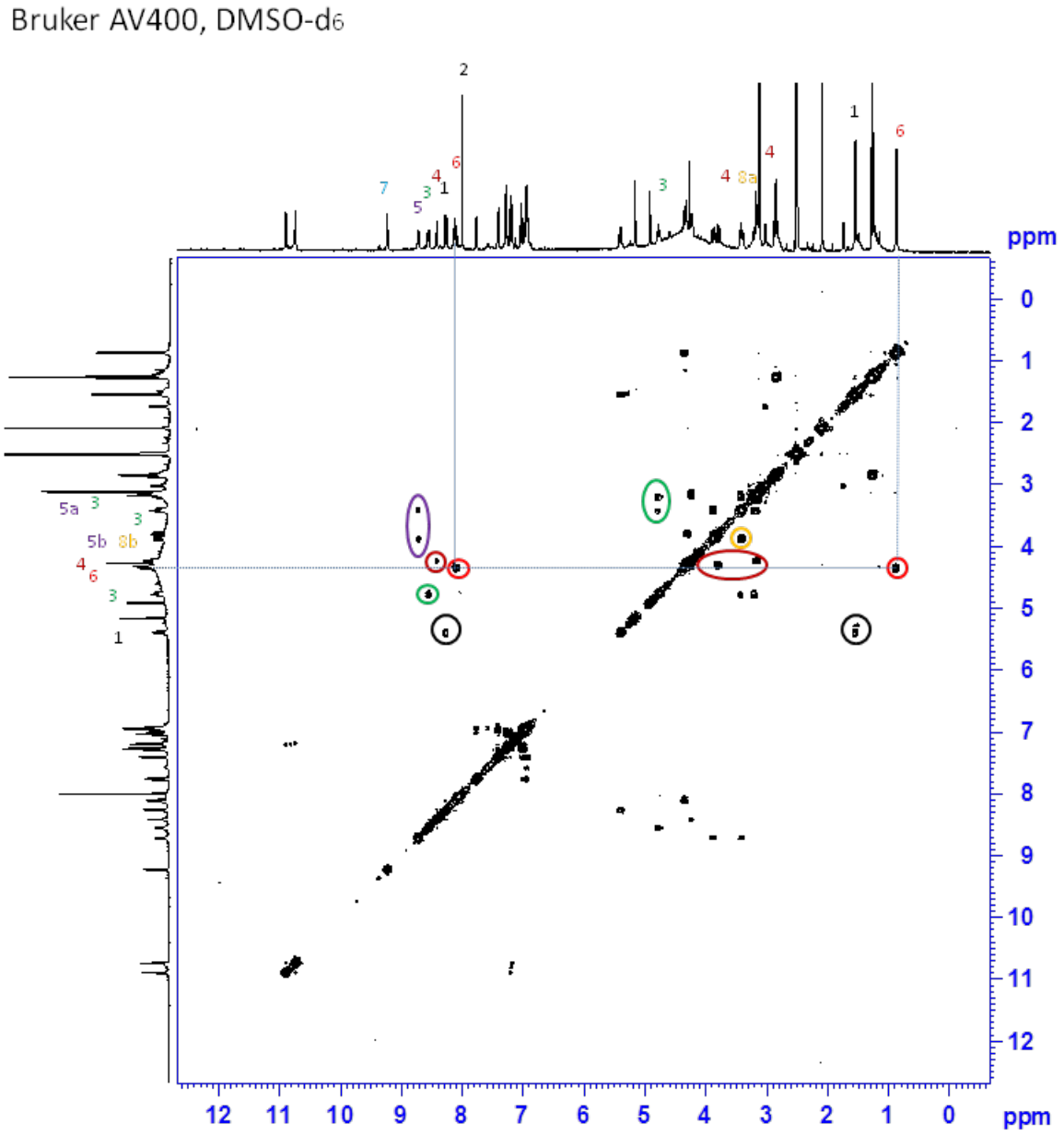

Figure 4-15 ^{1}H-^{1}H COSY spectrum of the argyrin A analogue 48e.

A summary of the retention times, yields and MS analysis of the six purified argyrin analogues is listed in Table 4-3. Although the reactions were clean and efficient, only moderate yields were obtained. Additionally, the cumulative yields from peptide assembling were only 4-11 %. The low cumulative yield may be attributed to the several work-up and purification steps. The poor solubility of peptides also reduced the yield. Therefore, in order to avoid tedious work-up steps and purification processes, an alternative strategy was investigated.

Table 4-3 Summary of the yields, RP-HPLC retention times and MS for the argyrin analogues 48a, 48b, 48c, 48e, 48f and 48h.

#	Sequence	Yield (%) [a]	t_R (min) [b]	ES-MS $[M+H]^+$ Calculated	ES-MS $[M+H]^+$ Measured	Cumulative yield (%) [c]
48a	***Cyclo*** [(*R*)-Ala^1-Thz^2-Trp^3-Trp^4-Gly^5-(*R*)-Ala^6-Dha^7-Sar^8]	66	6.8	795.3037	795.2959	11
48b	***Cyclo*** [(*R*)-Ala-Thz-Trp-(5-Br)-Trp-Gly-(*R*)-Ala-Dha-Sar]	58	8.0	875.2122	875.1877	6
48c	***Cyclo*** [(*R*)-Ala-Thz-Trp-(5-Cl)-Trp-Gly-(*R*)-Ala-Dha-Sar]	67	7.5	829.2647	829.2347	8
48e	***Cyclo*** [(*R*)-Ala-Thz-Trp-(7-Et)-Trp-Gly-(*R*)-Ala-Dha-Sar]	52	7.9	823.3350	823.3311	8
48f	***Cyclo*** [(*R*)-Ala-Thz-Trp-(5-Me)-Trp-Gly-(*R*)-Ala-Dha-Sar]	66	7.3	809.3193	809.3016	11
48g	***Cyclo*** [(*R*)-Ala-Thz-Trp-(5-MeO)-Trp-Gly-(*R*)-Ala-Dha-Sar]	58	6.5	825.3143	825.3056	4

[a] Yield refers to purified yields after the oxidative elimination step.
[b] RP-HPLC was performed on Onyx Monolithic analytical C_{18} column (100 x 4.6 mm). Eluent was monitored by UV absorbance at 216 nm. Linear gradient was 10-60 % B over 10 min at 3 mL /min.
[c] Cumulative yield refers to the accumulation of individual yields from peptide assembly.

Inspired by the previous observation that dehydroalanine moiety is stable in 50 % TFA acidolysis and peptide coupling processes (Section 4.3.3), it was therefore anticipated that oxidative elimination could be achieved while the linear peptide was still attached to the solid-support. In other words, instead of releasing the linear precursor into solution after peptide assembly, on-resin oxidative elimination was effected. The synthesis of **48d**, **48h** and **48k** is outlined in Scheme 4-3 and the purification was only required following the final reaction.

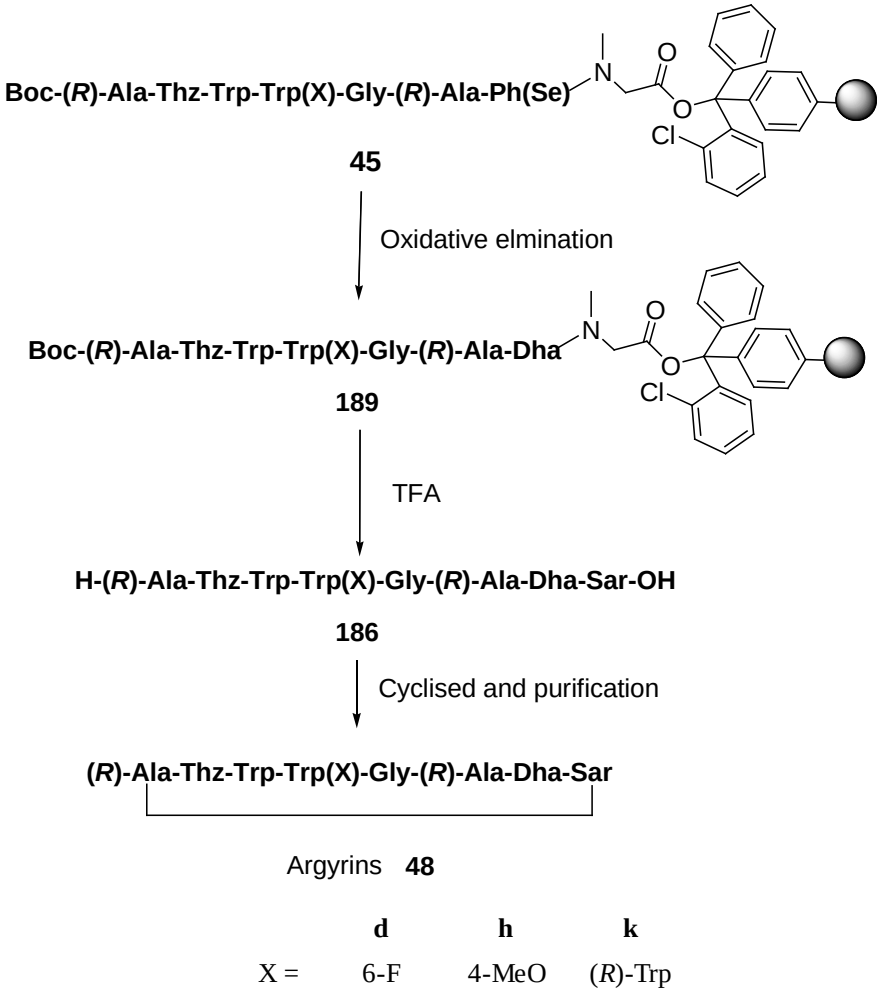

Scheme 4-3 Synthetic route for the cyclic peptides argyrin 48d, 48h and 48k.

After all amino acid residues were coupled to the peptidyl resin as described in Section 4.2.2, the resins were suspended in DMF/H_2O 0.5:0.2 and an aqueous solution of $NaIO_4$ (4 eq.) were added to the SPPS column. The reactions were stirred at room temperature for 16 h, after which more than 95 % of the starting material were reacted, as determined by RP-HPLC. Unexpectedly, elimination of phenylselenoxide occurred spontaneously without further base treatment. The reasons for this are unclear, however, analysis by RP-HPLC and MS revealed the completion of the elimination. The linear peptides **189d**, **189h** and **189k** were then cleaved from the resin and cyclised as previous described in Section 4.3.3 and Section 4.4, respectively.

The results of the three analogues are summarised in Table 4-4. Unfortunately, no improvement of yields was obtained using this approach. Nevertheless, this approach allows an overall reduction of time and purification efforts.

Table 4-4 Summary of the yields, RP-HPLC retention times and MS analysis for the argyrin analogues 48d, 48 h and 48k.

#	Sequence	Cumulative yield (%) [a]	t_R (min) [b]	ES-MS $[M+H]^+$ Calculated	ES-MS $[M+H]^+$ Measured
48d	***Cyclo*** [(*R*)-Ala-Thz-Trp-(6-F)-Trp-Gly-(*R*)-Ala-Dha-Sar]	4	7.0	813.2943	813.3016
48h	***Cyclo*** [(*R*)-Ala-Thz-Trp-(4-MeO)-Trp-Gly-(*R*)-Ala-Dha-Sar]	6	6.6	825.3143	825.3092
48k	***Cyclo*** [(*R*)-Ala-Thz-Trp-(*R*)-Trp-Gly-(*R*)-Ala-Dha-Sar]	16	5.9	795.3037	795.3020

[a] RP-HPLC was performed on Onyx Monolithic analytical C_{18} column (100 x 4.6 mm). Eluent was monitored by UV absorbance at 216 nm. Linear gradient was 10-60 % B over 12 min at 3 mL/min.
[b] Cumulative yield refers to the accumulation of individual yields from peptide assembly.

The structures of all nine argyrin analogues were elucidated by NMR spectroscopy. Analysis using solutions of argyrin analogues in DMSO-d_6 by ^{1}H NMR provided further evidence of their purity. Assignment of proton chemical shifts in argyrins was accomplished using ^{1}H and 2D COSY NMR analysis. It was somewhat surprising that all nine synthesised argyrin analogues showed poor solubility in $CDCl_3$, the solvent used in the reported literature.[152] Therefore, DMSO-d_6 was chosen as a suitable solvent.

4.6 Cytotoxicity evaluation of argyrin A and analogues

As described in Chapter 1, argyrin A exhibited potent inhibition of eukaryotic proteasome activity. Based on Nickeleit's studies, the concentration-dependent cytotoxicity effect of argyrin A was observed in several cancer cells of different origins, including colon carcinoma (HCT116, SW480), lung cancer (A549), breast adenocarcinoma (MCF7) and cervical cancer (Hela).[3] In addition, SAR study by Stauch *et al.* revealed that argyrin A and F were the most potent analogues, with IC_{50} values against SW480 up to 3.7 and 4.2 nM, respectively (Table 1-6).[155] They concluded that the presence of methoxy group in the 4-position of Trp^4 was essential for their biological activities. This hypothesis can be tested by using argyrin analogues incorporating various substituents at different position of the Trp^4 for further in-depth study.

In order to establish SAR of argyrins, the nine synthesised argyrin A and analogues (**48a-h** and **48k**) were tested in MTT cell viability assays. A detailed description of MTT assay and a discussion of the biological results obtained for the aforementioned nine argyrin derivatives are provided in the ensuing sections.

4.6.1 **MTT cell viability assay**

Viability of mammalian cells can be accurately monitored by a variety of viability assays. MTT is one of the most common and straightforward technique used to assess the cytotoxicity of substances.[302] Yellow 3-(4,5-dimethythiazol-2-yl)-2,5-diphenyl tetrazolium bromide (MTT) **190** is reduced to purple formazan **191** by succinate dehydrogenase in the mitochondria. Since reduction of MTT can only occur in metabolically active cells, the viability of the cells can be quantified by measuring of absorbance of this purple formazan solution.

Tetrazolium salt (yellow)

190

Formazan salt (purple)

191

Colon carcinoma cells have previously been reported to be sensitive to argyrin A treatment.[3, 151] Therefore, the cytotoxicity of synthetic argyrin A and analogues reported in this thesis was performed using an MTT assay against the HCT-116 human colon cancer cell line. Specifically, HCT-116 cells were seeded at a density of 2.5 x 10^3 cells per mL in 96-well plates and allowed to adhere overnight. The cells were treated with argyrins at various concentrations, from of 0.1 nM to 100 µM and incubated at 37 °C for 72 h. Proliferation activity was determined by treating the cells with MTT. It is anticipated that viable cells with active mitochondria would reduce the tetrazolium into purple formazan. The purple formazan crystals were dissolved in 150µL DMSO. Optical densities of the solutions were measured by absorbance at 500 nm in an ELISA plate reader. The GI_{50} values were determined according to an established methodology as described

in Section 6.5. All measurements were performed in triplicate and the results are reported as mean ± standard error of the mean.

4.6.2 **Results from the MTT cell viability assay**

The results of the GI_{50} values obtained from MTT cell viability assay with argyrin A and analogues are summarised in Table 4-5. The clinically used proteasome inhibitor bortezomib[58] was used as a positive control. GI_{50} values represent the concentration of argyrin analogue that inhibit the growth of cancer cells by 50 %.

Table 4-5 Inhibition of HCT-116 cell proliferation by argyrin analogues

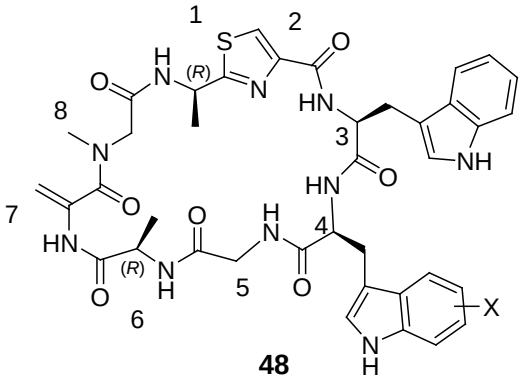

48

#	Argyrin analogues	GI_{50} (nM) [a]
48a	***Cyclo*** [(*R*)-Ala[1]-Thz[2]-Trp[3]-Trp[4]-Gly[5]-(*R*)-Ala[6]-Dha[7]-Sar[8]] / Argyrin E	227 ± 10.8
48b	***Cyclo*** [(*R*)-Ala-Thz-Trp-(5-Br)-Trp-Gly-(*R*)-Ala-Dha-Sar]	26 ± 4.1
48c	***Cyclo*** [(*R*)-Ala-Thz-Trp-(5-Cl)-Trp-Gly-(*R*)-Ala-Dha-Sar]	20 ± 1.3
48e	***Cyclo*** [(*R*)-Ala-Thz-Trp-(7-Et)-Trp-Gly-(*R*)-Ala-Dha-Sar]	133 ± 91
48f	***Cyclo*** [(*R*)-Ala-Thz-Trp-(5-Me)-Trp-Gly-(*R*)-Ala-Dha-Sar]	26 ± 0.2
48g	***Cyclo*** [(*R*)-Ala-Thz-Trp-(5-MeO)-Trp-Gly-(*R*)-Ala-Dha-Sar]	3.8 ± 2.7
48d	***Cyclo*** [(*R*)-Ala-Thz-Trp-(6-F)-Trp-Gly-(*R*)-Ala-Dha-Sar]	40 ± 6.0
48h	***Cyclo*** [(*R*)-Ala-Thz-Trp-(4-MeO)-Trp-Gly-(*R*)-Ala-Dha-Sar] / Argyrin A	1.8 ± 0.6
48k	***Cyclo*** [(*R*)-Ala-Thz-Trp-(*R*)-Trp-Gly-(*R*)-Ala-Dha-Sar]	335 ± 7
	Bortezomib [b]	2.5 ± 0.8

[a] Concentration needed to inhibit cell growth by 50% as determined from the dose-response curve. Determinations were made at 6 different concentrations of argyrins using MTT cell proliferation assays.
[b] This clinically used drug was purchased from Sigma-Aldrich.

The results show that all nine synthetic argyrin analogues display antiproliferative activity in the nanomolar range. The potency is comparable with those results reported from the other groups.[3, 151] Although the GI_{50} value determined for argyrin A with HCT116 cell line was 1.8 nM, which is slightly lower than the literature IC_{50} value of 2.8 nM,[3] this difference is presumably due to the cell line variability and experimental error.

Argyrin E (**48a**), which lack substitution in Trp^4, is less potent than other analogues. In addition, argyrin A (**48h**) and **48g**, which contain the methoxy substitution on Trp^4 residue are more potent than other analogues. As was discussed in Chapter 1.4.2, this observation is in agreement with the literature hypothesis that the methoxy substitution of Trp^4 is essential for activity. In fact, to investigate the influence of the key methoxy substituent at 4-position of Trp^4 on the potency, the methoxy group of argyrin **48g** was moved from the 4- to 5-postion. The results indicated that both **48h** and **48g** showed nearly equal potency. To the best of our knowledge, this is the first unique synthetic analogue of argyrin A, that displayed such high potency.

In contrast, replacement of the 4-methoxy group (**48g**) with a methyl group (**48f**) resulted in significant decreased in potency, by some 10-fold. Previous studies have suggested that the 4-methoxy group on Trp^4 residue is involved in electrostatic interaction with proteasome.[155] As illustrated in Figure 1-23, the methoxy oxygen atom participates in a hydrogen bond to the hydroxyl group of S118 in the C-L and CT-L pockets. Thus, this decrease in activity could be explained by the inability of the 4-Me to participate in a hydrogen bond.

Expectedly, another argyrin analogue **48e** with a 7-ethyl substituent on Trp^4 displayed even poorer activity than that of **48f**. It is postulated that, in addition to a lack of hydrogen bond, the introduction of an ethyl group at the 7-position of Trp^4 would sterically clash with the proteasome backbone (Figure 4-16). It is possible that this protrusion results in poorer binding affinity to the areas of the proteasome subunit.

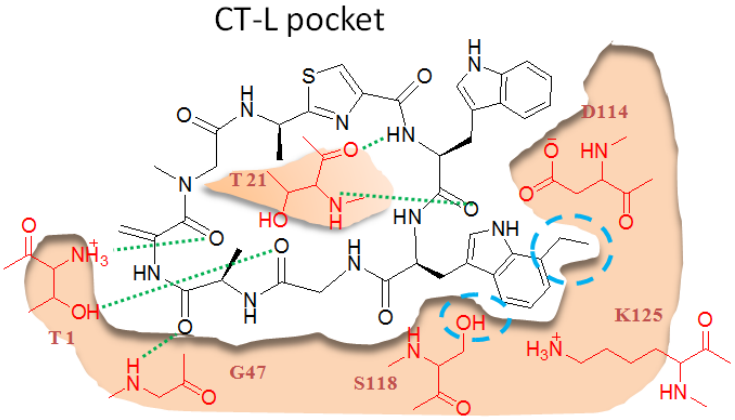

Figure 4-16 Proposed binding pose of argyrin 48e to the CT-L pocket.

Next, in order to investigate the electrostatic effect of the methoxy group on the potency, methoxy group (**48g**) was further replaced with an electron-withdrawing group. Argyrin **48b** bearing a bromine atom at 5-position of Trp^4 showed a GI_{50} value of 26 nM. The result showed a 10-fold less in potency compared to argyrin A. Incorporation of other halogen groups in the 5- and 6-postion of Trp^4 also resulted in diminished potency, as shown by argyrin **48b**, **48c** and **48d**. In addition, it seems that all halogenated argyrin analogous displayed similar degrees of potency. This is presumably due to hydrophobic characteristic of the halogen groups matches the hydrophobic side pocket of proteasome active site. However, good potency was maintained which is likely due to possible halogen bond interactions.

In fact, studies in the medicinal chemistry field have shown that the insertion of halogen atoms could provide two major interactions to their target proteins.[303] One of the most recognised interactions is the attachment of these bulky halogen atoms could occupy all the active site of target pockets, resulting in superior binding affinities to target proteins. For example, nemonapride (**192**), a chlorobenzamide, is a potent dopaminergic antagonist. The removal of the chlorine in this drug was found to be deleterious for the potency and reduce selectivity to the dopaminergic receptors.[304] Another effect of halogen atoms is the ability to contribute an intermolecular halogen bond in a fashion resembling the hydrogen bonds. The formation of halogen bonds provides favourable electrostatic interactions between ligand and protein. For example, the activity of 4,5,6,7,-tetrabromobenzotriazole

(**193**), an ATP competitive inhibitor of cyclin A-CDK2, was attributed to the involvement of three halogen bonds (Figure 4-17(b)).[305]

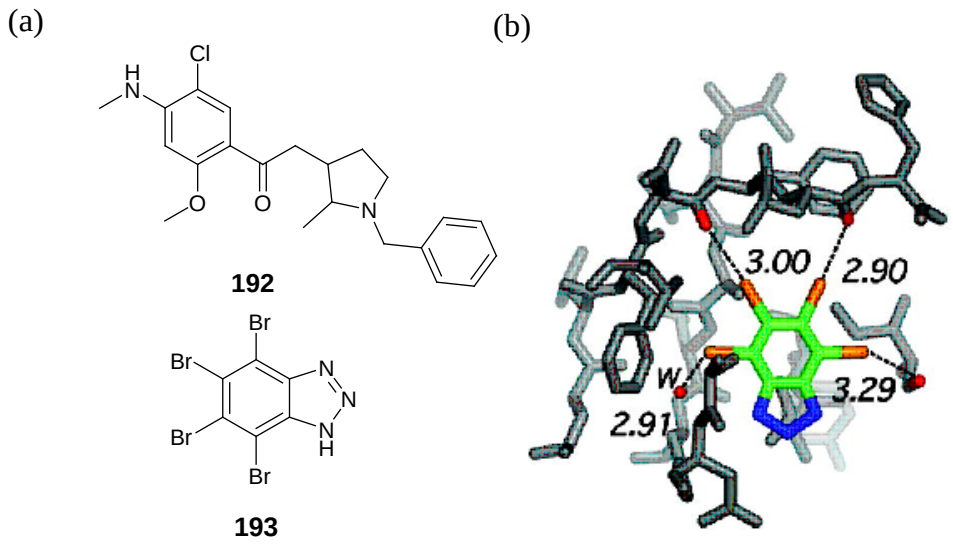

Figure 4-17 (a) Structure of nemonapride (192) and 4,5,6,7,-tetrabromobenzotriazole (193). (b) The 2.2 Å structure of cyclin A/CDK2 in complex with the inhibitor 184. The inhibitor is shown with three bromine halogen bonds to peptide carbonyl oxygens of the protein.[305]

On the basis of these experimental results, it can be concluded that the presence of methoxy group in the 4-position of Trp^4 is essential for biological activity. However, the methoxy group at 5-position of Trp^4 is also tolerated. Conversely, Argyrin E which lacked of substitution on Trp^4 showed considerable lost of activity. Other derivatives lacking the methoxy group on Trp^4 displayed less activity. The activities shown by halogenated compounds **48b**, **48c** and **48d** were not significantly different, but were typically 10-fold less potent than that of argyrin A.

In summary, the above results clearly demonstrate that argyrin A which contains 4-methoxy group on Trp^4 displayed the greatest degree of potency within the nine argyrin analogous. Both diastereoisomers of argyrin E which lack substitution on Trp^4 displayed the lowest activity.

4.7 Conclusion

A practical and robust solid-phase approach for the synthesis of argyrin A and analogues thereof has been developed. The described approaches enabled the production of linear precursors and the target cyclic peptides within a week. As a

result, the synthesis of nine argyrin A derivatives incorporating a wide range of functional group in an tryptophan residue was achieved. The high efficiency and reproducibility of the synthetic approach could be applied for the synthesis of other argyrin A analogues.

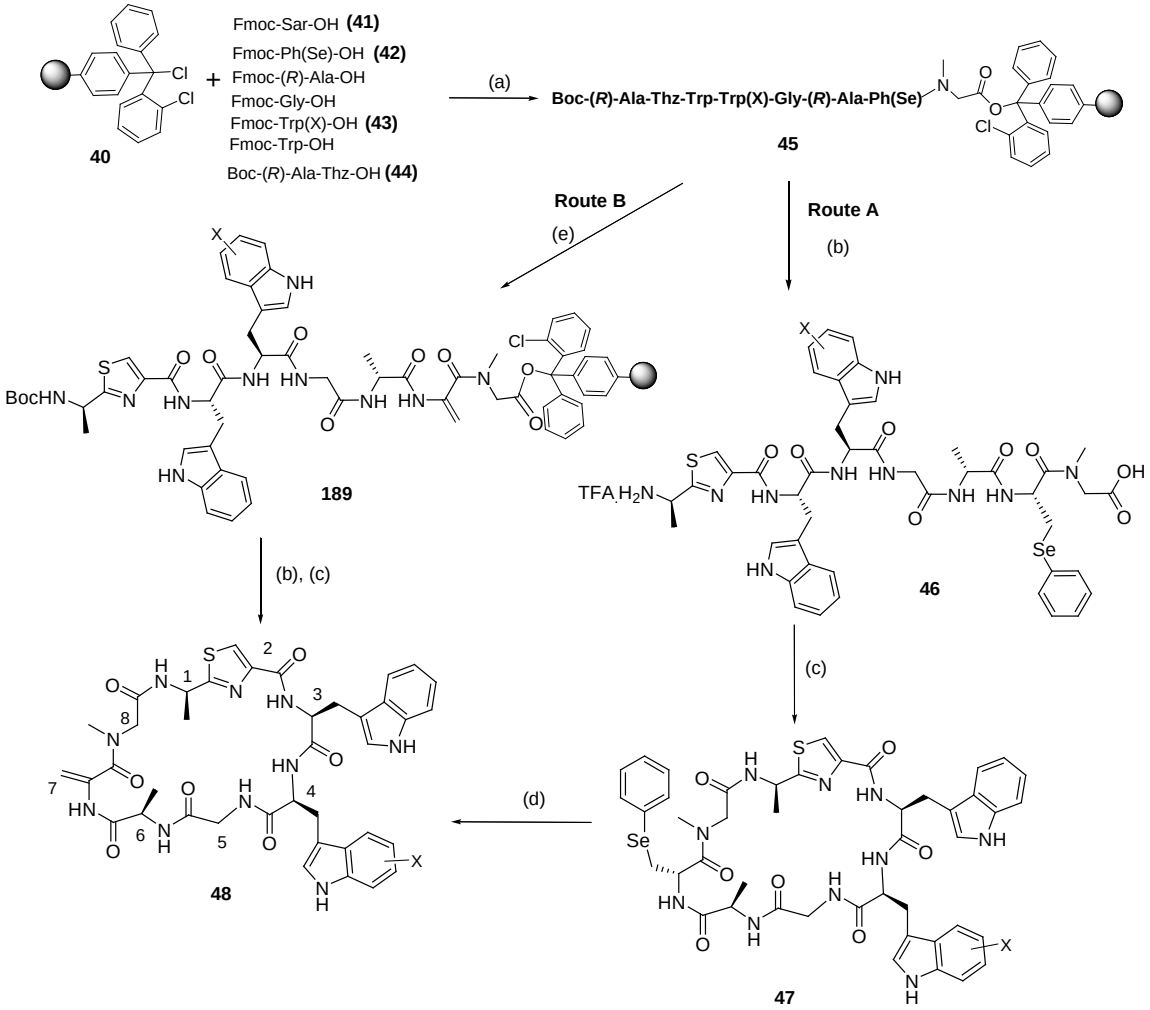

Route A	a	b	c	e	f	g	Route B	d	h	k
X =	H	5-Br	5-Cl	7-Et	5-Me	5-MeO	X =	6-F	4-MeO	(*R*)-Trp

Scheme 4-4 Synthesis of argyrin A and analogues thereof (48). Reagents and conditions: (a) i. piperidine/DMF (1:4); ii.Fmoc-amino acids, PyOxim or HATU, DIPEA; (b) TFA/DCM, H_2O, TIPS.; (c) PyBOP, HOBt, DIPEA; (d) i. $NaIO_4$, CH_3CN/H_2O; ii. Na_2CO_3, CH_3CN/H_2O; (e) $NaIO_4$, DMF/H_2O.

In summary, Fmoc-Sar (**41**) was chosen as the *C*-terminus amino acid residue which was tethered to the resin linker 2-chlorotrityl chloride polystyrene (**40**). All subsequent amino acids, including Fmoc-Ph(Se)-OH (**42**), Fmoc-(*R*)-Ala-OH, Fmoc-Gly-OH, Fmoc-Trp(X)-OH (**43**), Fmoc-Trp-OH and Boc-(*R*)-Ala-Thz-OH (**44**) were then coupled to the peptidyl resin using HATU- (**176**) or PyOxim-

mediated (**179**) carboxyl-activation to afford resin-bound linear peptides which were universally deprotected and cleaved form the resin by acidolysis using 50 % TFA to afford linear precursors **46** (Route A, Scheme 4-4). Cyclisation were then undertaken on high diluted solutions by treatment with PyBOP (**178**), HOBt and DIPEA to afford cyclic peptides **47**. RP-HPLC and MS confirmed the success of the cyclisation without oligomeric side-products being observed. Finally, conversion of phenylseleno moiety to the *exo*-methylene was achieved by oxidative elimination. Preparative RP-HPLC was used to purify the argyrin analogues in purity of > 95% and overall yields of 4-11 % (Table 4-5). As an alternative, on-resin oxidative elimination of the phenylselenocysteine residue was evaluated (Route B, Scheme 4-4). Unfortunately, the results showed that no significant improvements in yield were obtained in this approach (Table 4-4). However, this approach facilitated an overall reduction of time and purification efforts required to obtain the final desired products.

The purity and identity of nine synthesised argyrin analogues were established by RP-HPLC, MS and NMR. The purity and yield following RP-HPLC purification for each analogue are summarised in Table 4-5. The successful synthesis of argyrin A and eight analogues therefore allowed for further structure-activity studies.

The nine argyrin A and analogues described above were tested in a cell viability assay. HCT-116 human colon cancer cell line was chosen for the preliminary cytotoxicity study. The cells were treated with nine argyrin analogues for 72 h. The cytotoxic experiment was carried out using the MTT colorimetric assay. The results indicated that the synthesised argyrin analogues exhibited GI_{50} values in nanomolar range. The two most potent argyrins, argyrin A (**48h**) and argyrin **48g**, possessed GI_{50} values in 1.8 nM and 3.8 nM, respectively. It was found that replacing the 4-methoxy group with other groups greatly reduced the potency. Such results provide valuable evidence that the presence of the methoxy group on Trp^4 is crucial for biological activities of argyrin.

Table 4-5 Argyrin derivatives synthesised and purified by RP-HPLC with corresponding isolation yields and purity.

#	Sequence	Cumulative yield (%) [a]	Purity (%) [b]	t_R (min) [c]	GI_{50} (nM) [d]
48a	***Cyclo*** [(*R*)-Ala[1]-Thz[2]-Trp[3]-Trp[4]-Gly[5]-(*R*)-Ala[6]-Dha[7]-Sar[8]]/ Argyrin E	11	> 95	6.8	227 ± 10.8
48b	***Cyclo*** [(*R*)-Ala-Thz-Trp-(5-Br)-Trp-Gly-(*R*)-Ala-Dha-Sar]	6	> 95	8.0	26 ± 4.1
48c	***Cyclo*** [(*R*)-Ala-Thz-Trp-(5-Cl)-Trp-Gly-(*R*)-Ala-Dha-Sar]	8	> 95	7.5	20 ± 1.3
48e	***Cyclo*** [(*R*)-Ala-Thz-Trp-(7-Et)-Trp-Gly-(*R*)-Ala-Dha-Sar]	8	> 95	7.9	133 ± 91
48f	***Cyclo*** [(*R*)-Ala-Thz-Trp-(5-Me)-Trp-Gly-(*R*)-Ala-Ph(Se)-Sar]	11	> 95	7.3	26 ± 0.2
48g	***Cyclo*** [(*R*)-Ala-Thz-Trp-(5-MeO)-Trp-Gly-(*R*)-Ala-Dha-Sar]	4	> 95	6.5	3.8 ± 2.7
48d	***Cyclo*** [(*R*)-Ala-Thz-Trp-(6-F)-Trp-Gly-(*R*)-Ala-Dha-Sar]	4	> 95	7.0	40 ± 6.0
48h	***Cyclo*** [(*R*)-Ala-Thz-Trp-(4-MeO)-Trp-Gly-(*R*)-Ala-Dha-Sar] / Argyrin A	6	> 90	6.6	1.8 ± 0.6
48k	***Cyclo*** [(*R*)-Ala-Thz-Trp-(*R*)-Trp-Gly-(*R*)-Ala-Dha-Sar]	16	> 90	5.9	335 ± 7

[a.] Cumulative yield refers to the accumulation of individual yields from peptide assembly.

[b.] Peptide purity was determined from integration of RP-HPLC peaks.

[c.] RP-HPLC was performed on Onyx Monolithic analytical C_{18} column (100 x 4.6 mm). Eluent was monitored by UV absorbance at 216 nm. Linear gradient was 10-60 % B over 12 min at 3 mL/min.

[d.] Concentration needed to inhibit HCT-116 cell growth by 50% as determined from the dose-response curve. Determinations were made at 6 different concentrations of argyrins using MTT cell proliferation assays.

Chapter 5
General conclusion and further studies

Argyrin A is a cyclic octapeptide comprised of four natural amino acids and three unusual amino acids. To date, the total synthesis of argyrin A and its analogues have been achieved by three independent laboratories. In 2002, Ley *et al.* first described a total synthesis of argyrin B in 17 steps. After argyrin A was identified as a potent proteasome inhibitor by Nickeleit *et al.* in 2008, this natural occurring cyclic peptide has attracted the attention of chemists and biologists.[3] Preliminary studies also demonstrated that the dehydroalanine and 4-methoxy-tryptophan residues in this sequence are essential for their biological activities. In order to understand the structure-activity relationships of this complex molecule, Bülow *et al.* synthesised argyrin F and its eight Gly^5-modified analogues.[151] Wu *et al.* further modified the convergent strategy to achieve the total synthesis of argyrin A and E.[152]

However, the complexity of these syntheses limits both its availability and the scope for preparing structural analogues. In this thesis, the synthesis of three key unusual amino acid building blocks of argyrin A has been established, in particular a novel generic route for the synthesis of optically pure *N*-Fmoc tryptophan analogues. Additionally, the first solid-phase-based synthesis of the cyclic octapeptide argyrin A and analogues thereof was also established. This solid-phase strategy enabled the rapid and efficient synthesis of various argyrin analogues. Therefore, argyrin analogues obtained by this strategy provide valuable SAR concerning the key role played by the methoxy group in Trp^4.

5.1 **Synthesis of (*S*)-tryptophan and analogues**

The development of a novel synthetic route for the synthesis of *N*-Fmoc tryptophan analogues provided a key building block necessary for the synthesis of argyrin. As outlined in Scheme 5-1, a series of Fmoc tryptophan derivatives **43** were obtained from the corresponding indoles **49** in eight steps.

Commercially available indoles **49** were subjected to Vilsmeier formylation to give aldehydes **50**, which were then homologated *via* Wittig reaction followed by acid hydrolysis of the enol ether intermediates to afford aldehydes **51**. A practical one-pot diastereoselective Strecker amino acid synthesis using a chiral auxiliary amine in the presence of sodium cyanide led to the straightforward synthesis of a diastereoisomeric mixture of (*S*,*R*) and (*R*,*R*) α-aminonitriles **52** in 3:1 ratio. For the non-halogen substituted indoles, (*R*)-2-phenylglycinol (R' = OH, R'' = H) was used as a chiral auxiliary. In contrast, for the chlorine and bromine substituted indoles, 4-methoxy-α-methylbenzylamine (PMB) (R' = H, R''= OCH_3) was introduced as a chiral auxiliary reagent.

A number of acidic and basic conditions were found to be unsuccessful in their ability to effect hydrolysis of amino nitriles **52** to amino amides **53**; decomposition was the main observation. Thus, the mild peroxide hydrolysis was employed for the conversion of acid labile α-aminonitriles **52** to the corresponding α-amino amides **53**. Consequent separation of the desired (*S*,*R*) α-aminoamides **54** was readily achieved by silica chromatography or RP-HPLC.

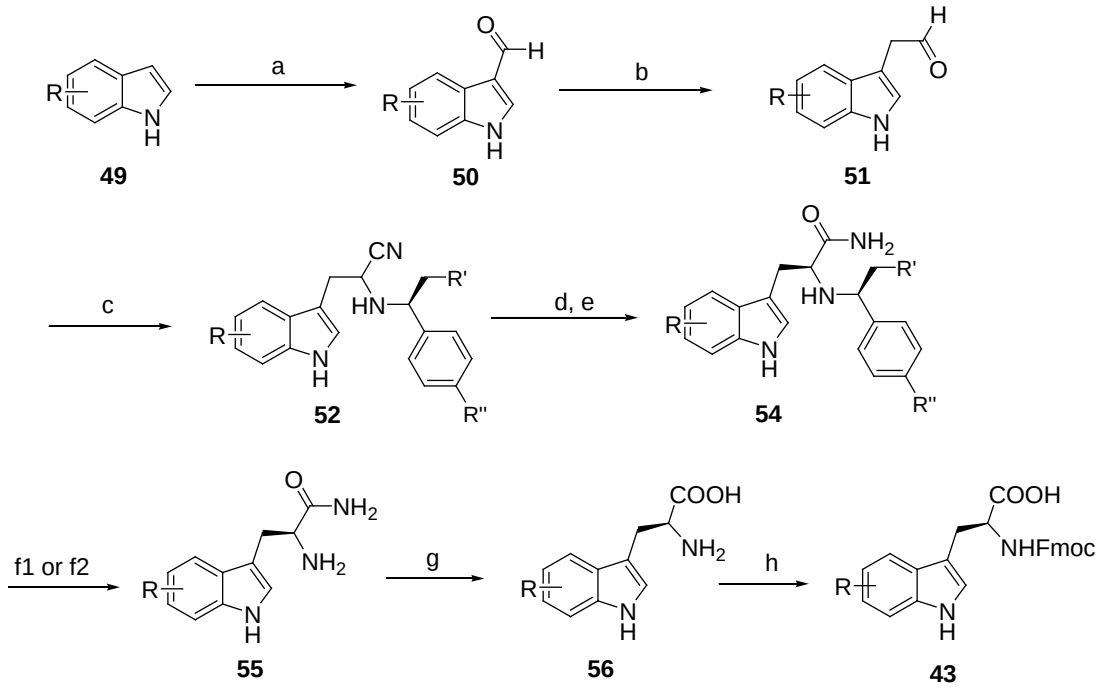

	a	**b**	**c**	**d**	**e**	**f**	**g**	**h**
R =	H	5-Br	5-Cl	6-F	7-Et	5-Me	5-MeO	4-MeO
R' =	OH	H	H	OH	OH	OH	OH	OH
R'' =	H	OCH_3	OCH_3	H	H	H	H	H

Scheme 5-1 Synthesis Fmoc-tryptophan derivatives (43); Reagents and conditions: (a) $POCl_3$, DMF, 0 °C then 45 °C; (b) i. $Ph_3PCH_2OCH_3$, n-BuLi; ii. HCl, THF, reflux; (c) Chiral auxiliary, NaCN, AcOH, MeOH; (d) H_2O_2, Na_2CO_3, DMSO; (e) Recrystallisation or HPLC; (f1) Pd/ C, NH_4HCO_2, MeOH, reflux; (f2) TFA, TIPS, 60 °C; (g) 1 M HCl, reflux; (h) Fmoc-OSu, $NaHCO_3$, THF/H_2O.

Having obtained the desired diastereomeric pure (*S,R*) α-aminoamides **54**, the chiral auxiliary was removed by two difference conditions: For the non-halogen substituted aminoamides (**54a**, **d-h**), removal of the *N*-benzyl group was achieved by catalytic transfer hydrogenation to afford (*S*)-tryptophan amide derivatives **55**. In contrast, for the chlorine and bromine substituted aminoamides (**54b** and **54c**), removal of the PMB group was achieved by TFA-mediated acidolysis. Subsequent hydrolysis of (*S*)-tryptophan amide derivatives **55** to the corresponding (*S*)-tryptophan derivatives **56** was accomplished in good yield (> 80 %) by refluxing in 1 M aqueous hydrochloric acid without causing decomposition. Finally, the *N*-terminal of amino acids was protected with Fmoc to afford **43** which were suitable for the Fmoc solid phase peptide synthesis.

The method described above was used for the synthesis of eight Fmoc-tryptophan derivatives with a broad range of substitutions in the indole ring. The overall yields over this eight-step synthesis ranged from 2 to 5 %. The low yield was due to sensitivity of indole moiety, especially for the indole with electron-donating substitutions.

In summary, a new generic method for the synthesis of optically pure *N*-Fmoc-tryptophan derivatives was established. This method employed inexpensive commercially available reagents, and avoided using expensive chiral auxiliaries or resolving reagents.

5.2 **Synthesis of *N*-Boc-(*R*)-Ala-Thz-OH**

The second unusual building block for the total synthesis of argyrin A is the thiazole-containing dipeptide. Therefore, *N*-Boc-(*R*)-Ala-Thz-OH dipeptide building block (**44**) was obtained using known procedures. As depicted in Scheme 5-2, *N*-Boc-(*R*)-Ala-Thz-OH (**44**) was prepared in four steps starting from *N*-Boc-(*R*)-Ala-OH.

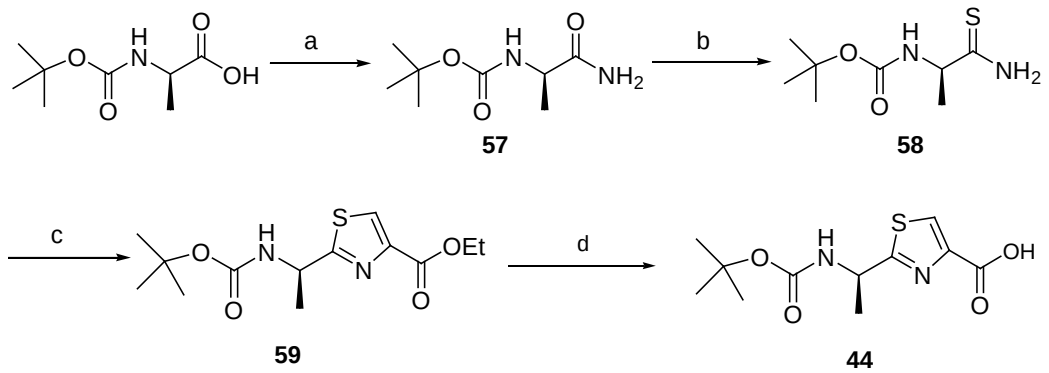

Scheme 5-2 Synthesis of *N*-Boc-(*R*)-Ala-Thz-OH (44); Reagents and conditions: (a) DCC, HOBt, NH_3, CH_2Cl_2, 0 °C; (b) Lawesson's reagent, THF, 0°C; (c) i. $BrCH_2COCO_2Et$, $KHCO_3$, DME, -15 °C; ii.TFAA, 2, 6-lutidine, DME, -15 °C; (d) LiOH, THF/ MeOH/ H_2O, room temp.

The key synthetic strategy of thiazole unit was achieved by using a modified Hantzsh-thiazole formation. Thioamide (**58**) was cyclised using ethyl bromopyruvate to afford thiazoline intermediate, followed by treatment of TFAA and 2,6-lutidine to give the desired thiazole dipeptide.

The overall yields over this four-step synthesis ranged from 26 to 30 %. The characterisation data of the thiazole dipeptide **44** was identical to that reported in the literature.[150] In addition, the specific rotation obtained for **44** indicated that thiazole formation occurred without racemisation. The optical purity of **44** was further confirmed by the Mosher's method. However, further modification of the thiazole subunit to oxazole derivative was unsuccessful, due to the epimerisation during the cyclisation step.

5.3 Synthesis of Fmoc-phenylselenocysteine, a dehydroalanine precursor

The third building block necessary for the total synthesis of argyrin A is the dehydroalanine precursor, phenylselenocysteine. It has been described that phenylselenocysteine can be incorporated into growing peptide chain *via* standard Fmoc SPPS procedure.[270] Therefore, Fmoc protected phenylselenocysteine was chosen as a masked precursor to the labile dehydroalanine building block. As outlined in Scheme 5-3, Fmoc-phenylselenocysteine (**42**) was prepared in four steps starting from *N*-Boc-Serine.

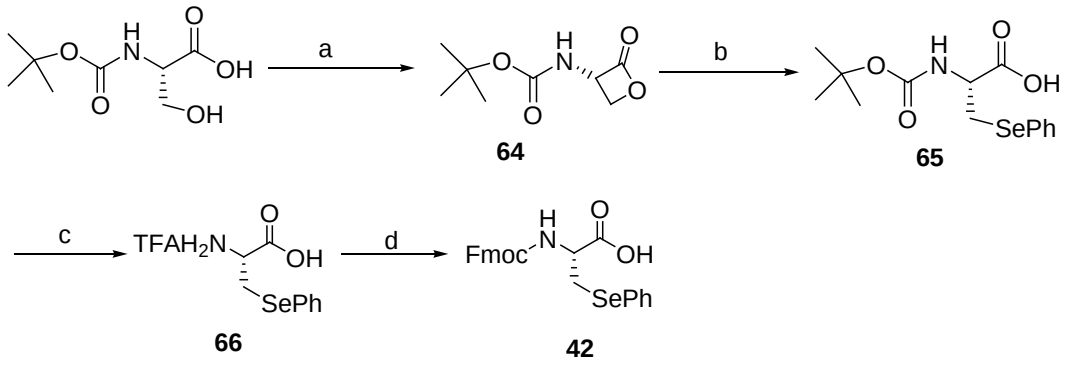

Scheme 5-3 Synthesis of a dehydroalanine precursor, Fmoc-phenylselenocysteine (42). Reagents and conditions: (a) DEAD, PPh_3, THF, -78 °C to room temp.; (b) PhSeSePh, $NaBH(OMe)_3$, EtOH, room temp.; (c) TFA/DCM, room temp.; (d) Fmoc-OSu, $NaHCO_3$, THF/H_2O, room temp.

N-Boc-Serine was firstly converted to its β-lactone (**64**) *via* intramolecular Misunobu reaction. This was followed by ring opening with phenylselenide anion which was generated by the reaction of diphenyl diselenide with sodium

trimethoxyborohydride. The resulting Boc-protected **65** was converted to its Fmoc derivatives **42** *via* standard conditions.

The overall yields over this four-step synthesis ranged from 35 to 40 %. The spectroscopic data of the *N*-Boc-phenylselenocysteine (**65**) was identical to that reported in the literature.[150] It should be noted that Fmoc-phenylselenocysteine (**42**) is stable to storage at room temperature without noticeable decomposition over at least several months. Unmasking of the dehydroalanine by oxidative elimination would be carried out in the ultimate step of the synthesis of argyrin.

5.4 Fmoc solid-phase synthesis of proteasome inhibitors argyrin A and analogues thereof

Having obtained the three unique amino acid building blocks, the work continued with the synthesis the cyclic peptide argyrin A. As outlined in Scheme 5-4, the strategy involved Fmoc solid phase peptide synthesis and in a solution-based head-to-tail cyclisation.

Fmoc SPPS was used for the synthesis of the linear argyrin precursors. Sarcosine was chosen as the *C*-terminal end to attach to the resin linker 2-chlorotrityl chloride polystyrene (**40**). Having determined the resin loading, all subsequent amino acids were coupled to the peptidyl resin manually. Sequential acylation reactions were carried out using appropriately *N*-protected amino acids, *N*-Fmoc amino acids (3-4 eq.) and carboxyl-activating reagent PyOxim or HATU (3-4 eq.) in the presence of DIPEA (6-8 eq.). Repetitive *N*-Fmoc deprotection was achieved by using 20 % *v/v* piperidine in DMF.

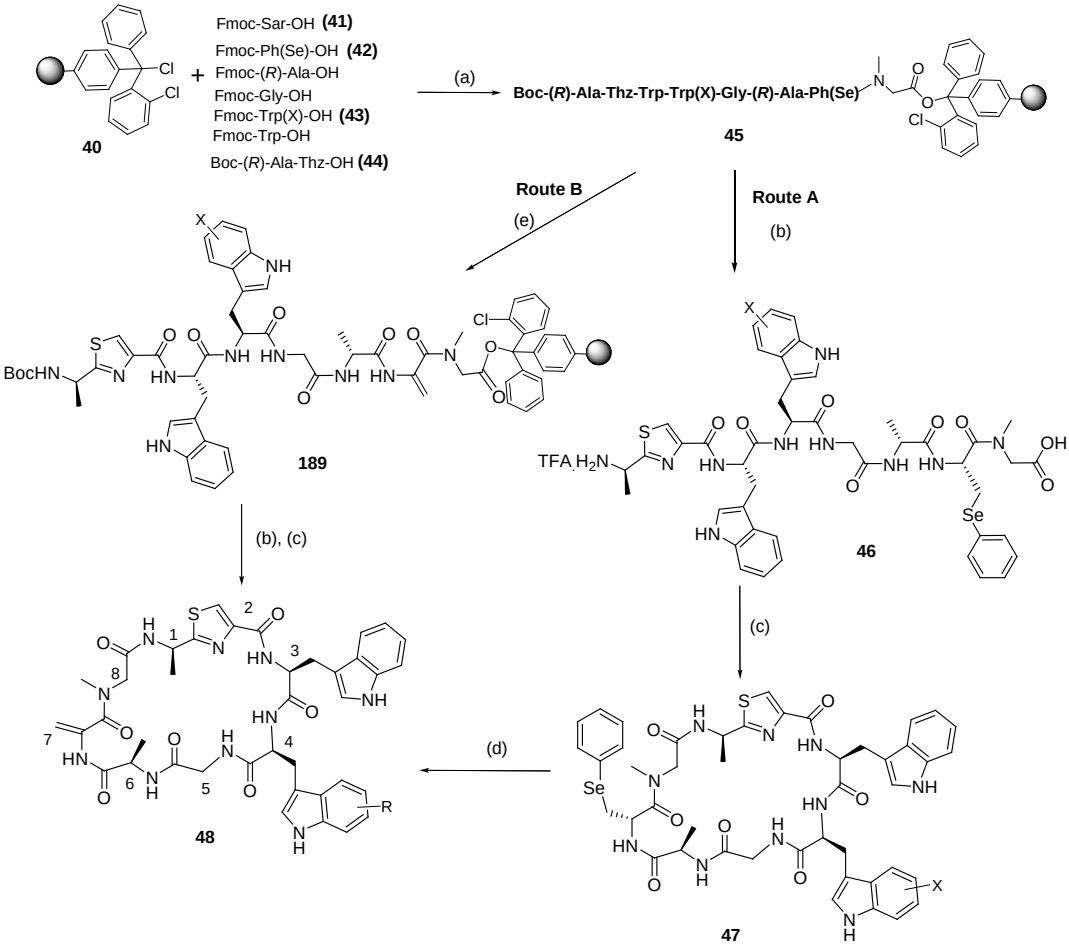

Route A	**a**	**b**	**c**	**e**	**f**	**g**	**Route B**	**d**	**h**	**k**
X =	H	5-Br	5-Cl	7-Et	5-Me	5-MeO		6-F	4-MeO	(*R*)-Trp
Yield (%)	11	6	8	8	11	4		4	6	16

Scheme 5-4 Synthesis of argryin A and analogues thereof (48). Reagents and conditions: (a) i. piperidine /DMF (1:4); ii.Fmoc-amino acids, PyOxim or HATU, DIPEA; (b) TFA/DCM, H_2O, TIPS.; (c) PyBOP, HOBt, DIPEA; (d) i. $NaIO_4$, CH_3CN/H_2O; ii. Na_2CO_3, CH_3CN/H_2O; (e) $NaIO_4$, DMF/H_2O.

In route A, the assembled **45** were universal deprotected and cleaved form the resin using 50 % *v/v* TFA in DCM. Subsequent cyclisation in high diluted solution for 3 days results in the cyclic peptides **47**. Finally, oxidative elimination of the phenylselenocysteine residue to *exo*-methylene afforded the final argyrin and analogues thereof in an overall yield of 4-11 %.

Alternatively, in route B, instead of releasing the linear precursor into solution after peptide assembly, on-resin oxidative elimination was employed to afford **180**. Subsequent cleavage of the resin followed by cyclisation in high diluted solution resulted in the final argyrin analogues in an overall yield of 4-16 %.

In summary, the first solid-phase-based synthesis of the cyclic octapeptide argyrin A and analogues was established. However, both route A and route B gave relatively low yields. Nevertheless, the purity and quantity achieved after preparative HPLC were suitable for preliminary biological test. All synthetic argyrin analogues were characterised by MS, ^{1}H and 2D COSY NMR spectrometry.

5.5 SAR study of argyrins

Synthetic argyrin A, argyrin E and seven novel argyrin analogues were tested in a cell viability assay using HCT-116 human colon cancer cell line. The obtained GI_{50} values are listed in Table 5-1.

Table 5-1 Inhibition of HCT-116 cell proliferation by argyrins.

#	Argyrin analogues	GI_{50} (nM) [a]
48a	***Cyclo*** [(*R*)-Ala^{1}-Thz^{2}-Trp^{3}-Trp^{4}-Gly^{5}-(*R*)-Ala^{6}-Dha^{7}-Sar^{8}] / Argyrin E	227 ± 10.8
48b	***Cyclo*** [(*R*)-Ala-Thz-Trp-(5-Br)-Trp-Gly-(*R*)-Ala-Dha-Sar]	26 ± 4.1
48c	***Cyclo*** [(*R*)-Ala-Thz-Trp-(5-Cl)-Trp-Gly-(*R*)-Ala-Dha-Sar]	20 ± 1.3
48e	***Cyclo*** [(*R*)-Ala-Thz-Trp-(7-Et)-Trp-Gly-(*R*)-Ala-Dha-Sar]	133 ± 91
48f	***Cyclo*** [(*R*)-Ala-Thz-Trp-(5-Me)-Trp-Gly-(*R*)-Ala-Dha-Sar]	26 ± 0.2
48g	***Cyclo*** [(*R*)-Ala-Thz-Trp-(5-MeO)-Trp-Gly-(*R*)-Ala-Dha-Sar]	3.8 ± 2.7
48d	***Cyclo*** [(*R*)-Ala-Thz-Trp-(6-F)-Trp-Gly-(*R*)-Ala-Dha-Sar]	40 ± 6.0
48h	***Cyclo*** [(*R*)-Ala-Thz-Trp-(4-MeO)-Trp-Gly-(*R*)-Ala-Dha-Sar] / Argyrin A	1.8 ± 0.6
48k	***Cyclo*** [(*R*)-Ala-Thz-Trp-(*R*)-Trp-Gly-(*R*)-Ala-Dha-Sar]	335 ± 7
	Bortezomib [b]	2.5 ± 0.8

[a] Concentration needed to inhibit cell growth by 50% as determined from the dose-response curve. Determinations were made at 6 different concentrations of argyrins using MTT cell proliferation assays.
[b] This clinically used drug was purchased from Sigma-Aldrich.

The results showed that most synthetic argyrin derivatives displayed growth inhibitory effects on HCT-116 human colon cancer cell line at nanomolar concentrations. These results are comparable to that reported by Nickeleit *et al*. It

has been proposed that the cytotoxic effect is due to inhibition of proteasomal activity. Among the nine argyrins, argyrin A which comprised 4-methoxy-Trp^4 displayed the greatest activity with GI_{50} value at 1.8 nM. Significantly, a comparable GI_{50} value was observed for argyrin **48g** which indicate 4-methoxy group on Trp^4 is tolerated at the 5-position.

However, other derivatives lacking the methoxy group on Trp^4 displayed less activity; the activity shown by halogenated compounds **48b**, **48c** and **48d** were not significantly different, but was 10-fold less potent when compared with argyrin A. Both isomers of argyrin E which lack substitution on Trp^4 displayed low activities.

In summary, the preliminary cytotoxicity study of argyrin A and analogues confirmed that a methoxy group at 4- or 5-position of Trp^4 showed the best cytotoxic activity. This finding is in agreement with the hypothesis that the methoxy moiety of Trp^4 is required to form a hydrogen bond with the active site of proteasome. Such result provided valuable information with respect to structure-activity relationship studies.

5.6 **Further studies**

The major goal of this thesis was the total synthesis of argyrin A and analogues thereof. This has been achieved by developing a generic route to the synthesis of *N*-Fmoc tryptophan analogues which is required for the argyrin synthesis. In addition, a convenient and efficient methodology to synthesise argyrin A has been established.

The ultimate goal of this project was to derive a library of rationally designed analogues of argyrin A. It is clear now that argyrin A and the eight analogues thereof have displayed anti-proliferative effect against HCT-116 tumour cell line. It is envisaged that these compounds will also show cytotoxic activity on other human tumour cell lines. Thus, further work in evaluating the biological properties would include (1) screening of a wider panel of human tumour cell lines against argyrin analogues to determine the sensitivity of individual cell line to the treatment of argyrin analogues, and (2) testing whether the cytotoxic effect is due to proteasome inhibition.

Besides HCT-116, a variety of cell lines, such as SW480 (colon adenocarcinoma), A549 (lung cancer), MCF7 (breast cancer), HeLa (cervical cancer) and human fibroblast cell lines could be tested against the nine synthetic argyrin analogues. The preliminary findings reported by Nickeleit *et al*. suggested that all these cell lines are sensitive to argyrin A with IC_{50} values in the low nanomolar range.[3] As revealed by the measurement of the sub-G1 DNA fraction in flow cytometry histograms, they suggested that argyrin A exhibits two different cellular phenotypes. Primary human fibroblast and A549 cells ceased to proliferate, whereas WS480, MDF7 and Hela cells underwent apoptosis.[3] Further time course experiments with these cell lines found that argyrin A treatment resulted in stabilisation of cellular p27 levels by preventing the turnover of the protein.[3]

Thus, in order to determine if proteasome inhibition is responsible for the cytotoxic effect of argyrin A and analogues, it is crucial to establish their proteasome inhibitory activity. To date, there are two available methods to monitor proteasome activity. One utilised purified human 20S proteasome from cell lysates.[104] 20S proteasome incubated with the argyrin analogues, and the CT-L, C-L and T-L activities of proteasome could be measured using fluorogenic peptide substrates specific for the three catalytic subunits The increase in fluorescence is proportional to the remaining proteasome activity. The other method is to assess proteasome activity in whole cells using site-specific proteasome probes.[306] Experiments are conducted using cell-permeable, fluorophore labelled proteasome inhibitors which specifically bind to and eventually label the active sites of the proteasome. The amount of fluorophore generated is proportional to the remaining proteasome activity.

In addition to the biological studies, further investigation into the structural modification of the other amino acid residues will be undertaken. Having established the SPPS of argyrin A, the main efforts towards the total synthesis of argyrin analogues are the preparation of the three unusual amino acid building blocks. Thus, a possible avenue for further investigation is to simplify the structure of argyrin A without compromising biological activities.

Since the methoxy group in Trp^4 was found to be crucial for the biological activity of argyrin A, the first logical progression is the synthesis of *O*-methyl-Tyr^4-argyrin

194 and **195**, in which the 4-methoxy-trypophan residue is respectively replaced by the *O*-methyl tyrosine and *O*-methyl-*m*-tyrosine (Figure 5-1).

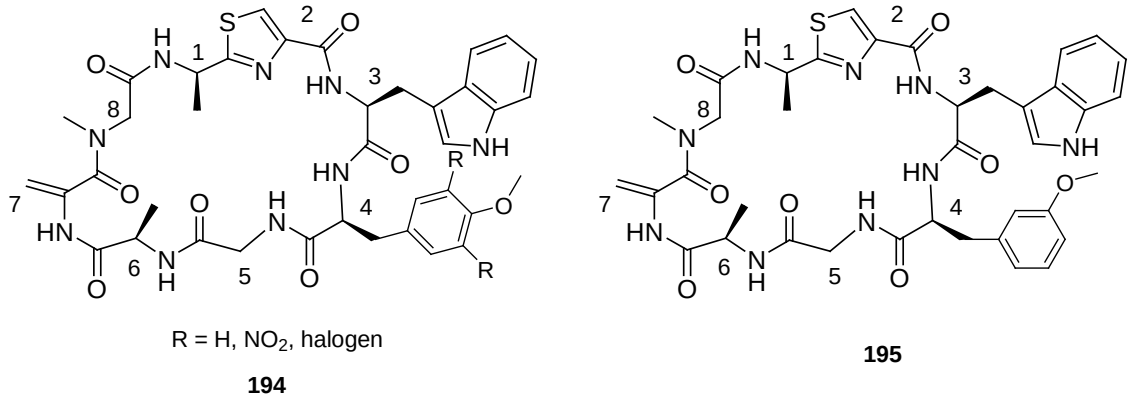

Figure 5-1 Chemical structure of two proposed (*O*-methyl-Tyr^4)-argyrin analogues.

It is anticipated that theses analogues would preserve the aryl methoxy group and physicochemical properties of the aromatic side-chain. The use of tyrosine as a Trp-mimetic residue is not only to avoid laborious preparation of tryptophan derivatives, but also to facilitate the derivatisation of 4-hydroxyphenyl side chain into a various different functional substitutions which are deemed suitable for further SAR studies.

Having examined the structural modifications of the unusual amino acid 4-methoxy-Trp^4, attention could now be focused on optimisation of the dipeptide (*R*)-Ala^1-Thz^2-OH. The computational docking studies of argyrin A bound to the proteasome revealed that the three active sites of proteasome were not involved in any interaction with the dipeptide, particularly with the thiazole moiety.[155] In order to test this hypothesis and to simplify the synthesis, analogues **196** and **197** can be respectively prepared using Ala^2 and Dha^2 in place of the Thz^2 residue. This modification is not expected to change the conformation of the argyrin backbone significantly.

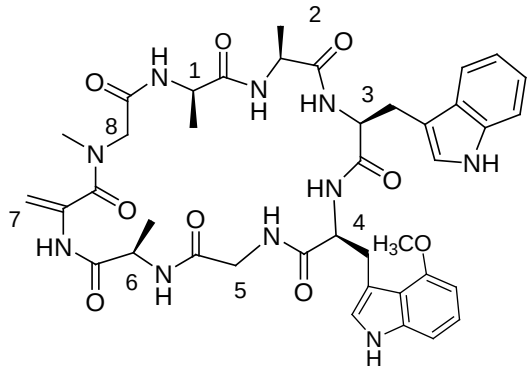

196

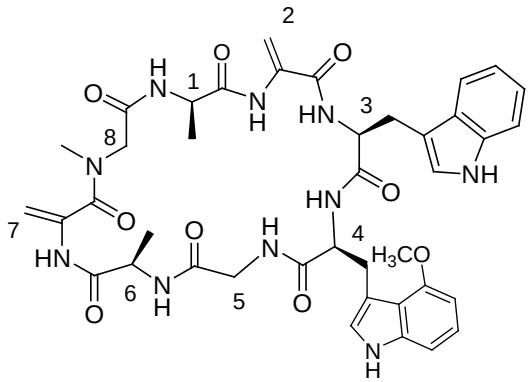

197

Based on previous SAR studies, absence of the dehydroalanine residue displayed significantly less activity due to reduction of conformational rigidity of the peptide backbone.[155] Nevertheless, as reported in the thesis, dehydroalanine moiety is stable in 50 % TFA acidolysis and other basic conditions during peptide coupling processes, it is therefore envisioned that it might not be necessary to prepare Fmoc-phenylselenocysteine as a precursor. Thus, an efficient method of introducing dehydroalanine into argyrin could be achieved using Fmoc-*S*-benzylcysteine (**198**), followed by oxidation and elimination to yield the Dha[7] residue.[307]

The proposed method for the synthesis of Dha[7] is outlined in Scheme 5-5. Sequential coupling of seven amino acid building blocks yields the on-resin linear precursor, which is then subjected to oxidation of the side chain of *S*-benzyl-Cys[7], followed by elimination, to yield the linear argyrin **199**. Subsequent cleavage from resin followed by cyclisation in high dilution affords argyrin A. The advantages of using this strategy are: (1) Fmoc-*S*-benzylcysteine (**198**) is commercially available, (2) *S*-benzylcysteine is stable in standard Fmoc deprotection conditions and (3) it is less toxic than selenocysteine.

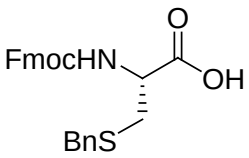

198

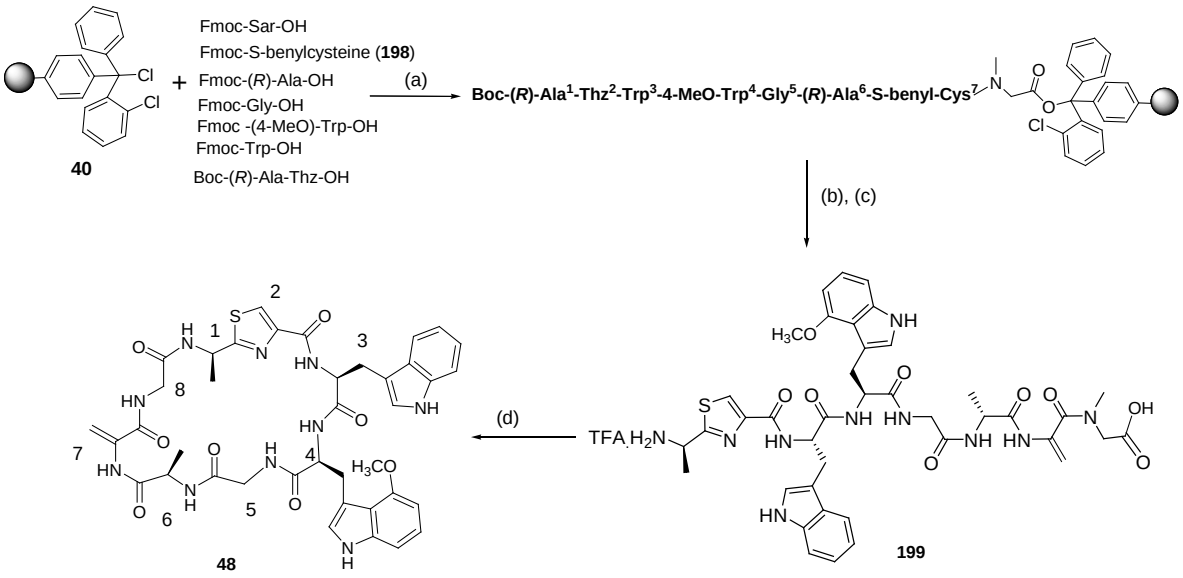

Scheme 5-5 Proposed scheme for the synthesis of argyrin A utilising *N*-Fmoc-*S*-benzylcysteine (198) as a dehydroalanine precursor. Reagents and conditions: (a) i. Piperidine /DMF (1:4); ii.Fmoc-amino acids, PyOxim or HATU, DIPEA; (b) i. *m*-CPBA, DCM, 0 °C; ii. DBU, MeOH or dioxane, reflux; (c) TFA/DCM, H_2O, TIPS; (d) PyBOP, HOBt, DIPEA.

As illustrated in Chapter 3.3, several attempts of obtaining the dipeptide analogue (*R*)-Ala-oxazole suitable for SPPS were unsuccessful, yielding a racemic mixture of (*R*)-Ala-oxazole and (*S*)-Ala-oxazole. It is deemed necessary either to optimise the conditions of the described processes or to investigate a different approach. As an alternative approach, oxazole derivatives could be accessed following a one-step oxazole synthesis established by Williams *et al.*.[308] They utilised bis(2-methoxyethyl)aminosulfur trifluoride (Deoxo-Fluor) (**200**) for the cyclo-dehydrative conversion of β-hydroxy amides to oxazole derivatives with no evidence of epimerisation.[308] Optically pure (*R*)-Ala-oxazole-OEt therefore could be synthesised following the proposed synthetic route shown in Scheme 5-6.

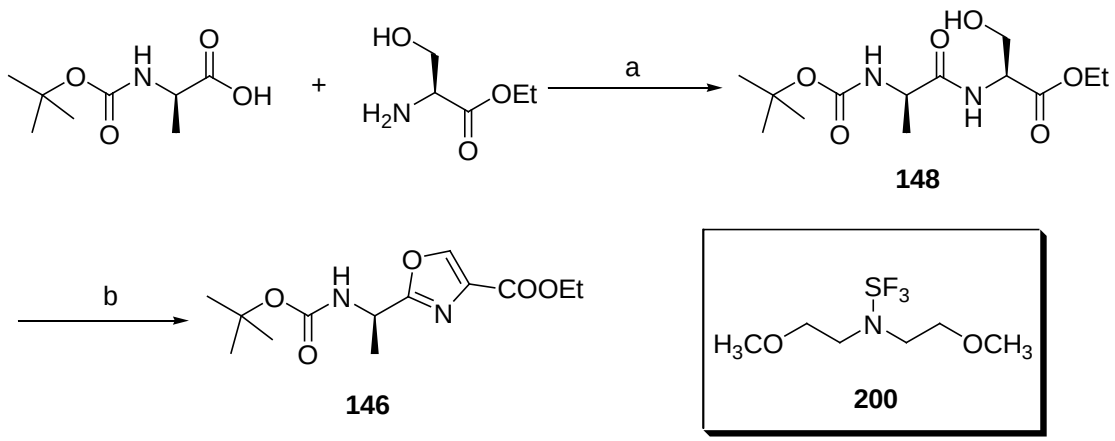

Scheme 5-6 Synthesis of *N*-Boc-(*R*)-Ala-oxazole-OEt (146) *via* Mitsunobu reaction. Reagents and conditions: (a) DCC, HOBt, DIPEA, DCM; (b) **200**, -20 °C; then $BrCCl_3$, DBU, 2-3 °C, 8 h.

As shown above, *N*-Boc-(*R*)-Ala-OH is first coupled with serine ethyl ester under standard conditions to give the amide **148**. Subsequent fluorination with Deoxo-Fluor (**200**) at -20 °C followed by oxidation, gives the desired (*R*)-Ala-oxazole-OEt **146**. The significance of this approach is the cyclisation and the oxidation performed under mild conditions, avoiding the potential epimerisation and hence giving a high optical purity (e.e. > 97 %) and good yields (> 60 %).[308]

In conclusion, the SPPS strategy established in this thesis has given access to argyrin A and a wide range of analogues.

Chapter 6

Experimental

6.1 **Materials and instrumentation**

Reagents which were used in the experiments were obtained from Sigma-Aldrich, Fisher scientific, Acros and TCI. 2-Chlorotrityl chloride resins were purchased from Novabiochem (100-200 mesh, 1% DVB, loading 1.2 mmol /g). The silica gel (sorbsil®, Group Rhone Poulene, UK) or ISOLUTE® scaffold (international sorbent technology, UK) were used for the column and flash chromatography respectively. Dried solvents such as DME, ethanol and THF, were used as supplied. All glassware was oven-dried overnight prior to use. TLC was carried out on Merck 60

F254 silica gel plates and visualised by UV irradiation 254 nm or by staining with $KMnO_4$ or ninhydrin solution if appropriate.

The identification of the prepared compound was done by using melting point apparatus, infrared spectra, polarimeter, nuclear magnetic resonance spectra and mass spectroscopy.

Melting points were measured on a Gallenkamp melting point apparatus and are uncorrected. Infrared spectra were obtained from an Avatar 360 Nicolet FT-IR spectrophotometer in the range of 4000-500 cm^{-1} using KBr discs. Absorption maxima (υ_{max}) are reported in wave numbers (cm^{-1}). Only signals representing functional groups are reported. Absorptions from the fingerprint region are not listed. Optical rotations were measured on an ADP220 model polarimeter. $[\alpha]_D$ values are reported in 10^{-1} deg. cm^{-2}. g^{-1}, concentration (*c*) is in gram per 100 mL.

Proton nuclear magnetic resonance (δ^{H}), carbon nuclear magnetic resonance (δ^{C}) and fluorine nuclear magnetic resonance (δ^{F}) spectra were obtained at room temperature on a Bruker 400 Ultrashield operating at 400.13 MHz, 101.62 MHz and 400.13 MHz, respectively. Deuterated solvents used were deuterium oxide, $CDCl_3$, acetone-d_6, CD_3OD and DMSO-d_6. Chemical shifts (δ) were recorded in ppm relative to TMS and coupling constants (*J*) were recorded in Hz. Abbreviations used in the description of spectra are: s, singlet; d, doublet; t, triplet; q, quartet and m, multiplet. ^{1}H and ^{13}C assignments were typically achieved using COSY, HSQC, DEPT 90 & 135. Mass spectra were recorded on a Waters 2759 spectrometer with both the positive and negative electrospray ionisation.

Analytical reverse-phase high performance liquid chromatography (RP-HPLC) was performed on an Onyx monolithic-C_{18} column (100 x 4.6 mm) at 3.0 mL min^{-1}. Eluent detection was monitored by UV absorbance at 214 nm. Solvent **A** was 100 % water + 0.06 % TFA and solvent **B** was 80 % aqueous acetonitrile + 0.06 % TFA. Preparative RP-HPLC was performed on an Onyx monolithic-C_{18} semi-preparative column (100 x 10 mm) at 9 mL min^{-1}.

Peptide synthesis was carried out using a NOVASYN® GEM manual peptide synthesiser with DMF to remove excess amino acid and coupling reagents. Fmoc deprotection was achieved by 20 % piperidine in DMF. The reaction progress was

monitored by UV absorbance at 344 nm. *N*-Fmoc deprotection profiles were recorded using a LKB Bromma 2210 recorder.

6.2 Experimental for Chapter 2

6.2.1 Preparation of indole-3-carbaldehyde derivatives

General procedure for the preparation of 6-fluoro-1*H*-indole-3-carbaldehyde (50d)

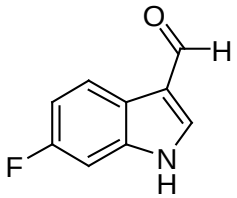

Phosphoryl chloride (1.2 mL, 13.4 mmol) was added dropwise to dry DMF (10 mL) at 0 °C. The mixture was stirred for 10 min. Then the solution of 5-fluoroindole (1.2 g, 9.0 mmol) in DMF (8 mL) was added dropwise to the mixture. The solution was heated to 45 °C and was stirred for 2 h. The reaction was poured onto ice water (50 mL), extracted with Et_2O (2 x 30 mL). The aqueous layer was treated with 1 M NaOH to pH = 9 and extracted with EtOAc (2 x 50 mL). The organic layers were combined, washed with brine, dried and concentrated to give **50d** as yellow crystals (0.9 g, 66 % yield) m.p. 174-178 °C; R_f = 0.2 (Hexane/EtOAc, 2:1); IR (KBr): ν = 2933, 1641, 1530, 1448, 1149 cm^{-1}. ^1H NMR (400 MHz, acetone-d_6): δ = 7.08 (td, J = 8, 2 Hz, 1H, H-5 or H-7), 7.31 (dd, J = 8 ,2 Hz, H-5 or H-7), 8.22 (dd, J = 8, 2 Hz,1H, H-4), 8.24 (s, 1H, H-2), 10.03 (s, 1H, CHO), 11.28 (br, 1H, NH) ppm. ^{13}C NMR (100 MHz, acetone-d_6): δ = 98.46 (d, J = 26 Hz, CH), 110.41 (d, J = 24 Hz, CH), 119.08 (C), 121.19 (C), 122.42 (d, J = 10 Hz, CH), 137.85 (CH), 159.18 (C), 161.54 (C), 184.43 (CHO) ppm; MS: *m/z* (+ESI) calcd for C_9H_7FNO 164.0512, found 164.0430 [MH^+].

7-Ethyl-1H-indole-3-carbaldehyde (50e)

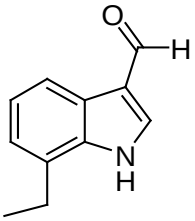

Procedure as described in the general procedure using phosphoryl chloride (1 mL, 10.9 mmol), 7-ethylindole (1 mL, 7.3 mmol) and DMF (8 mL) gave **50e** as brown powder (1.1 g, 95 % yield) m.p. 92-94 °C; R_f = 0.2 (Hexane/EtOAc, 2:1). IR (KBr): ν = 3166, 3054, 1628, 1456, 1228 cm^{-1}. ^1H NMR (400 MHz, $CDCl_3$): δ = 1.38 (t, J = 7.5 Hz, 3H, CH_2CH_3), 2.98 (q, J = 7.5 Hz, 2H, CH_2CH_3), 7.18 (d, J = 7 Hz, 1H, H-5 or H-6), 7.29 (t, J = 7 Hz, 1H, H-5 or H-6), 7.90 (d, J = 1 Hz,1H, H-2), 8.19 (d, J =7 Hz, 1H, H-4), 9.95 (br, 1H, NH), 10.05 (s, 1H, CHO) ppm. ^{13}C NMR (100 MHz, $CDCl_3$): δ = 14.11 (CH_3), 23.97 (CH_2), 119.33 (C), 119.70 (CH), 123.06(CH), 123.36 (CH), 127.63 (C), 135.91 (C), 136.31 (C), 146.54 (CH), 185.68 (CHO) ppm. MS: *m/z* (+ESI) calcd for $C_{11}H_{12}NO$ 174.0919, found 174.0805 [MH^+].

5-Methyl-1*H*-indole-3-carbaldehyde (50f)

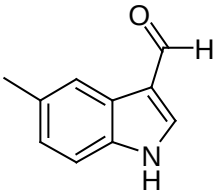

Procedure as described in the general procedure using phosphoryl chloride (1 mL, 11.3 mmol), 5-methylindole (1 g, 7.58 mmol) and DMF (10 mL) gave **50f** as yellow crystals (0.8 g, 65 % yield) m.p. 150- 151 °C; R_f = 0.2 (Hexane/EtOAc, 2:1). IR (KBr): ν = 3214, 1636, 1437, 1388 cm^{-1}. ^1H NMR (400 MHz, acetone-d_6): δ = 2.45 (s, 3H, CH_3), 7.12 (dd, J = 8, 2 Hz, 1H, H-6 or H-7), 7.44 (dd, J = 8 ,2 Hz, H-6 or H-7), 8.06 (d, J = 2 Hz, 1H, H-4), 8.15 (s, 1H, H-2), 10.02 (s, 1H, CHO), 11.08 (br, 1H, NH) ppm. ^{13}C NMR (100 MHz, acetone-d_6): δ = 20.71 (CH_3), 111.74 (CH), 118.90 (C), 121.11 (CH), 124.92 (C), 125.12 (CH), 131.47 (CH), 135.72 (C), 137.20 (C), 184.39 (CHO) ppm. MS: *m/z* (+ESI) calcd for $C_{10}H_{10}NO$ 160.0762, found 160.0667 [MH^+].

5-Methoxyl-1*H*-indole-3-carbaldehyde (50g)

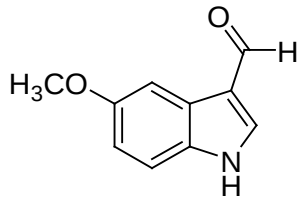

Procedure as described in the general procedure using phosphoryl chloride (2.87 mL, 30.6 mmol), 5-methoxylindole (3 g, 20.4 mmol) and DMF (10 mL) gave **50g** as yellow crystals (1.9 g, 54 % yield) m.p. 179-183 °C; R_f = 0.2 (Hexane/EtOAc, 2:1) IR (KBr): ν = 3170, 1641, 1432, 1263, 790 cm^{-1}. ^1H NMR (400 MHz, $CDCl_3$): δ = 3.89 (s, 3H, OCH_3), 6.95 (dd, J = 7, 2 Hz, 1H, H-6), 7.34 (d, J = 7 Hz, 1H, H-7), 7.78 (s, 1H, H-2), 7.79 (d, J = 2 Hz, 1H, H-4), 9.99 (s, 1H, CHO) ppm. ^{13}C NMR (100 MHz, $CDCl_3$): δ = 55.81 (OCH_3), 103.11 (CH), 112.50 (CH), 114.83 (CH), 119.42 (C), 125.23 (C), 131.60 (C), 136.31 (CH), 156.57 (C), 185.23 (CHO) ppm. MS: *m/z* (+ESI) calcd for $C_{10}H_{10}NO_2$ 176.0712, found 176.0650 [MH^+].

4-Methoxyl-1*H*-indole-3-carbaldehyde (50h)

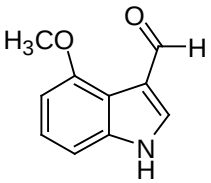

Procedure as described in the general procedure using phosphoryl chloride (0.9 mL, 10.2 mmol), 4-methoxylindole (1 g, 6.8 mmol) and DMF (10 mL) gave **50h** as a yellow powder (0.8 g, 70 % yield) m.p. 148-150 °C; R_f = 0.2 (Hexane/EtOAc, 2:1). IR (KBr): ν = 3250, 1642, 1361, 1323, 790 cm^{-1}. ^1H NMR (400 MHz, $CDCl_3$): δ = 4.01 (s, 3H, OCH_3), 6.77 (dd, J = 7, 2 Hz, 1H, H-6), 7.19 (d, J = 7 Hz, 1H, H-7), 7.19 (s, 1H, H-5), 8.04 (s, 1H, H-2), 10.51 (s, 1H, CHO) ppm. ^{13}C NMR (100 MHz, acetone-d_6): δ = 54.81(OCH_3), 102.09 (CH), 105.67 (CH), 116.16 (C), 119.08 (C), 123.73 (CH), 128.45 (CH), 138.22 (C), 154.43 (C), 186.72 (CHO) ppm. MS: *m/z* (+ESI) calcd for $C_{10}H_{10}NO_2$ 176.0712, found 176.0672 [MH^+].

1-Methyl-indole-3-carbaldehyde (50i)

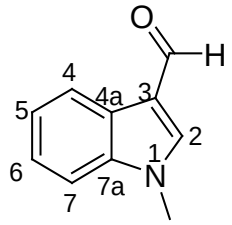

Procedure as described in the general procedure using phosphoryl chloride (2.1 mL, 23 mmol), 1-methylindole (1 g, 7.4 mmol) and DMF (10 mL) gave **50i** as purple crystals (2.07 g, 83 % yield); m.p. 67-70 °C; R_f = 0.2 (Hexane/EtOAc, 2:1); IR (KBr): ν = 3438, 1640, 1535, 1381, 1074 cm^{-1}. ^1H NMR (400 MHz, $CDCl_3$): δ = 3.66 (s, 3 H, CH_3), 7.27 (m, 3H, H-5, 6, 7), 7.46 (s, 1H, H-2), 8.27 (dd, J = 7.2, 1 Hz, H-4), 9.84 (s, 1 H, CHO) ppm. ^{13}C NMR (100 MHz, $CDCl_3$): δ = 33.51 (CH_3), 110.04 (C-7), 117.78 (C-3), 121.78 (C-4), 122.82 (C-5), 123.93 (C-6), 125.07 (C-4a), 137.83 (C-7a), 139.81 (C-2), 184.46 (CHO) ppm. MS: *m/z* (+ESI) calcd for $C_{10}H_{10}NO$ 160.0762, found 160.0650 [MH^+].

2-Methyl-1*H*-indole-3-carbaldehyde (50j)

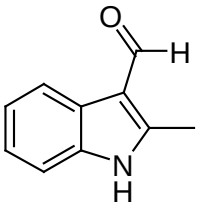

Procedure as described in the general procedure using phosphoryl chloride (2.1 mL, 22.8 mmol), 2-methylindole (2 g, 15.2 mmol) and DMF (10 mL) gave **50j** as a brown powder (1.8 g, 77 % yield) m.p. 204-205 °C; R_f = 0.2 (Hexane/EtOAc, 2:1); IR (KBr): ν = 3267, 1636, 1469, 1378, 1243 cm^{-1}. ^1H NMR (400 MHz, $CDCl_3$): δ = 2.77 (s, 3H, CH_3), 7.28 (m, 2H, H-5, 6), 7.35 (dd, 1H, J = 7.2, 1 Hz, H-7), 8.27 (dd, J = 7.2, 1 Hz, H-4), 8.70 (br, 1H, NH), 10.22 (s, 1 H, CHO) ppm. ^{13}C NMR (100 MHz, $CDCl_3$): δ = 12.28 (CH_3), 110.65 (CH), 114.83 (C), 120.88 (CH), 122.82 (CH), 123.46 (CH), 126.07 (C), 134.91 (C), 146.54 (C), 184.58 (CHO) ppm. MS: *m/z* (+ESI) calcd for $C_{10}H_{10}NO$ 160.0762, found 160.0592 [MH^+].

6.2.2 Preparation of 2-(2-hydroxy-1-phenylehtylamino)-3-(1*H*-indol-3-yl)propanenitrile derivatives

General procedure for the preparation of 2-(2-hydroxy-1-phenylehtylamino)-3-(1*H*-indol-3-yl)propanenitrile (52a)

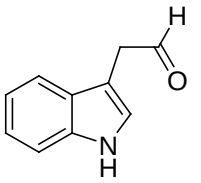

51a

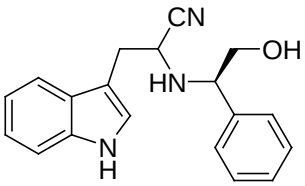

52a

A white suspension of (methoxymethyl)triphenylphosphonium chloride (2.3 g, 6.9 mmol) in dry THF (18 mL) was cooled to 0 °C under nitrogen, and treated with 2.5 M *n*-butyllithium in hexane (3.3 mL, 8.28 mmol). The reaction was stirred for 15 min then **50a** (500 mg, 3.45 mmol) in dry THF (15 mL) was added and stirred at room temperature for 2 h. Excess butyllithium was quenched by adding a few drops of MeOH. The mixture was acidified with 3 M HCl to pH = 7. The solvent was removed *in vacuo*. The residue was partitioned between EtOAc (100 mL) and brine (100 mL). The organic layer was dried and concentrated. The resultant residue was subjected to column chromatography (hexane/EtOAc, 1:1) to afford the enol ether intermediate. The enol ether intermediate was subsequently treated with THF (18 mL) and 1M HCl (12 mL). After being heated at reflux for 3 h, the solution was cooled and partitioned between Et_2O (80 mL) and brine (80 mL). The organic layer was dried and concentrated to afford **51a**.

(*R*)-2-phenylglycinol (449 mg, 3.3 mmol) and acetic acid (372 µL, 6.57 mmol) was added to a solution of **51a** (435 mg, 2.74 mmol) in MeOH (20 mL) at 0 °C. Sodium cyanide (160 mg, 3.28 mmol) was added to the solution immediately. The mixture was allowed to warm to room temperature and stirred for 16 h. The solvent was removed under reduced pressure, and the residue was partitioned between DCM (2 x 40 mL) and brine (80 mL). The organic layers were combined dried and concentrated. Purification of the residue by column chromatography ($CHCl_3$/MeOH, 30:1) gave **52a** as orange amorphous solid (307 mg, 29 % yield from **50a**); R_f = 0.3 (Hexane/EtOAc, 1:1); RP-HPLC 10-60 % B in 12 min, t_R 5.7

min for (*R*,*R*) isomer and 6.7 min for (*S*,*R*) isomer; IR (KBr): ν = 3413, 2924, 2873, 1455, 1356, 744 cm^{-1}. ^1H NMR (400 MHz, $CDCl_3$): δ = 2.58 (br, 1 H, NH), 3.23 (d, *J* = 4 Hz, 1H , CH_AH_B), 3.24 (d, *J* = 4 Hz, 1H , CH_AH_B), 3.52 (dd, *J* = 12, 8 Hz, 1H, CH_AH_BOH), 3.67 (dd, *J* = 4, 4 Hz, 1H, α-H), 3.70 (dd, *J* = 12, 8 Hz, 1H, CH_AH_BOH), 4.05 (dd, *J* = 8, 4 Hz, 1H, $CHCH_2OH$), 7.10- 7.59 (m, 10 H, arom. H), 8.30 (br, 1 H, NH) ppm. ^{13}C NMR (100 MHz, $CDCl_3$): δ = 29.47 (CH_2), 49.02 (CH), 63.03 (CH), 67.22 (CH_2), 109.13, 111.49, 118.60, 119.68, 120.53, 122.27, 123.75, 127.28, 127.63, 128.26, 128.87, 136.17, 138.31 ppm. MS: *m/z* (+ESI) calcd for $C_{19}H_{20}N_3O$ 306.1606, found 306.1680 [MH^+].

3-(5-Bromo-indol-3-yl)-2-[1-(4-methoxy-phenyl)-ethylamino]-propanenitrile (52b)

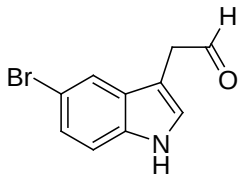

51b

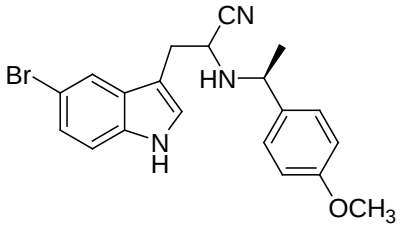

52b

Procedure as described in the general procedure using (methoxymethyl)triphenylphosphonium chloride (2.14 g, 6.3 mmol), 2.5 M *n*-butyllithium in hexane (3 mL, 7.5 mmol) and **50b** (700 mg, 3.1 mmol) afforded **51b.**

Procedure as described in the general procedure using **51b** (486 mg, 2.1 mmol), (*S*)-4-methoxy-α-methylbenzylamine (362 µL, 2.5 mmol), acetic acid (277 µL, 4.9 mmol) and sodium cyanide (120 mg, 2.5 mmol) gave **52b** as a yellow oil (442 mg, 39 % yield from **50b**); R_f = 0.4 (Hexane/EtOAc, 2:1); RP-HPLC 10-60 % B in 12 min, t_R 7.0 min for (*R*,*R*) isomer and 7.6 min for (*S*,*R*) isomer; IR (KBr): ν = 3418, 2960, 1459, 1244, 755 cm^{-1}. ^1H NMR (400 MHz, $CDCl_3$): δ = 1.35 (d, *J* = 6 Hz, 3H, CH_3), 1.68 (br, 1H, NH), 3.13 (d, *J* = 6 Hz, 2 H, CH_2), 3.56 (t, *J* = 6 Hz, 1H, α-H), 3.85 (s, 3H, OCH_3), 4.02 (q, *J* = 6 Hz, 1H, $CHCH_3$), 6.90- 7.30 (m, 7H, arom. H), 7.66 (d, *J* = 2 Hz, 1H, arom. H), 8.43 (br, 1H, NH) ppm. ^{13}C NMR (100 MHz, $CDCl_3$): δ = 24.85 (CH_3), 29.52 (CH_2), 49.27 (CH), 55.36 (OCH_3), 56.00 (CH),

109.19, 112.88, 113.01, 114.20, 120.64, 121.32, 124.76, 125.15, 127.89, 129.15, 134.80, 135.09, 159.10 ppm.

3-(5-Chloro-indol-3-yl)-2-[1-(4-methoxy-phenyl)-ethylamino]-propanenitrile (52c)

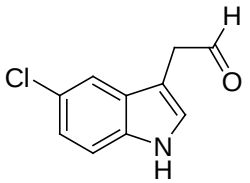

51c

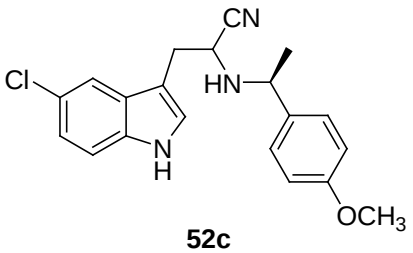

52c

Procedure as described in the general procedure using (methoxymethyl)triphenylphosphonium chloride (2.68 g, 7.8 mmol), 2.5 M *n*-butyllithium in hexane (3.7 mL, 9.4 mmol) and **50c** (700 mg, 3.9 mmol) afforded **51c.**

Procedure as described in the general procedure using **51c** (54 mg, 3.9 mmol), (*S*)-4-methoxy-α-methylbenzylamine (690 µL, 4.7 mmol) and acetic acid (530 µL, 9.4 mmol) and sodium cyanide (229 mg, 4.7 mmol) to give **52c** as a yellow oil (611 mg, 45 % yield from **50c**); R_f = 0.4 (Hexane/EtOAc, 2:1); RP-HPLC 10-60 % B in 12 min, t_R 7.0 min for (*R*,*R*) isomer and 7.6 min for (*S*,*R*) isomer; IR (KBr): ν = 3419, 2963, 1609, 1457, 756 cm^{-1}. ^{1}H NMR (400 MHz, $CDCl_3$): δ = 1.35 (d, J = 6 Hz, 3H, CH_3), 1.70 (br, 1H, NH), 3.14 (d, J = 6 Hz, 2 H, CH_2), 3.56 (t, J = 6 Hz, 1H, α-H), 3.84 (s, 3H, OCH_3), 4.02 (q, J = 6 Hz, 1H, C*H*CH_3), 6.90- 7.30 (m, 7H, arom. H), 7.50 (d, J = 2 Hz, 1H, arom. H), 8.41 (br, 1H, NH) ppm. ^{13}C NMR (100 MHz, $CDCl_3$): δ = 24.82 (CH_3), 29.51 (CH_2), 49.26 (CH), 55.33 (OCH_3), 55.99 (CH), 109.28, 112.41, 114.17, 118.22, 120.63, 122.63, 124.91, 125.49, 127.90, 128.50, 134.51, 135.10, 159.10 ppm.

3-(6-Fluoro-1*H*-indol-3-yl)-2-(2-hydroxy-1-phenyl-ethylamino)-propanenitrile (52d)

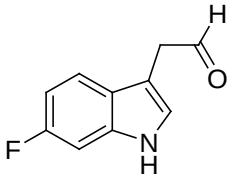

51d

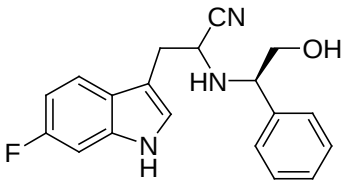

52d

Procedure as described in the general procedure using (methoxymethyl)triphenylphosphonium chloride (2.9 g, 8.6 mmol), 2.5 M *n*-butyllithium in hexane (4 mL, 10.2 mmol) and **50d** (700 mg, 4.3 mmol) afforded **51d**.

Procedure as described in the general procedure using **51d** (759 mg, 4.3 mmol), (*R*)-2-phenylglycinol (704 mg, 5.1 mmol), acetic acid (581 µL, 10.3 mmol) and sodium cyanide (251 mg, 5.1 mmol) gave **52d** as yellow amorphous solid (614 mg, 44 % yield from **50d**); R_f = 0.3 (Hexane/EtOAc, 1:1); RP-HPLC 10-60 % B in 12 min, t_R 6.0 min for (*R*,*R*) isomer and 7.2 min for (*S*,*R*) isomer; IR (KBr): ν = 3425, 3025, 2925, 1627, 758 cm^{-1}. ^1H NMR (400 MHz, $CDCl_3$): δ = 2.58 (br, 1 H, NH), 3.17 (d, *J* = 4 Hz, 1H, C$H_A$$H_B$), 3.19 (d, *J* = 4 Hz, 1H, C$H_A$$H_B$), 3.51 (dd, *J* = 12, 8 Hz, 1H, C$H_A$$H_B$OH), 3.64 (dd, *J* = 4, 4 Hz, 1H, α-H), 3.71 (dd, *J* = 12, 8 Hz, 1H, C$H_A$$H_B$OH), 4.04 (dd, *J* = 8, 4 Hz, 1H, C*H*CH_2OH), 7.10- 7.59 (m, 9 H, arom. H), 8.30 (br, 1 H, NH) ppm. ^{13}C NMR (100 MHz, $CDCl_3$): δ = 29.41 (CH_2), 48.89 (CH), 63.03 (CH), 67.20 (CH_2), 97.69 (d, *J* = 26 Hz), 108.75 (d, *J* = 24 Hz), 109.32, 119.39 (d, *J* = 11 Hz), 120.41, 123.87, 123.92 (d, *J* = 4 Hz), 127.58, 128.33, 128.89, 136.09 (d, *J* = 13 Hz), 138.15, 160.03 (d, *J* = 237 Hz) ppm. MS: *m/z* (+ESI) calcd for $C_{19}H_{19}FN_3O$ 324.1512, found 324.1248 [MH^+].

3-(7-Ethyl-1*H*-indol-3-yl)-2-(2-hydroxy-1-phenyl-ethylamino)-propanenitrile (52e)

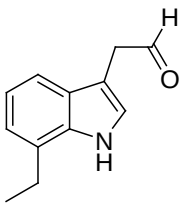

51e

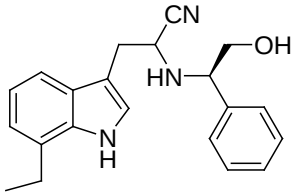

52e

Procedure as described in the general procedure using (methoxymethyl)triphenylphosphonium chloride (2.7 g, 8.0 mmol), 2.5 M *n*-butyllithium in hexane (3.8 mL, 9.7 mmol) and **50e** (700 mg, 4.04 mmol) afforded **51e**.

Procedure as described in the general procedure using **51e** (700 mg, 3.74 mmol), (*R*)-2-phenylglycinol (613 mg, 4.5 mmol), acetic acid (507 µL, 8.97 mmol) and sodium cyanide (219 mg, 4.48 mmol) gave **52e** as brown amorphous solid (444 mg, 33 % yield from **50e**); R_f = 0.3 (Hexane/EtOAc, 1:1); RP-HPLC 10-60 % B in 12 min, t_R 7.0 min for (*R*,*R*) isomer and 8.1 min for (*S*,*R*) isomer; IR (KBr): ν = 3415, 2964, 2930, 1453, 753 cm^{-1}. ^{1}H NMR (400 MHz, $CDCl_3$): δ = 1.37 (t, *J* = 8 Hz, 3H, CH_2CH_3), 2.52 (br, 1 H, NH), 2.85 (q, *J* = 8 Hz, 2H, CH_2CH_3), 3.26 (d, *J* = 4 Hz, 1H, CH_AH_B), 3.27 (d, *J* = 4 Hz, 1H, CH_AH_B), 3.57 (dd, *J* = 12, 8 Hz, 1H, CH_AH_BOH), 3.70 (dd, *J* = 4, 4 Hz, 1H, α-H), 3.74 (dd, *J* = 12, 8 Hz, 1H, CH_AH_BOH), 4.09 (dd, *J* = 8, 4 Hz, 1H, $CHCH_2OH$), 7.10- 7.59 (m, 9 H, arom. H), 8.28 (br, 1 H, NH) ppm. ^{13}C NMR (100 MHz, $CDCl_3$): δ = 13.84 (CH_3), 23.96 (CH_2), 29.71 (CH_2), 49.17 (CH), 63.10 (CH), 67.31 (CH_2), 109.72, 116.27, 120.03, 120.50, 120.81, 123.27, 126.87, 127.05, 127.64, 128.26, 128.87, 135.07, 138.35 ppm. MS: *m/z* (+ESI) calcd for $C_{21}H_{24}N_3O$ 334.1919, found 334.1843 [MH^+].

3-(5-Methyl-1*H*-indol-3-yl)-2-(2-hydroxy-1-phenyl-ethylamino)-propanenitrile (52f)

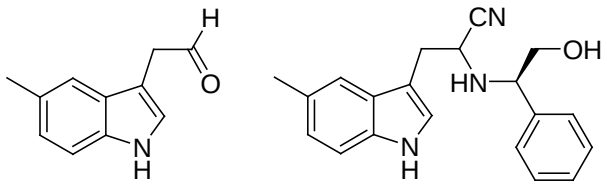

51f **52f**

Procedure as described in the general procedure using (methoxymethyl)triphenylphosphonium chloride (3 g, 8.8 mmol), 2.5 M *n*-butyllithium in hexane (4.2 mL, 10.5 mmol) and **50f** (700 mg, 4.4 mmol) afforded **51f**.

Procedure as described in the general procedure using **51f** (600 mg, 3.5 mmol), (*R*)-2-phenylglycinol (570 mg, 4.2 mmol), acetic acid (470 µL, 8.3 mmol) and sodium cyanide (203 mg, 4.2 mmol) gave **52f** as a brown oil (496 mg, 35 % yield from **50f**); R_f = 0.4 (Hexane/EtOAc, 1:1); RP-HPLC 10-60 % B in 12 min, t_R 6.5 min for (*R*,*R*) isomer and 7.2 min for (*S*,*R*) isomer; IR (KBr): ν = 3405, 3017, 2922, 1450, 756 cm^{-1}. ^1H NMR (400 MHz, $CDCl_3$): δ = 2.38 (br, 1 H, NH), 2.44 (s, 3H, CH_3), 3.22 (d, J = 4 Hz, 1H , CH_AH$_B$), 3.23 (s, 1H , CH$_A$$H_B$), 3.55 (dd, J = 12, 8 Hz, 1H, CH_AH$_B$OH), 3.68 (dd, J = 8, 8 Hz, 1H, α-H), 3.74 (dd, J = 12, 8 Hz, 1H, CH$_A$$H_B$OH), 4.08 (dd, J = 8, 4 Hz, 1H, C*H*CH$_2$OH), 7.03- 7.36 (m, 9 H, arom. H), 8.12 (br, 1H, NH) ppm. ^{13}C NMR (100 MHz, $CDCl_3$): δ = 21.52 (CH_3), 29.70 (CH_2), 48.91 (CH), 63.05 (CH), 67.29 (CH_2), 108.77, 111.08, 118.17, 120.51, 123.68, 123.93, 127.41, 127.62, 128.23, 128.83, 128.94, 134.52, 138.33 ppm. MS: *m/z* (+ESI) calcd for $C_{20}H_{22}N_3O$ 320.1763, found 320.1711 [MH^+].

3-(5-Methoxyl-1*H*-indol-3-yl)-2-(2-hydroxy-1-phenyl-ethylamino)-propanenitrile (52g)

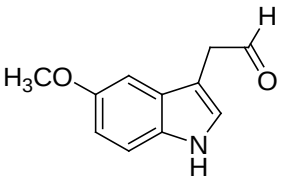

51g

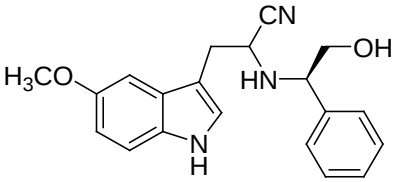

52g

Procedure as described in the general procedure using (methoxymethyl)triphenylphosphonium chloride (2.74 g, 8 mmol), 2.5 M *n*-butyllithium in hexane (3.8 mL, 9.6 mmol) and **50g** (700 mg, 4 mmol) afforded **51g**.

Procedure as described in the general procedure using **51g** (500 mg, 2.6 mmol), (*R*)-2-phenylglycinol (434 mg, 3.1 mmol), acetic acid (359 µL, 6.3 mmol) and sodium cyanide (155 mg, 3.2 mmol) gave **52g** as a brown oil (177 mg, 13 % yield from **50g**); R_f = 0.5 (Hexane/EtOAc, 1:1), RP-HPLC 10-60 % B in 12 min, t_R 5.5 min for (*R*,*R*) isomer and 6.4 min for (*S*,*R*) isomer; IR (KBr): ν = 3405, 3011, 2938, 1480, 757 cm^{-1}. ^1H NMR (400 MHz, $CDCl_3$): δ = 2.11 (br, 1 H, NH), 3.21 (d, J = 4 Hz, 1H , CH_AH$_B$), 3.22 (s, 1H , CH$_A$$H_B$), 3.55 (dd, J = 12, 8 Hz, 1H, CH_AH$_B$OH), 3.67 (dd, J = 8, 8 Hz, 1H, α-H), 3.75 (dd, J = 12, 8 Hz, 1H, CH$_A$$H_B$OH), 3.81 (s, 3H,$OCH_3$), 4.08 (dd, J = 8, 4 Hz, 1H, C*H*CH_2OH), 6.86- 7.34 (m, 9 H, arom. H), 8.11 (br, 1H, NH) ppm. ^{13}C NMR (100 MHz, $CDCl_3$): δ = 29.75 (CH_2), 48.88 (CH), 55.85 (OCH_3), 63.05 (CH), 67.33 (CH_2), 100.22, 109.09, 112.14, 112.77, 120.42, 124.31, 127.59, 128.24, 128.82, 131.29, 138.32, 154.15 ppm. MS: *m/z* (+ESI) calcd for $C_{20}H_{22}N_3O_2$ 336.1712, found 336.1786 [MH^+].

3-(4-Methoxyl-1*H*-indol-3-yl)-2-(2-hydroxy-1-phenyl-ethyamino)-propanenitrile (52h)

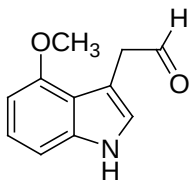

51h

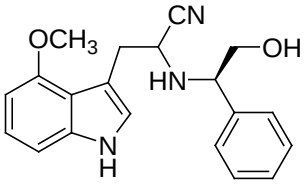

52h

Procedure as described in the general procedure using (methoxymethyl)triphenylphosphonium chloride (2.74 g, 8 mmol), 2.5 M *n*-butyllithium in hexane (3.8 mL, 9.6 mmol) and **50h** (700 mg, 4 mmol) afforded **51h**.

Procedure as described in the general procedure using **51h** (756 mg, 4.0 mmol), (*R*)-2-phenylglycinol (657 mg, 4.8 mmol), acetic acid (543 µL, 9.6 mmol) and sodium cyanide (235 mg, 4.8 mmol) gave **52h** as a brown oil (258 mg, 19 % yield from **50h**); R_f = 0.5 (Hexane/EtOAc, 1:1); RP-HPLC 10-60 % B in 12 min, t_R 5.8 min for (*R*,*R*) isomer and 6.2 min for (*S*,*R*) isomer; IR (KBr): ν = 3401, 2924, 1357, 1255, 733 cm^{-1}. ^1H NMR (400 MHz, $CDCl_3$): δ = 2.51 (br, 1 H, NH), 3.18 (dd, *J* = 14, 8 Hz, 1H , CH_AH$_B$), 3.47 (dd, *J* = 14, 8 Hz,1H , CH$_A$$H_B$), 3.58 (dd, *J* = 9, 8 Hz, 1H, CH_AH$_B$OH), 3.65 (s, 3H, OCH_3), 3.77 (dd, *J* = 4, 10 Hz, 1H, α-H), 3.93 (dd, *J* = 9, 6 Hz, 1H, CH$_A$$H_B$OH), 4.15 (dd, *J* = 9, 4 Hz, 1H, C*H*CH_2OH), 6.42 (d, *J* = 8 Hz, 1 H, arom. H), 6.97- 7.28 (m, 8 H, arom. H), 8.25 (br, 1H, NH) ppm. ^{13}C NMR (100 MHz, $CDCl_3$): δ = 31.60 (CH_2), 50.39 (CH), 54.75 (OCH_3), 63.11 (CH), 67.25 (CH_2), 99.42, 104.74, 109.86, 116.87, 120.88, 122.67, 123.05, 127.60, 128.00, 128.66, 138.06, 138.63, 154.15 ppm. MS: *m/z* (+ESI) calcd for $C_{20}H_{22}N_3O_2$ 336.1712, found 336.1656 [MH^+].

2-(2-Hydroxy-1-phenyl-ethylamino)-3-(1-methyl-1*H*-indol-3-yl)propanenitirle (52i)

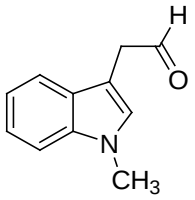

51i

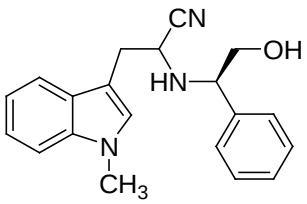

52i

Procedure as described in the general procedure using (methoxymethyl)triphenylphosphonium chloride (3 g, 8.8 mmol), 2.5 M *n*-butyllithium in hexane (4.2 mL, 10.5 mmol) and **50i** (700 mg, 4.4 mmol) afforded **51i**.

Procedure as described in the general procedure using **51i** (717 mg, 4.1 mmol), (*R*)-2-phenylglycinol (671 mg, 4.9 mmol), acetic acid (560 µL, 9.9 mmol) and sodium cyanide (240 mg, 4.9 mmol) gave **52i** as a brown oil (430 mg, 31 % yield from **50i**); R_f = 0.3 (Hexane/EtOAc, 2:1); RP-HPLC 10-60 % B in 12 min, t_R 6.8 min for (*R*,*R*) isomer and 7.8 min for (*S*,*R*) isomer; IR (KBr): ν = 3322, 3020, 2927, 1470, 751 cm^{-1}. ^1H NMR (400 MHz, $CDCl_3$): δ = 2.58 (br, 1 H, NH), 3.25 (d, *J* = 4 Hz, 1H , CH_AH$_B$), 3.26 (d, *J* = 4 Hz, 1H , CH$_A$$H_B$), 3.56 (dd, *J* = 12, 8 Hz, 1H, CH_AH$_B$OH), 3.67 (dd, *J* = 4, 4 Hz, 1H, α-H), 3.75 (dd, *J* = 12, 8 Hz, 1H, CH$_A$$H_B$OH), 3.78 (s, 3H, CH_3), 4.10 (dd, *J* = 8, 4 Hz, 1H, C*H*CH_2OH), 7.08- 7.57 (m, 10 H, arom. H) ppm. ^{13}C NMR (100 MHz, $CDCl_3$): δ = 29.55 (CH_2), 32.78 (CH_3), 49.29 (CH), 63.10 (CH), 67.33 (CH_2), 107.82, 109.45, 118.71, 119.27, 120.42, 121.97, 127.65, 127.83, 128.17, 128.24, 128.84, 136.97, 138.42 ppm; MS: *m/z* (+ESI) calcd for $C_{20}H_{22}N_3O$ 320.1763, found 320.1357 [MH^+].

2-(2-Hydroxy-1-phenyl-ethylamino)-3-(2-methyl-1*H*-indol-3-yl)propanenitirle (52j)

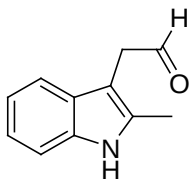

51j

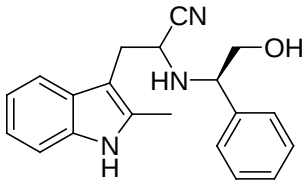

52j

Procedure as described in the general procedure using (methoxymethyl)triphenylphosphonium chloride (2.1 g, 6.3 mmol), 2.5 M *n*-butyllithium in hexane (3 mL, 7.5 mmol) and **50j** (500 mg, 3.1 mmol) afforded **51j**.

Procedure as described in the general procedure using **51j** (500 mg, 2.9 mmol), (*R*)-2-phenylglycinol (474 mg, 3.5 mmol), acetic acid (392 µL, 6.9 mmol) and sodium cyanide (69 mg, 3.5 mmol) gave **52j** as brown amorphous solid (388 mg, 39 % yield from **50j**); R_f = 0.5 (Hexane/EtOAc, 1:1), RP-HPLC 10-60 % B in 12 min, t_R 5.9 min for (*R*,*R*) isomer and 7.2 min for (*S*,*R*) isomer; IR (KBr): ν = 3399, 3016, 2923, 1456, 1219, 754 cm^{-1}. ^1H NMR (400 MHz, $CDCl_3$): δ = 2.38 (br, 1 H, NH), 2.41 (s, 3H, CH_3), 3.19 (d, J = 4 Hz, 1H , CH_AH$_B$), 3.21 (s, 1H , CH$_A$$H_B$), 3.53 (dd, J = 12, 8 Hz, 1H, CH_AH$_B$OH), 3.64 (dd, J = 8, 8 Hz, 1H, α-H), 3.73 (dd, J = 12, 8 Hz, 1H, CH$_A$$H_B$OH), 4.05 (dd, J = 8, 4 Hz, 1H, CHCH$_2$OH), 7.07- 7.42 (m, 9 H, arom. H), 7.99 (br, 1H, NH) ppm. ^{13}C NMR (100 MHz, $CDCl_3$): δ = 11.98 (CH_3), 28.76 (CH_2), 49.02 (CH), 62.96 (CH), 67.38 (CH_2), 105.22, 110.44, 117.76, 119.57, 120.62, 121.36, 127.45, 128.22, 128.48, 128.84, 133.62, 135.22, 138.33 ppm. MS: *m/z* (+ESI) calcd for $C_{20}H_{22}N_3O$ 320.1763, found 320.1670 [MH^+].

6.2.3 Preparation of (*S*)-2-((*R*)-2-Hydroxy-1-phenylethylamino)-3-(1*H*-indol-3-yl)-propanamide derivatives

General procedure for the preparation of (*S*)-2-((*R*)-2-Hydroxy-1-phenylethylamino)-3-(1*H*-indol-3-yl)-propanamide, (*S*,*R*)-54a

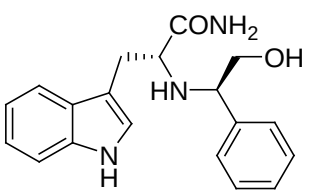

(*R*,*R*)-**53a**

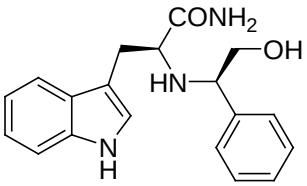

(*S*,*R*)-**54a**

To a solution of α-aminonitrile **52a** (257 mg, 0.8 mmol) in DMSO (3.5 mL), K_2CO_3 (138 mg, 1.3 mmol) and 30 % aqueous H_2O_2 (0.6 mL, 6.3 mmol) were added at 20 °C. After stirring at room temperature for 2 h, another portion of 30 % aqueous H_2O_2 (0.4 mL, 4.7 mmol) was added and stirred for a further hour. The resultant mixture was extracted with Et_2O (50 mL x 3) and brine (50 mL). The organic layers were combined, dried and concentrated. Purification of residue by column chromatography ($CHCl_3$/MeOH, 10:1) gave (*R*,*R*)-**53a** as a yellow oil (first eluting diastereoisomer, 35 mg, 13 % yield) and (*S*,*R*)-**54a** as a white foam (second eluting diastereoisomer, 101 mg, 38 % yield).

(*R*,*R*)-**53a** R_f = 0.5 ($CHCl_3$/MeOH, 6 :1), IR (KBr): ν = 3412, 2917, 1662, 744 cm^{-1}. ^1H NMR (400 MHz, acetone-d_6): δ = 3.13 (br, 1 H, NH), 3.24 (dd, J = 12, 8 Hz, 1H, CH_AH_B), 3.32 (dd, J = 12, 8 Hz, 1H, CH_AH_B), 3.36 (dd, J = 8, 8 Hz, 1H, α-H), 3.52 (dd, J = 12, 8 Hz, 1H, CH_AH_BOH), 3.60 (dd, J = 12, 8 Hz, 1H, CH_AH_BOH), 3.96 (dd, J = 8, 4 Hz, 1H, $CHCH_2OH$), 6.40 (br, 1H, NH), 6.98 (t, 1H, arom. H), 7.01 (t, 1H, arom. H), 7.08- 7.68 (m, 7H, arom. H), 7.70 (d, 1H, arom. H), 10.18 (br, 1H, NH) ppm. ^{13}C NMR (100 MHz, acetone-d_6): δ = 26.62 (CH_2), 59.46 (CH), 63.63 (CH), 66.74 (CH_2), 110.39, 111.14, 118.53, 119.17, 121.16, 124.28, 127.30, 127.95, 128.02, 128.23, 136.76, 141.25, 176.26 ppm. MS: *m/z* (+ESI) calcd for $C_{19}H_{22}N_3O_2$ 324.1712, found 324.1638 [MH^+].

(*S*,*R*)-**54a** R_f = 0.4 ($CHCl_3$/MeOH, 6:1), IR (KBr): ν = 3412, 2917, 1662, 744 cm^{-1}. ^1H NMR (400 MHz, acetone-d_6): δ = 2.97 (dd, J = 16, 8 Hz, 1H, CH_AH_B), 3.22 (dd,

J = 16, 8 Hz, 1H, CH_AH_B), 3.31 (dd, *J* = 8, 4 Hz, 1H, α-H), 3.46 (dd, *J* = 12, 8 Hz, 1H, CH_AH_BOH), 3.60 (dd, *J* = 12, 8 Hz, 1H, CH_AH_BOH), 3.77 (dd, *J* = 8, 4 Hz, 1H, $CHCH_2OH$), 6.71 (br, 1H, NH), 6.92- 7.15 (m, 7H, arom. H), 7.42- 7.48 (m, 3H, arom. H), 10.17 (br, 1H, NH) ppm. ^{13}C NMR (100 MHz, acetone-d_6): δ = 30.00 (CH_2), 60.36 (CH), 63.50 (CH), 67.18 (CH_2), 111.06, 111.27, 118.61, 121.25, 123.64, 126.82, 127.22, 127.81, 127.94, 136.84, 140.93, 177.15 ppm. MS: *m/z* (+ESI) calcd for $C_{19}H_{22}N_3O_2$ 324.1712, found 324.1365 [MH^+].

(*S*)-3-(5-Bromo-indol-3-yl)-2-[(*S*)-1-(4-methoxy-phenyl)ethylamino]-propanamide, (*S*,*S*)-125b

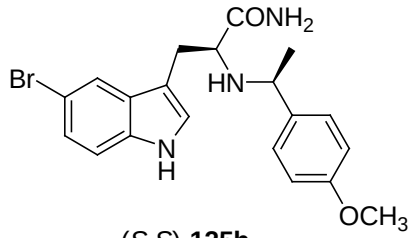

(*S*,*S*)-**125b**

Procedure as described in the general procedure used α-aminonitrile **52b** (356 mg, 0.9 mmol) in DMSO (3.5 mL), K_2CO_3 (172 mg, 1.2 mmol) and 30 % H_2O_2 (0.8 mL, 7.3 mmol), 30 % H_2O_2 (0.4 mL, 2.3 mmol). Purification of residue by column chromatography (Hexane/EtOAc, 1 : 4) followed by RP-HPLC (Onyx Monolithic C_{18}, 100 x 10 mm) gave (*S*,*S*)-**125b** as yellow foam (196 mg, 53 %); R_f = 0.2 (Hexane/EtOAc, 1 : 4) IR (KBr): ν = 3267, 3006, 2961, 1669, 1244, 755 cm^{-1}. ^{1}H NMR (400 MHz, $CDCl_3$): δ = 1.24 (d, *J* = 6 Hz, 3H, CH_3), 1.83 (br, 1H, NH), 2.79 (dd, *J* = 14, 9 Hz, 1H, CH_AH_B), 3.22 (m, 2H, CH_AH_B, α-H), 3.55 (q, *J* = 6 Hz, 1H, $CHCH_3$), 3.76 (s, 3H, OCH_3), 6.10 (br, 1H, NH), 6.53 (d, *J* = 8 Hz, 2H, arom. H), 6.63 (d, *J* = 8 Hz, 2H, arom. H), 6.90 (d, *J* = 2 Hz, 1H, arom. H), 7.21 (s, 1H, arom. H), 7.23 (d, *J* = 2 Hz, 1H, arom.H), 7.48 (d, *J* = 2 Hz, 1H, arom. H), 8.75 (br, 1H, NH) ppm. ^{13}C NMR (100 MHz $CDCl_3$): δ = 24.14 (CH_3), 29.55 (CH_2), 55.18 (OCH_3), 56.38 (CH), 59.82 (CH), 110.86, 112.69, 112.77, 113.53, 121.45, 124.34, 125.00, 127.03, 128.92, 135.11, 135.73, 158.42, 178.18 ppm. MS: *m/z* (+ESI) calcd for $C_{20}H_{23}BrN_3O_2$ 416.0974, found 416.0773 [MH^+].

(*S*)-3-(5-Chloro-indol-3-yl)-2-[(*S*)-1-(4-methoxy-phenyl)-ethylamino]-propanamide, (*S*,*S*)-125c

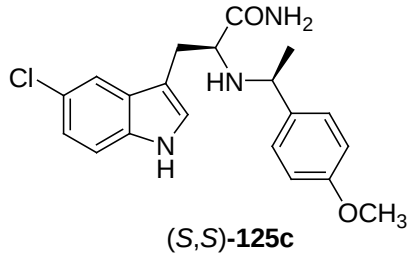

(*S*,*S*)-**125c**

Procedure as described in the general procedure used α-aminonitrile **52c** (542 mg, 1.5 mmol) in DMSO (3.5 mL), K_2CO_3 (275 mg, 2.0 mmol) and 30 % H_2O_2 (1.1 mL, 11.6 mmol), 30 % H_2O_2 (0.4 mL, 2.3 mmol). Purification of residue by column chromatography (Hexane/EtOAc, 1 : 4) followed by RP-HPLC (Onyx Monolithic C_{18}, 100 x 10 mm) gave (*S*,*S*)-**125c** as yellow foam (406 mg, 71 %); R_f = 0.4 (Hexane/EtOAc, 2:1) IR (KBr): ν = 3269, 2961, 2928, 1670, 1279, 755 cm^{-1}. ^1H NMR (400 MHz, $CDCl_3$): δ = 1.24 (d, J = 6 Hz, 3H, CH_3), 1.85 (br, 1H, NH), 2.79 (dd, J = 14, 9 Hz, 1H, CH_AH_B), 3.22 (m, 2H, CH_AH_B, α-H), 3.54 (q, J = 6 Hz, 1H, $CHCH_3$), 3.75 (s, 3H, OCH_3), 6.12 (br, 1H, NH), 6.52 (d, J = 8 Hz, 2H, arom. H), 6.62 (d, J = 8 Hz, 2H, arom. H), 6.91 (d, J = 2 Hz, 1H, arom. H), 7.09- 7.31 (m, 3H, arom. H), 8.75 (br, 1H, NH) ppm. ^{13}C NMR (100 MHz $CDCl_3$): δ = 24.12 (CH_3), 29.57 (CH_2), 55.14 (OCH_3), 56.38 (CH), 59.82 (CH), 110.93, 112.23, 113.51, 118.38, 121.45, 124.51, 125.17, 127.04, 128.26, 134.83, 135.76, 158.42, 178.24 ppm. MS: *m/z* (+ESI) calcd for $C_{20}H_{23}ClN_3O_2$ 372.1479, found 372.1255 [MH^+].

(*S*)-3-(6-Fluoro-1*H*-indol-3-yl)-2-((*R*)-2-hydroxy-1-phenylethyamino)-propanamide, **(*S*,*R*)-54d**

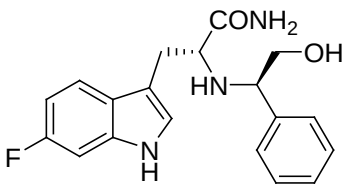

(*R*,*R*)-**53d**

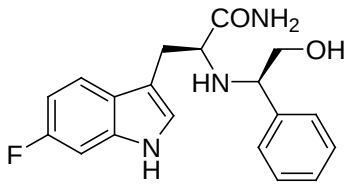

(*S*,*R*)-**54d**

Procedure as described in the general procedure using α-aminonitrile **52d** (557 mg, 1.7 mmol) in DMSO (4 mL), K_2CO_3 (308 mg, 2.2 mmol) and 30 % H_2O_2 (1.3 mL,

13 mmol), 30 % H_2O_2 (0.4 mL, 4.7 mmol) gave (*R*,*R*)-**53d** as yellow foam (first eluting diastereoisomer, 71 mg, 12 % yield) and (*S*,*R*)-**54d** as white foam (second eluting diastereoisomer, 207 mg, 35 % yield).

(*R*,*R*)-**53d** R_f = 0.5 ($CHCl_3$/MeOH, 6:1), IR (KBr): ν = 3423, 3311, 2919, 1664, 759 cm^{-1}. ^1H NMR (400 MHz, acetone-d_6): δ = 3.24 (dd, *J* = 12, 8 Hz, 1H, CH_AH_B), 3.34 (dd, *J* = 12, 8 Hz, 1H, CH_AH_B), 3.35 (dd, *J* = 8, 8 Hz, 1H, α-H), 3.52 (dd, *J* = 12, 8 Hz, 1H, CH_AH_BOH), 3.62 (dd, *J* = 12, 8 Hz, 1H, CH_AH_BOH), 3.97 (dd, *J* = 8, 4 Hz, 1H, $CHCH_2OH$), 6.58 (br, 1H, NH), 6.80 (td, *J* = 4, 2 Hz, 1H, arom. H), 7.14 (dd, *J* = 8, 2 Hz, 1H, arom. H), 7.25- 7.66 (m, 6H, arom. H), 7.66 (dd, *J* = 8, 4 Hz, 1H, arom. H), 10.29 (br, 1H, NH) ppm. ^{13}C NMR (100 MHz, acetone-d_6): δ = 26.50 (CH_2), 59.32 (CH), 63.60 (CH), 66.89 (CH_2), 97.13 (d, *J* = 26 Hz), 106.92 (d, *J* = 24 Hz), 110.65, 120.24 (d, *J* = 10 Hz), 124.78, 124.90 (d, *J* = 3 Hz), 127.34, 127.92, 128.28, 136.65 (d, *J* = 13 Hz), 140.30, 159.66 (d, *J* = 233 Hz), 176.83 ppm. MS: *m/z* (+ESI) calcd for $C_{19}H_{21}FN_3O_2$ 342.1618, found 342.1321 [MH^+].

(*S*,*R*)-**54d** R_f = 0.4 ($CHCl_3$/MeOH, 6:1), IR (KBr): ν = 3423, 3311, 2919, 1664, 759 cm^{-1}. ^1H NMR (400 MHz, acetone-d_6): δ = 2.96 (dd, *J* = 16, 8 Hz, 1H, CH_AH_B), 3.22 (dd, *J* = 16, 8 Hz, 1H, CH_AH_B), 3.31 (dd, *J* = 8, 4 Hz, 1H, α-H), 3.48 (dd, *J* = 12, 8 Hz, 1H, CH_AH_BOH), 3.62 (dd, *J* = 12, 8 Hz, 1H, CH_AH_BOH), 3.77 (dd, *J* = 8, 4 Hz, 1H, $CHCH_2OH$), 6.73 (td, *J* = 4, 2 Hz, 1H, arom. H), 6.76 (br, 1H, NH), 6.76- 7.17 (m, 7H, arom. H), 7.40 (td, *J* = 4, 2 Hz, 1H, arom. H), 8.02 (br, 1H, NH), 10.29 (br, 1H, NH) ppm. ^{13}C NMR (100 MHz, acetone-d_6): δ = 29.97 (CH_2), 60.23 (CH), 63.53 (CH), 67.12 (CH_2), 97.24 (d, *J* = 26 Hz), 106.96 (d, *J* = 24 Hz), 111.32, 119.59 (d, *J* = 10 Hz), 124.27 (d, *J* = 3 Hz), 124.53, 126.88, 127.21, 127.95, 136.73 (d, *J* = 13 Hz), 140.93, 159.68 (d, *J* = 233 Hz), 177.37 ppm. MS: *m/z* (+ESI) calcd for $C_{19}H_{21}FN_3O_2$ 342.1618, found 342.1298 [MH^+].

(*S*)-3-(7-Ethyl-1*H*-indol-3-yl)-2-((*R*)-2-hydroxy-1-phenylethylamino)-propanamide, **(*S*,*R*)-54e**

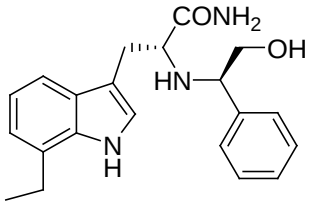

(*R*,*R*)-**53e**

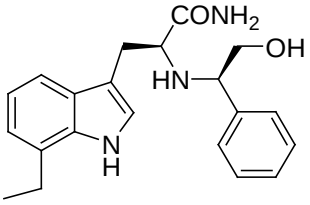

(*S*,*R*)-**54e**

Procedure as described in the general procedure using α-aminonitrile **52e** (396 mg, 1.1 mmol) in DMSO (3 mL), K_2CO_3 (172 mg, 1.4 mmol) and 30 % H_2O_2 (0.8 mL, 8.4 mmol), 30 % H_2O_2 (0.4 mL, 4.7 mmol) gave (*R*,*R*)-**53e** as a yellow oil (first eluting diastereoisomer, 71 mg, 17 % yield) and (*S*,*R*)-**54e** as yellow foam (second eluting diastereoisomer, 196 mg, 47 % yield).

(*R*,*R*)-**53e** R_f = 0.5 ($CHCl_3$/MeOH, 6:1), IR (KBr): ν = 3417, 3311, 2929, 1665, 749 cm^{-1}. ^{1}H NMR (400 MHz, acetone-d_6): δ = 1.32 (t, *J* = 8 Hz, 3H, CH_2CH_3), 2.91 (q, *J* = 8 Hz, 2H, CH_2CH_3), 3.24 (dd, *J* = 12, 8 Hz, 1H, CH_AH_B), 3.34 (dd, *J* = 12, 8 Hz, 1H, CH_AH_B), 3.35 (dd, *J* = 8, 8 Hz, 1H, α-H), 3.51 (dd, *J* = 12, 8 Hz, 1H, CH_AH_BOH), 3.61 (dd, *J* = 12, 8 Hz, 1H, CH_AH_BOH), 3.98 (dd, *J* = 8, 4 Hz, 1H, $CHCH_2OH$), 6.49 (br, 1H, NH), 6.96 (d, *J* = 4 Hz, 2H, arom. H), 7.24- 7.40 (m, 6H, arom. H), 7.55 (dd, *J* = 4, 4 Hz, 1H, arom. H), 10.18 (br, 1H, NH) ppm. ^{13}C NMR (100 MHz, acetone-d_6): δ = 13.80 (CH_3), 23.88 (CH_2), 26.71 (CH_2), 59.51 (CH), 63.61 (CH), 66.85 (CH_2), 110.81, 116.94, 118.95, 119.90, 123.94, 126.61, 127.28, 127.95, 127.98, 128.23, 135.39, 141.42, 176.60 ppm. MS: *m/z* (+ESI) calcd for $C_{21}H_{26}N_3O_2$ 352.1947, found 352.1683 [MH^+].

(*S*,*R*)-**54e** R_f = 0.4 ($CHCl_3$/MeOH, 6:1), IR (KBr): ν = 3417, 3311, 2929, 1665, 749 cm^{-1}. ^{1}H NMR (400 MHz, acetone-d_6): δ = 1.35 (t, *J* = 8 Hz, 3H, CH_2CH_3), 2.93 (q, *J* = 8 Hz, 2H, CH_2CH_3), 2.96 (dd, *J* = 16, 8 Hz, 1H, CH_AH_B), 3.23 (dd, *J* = 16, 8 Hz, 1H, CH_AH_B), 3.30 (dd, *J* = 8, 4 Hz, 1H, α-H), 3.45 (dd, *J* = 12, 8 Hz, 1H, CH_AH_BOH), 3.61 (dd, *J* = 12, 8 Hz, 1H, CH_AH_BOH), 3.76 (dd, *J* = 8, 4 Hz, 1H, $CHCH_2OH$), 6.73 (br, 1H, NH), 6.89- 7.12 (m, 8H, arom. H), 7.32 (d, *J* = 8 Hz, 1H, arom. H), 7.45 (br, 1H, NH), 10.15 (br, 1H, NH) ppm. ^{13}C NMR (100 MHz, acetone-d_6): δ = 13.93 (CH_3), 23.96 (CH_2), 30.09 (CH_2), 60.49 (CH), 63.56 (CH),

67.21 (CH_2), 111.52, 116.37, 119.03, 120.04, 123.22, 126.80, 127.19, 127.75, 127.92, 135.45, 140.96, 177.24 ppm. MS: *m/z* (+ESI) calcd for $C_{21}H_{26}N_3O_2$ 352.1947, found 352.1595 [MH^+].

(*S*)-3-(5-Methyl-1*H*-indol-3-yl)-2-((*R*)-2-hydroxy-1-phenylethyamino)-propanamide, **(*S*,*R*)-54f**

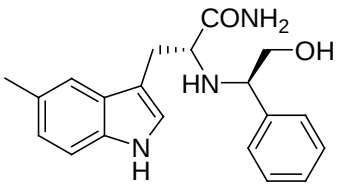

(*R*,*R*)-**53f**

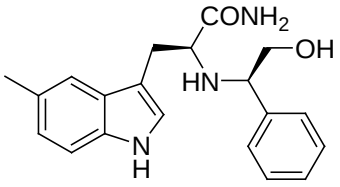

(*S*,*R*)-**54f**

Procedure as described in the general procedure using α-aminonitrile **52f** (468 mg, 1.5 mmol) in DMSO (3 mL), K_2CO_3 (261 mg, 1.9 mmol) and 30 % H_2O_2 (1.3 mL, 11.1 mmol), 30 % H_2O_2 (0.4 mL, 4.7 mmol) gave (*R*,*R*)-**53f** as a yellow oil (first eluting diastereoisomer, 12 mg, 2 % yield) and (*S*,*R*)-**54f** as yellow foam (second eluting diastereoisomer, 48 mg, 10 % yield).

(*R*,*R*)-**53f** R_f = 0.6 ($CHCl_3$/MeOH, 6:1), IR (KBr): ν = 3310, 2919, 1662, 756 cm^{-1}. ^{1}H NMR (400 MHz, acetone-d_6): δ = 2.39 (s, 3H, CH_3), 3.20 (dd, *J* = 12, 8 Hz, 1H, CH_AH_B), 3.22 (dd, *J* = 12, 8 Hz, 1H, CH_AH_B), 3.32 (dd, *J* = 8, 8 Hz, 1H, α-H), 3.49 (dd, *J* = 12, 8 Hz, 1H, CH_AH_BOH), 3.58 (dd, *J* = 12, 8 Hz, 1H, CH_AH_BOH), 3.93 (dd, *J* = 8, 4 Hz, 1H, $CHCH_2OH$), 6.32 (br, 1H, NH), 6.94 (dd, 1H, arom. H), 7.22-7.44 (m, 8H, arom. H), 9.95 (br, 1H, NH) ppm. ^{13}C NMR (100 MHz, acetone-d_6): δ = 20.82 (CH_3), 26.83 (CH_2), 59.49 (CH), 63.56 (CH), 66.84 (CH_2), 110.10, 110.82, 118.75, 122.78, 124.22, 127.20, 127.22, 127.94, 128.19, 128.26, 135.15, 141.49, 176.27 ppm. MS: *m/z* (+ESI) calcd for $C_{20}H_{24}N_3O_2$ 338.1869, found 338.1823 [MH^+].

(*S*,*R*)-**54f** R_f = 0.5 ($CHCl_3$/MeOH, 6:1), IR (KBr): ν = 3310, 2919, 1662, 756 cm^{-1}. ^{1}H NMR (400 MHz, acetone-d_6): δ = 2.33 (s, 3H, CH_3), 2.91 (dd, *J* = 16, 8 Hz, 1H, CH_AH_B), 3.18 (dd, *J* = 16, 8 Hz, 1H, CH_AH_B), 3.29 (dd, *J* = 8, 4 Hz, 1H, α-H), 3.45 (dd, *J* = 12, 8 Hz, 1H, CH_AH_BOH), 3.59 (dd, *J* = 12, 8 Hz, 1H, CH_AH_BOH), 3.75 (dd, *J* = 8, 4 Hz, 1H, $CHCH_2OH$), 6.63 (br, 1H, NH), 6.90- 7.30 (m, 9H, arom. H), 7.36 (br, 1H, NH), 10.02 (br, 1H, NH) ppm. ^{13}C NMR (100 MHz, acetone-d_6): δ =

20.79(CH_3), 30.08 (CH_2), 60.22 (CH), 63.51 (CH), 67.12 (CH_2), 110.53, 110.95, 118.29, 122.90, 123.71, 126.77, 127.24, 127.29, 127.88, 127.98, 135.26, 140.98, 176.97 ppm. MS: *m/z* (+ESI) calcd for $C_{20}H_{24}N_3O_2$ 338.1869, found 338.1942 [MH^+].

(*S*)-3-(5-Methoxyl-1*H*-indol-3-yl)-2-((*R*)-2-hydroxy-1-phenylethyamino)-propanamide, **(*S*,*R*)-54g**

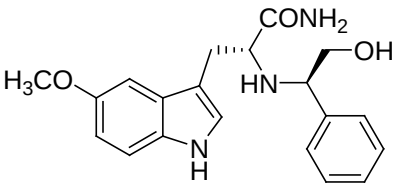

(*R*,*R*)-**53g**

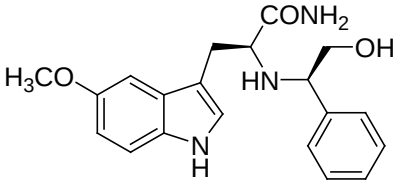

(*S*,*R*)-**54g**

Procedure as described in the general procedure using α-aminonitrile **52g** (266 mg, 0.8 mmol) in DMSO (3 mL), K_2CO_3 (141 mg, 1.0 mmol) and 30 % H_2O_2 (0.6 mL, 5.9 mmol), 30 % H_2O_2 (0.4 mL, 4.7 mmol) gave (*R*,*R*)-**53g** as a yellow oil (first eluting diastereoisomer, 17 mg, 6 % yield) and (*S*,*R*)-**54g** as yellow foam (second eluting diastereoisomer, 30 mg, 10 % yield).

(*R*,*R*)-**53g** R_f = 0.6 ($CHCl_3$/MeOH, 6:1), IR (KBr): ν = 3331, 2931, 1661, 1481, 1216, 756 cm^{-1}. ^{1}H NMR (400 MHz, acetone-d_6): δ = 2.93 (br, 1H, NH), 3.18 (dd, *J* = 16, 8 Hz, 1H, CH_AH_B), 3.29 (dd, *J* = 16, 8 Hz, 1H, CH_AH_B), 3.30 (dd, *J* = 8, 8 Hz, 1H, α-H), 3.50 (dd, *J* = 8, 8 Hz, 1H, CH_AH_BOH), 3.60 (dd, *J* = 12, 4 Hz, 1H, CH_AH_BOH), 3.78 (s, 3H, OCH_3), 3.98 (dd, *J* = 8, 4 Hz, 1H, $CHCH_2OH$), 6.31 (br, 1H, NH), 6.74 (dd, 1H, arom. H), 7.20- 7.40 (m, 8H, arom. H), 9.95 (br, 1H, NH) ppm. ^{13}C NMR (100 MHz, acetone-d_6): δ = 26.52 (CH_2), 54.92 (OCH_3), 59.20 (CH), 63.54 (CH), 66.89 (CH_2), 100.84, 110.21, 111.65, 111.67, 124.99, 127.27, 127.92, 128.21, 128.35, 131.86, 141.41, 153.77, 176.22 ppm. MS: *m/z* (+ESI) calcd for $C_{20}H_{24}N_3O_3$ 354.1818, found 354.1886 [MH^+].

(*S*,*R*)-**54g** R_f = 0.4 ($CHCl_3$/MeOH, 6:1), IR (KBr): ν = 3331, 2931, 1661, 1481, 1216, 756 cm^{-1}. ^{1}H NMR (400 MHz, acetone-d_6): δ = 2.93 (dd, *J* = 16, 8 Hz, 1H, CH_AH_B), 3.15 (dd, *J* = 16, 8 Hz, 1H, CH_AH_B), 3.28 (dd, *J* = 8, 4 Hz, 1H, α-H), 3.45 (dd, *J* = 12, 8 Hz, 1H, CH_AH_BOH), 3.59 (dd, *J* = 12, 8 Hz, 1H, CH_AH_BOH), 3.70 (s,

3H, OCH_3) 3.76 (dd, *J* = 8, 4 Hz, 1H, C*H*CH_2OH), 6.56 (br, 1H, NH), 6.76 (dd, *J* = 8, 4 Hz, 1H, arom. H), 6.76-7.30 (m, 8H, arom. H), 7.33 (br, 1H, NH), 9.98 (br, 1H, NH) ppm. ^{13}C NMR (100 MHz, acetone-d_6): δ = 30.09 (CH_2), 54.92 (OCH_3), 60.14 (CH), 63.55 (CH), 67.16 (CH_2), 100.30, 110.83, 111.72, 111.86, 124.27, 126.80, 127.26, 127.91, 128.01, 131.95, 141.06, 153.77, 176.80 ppm. MS: *m/z* (+ESI) calcd for $C_{20}H_{24}N_3O_3$ 354.1818 found 354.1914 [MH^+].

(*S*)-3-(4-Methoxyl-1*H*-indol-3-yl)-2-((*R*)-2-hydroxy-1-phenylethyamino)-propanamide, **(*S,R*)-54h**

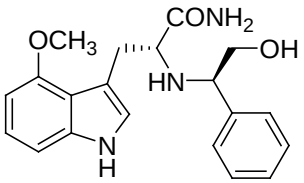

(*R*,*R*)-**53h**

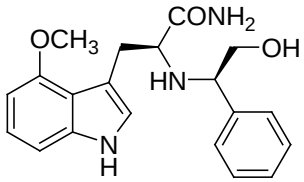

(*S*,*R*)-**54h**

Procedure as described in the general procedure using α-aminonitrile **52h** (213 mg, 0.6 mmol) in DMSO (3 mL), K_2CO_3 (113 mg, 0.8 mmol) and 30 % H_2O_2 (0.5 mL, 4.7 mmol), 30 % H_2O_2 (0.4 mL, 4.7 mmol) gave (*R,R*)-**53h** as a yellow oil (first eluting diastereoisomer, 16 mg, 7 % yield) and (*S,R*)-**54h** as yellow foam (second eluting diastereoisomer, 25 mg, 11 % yield).

(*R,R*)-**53h** R_f = 0.6 ($CHCl_3$/MeOH, 6 :1), IR (KBr): ν = 3317, 2932, 1665, 1086, 755 cm^{-1}. ^{1}H NMR (400 MHz, acetone-d_6): δ = 2.90 (br, 2H, NH), 3.16 (ddd, *J* = 12, 8, 8 Hz, 1H, CH_AH_B), 4.16 (m, 4 H, CH_AH_B, α-H, CH_AH_BOH, CH_AH_BOH), 3.69 (dd, , *J* = 8, 4 Hz, 1H), 3.86 (s, 3H, OCH_3), 6.22 (br, 1H, NH), 6.49 (dd, 6,1 Hz, 1H, arom. H), 7.00- 7.06 (m, 3H, arom. H), 7.11 (br, 1H, NH), 7.21- 7.27 (m, 5 H, arom. H), 10.07 (br, 1H, NH) ppm. ^{13}C NMR (100 MHz, acetone-d_6): δ = 29.91 (CH_2), 54.34 (CH), 60.97 (OCH_3), 63.59 (CH), 66.44 (CH_2), 98.83, 104.85, 111.57, 117.74, 122.01, 122.53, 126.97, 127.88, 128.00, 138.44, 141.90, 154.66, 176.52 ppm. MS: *m/z* (+ESI) calcd for $C_{20}H_{24}N_3O_3$ 354.1818, found 354.1598 [MH^+].

(*S,R*)-**54h** R_f = 0.5 ($CHCl_3$/MeOH, 6 :1), IR (KBr): ν = 3317, 2932, 1665, 1086, 755 cm^{-1}. ^{1}H NMR (400 MHz, acetone-d_6): δ = 2.90 (br, 1H, NH), 3.01 (dd, *J* = 12, 8 Hz, 1H, CH_AH_B), 3.29 (dd, *J* = 16, 8 Hz, 1H, CH_AH_B), 3.32 (dd, *J* = 16, 4 Hz, 1H, α-H), 3.44 (dd, *J* = 12, 8 Hz, 1H, CH_AH_BOH), 3.59 (dd, *J* = 12, 8 Hz, 1H,

CH_AH_BOH), 3.70 (s, 3H, OCH_3), 3.71 (dd, *J* = 8, 4 Hz, 1H, C*H*CH_2OH), 6.40 (dd, *J* = 4, 1 Hz, 1H, arom. H), 6.51 (br, 1H, NH), 6.04- 7.09 (m, 8 H, arom. H), 7.22 (br, 1H, NH), 10.10 (br, 1H, NH) ppm. ^{13}C NMR (100 MHz, acetone-d_6): δ = 31.39 (CH_2), 54.24 (CH), 61.15 (CH), 63.60 (OCH_3), 67.20 (CH_2), 98.97, 104.78, 111.45, 117.65, 122.09, 122.57, 126.66, 127.23, 127.83, 138.57, 141.27, 154.56, 177.22 ppm. MS: *m/z* (+ESI) calcd for $C_{20}H_{24}N_3O_3$ 354.1818, found 354.1441 [MH^+].

(*S*)-2-((*R*)-2-Hydroxy-1-phenylethylamino)-3-(1-methylindol-3-yl)-propanamide, **(*S,R*)-54i**

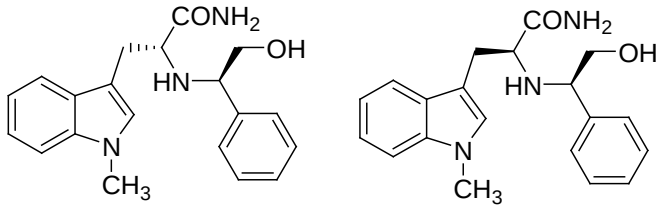

(*R,R*)-**53i** (*S,R*)-**54i**

Procedure as described in the general procedure using α-aminonitrile **52i** (391 mg, 1.2 mmol) in DMSO (3.5 mL), K_2CO_3 (220 mg, 1.6 mmol) and 30 % H_2O_2 (1.0 mL, 9.3 mmol), 30 % H_2O_2 (0.4 mL, 4.7 mmol) gave (*R,R*)-**53i** as a yellow oil (first eluting diastereoisomer, 48 mg, 11 % yield) and (*S,R*)-**54i** as white foam (second eluting diastereoisomer, 122 mg, 29 % yield).

(*R,R*)-**53i** R_f = 0.5 ($CHCl_3$/MeOH, 20 :1), IR (KBr): ν = 3424, 3314, 2925, 1673, 752 cm^{-1}. ^{1}H NMR (400 MHz, acetone-d_6): δ = 2.98 (br, 1 H, NH), 3.21 (dd, *J* = 12, 8 Hz, 1H, CH_AH_B), 3.29 (dd, *J* = 12, 8 Hz, 1H, CH_AH_B), 3.31 (dd, *J* = 8, 8 Hz, 1H, α-H), 3.50 (dd, *J* = 12, 8 Hz, 1H, CH_AH_BOH), 3.60 (dd, *J* = 12, 8 Hz, 1H, CH_AH_BOH), 3.75 (s, 3H, CH_3), 3.96 (dd, *J* = 8, 4 Hz, 1H, C*H*CH_2OH), 6.40 (br, 1H, NH), 7.01 (t, 1H, arom. H), 7.04 (t, 1H, arom. H), 7.14- 7.68 (m, 7H, arom. H), 7.70 (d, 1H, arom. H) ppm. ^{13}C NMR (100 MHz, acetone-d_6): δ = 26.28 (CH_2), 31.84 (CH_3), 59.34 (CH), 63.56 (CH), 66.92 (CH_2), 109.05, 109.59, 118.44, 119.46, 121.15, 127.27, 127.91, 128.23, 128.48, 128.69, 137.17, 141.42, 176.33 ppm. MS: *m/z* (+ESI) calcd for $C_{20}H_{24}N_3O_2$ 338.1869, found 338.1843 [MH^+].

(*S,R*)-**54i** R_f = 0.4 ($CHCl_3$/MeOH, 20 :1), IR (KBr): ν = 3424, 3314, 2925, 1673, 752 cm^{-1}. ^{1}H NMR (400 MHz, acetone-d_6): δ = 2.93 (dd, *J* = 16, 8 Hz, 1H, CH_AH_B),

3.17 (dd, *J* = 16, 8 Hz, 1H, CH_AH_B), 3.27 (dd, *J* = 8, 4 Hz, 1H, α-H), 3.47 (dd, *J* = 12, 8 Hz, 1H, CH_AH_BOH), 3.59 (dd, *J* = 12, 8 Hz, 1H, CH_AH_BOH), 3.73 (dd, *J* = 8, 4 Hz, 1H, $CHCH_2OH$), 3.75 (s, 3H, CH_3), 6.63 (br, 1H, NH), 6.95- 6.69 (m, 4H, arom. H), 7.05- 7.18 (m, 4H, arom. H), 7.36 (d, *J* = 8 Hz, 1H, arom. H), 7.40 (br, 1H, NH), 7.48 (d, *J* = 8 Hz, 1H, arom. H) ppm. ^{13}C NMR (100 MHz, acetone-d_6): δ = 29.75 (CH_2), 31.85 (CH_3), 60.54 (CH), 63.64 (CH), 67.09 (CH_2), 109.17, 110.34, 118.51, 118.80, 121.22, 126.86, 127.29, 127.84, 127.93, 128.29, 137.20, 141.09, 176.95 ppm. MS: *m/z* (+ESI) calcd for $C_{20}H_{24}N_3O_2$ 338.1869, found 338.1441 [MH^+].

(*S*)-2-((*R*)-2-Hydroxy-1-phenylethylamino)-3-(2-methyl-1*H*-indol-3-yl)-propanamide, **(*S*,*R*)-54j**

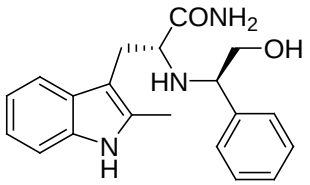

(*R*,*R*)-**53j**

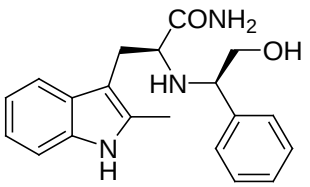

(*S*,*R*)-**54j**

Procedure as described in the general procedure using α-aminonitrile **52j** (355 mg, 1.1 mmol) in DMSO (3 mL), K_2CO_3 (199 mg, 1.4 mmol) and 30 % H_2O_2 (0.9 mL, 8.4 mmol), 30 % H_2O_2 (0.4 mL, 4.7 mmol) to give (*R*,*R*)-**53j** as a yellow foam (first eluting diastereoisomer, 18 mg, 5 % yield) and (*S*,*R*)-**54j** as a yellow foam (second eluting diastereoisomer, 150 mg, 40 % yield).

(*R*,*R*)-**53j** R_f = 0.6 ($CHCl_3$/MeOH, 6 :1), IR (KBr): ν = 3311, 2926, 1667, 1453, 752 cm^{-1}. ^{1}H NMR (400 MHz, acetone-d_6): δ = 2.44 (s, 3H, CH_3), 2.98 (br, 1 H, NH), 3.10 (dd, *J* = 12, 8 Hz, 1H, CH_AH_B), 3.22 (dd, *J* = 12, 8 Hz, 1H, CH_AH_B), 3.35 (dd, *J* = 8, 8 Hz, 1H, α-H), 3.45 (dd, *J* = 12, 8 Hz, 1H, CH_AH_BOH), 3.48 (dd, *J* = 12, 8 Hz, 1H, CH_AH_BOH), 3.75 (dd, *J* = 8, 4 Hz, 1H, $CHCH_2OH$), 6.38 (br, 1H, NH), 6.93 (t, 1H, arom. H), 7.02 (t, 1H, arom. H), 7.14- 7.68 (m, 6H, arom. H), 7.49 (d, *J* = 8 Hz ,1H, arom. H), 9.95 (br, 1H, NH) ppm. ^{13}C NMR (100 MHz, acetone-d_6): δ = 11.00 (CH_3), 27.60 (CH_2), 60.01 (CH), 63.69 (CH), 66.54 (CH_2), 106.99, 110.17, 118.10, 118.39, 120.25, 127.11, 127.88, 128.09, 128.99, 133.26, 135.85, 141.59, 176.64 ppm. MS: *m/z* (+ESI) calcd for $C_{20}H_{24}N_3O_2$ 338.1869, found 338.1766 [MH^+].

(*S*,*R*)-**54j** R_f = 0.5 ($CHCl_3$/MeOH, 6 :1), IR (KBr): ν = 3311, 2926, 1667, 1453, 752 cm^{-1}. ^1H NMR (400 MHz, acetone-d_6): δ = 2.31 (s, 3H, CH_3), 2.95 (dd, J = 16, 8 Hz, 1H, CH_AH_B), 3.17 (dd, J = 16, 8 Hz, 1H, CH_AH_B), 3.24 (dd, J = 8, 4 Hz, 1H, α-H), 3.39 (dd, J = 12, 8 Hz, 1H, CH_AH_BOH), 3.58 (dd, J = 12, 8 Hz, 1H, CH_AH_BOH), 3.74 (dd, J = 8, 4 Hz, 1H, $CHCH_2OH$), 6.76 (br, 1H, NH), 6.84- 7.09 (m, 6H, arom. H), 7.31- 7.40 (m, 3H, arom. H), 10.02 (br, 1H, NH) ppm. ^{13}C NMR (100 MHz, acetone-d_6): δ = 10.86 (CH_3), 29.62 (CH_2), 60.64 (CH), 63.47 (CH), 67.33 (CH_2), 106.87, 110.30, 117.65, 118.55, 120.34, 126.76, 127.10, 127.93, 129.15, 133.08, 135.76, 140.96, 177.00 ppm. MS: *m/z* (+ESI) calcd for $C_{20}H_{24}N_3O_2$ 338.1869, found 338.1903 [MH^+].

6.2.4 Preparation of (S)-2-Amino-3-(indol-3-yl)-propanamide derivatives

General procedure for the preparation of (S)-2-Amino-3-(indol-3-yl)-propanamide, (55a)

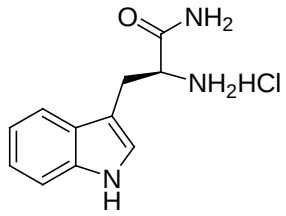

55a

To a stirred solution of **54a** (101 mg, 0.3 mmol), 10 % Pd/C (50 mg, 50 % *w/w*) in MeOH (10 mL) and ammonium formate (98 mg, 1.56 mmol) were added under nitrogen. The resulting mixture was stirred at reflux for 4 h. The catalyst was removed by filtration through a celite pad and washed with MeOH (5 mL). The filtrate was dried and concentrated. Purification of the residue by column chromatography (CH_2Cl_2/MeOH, 4:1) gave amino amide. The amino amide was acidified with 1M HCl to give **55a** hydrochloric salt as a white solid (30 mg, 41 %) m.p. 256-257 °C; R_f = 0.2 ($CHCl_3$/MeOH, 4:1). IR (KBr): ν = 3388, 3247, 2914, 1693, 1492, 751 cm^{-1}. ^1H NMR (400 MHz, D_2O): δ = 3.23 (dd, J = 14, 7 Hz, 1H, CH_AH_B), 3.30 (dd, J = 14, 7 Hz, 1H, CH_AH_B), 4.20 (t, J = 7 Hz, 1H, α-H), 7.10 (td, J = 8, 1 Hz, 1H, arom. H), 7.22 (s, 1H, C2H), 7.18 (td, J = 8, 1 Hz, 1H, arom. H), 7.44 (d, J = 8 Hz, 1H, arom. H), 7.60 (d, J = 8 Hz, 1H, arom. H) ppm. ^{13}C NMR

(100 MHz, D_2O): δ = 26.83 (CH_2), 53.21 (CH), 106.26, 111.99, 118.24, 119.50, 122.15, 125.36, 126.53, 136.22, 171.84 ppm. MS: *m/z* (+ESI) calcd for $C_{11}H_{14}N_3O$ 204.1137, found 204.1016 [MH^+].

(S)-2-Amino-3-(5-bromo-indol-3-yl)propanamide, (55b)

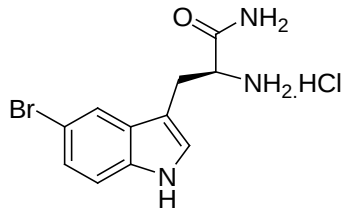

55b

A solution of **125b** (510 mg, 1.2 mmol) and triisopropylsilane (252 µL, 1.2 mmol) in trifluoroacetic acid (4 mL) was stirred at 60 °C for 42 h. The crude mixture was triturated with cold ether. The crude **55b** was use used directly to the acid hydrolysis.

(*S*)-2-Amino-3-(5-chloro-indol-3-yl)propanamide, **(55c)**

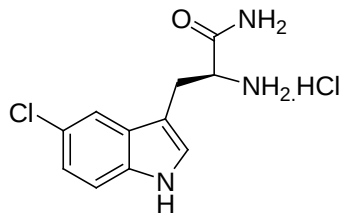

55c

A solution of **125c** (446 mg, 1.2 mmol) and triisopropylsilane (246 µL, 1.2 mmol) in trifluoroacetic acid (4 mL) was stirred at 60 °C for 40 h. The crude mixture was triturated with cold ether. The crude **55c** was use used directly to the acid hydrolysis.

(*S*)-2-Amino-3-(6-fluoro-indol-3-yl)-propanamide, (55d)

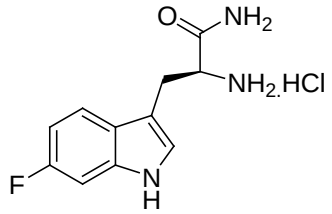

55d

Procedure as described in the general procedure using **54d** (207 mg, 0.6 mmol), 10 % Pd/C (62 mg, 35 % *w/w*) in MeOH (8 mL), ammonium formate (190 mg, 3.0 mmol) gave **55d** hydrochloric salt as a pale orange solid (102 mg, 65 %). m.p. 232-233 °C; R_f = 0.2 ($CHCl_3$/MeOH, 4:1), IR (KBr): ν = 3472, 3271, 2983, 1658, 1451 cm^{-1}. ^1H NMR (400 MHz, D_2O): δ = 3.13 (dd, J = 14, 7 Hz, 1H, CH_AH_B), 3.20 (dd, J = 14, 7 Hz, 1H, CH_AH_B), 4.17 (t, J = 7 Hz, 1H, α-H), 6.81 (m, 1H, arom. H), 7.04 (dd, J = 10, 4 Hz, 1H, arom. H), 7.12 (s, 1H, C2H), 7.43 (dd, 10, 4 Hz, 1H, arom. H) ppm. ^{13}C NMR (100 MHz, D_2O): δ = 26.75 (CH_2), 53.12 (CH), 97.76 (d, J = 26 Hz), 106.34, 107.91 (d, J = 25 Hz), 118.97 (d, J = 10 Hz), 123.19, 125.54 (d, J = 3 Hz), 136.10 (d, J = 12 Hz), 159.58 (d, J = 233 Hz), 171.76 ppm. MS: *m/z* (+ESI) calcd for $C_{11}H_{12}FN_3O$ 222.1043, found 222.0912 [MH^+].

(*S*)-2-Amino-3-(7-ethyl-indol-3-yl)propanamide, (55e)

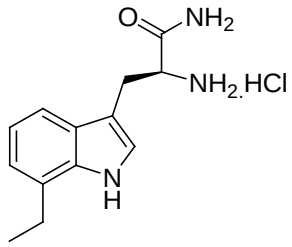

55e

Procedure as described in the general procedure using **54e** (275 mg, 0.8 mmol), 10 % Pd/C (90 mg, 35 % *w/w*) in MeOH (10 mL), ammonium formate (246 mg, 3.9 mmol) gave **55e** hydrochloric salt as a pale purple solid (102 mg, 65 %). m.p. 160-161 °C; R_f = 0.2 ($CHCl_3$/MeOH, 4:1), IR (KBr): ν = 3411, 3154, 3045, 1687, 1413 cm^{-1}. ^1H NMR (400 MHz, D_2O): δ = 1.12 (t, J = 8 Hz, 3H, CH_2CH_3), 2.68 (q, J = 8 Hz, 2H, CH_2CH_3), 3.15 (dd, J = 14, 7 Hz, 1H, CH_AH_B), 3.20 (dd, J = 14, 7 Hz, 1H, CH_AH_B), 4.17 (t, J = 7 Hz, 1H, α-H), 6.88 (d, J = 6 Hz, 1H, arom. H), 6.98 (t, J = 7 Hz, 1H, arom. H), 7.18 (s, 1H, C2H), 7.40 (d, J = 8 Hz, 1H, arom. H) ppm. ^{13}C

NMR (100 MHz, D_2O): δ = 13.45 (CH_3), 23.64 (CH_2), 26.93 (CH_2), 53.21 (CH), 106.68, 115.98, 119.90, 120.51, 125.01, 126.50, 128.22, 134.86, 171.76 ppm. MS: *m/z* (+ESI) calcd for $C_{13}H_{18}N_3O$ 232.1450, found 232.1390 [MH^+].

(*S*)-2-Amino-3-(5-indol-3-yl)propanamide, (55f)

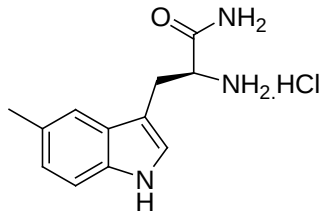

55f

Procedure as described in the general procedure using **54f** (94 mg, 0.3 mmol), 10 % Pd/C (32 mg, 35 % *w/w*) in MeOH (6 mL), ammonium formate (88 mg, 1.4 mmol) gave **55f** hydrochloric salt as a colourless film (26 mg, 37 %) m.p. 82-84 °C; R_f = 0.2 ($CHCl_3$/MeOH, 4:1). IR (KBr): ν = 3402, 2916, 1668, 1431 cm^{-1}. ^1H NMR (400 MHz, D_2O): δ = 2.33 (s, 3H, CH_3), 3.04 (dd, *J* = 15, 6 Hz, 1H, CH_AH_B), 3.12 (dd, *J* = 15, 6 Hz, 1H, CH_AH_B), 3.83 (t, *J* = 6 Hz, 1H, α-H), 7.00 (dd, *J* = 8, 1 Hz, 1H, arom. H), 7.12 (s, 1H, C-2H), 7.30 (d, *J* = 8 Hz, 1H, arom. H), 7.38 (s, 1H, arom. H) ppm. ^{13}C NMR (100 MHz, D_2O): δ = 20.41 (CH_3), 28.64 (CH_2), 54.05 (CH), 107.50, 111.69, 117.71, 123.46, 125.01, 127.03, 129.00, 134.45, 176.44 ppm. MS: *m/z* (+ESI) calcd for $C_{12}H_{16}N_3O$ 218.1293, found 218.1220 [MH^+].

(*S*)-2-amino-3-(5-methoxyl-indol-3-yl)propanamide, (55g)

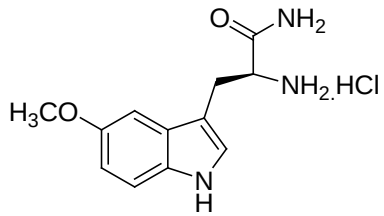

55g

Procedure as described in the general procedure using **54g** (80 mg, 0.2 mmol), 10 % Pd/C (30 mg, 35 % *w/w*) in MeOH (8 mL), ammonium formate (71 mg, 1.1 mmol) gave **55g** hydrochloric salt as a pale purple solid (38 mg, 64 %). m.p. 247-249 °C; R_f = 0.2 ($CHCl_3$/MeOH, 4:1). IR (KBr): ν = 3354, 3167, 2954, 1687, 1462 cm^{-1}. ^1H NMR (400 MHz, D_2O): δ = 3.17 (dd, *J* = 15, 7 Hz, 1H, CH_AH_B), 3.23 (dd,

J = 15, 7 Hz, 1H, CH_AH_B), 3.75 (s, 3H, OCH_3), 4.18 (t, *J* = 7 Hz, 1H, α-H), 6.78 (dd, *J* = 8, 2 Hz, 1H, C6H), 7.05 (d, *J* = 2 Hz, 1H, C4H), 7.17 (s, 1H, C2H), 7.29 (d, *J* = 8 Hz, 1H, C7H) ppm. ^{13}C NMR (100 MHz, D_2O): δ = 26.80 (CH_2), 53.08 (CH), 56.03 (OCH_3), 100.59, 106.02, 111.74, 112.78, 126.19, 126.93, 131.62, 152.90, 171.88 ppm. MS: *m/z* (+ESI) calcd for $C_{12}H_{16}N_3O_2$ 234.1243 found 234.1187 [MH^+].

(*S*)-2-Amino-3-(4-methoxyl-indol-3-yl)propanamide, (55h)

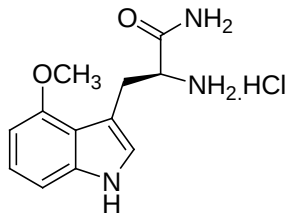

55h

Procedure as described in the general procedure using **54h** (55 mg, 0.2 mmol), 10 % Pd/C (20 mg, 35 % *w/w*) in MeOH (8 mL), ammonium formate (49 mg, 0.8 mmol) gave **55h** hydrochloric salt as a pale yellow solid (28 mg, 68 %) m.p. 231-233 °C; R_f = 0.2 ($CHCl_3$/MeOH, 4:1). IR (KBr): *v* = 3354, 3168, 2955, 1687, 1463 cm^{-1}. ^{1}H NMR (400 MHz, D_2O): δ = 3.22 (dd, *J* = 15, 7 Hz, 1H, CH_AH_B), 3.35 (dd, *J* = 15, 7 Hz, 1H, CH_AH_B), 3.84 (s, 3H, OCH_3), 4.24 (t, *J* = 7 Hz, 1H, α-H), 6.53 (dd, *J* = 8, 1 Hz, 1H, arom. H), 7.02 (dd, *J* = 8, 1 Hz, 1H, arom. H), 7.04 (s, 1H, C2H), 7.06 (d, *J* = 8 Hz, 1H, arom. H) ppm. ^{13}C NMR (100 MHz, D_2O): δ = 28.21(CH_2), 54.37 (CH), 55.12 (OCH_3), 99.74, 105.41, 106.26, 116.19, 123.11, 124.24, 138.02, 153.51, 171.88 ppm. MS: *m/z* (+ESI) calcd for $C_{12}H_{16}N_3O_2$ 234.1243 found 234.1096 [MH^+].

(*S*)-2-Amino-3-(1-methyl-indol-3-yl)propanamide, (55i)

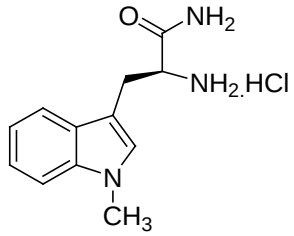

55i

To a stirred solution of **54i** (122 mg, 0.3 mmol) and 10 % Pd/C (42 mg, 35 % *w/w*) in MeOH (8 mL), ammonium formate (113 mg, 1.8 mmol) were added under nitrogen. The resulting mixture was stirred at reflux for 4 h. Another 10 % Pd/C (42 mg, 35 % *w/w*) and ammonium formate (113 mg, 1.8 mmol) were added and stirred for 16 h. The catalyst was removed by filtration through a celite pad and washed with MeOH (5 mL). The filtrate was dried and concentrated. Purification of the residue by column chromatography (CH_2Cl_2/MeOH, 4:1) gave amino amide. The amino amide was acidified with 1M HCl to give **55i** hydrochloric salt as a white solid (46 mg, 53 %) m.p. 260-261 °C; R_f = 0.4 ($CHCl_3$/MeOH, 9:1) IR (KBr): ν = 3376, 3175, 1687, 1480, 742 cm^{-1}. ^1H NMR (400 MHz, acetone-d_6): δ = 2.93 (dd, *J* = 14, 9 Hz, 1H, CH_AH$_B$), 3.37 (dd, *J* = 14, 3 Hz, 1H, CH$_A$$H_B$), 3.77 (s, 3H, CH_3), 4.10 (dd, *J* = 9, 3 Hz, 1H, α-H), 6.65 (br, 1H, NH), 6.97 (s, 1H, C2H), 7.04 (td, *J* = 8, 1 Hz, 1H, arom. H), 7.15 (td, *J* = 8, 1 Hz, 1H, arom. H), 7.33 (d, *J* = 8 Hz, 1H, arom. H), 7.60 (d, *J* = 8 Hz, 1H, arom. H) ppm. ^{13}C NMR (100 MHz, acetone-d_6): δ = 29.97 (CH_2), 31.77 (CH_3), 65.68 (CH), 109.13, 110.95, 118.40, 118.99, 121.14, 127.96, 128.39, 137.02, 175.22 ppm. MS: *m/z* (+ESI) calcd for $C_{12}H_{16}N_3O$ 218.1293, found 218.1318 [MH^+].

(*S*)-2-Amino-3-(2-methyl-indol-3-yl)propanamide, (55j)

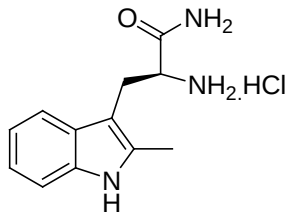

55j

To a stirred solution of **54j** (150 mg, 0.4 mmol) and 10 % Pd/C (52 mg, 35 % *w/w*) in MeOH (8 mL) and ammonium formate (138 mg, 2.2 mmol) were added under nitrogen. The resulting mixture was stirred at reflux for 4 h. Another 10 % Pd/C (32 mg, 20 % *w/w*) and ammonium formate (138 mg, 2.2 mmol) were added and stirred for 16 h. The catalyst was removed by filtration through a celite pad and washed with MeOH (5 mL). The filtrate was dried and concentrated. Purification of the residue by column chromatography (CH_2Cl_2/MeOH, 4:1) gave amino amide. The amino amide was acidified with 1M HCl to give **55j** hydrochloric salt as a purple solid (90 mg, 81 %). m.p. 210-211°C; R_f = 0.4 ($CHCl_3$/MeOH, 4:1), IR

(KBr): ν = 3397, 3174, 1687, 1461, 749 cm^{-1}. ^{1}H NMR (400 MHz, D_2O): δ = 2.18 (s, 3H, CH_3), 3.02 (dd, J = 11, 7 Hz, 1H, CH_AH_B), 3.06 (dd, J = 11, 7 Hz, 1H, CH_AH_B), 4.04 (t, J = 7 Hz, 1H, α-H), 7.01 (td, J = 8, 1 Hz, 1H, arom. H), 7.05 (td, J = 8, 1 Hz, 1H, arom. H), 7.27 (d, J = 8 Hz, 1H, arom. H), 7.41 (d, J = 8 Hz, 1H, arom. H) ppm. ^{13}C NMR (100 MHz, D_2O): δ = 10.47 (CH_3), 25.87 (CH_2), 53.09 (CH), 102.22, 110.98, 117.25, 119.26, 121.10, 127.60, 135.17, 135.42, 171.76 ppm. MS: *m/z* (+ESI) calcd for $C_{12}H_{16}N_3O$ 218.1293, found 218.1079 [MH^+].

6.2.5 Preparation of (*S*)-2-Amino-3-(indol-3-yl)propanic acid derivatives

General procedure for the preparation of (*S*)-2-Amino-3-(indol-3-yl)propanic acid, (56a)

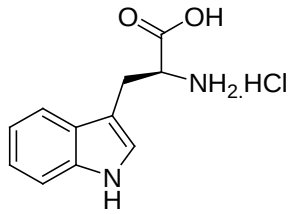

56a

To a two neck round bottom flask containing the α-aminoamide **55a** (86 mg, 0.4 mmol) was added a solution of 1M HCl (6 mL). The reaction mixture was heated at reflux for 5 h and was cooled to room temperature. The residue was lyophilised to give **56a** as a white solid (100 mg, 83 % yield). m.p. 246-247 °C; IR (KBr): ν = 3386, 2941, 1735 cm^{-1}. ^{1}H NMR (400 MHz, D_2O): δ = 3.23 (dd, J = 15, 7 Hz, 1H, CH_AH_B), 3.32 (dd, J = 15, 5 Hz, 1H, CH_AH_B), 4.13 (dd, J = 7, 5 Hz, 1H, α-H), 7.04 (td, J = 8, 1 Hz, 1H, arom. H), 7.13 (td, J = 8, 1 Hz, 1H, arom. H), 7.16 (s, 1H, C-2H), 7.39 (d, J = 8 Hz, 1H, arom. H), 7.51 (d, J = 8 Hz, 1H, arom. H) ppm. ^{13}C NMR (100 MHz, D_2O): δ = 25.65 (CH_2), 53.19 (CH), 106.17, 111.97, 118.16, 119.48, 122.12, 125.31, 126.44, 136.24, 171.80 ppm. MS: *m/z* (+ESI) calcd for $C_{11}H_{13}N_2O_2$ 205.0977, found 205.0953 [MH^+].

(*S*)-2-Amino-3-(5-bromo-indol-3-yl)propanic acid, (56b)

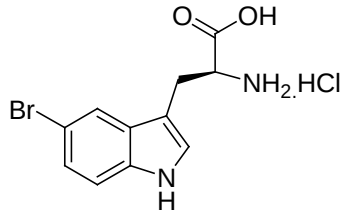

56b

To a two neck round bottom flask containing α-aminoamide **55b** (90 mg, 0.2 mmol) was added a solution of 1M HCl (5 mL). The reaction mixture was heated at reflux for 18 h and was cooled to room temperature. The residue was lyophilised to give **56b** as a yellow solid (78 mg, 99 % yield). m.p. 220-221 °C; ^{1}H NMR (400 MHz, D_2O): δ = 3.20 (dd, J = 15, 7 Hz, 1H, CH_AH$_B$), 3.28 (dd, J = 15, 5 Hz, 1H, CH$_A$$H_B$), 4.18 (dd, J = 7, 5 Hz, 1H, α-H), 7.17 (dd, J = 8, 2 Hz, 1H, arom. H), 7.17 (s, 1H, C-2H), 7.25 (d, J = 8 Hz, 1H, arom. H), 7.63 (d, J = 2 Hz, 1H, arom. H) ppm. ^{13}C NMR (100 MHz, D_2O): δ = 25.64 (CH_2), 53.31 (CH), 106.03, 112.01, 113.46, 120.52, 124.55, 126.46, 128.19, 134.91, 172.00 ppm. MS: *m/z* (+ESI) calcd for $C_{11}H_{12}BrN_2O_2$ 283.0082, found 283.0150 [MH$^+$].

(*S*)-2-Amino-3-(5-chloro-indol-3-yl)propanic acid, (56c)

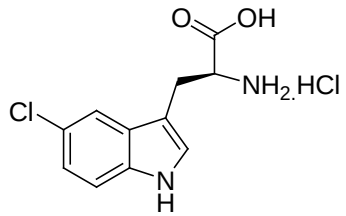

56c

To a two neck round bottom flask containing α-aminoamide **55c** (62 mg, 0.3 mmol) was added a solution of 1M HCl (5 mL). The reaction mixture was heated at reflux for 18 h and was cooled to room temperature. The residue was lyophilised to give **56c** as a yellow solid (59 mg, 95 % yield). m.p. 230-233 °C; IR (KBr): ν = 3456, 3138, 3037, 1730, 1407 cm^{-1}. ^{1}H NMR (400 MHz, D_2O): δ = 3.16 (dd, J = 15, 7 Hz, 1H, CH_AH$_B$), 3.23 (dd, J = 15, 5 Hz, 1H, CH$_A$$H_B$), 4.16 (dd, J = 7, 5 Hz, 1H, α-H), 7.00 (dd, J = 8, 2 Hz, 1H, arom. H), 7.16 (s, 1H, C-2H), 7.25 (d, J = 8 Hz, 1H, arom. H), 7.41 (d, J = 2 Hz, 1H, arom. H) ppm. ^{13}C NMR (100 MHz, D_2O): δ = 25.59 (CH_2), 53.24 (CH), 106.02, 113.00, 117.34, 121.95, 124.41, 126.59, 127.49,

134.61, 171.88 ppm. MS: *m/z* (+ESI) calcd for $C_{11}H_{12}ClN_2O_2$ 239.0587, found 239.0587 [MH^+].

(*S*)-2-Amino-3-(6-fluoro-indol-3-yl)propanic acid, (56d)

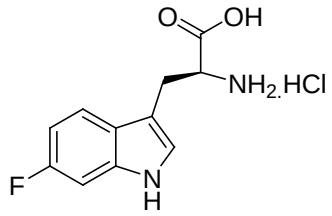

56d

To a two neck round bottom flask containing α-aminoamide **55d** (102 mg, 0.4 mmol) was added a solution of 1M HCl (6 mL). The reaction mixture was heated at reflux for 5 h and was cooled to room temperature. The residue was lyophilised to give **56d** as a white solid (92 mg, 90 % yield). m.p. 218-220 °C; IR (KBr): ν = 3458, 3015, 1732, 1412 cm^{-1}. ^{1}H NMR (400 MHz, D_2O): δ = 3.26 (dd, J = 15, 7 Hz, 1H, CH_AH$_B$), 3.33 (dd, J = 15, 5 Hz, 1H, CH$_A$$H_B$), 4.13 (dd, J = 7, 5 Hz, 1H, α-H), 6.84 (ddd, J = 10, 9, 2 Hz, 1H, arom. H), 7.10 (dd, J = 10, 2 Hz, 1H, arom. H), 7.15 (s, 1H, C-2H), 7.45 (dd, J = 9, 5 Hz, 1H, arom. H) ppm. ^{13}C NMR (100 MHz, D_2O): δ = 25.66 (CH_2), 53.24 (CH), 97.81 (d, J = 26 Hz), 106.43, 108.00 (d, J = 25 Hz), 118.95 (d, J = 10 Hz), 123.11, 125.54 (d, J = 3 Hz), 136.17 (d, J = 13 Hz), 159.64 (d, J = 234 Hz), 171.92 ppm. MS: *m/z* (+ESI) calcd for $C_{11}H_{12}FN_2O_2$ 223.0883, found 223.0752 [MH^+].

(*S*)-2-Amino-3-(7-ethyl-indol-3-yl)propanic acid, (56e)

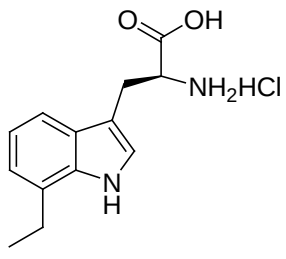

56e

To a two neck round bottom flask containing α-aminoamide **55e** (151 mg, 0.6 mmol) was added a solution of 1M HCl (8 mL). The reaction mixture was heated at reflux for 5 h and was cooled to room temperature. The residue was lyophilised to give **56e** as a white solid (151 mg, 99 % yield). m.p. 216-218 °C; IR (KBr): ν =

3393, 3137, 3041, 1728, 1407 cm^{-1}. ^1H NMR (400 MHz, D_2O): δ = 1.14 (t, J = 8 Hz, 3H, CH_2CH_3), 2.71 (q, J = 8 Hz, 2H, CH_2CH_3), 3.22 (dd, J = 15, 7 Hz, 1H, CH_AH_B), 3.31 (dd, J = 15, 5 Hz, 1H, CH_AH_B), 4.20 (dd, J = 7, 5 Hz, 1H, α-H), 6.93 (t, J = 8 Hz, 1H, arom. H), 6.98 (t, J = 8 Hz, 1H, arom. H), 7.17 (s, 1H, C-2H), 7.36 (d, J = 8 Hz, 1H, arom. H) ppm. ^{13}C NMR (100 MHz, D_2O): δ = 13.44 (CH_3), 23.65 (CH_2), 25.81 (CH_2), 53.28 (CH), 106.68, 115.91, 119.91, 120.55, 125.02, 126.42, 128.29, 134.90, 171.88 ppm. MS: *m/z* (+ESI) calcd for $C_{13}H_{17}N_2O_2$ 233.1290, found 233.1174 [MH^+].

(*S*)-2-Amino-3-(5-methoxyl-indol-3-yl)propanic acid, (56f)

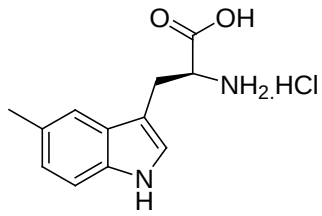

56f

To a two neck round bottom flask containing α-aminoamide **55f** (28 mg, 0.1 mmol) was added a solution of 1M HCl (5 mL). The reaction mixture was heated at reflux for 16 h and was cooled to room temperature. The residue was lyophilised to give **56f** as a white solid (27 mg, 96 % yield). m.p. 112-114 °C; IR (KBr): v = 3406, 2918, 1736, 1485 cm^{-1}. ^1H NMR (400 MHz, D_2O): δ = 2.32 (s, 3H, CH_3), 3.25 (dd, J = 15, 7 Hz, 1H, CH_AH_B), 3.35 (dd, J = 15, 5 Hz, 1H, CH_AH_B), 4.21 (dd, J = 7, 5 Hz, 1H, α-H), 7.00 (dd, J = 8, 1 Hz, 1H, arom. H), 7.16 (s, 1H, arom. H), 7.30 (d, J = 8 Hz, 1H, arom. H), 7.36 (s, 1H, arom. H) ppm. ^{13}C NMR (100 MHz, D_2O): δ = 20.42 (CH_3), 25.76 (CH_2), 53.25 (CH), 105.74, 111.79, 117.60, 123.65, 125.45, 126.70, 129.21, 134.57, 171.96 ppm. MS: *m/z* (+ESI) calcd for $C_{12}H_{15}N_2O_2$ 219.1134, found 219.1036 [MH^+].

(*S*)-2-Amino-3-(5-methoxyl-indol-3-yl)propanic acid, (56g)

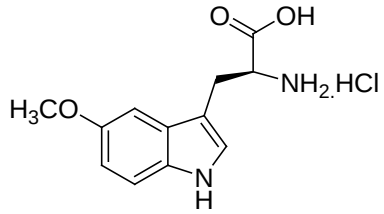

56g

To a two neck round bottom flask containing α-aminoamide **55g** (38 mg, 0.1 mmol) was added a solution of 1M HCl (4 mL). The reaction mixture was heated at reflux for 5 h and was cooled to room temperature. The residue was lyophilised to give **56g** as a white solid (38 mg, 99 % yield). m.p. 224-225 °C; IR (KBr): ν = 3358, 2909, 1728, 1478, 1214 cm^{-1}. ^1H NMR (400 MHz, D_2O): δ = 3.22 (dd, J = 15, 7 Hz, 1H, CH_AH$_B$), 3.30 (dd, J = 15, 5 Hz, 1H, CH$_A$$H_B$), 3.74 (s, 3H, OCH_3), 4.21 (dd, J = 7, 5 Hz, 1H, α-H), 6.78 (dd, J = 8, 2 Hz, 1H, arom. H), 7.02 (d, J = 2 Hz, 1H, arom. H), 7.15 (s, 1H, C-2H), 7.28 (d, J = 8 Hz, arom. H) ppm. ^{13}C NMR (100 MHz, D_2O): δ = 25.81 (CH_2), 53.28 (CH), 55.97 (OCH_3), 100.44, 106.04, 111.82, 112.81, 126.14, 126.82, 131.67, 152.91, 171.97 ppm. MS: *m/z* (+ESI) calcd for $C_{12}H_{15}N_2O_3$ 235.1083, found 235.1068 [MH^+].

(*S*)-2-Amino-3-(4-methoxyl-indol-3-yl)propanic acid, (56h)

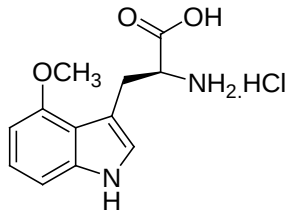

56h

To a two neck round bottom flask containing α-aminoamide **55h** (28 mg, 0.1 mmol) was added a solution of 1M HCl (4 mL). The reaction mixture was heated at reflux for 5 h and was cooled to room temperature. The residue was lyophilised to give **56h** as a white solid (36 mg, 99 % yield). m.p. 220-222 °C; IR (KBr): ν = 3358, 2906, 1728, 1480, 1215 cm^{-1}. ^1H NMR (400 MHz, D_2O): δ = 3.24 (dd, J = 15, 7 Hz, 1H, CH_AH$_B$), 3.37 (dd, J = 15, 7 Hz, 1H, CH$_A$$H_B$), 3.86 (s, 3H, OCH_3), 4.28 (t, J = 7 Hz, 1H, α-H), 6.55 (dd, J = 8, 1 Hz, 1H, arom. H), 7.04 (dd, J = 8, 1 Hz, 1H, arom. H), 7.06 (s, 1H, C2H), 7.09 (d, J = 8 Hz, 1H, arom. H) ppm. ^{13}C NMR (100

MHz, D_2O): δ = 28.21(CH_2), 54.37 (CH), 55.13 (OCH_3), 99.74, 105.41, 106.26, 116.20, 123.09, 124.24, 138.02, 153.56, 171.84 ppm. MS: *m/z* (+ESI) calcd for $C_{12}H_{15}N_2O_3$ 235.1083, found 235.1068 [MH^+].

(*S*)-2-Amino-3-(1-methyl-indol-3-yl)propanic acid, (56i)

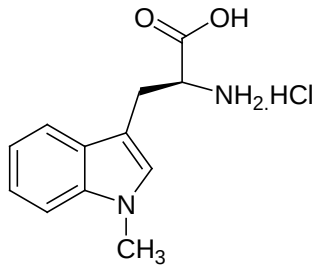

56i

To a two neck round bottom flask containing α-aminoamide **55i** (42 mg, 0.2 mmol) was added a solution of 1M HCl (6 mL). The reaction mixture was heated at reflux for 5 h and was cooled to room temperature. The residue was lyophilised to give **56i** as a white solid (41 mg, 97 % yield). m.p. 210-212 °C; IR (KBr): ν = 3420, 3127, 3047, 1731, 1412 cm^{-1}. ^1H NMR (400 MHz, D_2O): δ = 3.25 (dd, J = 16, 7 Hz, 1H, CH_AH$_B$), 3.32 (dd, J = 16, 5 Hz, 1H, CH$_A$$H_B$), 3.62 (s, 3H, CH_3), 4.20 (dd, J = 7, 5 Hz, 1H, α-H), 7.06 (s, 1H, C-2H), 7.08 (dd, J = 8, 1 Hz, 1H, arom. H), 7.19 (td, J = 8, 1 Hz, 1H, arom. H), 7.33 (d, J = 8 Hz, 1H, arom. H), 7.53 (d, J = 8 Hz, 1H, arom. H) ppm. ^{13}C NMR (100 MHz, D_2O): δ = 25.54 (CH_2), 32.10 (CH_3), 53.34 (CH), 105.12, 110.05, 118.36, 119.31, 121.94, 126.90, 129.55, 136.92, 171.92 ppm. MS: *m/z* (+ESI) calcd for $C_{12}H_{15}N_2O_2$ 219.1134, found 219.1115 [MH^+].

(*S*)-2-amino-3-(2-methyl-indol-3-yl)propanic acid, (56j)

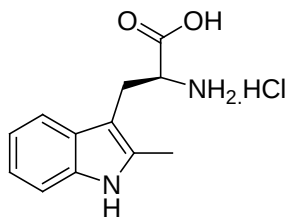

56j

To a two neck round bottom flask containing α-aminoamide **55j** (68 mg, 0.4 mmol) was added a solution of 1M HCl (6 mL). The reaction mixture was heated at reflux for 5 h and was cooled to room temperature. The residue was lyophilized to give

56j as a purple solid (68 mg, 99 % yield). m.p. 200-202 °C; IR (KBr): ν = 3397, 3033, 1730, 1422 cm^{-1}. ^1H NMR (400 MHz, D_2O): δ = 2.19 (s, 3H, CH_3), 3.08 (dd, J = 16, 7 Hz, 1H, CH_AH_B), 3.19 (dd, J = 16, 6 Hz, 1H, CH_AH_B), 4.13 (t, J = 6 Hz, 1H, α-H), 7.00 (td, J = 7, 1 Hz, 1H, arom. H), 7.05 (td, J = 7, 1 Hz, 1H, arom.), 7.27 (d, J = 8 Hz, 1H, arom. H), 7.38 (d, J = 8 Hz, 1H, arom. H) ppm. ^{13}C NMR (100 MHz, D_2O): δ = 10.49 (CH_3), 24.85 (CH_2), 53.29 (CH), 102.10, 111.01, 117.17, 119.29, 121.15, 127.53, 135.23, 135.37, 171.65 ppm. MS: *m/z* (+ESI) calcd for $C_{12}H_{15}N_2O_2$ 219.1134, found 219.1122 [MH^+].

6.2.6 Preparation of *N*-[(fluoren-9-ylmethoxy)carbonyl]tryptophan derivatives

General procedure for the preparation of *N*-[(fluoren-9-ylmethoxy) carbonyl]tryptophan, (43a)

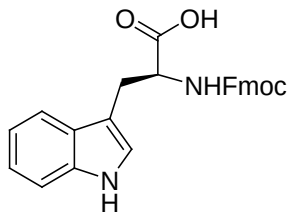

43a

Tryptophan hydrochloric salt **56a** (100 mg, 0.42 mmol) was added to an aqueous solution of sodium carbonate (89 mg, 0.84 mmol) 10 mL. 9-Fluorenylmethyl succinimidyl carbonate (141 mg, 0.42 mmol) in THF (3 mL) was added to the solution. The mixture was stirred for 2 h at room temperature. THF was removed *in vacuo* and the crude was poured into water (15 mL) and extracted with Et_2O (15 mL x 2). The pH of the aqueous layer was adjusted to 2 using 3 M HCl and was extracted with DCM (20 mL x 2). The organic layer were combined, washed with brine, dried and concentrated to give **43a** as a pale yellow solid (114 mg, 44 % yield). m.p. 182-185 °C; $[\alpha]^{24}_D$ = -29 (*c* 1, MeOH); IR (KBr): ν = 3416, 3057, 2950, 1710, 743 cm^{-1}. ^1H NMR (400 MHz, acetone-d_6): δ = 3.31 (dd, J = 15, 8 Hz, 1H, CH_AH_B), 3.46 (dd, J = 15, 5 Hz, 1H, CH_AH_B), 4.20 (t, J = 8 Hz, 1H, Fmoc CH), 4.31 (m, 2H, Fmoc CH_2), 4.69 (m, 1H, α-H), 6.68 (d, J = 8 Hz, 1H, NH), 7.07 (t, J = 7 Hz, 1H, arom. H), 7.14 (t, J = 7 Hz, 1H, arom. H), 7.28 (s, 1H, C-2H), 7.30 (m,

2H, arom. H), 7.41 (m, 3H, arom. H), 7.69 (m, 3H, arom. H), 7.84 (d, *J* = 7 Hz, 2H. arom. H), 10.10 (br, 1H, NH) ppm. ^{13}C NMR (100 MHz, acetone-d_6): δ = 27.52 (CH_2), 47.09 (CH), 54.83 (CH), 66.36 (CH_2), 110.30, 111.41, 118.39, 118.88, 119.91, 121.38, 123.63, 125.29, 125.33, 127.08, 127.64, 127.79, 136.75, 141.18, 144.11, 144.15, 156.07, 173.04 ppm. MS: m/z (+ESI) calcd for $C_{26}H_{23}N_2O_4$ 427.1658, found 427.1743 [MH^+].

***N*-[(fluoren-9-ylmethoxy)carbonyl]-5-bromo-tryptophan, (43b)**

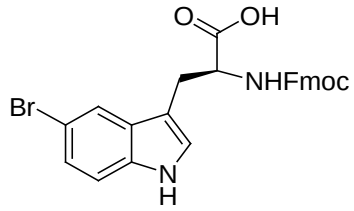

43b

Procedure as described in the general procedure using **56b** (66 mg, 0.21 mmol), sodium carbonate (65 mg, 0.62 mmol) and 9-fluorenylmethyl succinimidyl carbonate (71 mg, 0.21 mmol) gave **43b** as a white solid (23 mg, 20 % yield). m.p. 130-132 °C; $[\alpha]^{24}_D$ = -23 (*c* 1, MeOH); IR (KBr): *v* = 3411, 3060, 2950, 1709, 737 cm^{-1}. ^{1}H NMR (400 MHz, acetone-d_6): δ = 3.25 (dd, *J* = 16, 8 Hz, 1H, CH_AH$_B$), 3.41 (dd, *J* = 16, 5 Hz, 1H, CH_AH$_B$), 4.20 (t, *J* = 8 Hz, 1H, Fmoc CH), 4.31 (m, 2H, Fmoc CH_2), 4.60 (m, 1H, α-H), 6.70 (d, *J* = 8 Hz, 1H, NH), 7.23 (dd, *J* = 8, 2 Hz, 1H, arom. H), 7.30 (m, 3H, arom. H), 7.40 (m, 3H, arom. H), 7.66 (dd, *J* = 8, 2 Hz, 2H, arom. H), 7.86 (m, 3H, arom. H), 10.34 (br, 1H, NH) ppm. ^{13}C NMR (100 MHz, acetone-d_6): δ = 27.13 (CH_2), 47.07 (CH), 54.67 (CH), 66.32 (CH_2), 110.25, 111.77, 113.15, 119.87, 120.96, 123.92, 125.14, 125.25, 125.33, 127.05, 127.60, 129.66, 135.17, 141.15, 141.17, 144.11, 144.15, 155.94, 172.64 ppm. MS: m/z (+ESI) calcd for $C_{26}H_{22}BrN_2O_4$ 505.0763, found 505.0978 [MH^+].

***N*-[(fluoren-9-ylmethoxy)carbonyl]-5-chloro-tryptophan, (43c)**

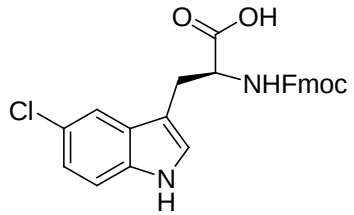

43c

Procedure as described in the general procedure using **56c** (59 mg, 0.25 mmol), sodium carbonate (79 mg, 0.75 mmol) and 9-fluorenylmethyl succinimidyl carbonate (84 mg, 0.25 mmol) gave **43c** as a white solid (23 mg, 20 % yield). m.p. 98-99°C; $[\alpha]^{24}_{D}$ = -16 (*c* 1, MeOH); IR (KBr): *v* = 3414, 3058, 2953, 1710, 748 cm^{-1}. ^{1}H NMR (400 MHz, acetone-d_6): δ = 3.27 (dd, *J* = 15, 8 Hz, 1H, CH_AH$_B$), 3.42 (dd, *J* = 15, 5 Hz, 1H, CH_AH$_B$), 4.20 (t, *J* = 8 Hz, 1H, Fmoc CH), 4.31 (m, 2H, Fmoc CH_2), 4.63 (m, 1H, α-H), 6.73 (d, *J* = 8 Hz, 1H, NH), 7.12 (dd, *J* = 8, 2 Hz, 1H, arom. H), 7.27- 7.42 (m, 6H, arom. H), 7.66 (dd, *J* = 8, 4 Hz, 2H, arom. H), 7.71 (m, 1H, arom. H), 7.85 (d, *J* = 8 Hz, 2H, arom. H), 10.31 (br, 1H, NH) ppm. ^{13}C NMR (100 MHz, acetone-d_6): δ = 27.17 (CH_2), 47.07 (CH), 54.65 (CH), 66.32 (CH_2), 100.30, 112.69, 117.84, 119.87, 119.88, 121.36, 124.19, 125.24, 125.31, 127.05, 127.60, 128.95, 134.93, 141.15, 141.17, 144.11, 144.14, 155.95, 172.65 ppm. MS: m/z (+ESI) calcd for $C_{26}H_{22}ClN_2O_4$ 461.1268, found 461.1317 [MH^+].

***N*-[(fluoren-9-ylmethoxy)carbonyl]-6-fluoro-tryptophan, (43d)**

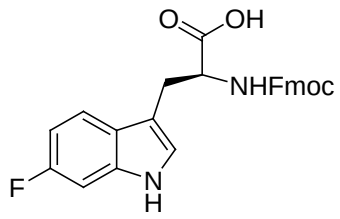

43d

Procedure as described in the general procedure using **56d** (90 mg, 0.35 mmol), sodium carbonate (74 mg, 0.70 mmol) and 9-fluorenylmethyl succinimidyl carbonate (117 mg, 0.35 mmol) gave **43d** as a white solid (77 mg, 50 % yield). m.p. 102-104 °C; $[\alpha]^{24}_{D}$ = -19 (*c* 1, MeOH); IR (KBr): *v* =3419, 3064, 2952, 1710, 745 cm^{-1}. ^{1}H NMR (400 MHz, acetone-d_6): δ = 3.26 (dd, *J* = 14, 8 Hz, 1H, CH_AH$_B$), 3.41 (dd, *J* = 14, 5 Hz, 1H, CH$_A$$H_B$), 4.20 (t, *J* = 8 Hz, 1H, Fmoc CH), 4.31 (m, 2H, Fmoc CH_2), 4.6 (m, 1H, α-H), 6.68 (d, *J* = 8 Hz, NH), 6.89 (td, *J* = 10, 2 Hz, 1H, arom. H), 7.15 (dd, *J* = 10, 2 Hz, 1H, arom. H), 7.27 (s, 1H, C-2H), 7.30 (m, 2H, arom.H), 7.41 (t, *J* = 7 Hz, 2H, arom. H), 7.66 (m, 3H, arom. H), 7.85 (d, *J* = 8 Hz, 2H, arom. H), 10.19 (br, 1H, NH) ppm. ^{13}C NMR (100 MHz, acetone-d_6): δ = 27.41 (CH_2), 47.08 (CH), 54.74 (CH), 66.30 (CH_2), 97.33 (d, *J* = 26 Hz), 107.22 (d, *J* = 25 Hz), 110.63, 119.89, 119.35 (d, *J* = 10 Hz), 124.16(d, *J* = 3 Hz), 124.56, 125.26, 125.29, 127.04, 127.62, 136.60 (d, *J* = 13 Hz), 141.18, 144.11, 144.15,

156.00, 159.70 (d, *J* = 233 Hz), 172.82 ppm. MS: m/z (+ESI) calcd for $C_{26}H_{22}FN_2O_4$ 445.1564, found 445.1790 [MH^+].

***N*-[(fluoren-9-ylmethoxy)carbonyl]-7-ethyl-tryptophan, (43e)**

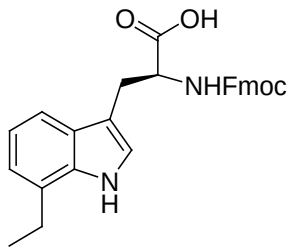

43e

Procedure as described in the general procedure using **56e** (102 mg, 0.38 mmol), sodium carbonate (80 mg, 0.76 mmol) and 9-fluorenylmethyl succinimidyl carbonate (128 mg, 0.38 mmol) gave **43e** as a white solid (83 mg, 50 % yield). m.p. 146-148 °C; $[\alpha]^{24}_D$ = -26 (c 1, MeOH); IR (KBr): ν = 3422, 3057, 2964, 1711, 746 cm^{-1}. ^{1}H NMR (400 MHz, acetone-d_6): δ = 1.31 (t, *J* = 8 Hz, 3H, CH_2CH_3), 2.91 (q, *J* = 8 Hz, 2H, CH_2CH_3), 3.27 (dd, *J* = 15, 8 Hz, 1H, CH_AH_B), 3.43 (dd, *J* = 15, 5 Hz, 1H, CH_AH_B), 4.20 (t, *J* = 7 Hz, 1H, Fmoc CH), 4.29 (m, 2H, Fmoc CH_2), 4.66 (m, 1H, α-H), 6.65 (d, *J* = 8 Hz, 1H, NH), 7.01 (m, 2H, arom. H), 7.27 (s, 1H, C-2H), 7.30 (m, 2H, arom. H), 7.40 (t, *J* = 7 Hz, 2H, arom. H), 7.54 (d, *J* = 7 Hz, 1H, arom. H), 7.66 (m, 2H, arom. H), 7.85 (d, *J* = 7 Hz, 2H, arom. H), 10.08 (br, 1H, NH) ppm. ^{13}C NMR (100 MHz, acetone-d_6): δ = 13.72 (CH_3), 23.85 (CH_2), 27.62 (CH_2), 47.07 (CH), 54.79 (CH), 66.34 (CH_2), 110.73, 116.16, 119.26, 119.88, 120.13, 123.19, 125.29, 125.33, 126.87, 127.05, 127.61, 135.37, 141.16, 144.14, 156.01, 172.95 ppm. MS: m/z (+ESI) calcd for $C_{28}H_{27}N_2O_4$ 455.1971, found 455.2142 [MH^+].

***N*-[(fluoren-9-ylmethoxy)carbonyl]-5-methyl-tryptophan, (43f)**

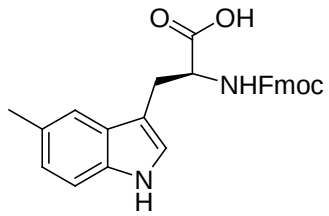

43f

Procedure as described in the general procedure using **56f** (48 mg, 0.19 mmol), sodium carbonate (40 mg, 0.38 mmol) and 9-fluorenylmethyl succinimidyl carbonate (64 mg, 0.19 mmol) gave **43f** as a colourless film (55 mg, 66 % yield). m.p. 178 °C; $[\alpha]^{24}_{D}$ = -15 (c 1, MeOH); IR (KBr): ν = 3424, 3038, 2920, 1708, 1448 cm^{-1}. ^{1}H NMR (400 MHz, acetone-d_6): δ = 2.42 (s, 3H, CH_3), 3.25 (dd, J = 15, 8 Hz, 1H, CH_AH$_B$), 3.43 (dd, J = 15, 5 Hz, 1H, CH_AH$_B$), 4.20 (t, J = 7 Hz, 1H, Fmoc CH), 4.29 (m, 2H, Fmoc CH_2), 4.65 (m, 1H, α-H), 6.65 (d, J = 8 Hz, 1H, NH), 6.97 (dd, J = 8, 1 Hz, 1H, arom. H), 7.23 (d, J = 2 Hz, 1H, arom. H), 7.28 (s, 1H, C-2H), 7.30 (m, 2H, arom. H), 7.40 (t, J = 7 Hz, 2H, arom. H), 7.48 (s, 1H, arom. H), 7.66 (d, J = 7 Hz, 2H, arom. H), 7.85 (d, J = 7 Hz, 2H, arom. H), 9.97 (br, 1H, NH) ppm. ^{13}C NMR (100 MHz, acetone-d_6): δ = 20.88 (CH_3), 27.47 (CH_2), 47.08 (CH), 54.80 (CH), 66.34 (CH_2), 109.75, 111.11, 117.98, 119.89, 122.99, 123.69, 125.27, 127.06, 127.59, 127.62, 128.03, 135.13, 141.16, 144.14, 156.03, 173.02 ppm. MS: m/z (+ESI) calcd for $C_{27}H_{25}N_2O_4$ 441.1814, found 441.2083 [MH^+].

***N*-[(fluoren-9-ylmethoxy)carbonyl]-5-methoxyl-tryptophan, (43g)**

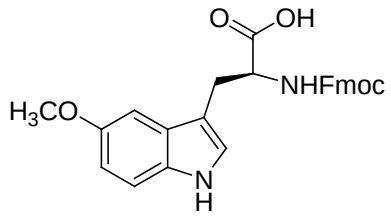

43g

Procedure as described in the general procedure using **56g** (300 mg, 1.28 mmol), sodium carbonate (271 mg, 2.56 mmol) and 9-fluorenylmethyl succinimidyl carbonate (431 mg, 1.28 mmol) gave **43g** as a white powder (479 mg, 82 % yield). m.p. 198 °C; $[\alpha]^{24}_{D}$ = -23 (c 1, MeOH); IR (KBr): ν = 3415, 2949, 1703, 1493,

1218 cm^{-1}. ^1H NMR (400 MHz, acetone-d_6): δ = 3.25 (dd, J = 15, 8 Hz, 1H, CH_AH$_B$), 3.39 (dd, J = 15, 5 Hz, 1H, CH_AH$_B$), 3.82 (s, 3H, OCH_3), 4.20 (t, J = 7 Hz, 1H, Fmoc CH), 4.29 (m, 2H, Fmoc CH_2), 4.61 (m, 1H, α-H), 6.63 (d, J = 8 Hz, 1H, NH), 6.79 (dd, J = 8, 1 Hz, 1H, arom. H), 7.21 (m, 1H, arom. H), 7.30 (m, 4H, arom. H), 7.40 (t, J = 7 Hz, 2H, arom. H), 7.66 (d, J = 7 Hz, 2H, arom. H), 7.85 (d, J = 7 Hz, 2H, arom. H), 9.96 (br, 1H, NH) ppm. ^{13}C NMR (100 MHz, acetone-d_6): δ = 27.45 (CH_2), 47.07 (CH), 54.65 (CH), 54.97 (OCH_3), 66.32 (CH_2), 100.18, 110.01, 111.60, 111.92, 119.87, 124.06, 125.28, 125.32, 127.05, 127.60, 128.14, 131.66, 141.15, 144.12, 144.15, 153.98, 155.93, 172.83 ppm. MS: m/z (+ESI) calcd for $C_{27}H_{25}N_2O_5$ 457.1763, found 457.1913 [MH^+].

***N*-[(fluoren-9-ylmethoxy)carbonyl]-4-methoxyl-tryptophan, (43h)**

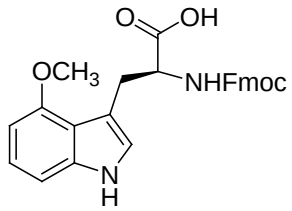

43h

Procedure as described in the general procedure using **56h** (38 mg, 0.14 mmol), sodium carbonate (29 mg, 0.28 mmol) and 9-fluorenylmethyl succinimidyl carbonate (47 mg, 0.14 mmol) gave **43h** as a white powder (39 mg, 62 % yield). m.p. 168 °C; $[\alpha]^{24}_D$ = -27 (c 1, MeOH); IR (KBr): ν = 3415, 2949, 1703, 1494, 1218 cm^{-1}. ^1H NMR (400 MHz, acetone-d_6): δ = 3.26 (dd, J = 15, 8 Hz, 1H, CH_AH$_B$), 3.41 (dd, J = 15, 5 Hz, 1H, CH_AH$_B$), 3.82 (s, 3H, OCH_3), 4.20 (t, J = 7 Hz, 1H, Fmoc CH), 4.29 (m, 2H, Fmoc CH_2), 4.62 (m, 1H, α-H), 6.59 (d, J = 8 Hz, 1H, NH), 6.56 (dd, J = 8, 1 Hz, 1H, arom. H), 7.25 (m, 1H, arom. H), 7.26 (m, 4H, arom. H), 7.41 (t, J = 7 Hz, 2H, arom. H), 7.66 (d, J = 7 Hz, 2H, arom. H), 7.85 (d, J = 7 Hz, 2H, arom. H), 9.96 (br, 1H, NH) ppm. ^{13}C NMR (100 MHz, acetone-d_6): δ = 27.45 (CH_2), 47.07 (CH), 54.63 (CH), 54.95 (OCH_3), 66.33 (CH_2), 99.76, 110.11, 111.65, 116.20, 119.85, 121.34, 123.41, 125.26, 125.29, 127.06, 127.61, 137.94, 141.15, 144.12, 144.15, 154.98, 156.02, 172.83 ppm. MS: m/z (+ESI) calcd for $C_{27}H_{25}N_2O_5$ 457.1763, found 457.1781 [MH^+].

***N*-[(fluoren-9-ylmethoxy)carbonyl]-1-methyl-tryptophan, (43i)**

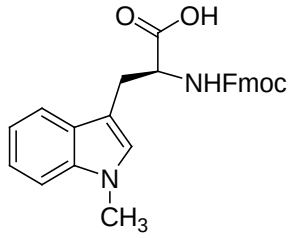

43i

Procedure as described in the general procedure using **56i** (300 mg, 1.37 mmol), sodium carbonate (290 mg, 2.75 mmol) and 9-fluorenylmethyl succinimidyl carbonate (461 mg, 1.37 mmol) gave **43i** as a white powder (447 mg, 74 % yield). m.p. 92-94 °C; $[\alpha]^{24}_{D}$ = -24 (c 1, MeOH); IR (KBr): ν = 3416, 3058, 2937, 1708, 741 cm^{-1}. ^{1}H NMR (400 MHz, DMSO-d_6): δ = 3.04 (dd, J = 14, 10 Hz, 1H, CH_AH$_B$), 3.20 (dd, J = 14, 5 Hz, 1H, CH$_A$$H_B$), 3.71 (s, 3H, CH_3), 4.22 (m, 4H, α-H, Fmoc CH, CH_2), 7.03 (t, J = 6 Hz, 1H, arom. H), 7.14 (s, 1H, C-2H), 7.14 (t, J = 8 Hz, arom. H), 7.25- 7.43 (m, 5H, arom. H), 7.60 (d, J = 8 Hz, 1H, arom. H), 7.69 (m, 2H, arom. H), 7.89 (d, J = 8 Hz, 2H, arom. H), 12.7 (br, 1H, NH) ppm. ^{13}C NMR (100 MHz, DMSO-d_6): δ = 27.25 (CH_2), 32.75 (CH), 40.05 (CH_3), 55.47 (CH), 66.12 (CH_2), 110.06, 118.89, 118.98, 120.57, 121.52, 125.76, 127.51, 127.93, 128.09, 128.47, 137.01, 141.15, 144.24, 156.46, 174.11 ppm. MS: *m/z* (+ESI) calcd for $C_{27}H_{25}N_2O_4$ 441.1814, found 441.1994 [MH^+].

***N*-[(fluoren-9-ylmethoxy)carbonyl]-2-methyl-tryptophan, (43j)**

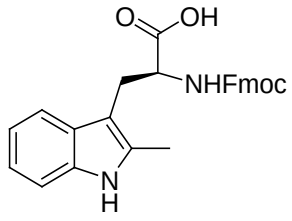

43j

Procedure as described in the general procedure using **56j** (68 mg, 0.31 mmol), sodium carbonate (65 mg, 0.62 mmol) and 9-fluorenylmethyl succinimidyl carbonate (104 mg, 0.31 mmol) gave **43j** as a white solid (53 mg, 40 % yield). m.p. 182-185 °C; $[\alpha]^{24}_{D}$ = -15 (c 1, MeOH); IR (KBr): ν =3412, 3057, 2924, 1712, 743 cm^{-1}. 1H NMR (400 MHz, acetone-d_6): δ = 2.43 (s, 3H, CH_3), 3.26 (dd, J = 14, 7

Hz, 1H, CH_AH$_B$), 3.37 (dd, J = 14, 6 Hz, 1H, CH_AH$_B$), 4.19 (t, J = 8 Hz, 1H, Fmoc CH), 4.29 (d, J = 8 Hz, 2H, Fmoc CH_2), 4.62 (m, 1H, α-H), 6.57 (d, J = 8 Hz, NH), 7.03 (m, 2H, arom. H), 7.30 (m, 3H, arom. H), 7.40 (t, J = 7 Hz, 2H, arom. H), 7.62 (d, J = 7 Hz, 1H, arom. H), 7.67 (m, 2H, arom. H), 7.85 (d, J = 8 Hz, 2H, arom. H), 9.91 (br, 1H, NH) ppm. ^{13}C NMR (100 MHz, acetone-d_6): δ = 10.88 (CH_3), 26.88 (CH_2), 47.06 (CH), 54.92 (CH), 66.39 (CH_2), 106.11, 110.35, 117.68, 118.71, 119.89, 120.41, 125.32, 125.33, 127.06, 127.62, 129.02, 133.31, 135.81, 141.17, 144.10, 144.19, 155.92, 172.97 ppm. MS: m/z (+ESI) calcd for $C_{27}H_{25}N_2O_4$ 441.1814, found 441.2033 [MH^+].

6.3 Experimental for Chapter 3

6.3.1 Synthesis of (*R*)-Ala-Thz-OH

(*R*)-*tert*-Butyl 1-amino-1-oxopropan-2-ylcarbamate, (57)

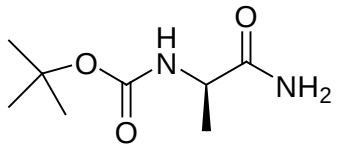

57

DCC (6.57 g, 31.9 mmol) was added to a suspension of Boc-(*R*)-alanine (5.03 g, 26.6 mmol) and 1-hydroxybenzotriazole (4.3 g, 31.9 mmol) in CH_2Cl_2 (80 mL) at 0°C. The solution was warmed to room temperature and stirred for 1 h. The solution was cooled to 0 °C again and 0.5 M ammonia in dioxane (69 mL) was added into the solution, The reaction mixture was warmed to room temperature, stirred for 1 h and then filtered. The mother liquor was concentrated and purified by column chromatography ($CHCl_3$/ MeOH, 96:4) to give the amide **57** as a white solid (4.81 g, 96 % yield); m.p. 100-104 °C (ref.[309] m.p. 120-121 °C); R_f = 0.25 ($CHCl_3$/ MeOH, 96:4). IR (KBr): ν = 3390, 3353, 3200, 1682, 1644, 1522, 1325, 1251, 1167 cm^{-1}. ^{1}H NMR (400 MHz, $CDCl_3$): δ = 1.37 (d, J = 7 Hz, 3H, CHCH_3), 1.43 (s, 9H, C(CH_3)$_3$), 4.23 (br, 1H, CHCH$_3$), 5.29 (br, 1H, α-NH), 6.07 (br, 1H, NH_AH$_B$), 6.56 (br, 1H, NH$_A$$H_B$) ppm. ^{13}C NMR (100 MHz, $CDCl_3$): δ = 18.45 (CHCH$_3$), 28.31 (C(CH$_3$)), 49.71 (CHCH$_3$), 80.14 (C(CH$_3$)), 155.62 (CO), 176.03

(CO) ppm. MS: *m/z* (+ESI) calcd for $C_8H_{16}N_2O_3Na^+$ 211.1161, found 211.1191[MNa^+].

***tert*-Butyl -(*R*)-(1-thiocarbamoylethyl)carbamate, (58)**

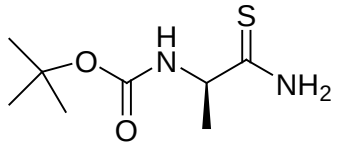

58

Lawesson's reagent (3.1 g, 7.6 mmol) was added to a solution of the amide **57** (2.4 g, 12.7 mmol) in THF (50 mL) cooled at 0 °C. The mixture was stirred at room temperature for 40 min. The solution was poured into a separating funnel which contains ice (50 mL) and saturated aqueous $NaHCO_3$ (50 mL), and the mixture was extracted with Et_2O (50 mL × 3). The organic layers were combined, washed with brine (100 mL), dried with $MgSO_4$ and concentrated. The residue was purified by column chromatography (n-hexane/EtOAc) to give **58** as a white solid (1.71 g, 66 % yield); m.p. 64- 66 °C (ref.[150] m.p. 104- 105 °C); R_f = 0.30 (n-hexane/EtOAc, 3:2). IR (KBr): ν = 3378, 3288, 3181, 1675, 1523, 1241, 1158 cm^{-1}. ^1H NMR (400 MHz, $CDCl_3$): δ = 1.44 (s, 9H, C(CH_3)$_3$), 1.47 (d, J = 7 Hz, 3H, CHCH_3), 4.58 (br, 1H, CHCH$_3$), 5.45 (br, 1H, α-NH), 7.85 (br, 1H, NH_AH$_B$), 8.23 (br, 1H, NH$_A$$H_B$) ppm. ^{13}C NMR (100 MHz, $CDCl_3$): δ = 21.73 (CHCH$_3$), 28.34 (C(CH$_3$)), 55.14 (CHCH$_3$), 80.56 (C(CH$_3$)), 155.57 (CO), 210.58 (CS) ppm.

Ethyl-2-(1-(*tert*-butoxycaronylamino)ethyl)-4-hydroxy-4,5-dihydrothiazole-4-carboxylate, (138)

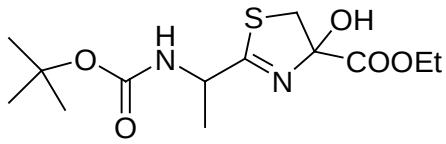

138

Thioamide **58** (100 mg, 0.5 mmol) was dissolved in DME (5mL). After stirring vigorously for 10 min at -15 °C, the ground $KHCO_3$ (400 mg, 4 mmol) fine powder was added to a suspension solution. The mixture was stirred for 30 min and then ethyl bromopyruvate (0.2 mL, 1.5 mmol) was added. The solution was poured into water (10 mL) and was extracted with Et_2O (10 mL × 3). The combined dry with

$MgSO_4$ and concentrated. The residue was purified by column chromatography (n-hexane/EtOAc, 1:1) to give hydroxythiazoline **138** as a colourless oil (60 mg, 38 % yield), R_f = 0.10 (n-hexane/EtOAc, 3:1). ^{1}H NMR (400 MHz, $CDCl_3$, isomer ratio = 1:1, the asterisk denotes isomer peak): δ =1.33 and 1.34* (t, J = 7 Hz, 3H, OCH_2CH_3), 1.46 (d, J = 7 Hz, 3H, $CHCH_3$) 1.47 (s, 9H, $C(CH_3)_3$), 3.41 (d, J = 12 Hz, SCH_AH_B), 3.87 (d, J = 12 Hz, SCH_AH_B), 4.31 and 4.32* (q, J = 7.2 Hz, 2H, OCH_2CH_3), 4.63 (br, 1H, $CHCH_3$), 5.31 (br, 1H, α-NH) ppm. ^{13}C NMR (100 MHz, $CDCl_3$): δ = 14.04 (CH_2CH_3), 20.24 and 20.61* ($CHCH_3$), 28.23 and 28.31* ($C(CH_3)_3$), 40.8 (C5-H), 49.06 and 49.29* (α-CH), 62.90 and 62.99* (CH_2CH_3), 79.92 ($C(CH_3)_3$), 105.35 (C-OH), 154.83 (C=O), 170.71 (C=O), 179.90 (C=N) ppm.

Ethyl (*R*)-2-(1-*tert*-butoxycarbonylaminoethyl)thiazole-4-carboxylate, (59)

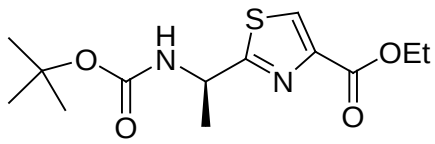

59

Thioamide **58** (500 mg, 2.45 mmol) was dissolved in DME (12 mL). After stirring vigorously at -15 °C for 10 min, finely ground $KHCO_3$ (1.96 g, 19.6 mmol) was added to a suspension solution. The mixture was stirred for 30 min and ethyl bromopyruvate (0.2 mL, 1.5 mmol) was added. After 5 min, the solution of 2,6-lutidine (2.43 mL, 20.8 mmol) and trifluoroacetic anhydride (1.37 mL, 9.8 mmol) in DME (2 mL) was added at -15 °C. After stirring at -15 °C for 1 h, the mixture was poured into water (20 mL) and extracted with Et_2O (10 mL × 3). The organic layers were combined, dried ($MgSO_4$) and concentrated. The residue was purified by column chromatography (n-hexane/EtOAc, 4:1) to give thiazole **59** as a light yellow solid (361 mg, 49 % yield), m.p. 80-82 °C (ref.[150] 85-86 °C); R_f = 0.5 (n-hexane/EtOAc, 3:2). $[\alpha]_D^{21}$ = +32 (c =1.0, $CHCl_3$). IR (KBr): ν = 3368, 3114, 1717, 1687, 1494, 1229, 1059 cm^{-1}. ^{1}H NMR (400 MHz, $CDCl_3$): δ = 1.40 (t, J = 7 Hz, 3H, CH_2CH_3), 1.44 (s, 9H, $C(CH_3)_3$), 1.62 (d, J = 6.4 Hz, 3H, $CHCH_3$), 4.40 (q, J = 7 Hz, 2H, CH_2CH_3), 5.10 (br, s, 1H, α-CH), 5.30 (br, s, 1H, α-NH), 8.08 (s, 1H, C^5H) ppm. ^{13}C NMR (100 MHz, $CDCl_3$): δ = 14.36 (CH_2CH_3), 21.79 ($CHCH_3$), 28.31 ($C(CH_3)_3$), 48.93 (α-CH), 61.43 (CH_2CH_3), 80.25 ($C(CH_3)_3$), 127.14 (C5-H),

147.21 (C=C), 154.88 (C=O), 161.35 (C=O), 174.90 (C=N) ppm. MS: *m/z* (+ESI) calcd for $C_{13}H_{20}N_2O_4SNa^+$ 323.1144, found 323.0970 [MNa^+].

(*R*)-2-(1-*tert*-Butoxycarbonylaminoethyl)thiazole-4-carboxylic acid, (44)

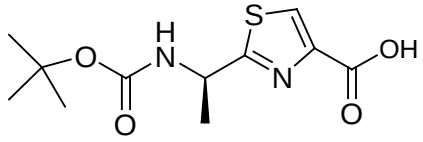

44

Boc-(*R*)-Ala-Thz-OEt **(59)** (1.24 g, 4.1 mmol) was dissolved in solution of THF/ MeOH/ H_2O 9:6:6 mL. Lithium hydroxide (118 mg, 4.9 mmol) in water (2 mL) was added at 0 °C. The mixture was warmed to room temperature and stirred overnight. The solvent was removed *in vacuo*. The residue was dissolved in H_2O (40 mL) and extracted with EtOAc (20 mL × 2). The aqueous layer was acidified with saturated aqueous $KHSO_4$ to pH = 2 and extracted with DCM (40 mL × 3). The organic layers were washed with brine, dried and concentrated. The residue was recrystallised with DCM/ Hexane to give the carboxylic acid **44** as a pale yellow solid (986 mg, 88 % yield), m.p. 58-61 °C; $[\alpha]_D^{26}$ = + 31 (*c* = 1.0, $CHCl_3$). IR (Solid): *v* = 3362, 3105, 2979, 1692, 1517, 1366, 1242, 1058 cm^{-1}. ^1H NMR (400 MHz, $CDCl_3$): δ = 1.47 (s, 9H, C(CH_3)$_3$), 1.66 (d, *J* = 6 Hz, 3H, CHCH_3), 5.10 (br, s, 1H, α-CH), 5.30 (br, s, 1H, α-NH), 8.23 (s, 1H, C^5H) ppm. ^{13}C NMR (100 MHz, $CDCl_3$): 21.7 (CH_3), 28.4 (C(*C*H_3)$_3$), 60.5 (α-*C*H), 80.2 (*C*(CH_3)$_3$), 128.7 (C_5-H), 146.6 (C=C), 155.0 (C=O), 164.1 (C=O), 171.4 (C=N) ppm. MS: *m/z* (+ESI) calcd for $C_{11}H_{17}N_2O_4SNa^+$ 295.0562, found 295.0352 [MNa^+].

Ethyl-2-((*R*)-1-((*S*)-3,3,3-trifluoro-2-methoxy-2-phenylpropanamido)ethyl)-thiazole-4-carboxylate, (*R*,*S*)-145

Ethyl-2-((*S*)-1-((*S*)-3,3,3-trifluoro-2-methoxy-2-phenylpropanamido)ethyl)-thiazole-4-carboxylate, (*S*,*S*)-145

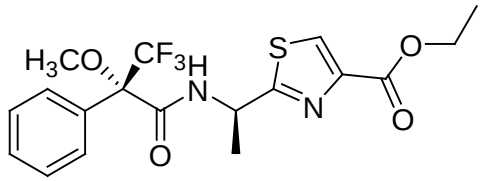

(*R*,*S*)-**145**

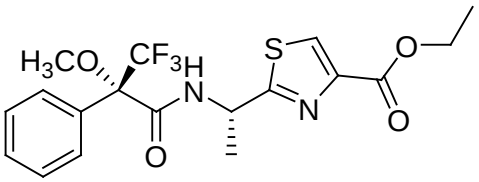

(*S*,*S*)-**145**

Recemic Boc-(*R*)-Ala-Thz-OEt **(59)** (20 mg, 0.06 mmol) was treated with TFA/DCM (1 mL/ 1 mL). The reaction mixture was stirred at room temperature for 1 h. The solvent was removed *in vacuo*. The residue oil was treated with (*R*)-(−)-α-Methoxy-α-(trifluoromethyl)phenylacetyl chloride (12.5 µL, 0.06 mmol) and DIPEA (23 µL, 0.12 mmol) in DCM (1 mL) and was stirred at room temperature for 1 h. The solvent was removed *in vacuo* to give the Mosher's derivatives (*R*,*S*)-**145** and (*R*,*R*)-**145** as colourless oils (27 mg, 96 % yield).

(*R*,*S*)-**145**: ^{1}H NMR (400 MHz, $CDCl_3$): δ = 1.41 (t, *J* = 7 Hz, 3H, OCH_2CH_3), 1.75 (d, *J* = 8 Hz, 3H, α-CH_3), 3.41 (t, *J* = 1 Hz, 3H, OCH_3), 4.43 (q, *J* = 7 Hz, 3H, OCH_2CH_3), 5.49 (td, *J* = 2, 8 Hz, 1 H, α-H), 7.38-7.53 (m, 5 H, arom. H), 8.09 (s, 1H, C-5H) ppm. ^{19}F NMR (375 MHz, $CDCl_3$): δ = - 68.94 ppm.

(*R*,*R*)-**145**: ^{1}H NMR (400 MHz, $CDCl_3$): δ = 1.41 (t, *J* = 7 Hz, 3H, OCH_2CH_3), 1.69 (d, *J* = 8 Hz, 3H, α-CH_3), 3.47 (t, *J* = 1 Hz, 3H, OCH_3), 4.42 (q, *J* = 7 Hz, 3H, OCH_2CH_3), 5.49 (td, *J* = 2, 8 Hz, 1 H, α-H), 7.38-7.53 (m, 5 H, arom. H), 8.13 (s, 1H, C-5H) ppm. ^{19}F NMR (375 MHz, $CDCl_3$): δ = - 68.57 ppm.

6.3.2 **Synthesis of (*R*)-Ala-oxazole-OH**

(*S*)-Ethyl 2-((*R*)-2-(*tert*-butoxycarbonylamino)propanamido)-3-hydropropanoate, (148)

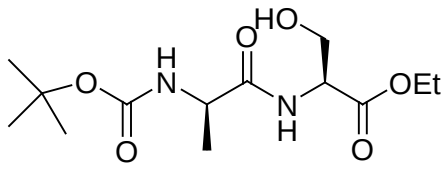

148

Boc-(*R*)-Alanine (1.23 g, 6.5 mmol) and serine ethyl ester hydrochloride were dissolved in CH_2Cl_2 (15 mL). *N*,*N*-diisopropylethylamine (1.70 mL, 9.7 mmol) was added into the solution and cooled to 0 °C. Then hydroxybenzotriazole (0.878 g, 6.5 mmol) and *N*,*N'*-dicyclohexylcarbodiimide (1.34 g, 6.5 mmol) were added. The reaction mixture was warmed to room temperature and stirred for 2 h. The solution was partitioned with 0.1 N HCl (10 mL) and CH_2Cl_2 (10 mL × 3). The organic layer was washed with saturated $NaHCO_3$ (10 mL), dried ($MgSO_4$) and concentrated. The residue was purified by column chromatography ($CHCl_3$/MeOH, 96:4) to give Boc-(*R*)-Ala-Ser-OEt (**148**) as a white solid (1.37 g, 69 % yield); m.p. 86-87 °C; R_f = 0.25 ($CHCl_3$/MeOH, 96:4). IR (KBr): ν = 3510, 3363, 3263, 1706, 1678, 1530, 1327 cm^{-1}. ^1H NMR (400 MHz, $CDCl_3$): δ = 1.30 (t, J = 7 Hz, 3H, CH_2CH_3), 1.40 (d, J = 7 Hz, 3H, $CHCH_3$), 1.45 (s, 9H, $C(CH_3)_3$), 2.82 (t, J = 6 Hz, 1H, OH), 3.96 (br, 1H, CH_AH_BOH), 4.04 (br, 1H, CH_AH_BOH), 4.18 (t, J = 6 Hz, 1H, $CHCH_2$), 4.26 (q, J = 7 Hz, 2H, CH_2CH_3), 4.61 (br, 1H, $CHCH_3$), 5.04 (d, J = 4 Hz, 1H, NH), 7.08 (d, J = 4 Hz, 1H, NH). ^{13}C NMR (100 MHz, $CDCl_3$): δ = 14.10 (CH_2CH_3), 18.23 ($CHCH_3$), 28.28 ($C(CH_3)$), 50.69 (α-CH), 54.86 (α-CH), 61.80 (OCH_2), 62.70 (OCH_2), 80.48 ($C(CH_3)$), 155.81 (CO), 170.38 (CO), 172.92 (CO) ppm. MS: *m/z* (+ESI) calcd for $C_{13}H_{24}N_2O_6Na^+$ 305.0634, found 305.0638 [MNa^+].

Ethyl 2-((*R*)-1-(*tert*-butoxycarbonylamino)ethyl)-4,5-dihydrooxazole-4-carboxylate, (149)

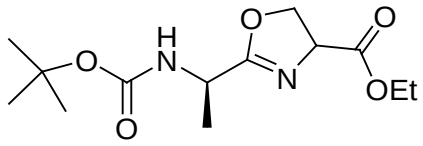

149

Burgess reagent (methoxycarbonylsulphamoyl-triethylammoniumm hydroxide) was added to a solution of Boc-(*R*)-Ala-Ser-OEt (**148**) (200 mg, 0.66 mmol) in dry THF (5 mL) in 7 mL microwave tube. The tube was capped; the mixture was stirred for 10 min and was microwaved (100 W) for 30 min at 70 °C under 250 psi pressure. The solution was allowed to cool to room temperature. The pale yellow solution was concentrated and purified by column chromatography (n-Hexane/EtOAc, 2:3) to give Boc-(*R*)-Ala-dehydrooxazole **149** as a yellow oil (145 mg, 77 % yield), R_f = 0.5 (n-Hexane/EtOAc, 2:3). ^{1}H NMR (400 MHz, $CDCl_3$): δ = 1.32 (t, J = 7 Hz, 3H, OCH_2CH_3), 1.41 (d, J = 7 Hz, 3H, $CHCH_3$), 1.45 (s, 9H, $C(CH_3)_3$), 4.25 (q, J = 7 Hz, 2H, OCH_2CH_3), 4.47 (br, 1H, $CHCH_3$), 4.48 (t, J = 8 Hz, 1H, OCH_AH_B), 4.57 (t, J = 8 Hz, 1H, OCH_AH_B), 4.74 (dd, J = 4, 8 Hz, 1H, NCH), 5.21 (br, 1H, NH). ^{13}C NMR (100 MHz, $CDCl_3$, isomer ratio = 1:1, the asterisk denotes isomer peak): δ = 14.12 (OCH_2CH_3), 19.57 and 19.63* ($CHCH_3$), 28.31 ($C(CH_3)$), 44.78 ($CHCH_3$), 61.76 (OCH_2CH_3), 67.98 (NCH), 70.21 (CH_2CH), 79.73 ($C(CH_3)$), 154.89 (CO), 170.8 (CO), 170.78 (CN) ppm.

(*R*)-Ethyl 2-(1-(*tert*-butoxycarbonylamino)ethyl)oxazole-4-carboxylate, (150)

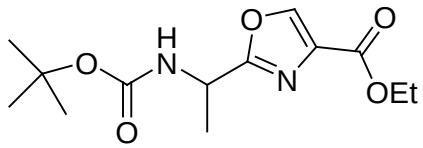

150

tert-Butyl perbenzoate (74.6 µL, 0.65 mmol) was added dropwise to a boiling solution, which is a mixture of the Boc-(*R*)-Ala-dehydrooxazole (**149**) and CuBr (74.6 mg, 0.52 mmol) in benzene (4 mL) over 1 h. The solution was further refluxed for 1 h. Then the reaction mixture was poured into saturated aqueous $NaHCO_3$ (10 mL) and extracted with ether (10 mL × 2), dried with $MgSO_4$ and

concentrated. The residue oil was purified by column chromatography (n-Hexane/EtOAc, 7:3) to give oxazole **150** as a colourless oil (86 mg, 72 % yield), R_f = 0.4 (n-Hexane/EtOAc, 7:3). $[\alpha]_D^{21}$ = + 13 (*c* = 1.0, $CHCl_3$). IR (KBr): *v* =3346, 3016, 1716, 1683, 1523, 1110, 1063 cm^{-1}. ^1H NMR (400 MHz, $CDCl_3$): δ = 1.39 (t, *J* = 7 Hz, 3H, CH_2CH_3), 1.46 (s, 9H, $C(CH_3)_3$), 1.60 (d, *J* = 7.2 Hz, 3H, $CHCH_3$), 4.41 (q, *J* = 7 Hz, 2H, CH_2CH_3), 5.03 (br, 1H, $CHCH_3$), 5.23 (br, 1H, NH), 8.18 (s, 1H, C=CH). ^{13}C NMR (100 MHz, $CDCl_3$): δ = 14.32 (OCH_2CH_3), 20.25 ($CHCH_3$), 28.30 ($C(CH_3)$), 44.80 ($CHCH_3$), 61.30 (OCH_2CH_3), 80.17 ($C(CH_3)$), 133.48 (C=CH), 143.86 (C=CH), 161.14 (CO), 165.87 (CO) ppm. MS: *m/z* (+ESI) calcd for $C_{13}H_{20}N_2O_5Na^+$ 307.1372, found 307.1220 [MNa^+].

Ethyl-2-((*R*)-1-((*S*)-3,3,3-trifluoro-2-methoxy-2-phenylpropanamido)ethyl)-oxazole-4-carboxylate, (*R*,*S*)-155

Ethyl-2-((*S*)-1-((*S*)-3,3,3-trifluoro-2-methoxy-2-phenylpropanamido)ethyl)-oxazole-4-carboxylate, (*S*,*S*)-155

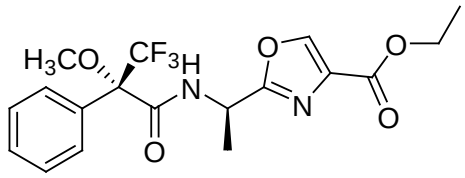

(*R*,*S*)-**155**

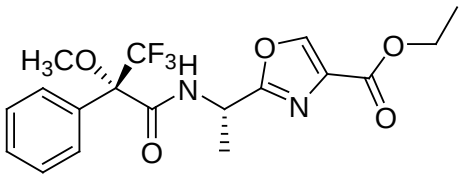

(*S*,*S*)-**155**

Boc-Ala-oxazole-OEt (**150**) (4 mg, 0.014 mmol) was treated with TFA/DCM (1 mL/ 1mL). The reaction mixture was stirred at room temperature for 1 h. The solvent was removed *in vacao*. The residue oil was treated with (*R*)-(−)-α-Methoxy-α-(trifluoromethyl)phenylacetyl chloride (2.6 µL, 0.014 mmol) and DIPEA (4.8 µL, 0.028 mmol) in DCM (1 mL) and was stirred at room temperature for 1 h. The solvent was removed *in vacao* to give the Mosher's derivatives (*R*,*S*)-**155** and (*S*,*S*)-**155** as a colourless oil (5 mg, 90 % yield). ^1H NMR (400 MHz, $CDCl_3$, isomer ratio = 2:1, the asterisk denotes isomer peak): δ = 1.39 and 1.40* (t, *J* = 7 Hz, 3H, OCH_2CH_3), 1.61* and 1.67 (d, *J* = 8 Hz, 3H, α-CH_3), 3.93* and 3.48 (t, *J* = 1 Hz, 3H, OCH_3), 4.42 (q, *J* = 7 Hz, 3H, OCH_2CH_3), 5.39 (m, , 1 H, α-H), 7.41-7.45 (m, 5 H, arom. H), 8.17* and 8.20(s, 1H, C-5H) ppm. ^{19}F NMR (375 MHz, $CDCl_3$): δ = -68.99 and -68.74* ppm.

6.3.3 **Synthesis of *N*-Fmoc-phenylselenocysteine**

***N*-(*tert*-Butoxycarbonyl)-(*S*)-serine β-lactone, (64)**

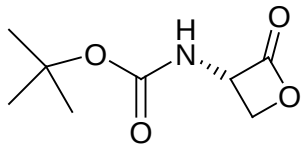

64

Two-Neck round-bottom flask was equipped with a stir bar, nitrogen bubbler and a rubber septum. The flask was charged with dry THF (8 mL) and triphenylphosphine (257 mg, 0.98 mmol). The triphenylphosphine was dissolved by stirring and was cooled to -78 °C. Diethyl azodicarboxylate (445 µL, 0.98 mmol) was added to the solution. The result pale solution was stirred at -78 °C for 10 min. The rubber septum was quickly replaced by a dropping funnel containing a solution of Boc-(*S*)-serine (200 mg, 0.98 mmol) in THF (2 mL) which was further added dropwise to the mixture over more than 30 min. After completion of addition, the mixture was stirred at -78 °C for 20 min. The cooling bath was removed, and the mixture was slowly warmed to room temperature over 2.5 h, then concentrated. The yellow residual oil was suspended in n-hexane/EtOAc (1:1, 20 mL) and filtered. The filtrate was concentrated and further purified by column chromatography (n-hexane/EtOAc, 7:3) to give **64** as a white solid (76 mg, 42 % yield). R_f = 0.25 (n-Hexane/EtOAc, 7:3). $[\alpha]_D^{23}$ = -17 (*c* 1.0, $CHCl_3$). IR (KBr): ν = 3358, 3011, 2977, 1842, 1680, 1531, 1289 cm^{-1}. ^1H NMR (400 MHz, $CDCl_3$): δ = 1.45 (s, 9H, $C(CH_3)_3$), 4.43 (br, 2H, CH_2), 5.09 (br, 1H, NC*H*), 5.58 (d, *J* = 8 Hz, 1H, N*H*) ppm. ^{13}C NMR (100 MHz, $CDCl_3$): δ = 28.18 ($C(CH_3)$), 59.44 (*C*H), 66.55 (CH_2), 81.30 ($C(CH_3)$), 154.66 (CO), 169.71 (CO) ppm.

***N*-(*tert*-Butoxycarbonyl)-(*R*)-phenylselenocysteine, (65)**

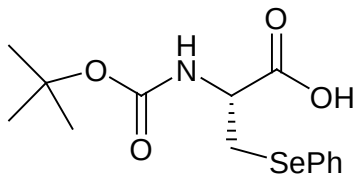

65

Sodium trimethylborohydride (358 mg, 2.8 mmol) was added to a solution of diphenyl diselenide (437 mg, 1.4 mmol) in dry ethanol (12 mL) at room temperature under nitrogen. The resulting yellow solution was stirred for 30 min then a solution of β-lactone (**64**) (374 mg, 2 mmol) in dry ethanol (5 mL) was added. The reaction mixture was stirred for 2 h and concentrated. The residue was partitioned between saturated $NaHCO_3$ (20 mL) and Et_2O (20 mL). The aqueous layer was washed by Et_2O (5 mL × 2) to remove excess diphenyl diselenide. The aqueous layer was acidified with 3M aqueous HCl to pH = 2, extracted with EtOAc (20 mL × 3). The organic layers were combined, washed with brine, dried ($MgSO_4$) and concentrated to give **65** as a white solid (685 mg, 99 % yield). m.p. 87-90 °C (ref.[150] m.p. 94-95 °C); R_f = 0.4 ($CHCl_3$/MeOH, 9:1 with 1 drop AcOH). $[\alpha]_D^{23}$ = -34 (*c* = 1.0, MeOH). ^{1}H NMR (400 MHz, $CDCl_3$): δ = 1.43 (s, 9H, C(C*H*$_3$)$_3$), 3.38 (br, 2H, CH_2), 4.66 (br, 1H, α-CH), 5.37 (br, 1H, NH), 7.28 (br, 3H, arom. CH), 7.57 (br, 2H, arom. CH) ppm. ^{13}C NMR (100 MHz, $CDCl_3$): δ = 28.27 (C(*C*H$_3$)), 30.16 (CH_2), 53.57 (α-CH), 80.43 (*C*(CH$_3$)), 127.61 (arom. CH), 129.02 (arom. C), 133.62 (arom. CH), 155.27 (CO), 175.43 (CO) ppm. MS: *m/z* (+ESI) calcd for $C_{14}H_{19}NNaO_4Se^+$ 368.0377, found 368.0130 [MNa^+].

(*R*)-β-Phenylselenocysteine, (66)

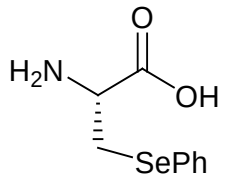

66

Trifluroroacetic acid (15 mL) was added dropwise to a solution of Boc-phenyselenocycsteine (**65**) (3.65 g, 10.6 mmol) in CH_2Cl_2 (15 mL) at room temperature. The reaction mixture was stirred for 1 h and concentrated. The white solid was wash with *n*-hexane to give **66** trifluoroacetate salt as a white solid (3.7 g, 97 % yield). m.p. 166-170 °C. ^{1}H NMR (400 MHz, MeOD): δ = 3.11 (dd, *J* = 16, 4 Hz, 1H, C*H*$_A$H$_B$), 3.29 (dd, *J* = 16, 4 Hz, 1H, CH$_A$*H*$_B$), 3.91 (dd, *J* = 4, 4 Hz, 1H, α-H), 7.13 (m, 3H, arom. CH), 7.42 (m, 3H, arom. CH) ppm. MS: *m/z* (+ESI) calcd for $C_9H_{12}NO_2Se^+$ 246.0033, found 246.0019 [MH^+].

***N*-(9-Fluorenylmethoxycarbonyl)-(*R*)-β-phenylselenocysteine, (67)**

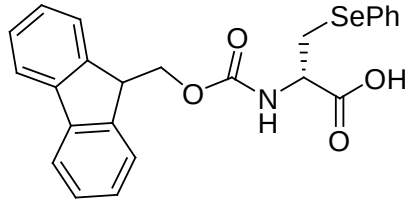

67

N-(9-Fluorenylmethyoxycarbonyloxy) succinimide (2.77 g, 8.2 mmol) was dissolved in THF (20 mL) and was added to a stirred solution of phenyselenocycsteine **(66)** (2.87 g, 8 mmol) and $NaHCO_3$ (2.3 g, 28 mmol) in water (25 mL) over 10 min. The reaction mixture was stirred overnight at room temperature. The solvent was removed *in vacuo*. The residue was dissolved in H_2O (40 mL), acidified with saturated aqueous $KHSO_4$ (30 mL), extracted with ethyl acetate (3 × 40 mL), washed with brine, dried and concentrated. The oil residue was purified by column chromatography ($CHCl_3$/MeOH, 19:1) to give Fmoc-phenylselenocysteine (**67**) as a white solid (3.49 g, 93 % yield); m.p. 98-99 °C; R_f = 0.5 ($CHCl_3$/ MeOH, 9:1 + 1 % AcOH). IR (KBr): ν = 3358, 3063, 1727, 1711, 1682, 1522, 1449, 1248 and 758 cm^{-1}. ^1H NMR (400MHz, $CDCl_3$): δ = 3.37 (dd, J = 4, 16 Hz, 1H, CH_AH$_B$), 3.45 (dd, J = 4, 16 Hz, 1H, CH_AH$_B$), 4.20 (t, J = 8 Hz, 1H, OCH$_2$CH), 4.36 (m, 2H, OCH_2CH), 4.77 (br, 1H, α-H), 5.58 (d, J = 8 Hz, 1H, NH), 7.26 (m, 4H, arom. CH), 7.34 (m, 2H, arom. CH), 7.43 (m, 2H, arom. CH), 7.54 (m, 3H, arom. CH), 7.79 (m, 2H, arom. CH) ppm. ^{13}C NMR (100MHz, $CDCl_3$): δ = 29.73 (SeCH$_2$), 47.05 (α-CH), 53.91 (CHCH$_2$), 67.38 (CHCH$_2$), [120.03, 125.14, 127.12, 127.79, 127.86, 128.58, 129.30, 133.79, 141.31, 143.66, 143.71] (arom.CH), 155.75 (CO), 174.93 (CO) ppm. MS: *m/z* (+ESI) calcd for $C_{24}H_{22}NO_4Se^+$ 468.0636 found 468.0135 [MH^+].

6.4 Experimental for Chapter 4

(*S*)-2-Chlorotrityl[*N*-(fluoren-9-ylmethoxycarbonyl)methyl-amino]-acetic acid polystyrene, (185)

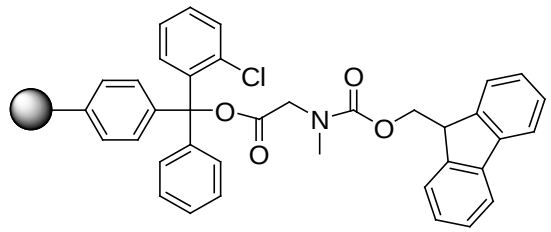

185

2-Chlorotrityl chloride resin (1 g, 1.2 mmol, theoretical loading 1.2 mmol g^{-1}) was swollen in DCM (6 mL) for 1 h. Fmoc-sarcosine (373 mg, 1.2 mmol) and DIPEA (418 µL, 2.4 mmol) in DCM (2 mL) then added to the resin suspension. The reaction mixture was gently stirred at room temperature for 2 h. MeOH (500 µL) was added and the suspension was stirred for another 15 min. The derivatised resin was collected in a Buchner funnel, washed with DMF, DCM and hexane and dried *in vacuo* to give the desired product **185** (1.363 g, Fmoc substitution 0.84 mmol g^{-1}, 70 %).

Determination of resin substation based on the Fmoc-substitution.

An accurately weighted sample of the dry Fmoc-substituted resin (*ca*.1-2 mg) was exposed to a solution of 20 % *v/v* peperidine in DMF (3 mL) for 1 h, with occasional agitation. Te UV absorbance reading at 290 nm was taken and used in the Beer-Lamber's law.

$A_{290} = \varepsilon\ c\ l$

A = absorbance wavelength at 209 nm

ε = molar extinction coefficient (5253 $mol^{-1}\ cm^{-1}$ for Fmoc piperidine adduct)

c = concentration (mol^{-1})

l = path length (1 cm)

Since l and ε are known and A can be measured, the concentration of the Fmoc-piperidein adduct released from the resin can be determined.

The theoretical loading can be calculated using the follow equation

Theoretical loading = x /(1+(xy / 1000)) mmol g^{-1}

X = initial loading of resin (mmol)

Y = molecular weight added on to resin

The percentage efficiency of resin loading can then be evaluated from the following equation:

% loading efficiency = (actual loading / theoretical loading) x 100

Standard Protocal A for linear peptide synthesis

The derivatised resin **185** (1 eq.) was placed in a reaction column, swollen with DMF/DCM (1 mL) for 12 h, and Fmoc-deprotection was carried out on a continuous flow of 20 % *v/v* piperidein in DMF (2.8 mL min^{-1}, 10 min) using NOVA SYN® GEM manual peptide synthesiser. The reaction was monitored post-column at 355 nm. The resin was then washed with DMF (2.8 mL min^{-1}, 5 min), and the peptide sequence (*R*)-Ala^1-Thz^2-Trp^3-Trp^4(X)–Gly^5-(*R*)-Ala^6-$Ph(Se)^7$-Sar^8-OH was assembled manually using NOVA SYN® GEM manual peptide synthesiser.

Sequential acylation reactions were carried out at ambient temperature for 4 h using appropriate N^{α}-Fmoc-protected amino acids (4 eq.) [Fmoc-Ph(Se)-OH (**42**), Fmoc-(*R*)-Ala-OH, Fmoc-Gly-OH, Fmoc-Trp(X)-OH (**43**), Fmoc-Trp-OH, Boc-(*R*)-Ala-Thz-OH (**44**)] and carboxylated-activating reagent, PyOxim (4 eq.) or HATU (3.9 eq.) and DIPEA (8 eq.) in DMF (0.5 mL). Sequential Fmoc-deprotection was achieved using 20 % *v/v* piperidine in DMF (2.8 mL min^{-1}, 10 min).

After final acylation reaction, the peptidyl-resin was filtered, washed successively with DMF, DCM and hexane, and dried *in vacuo*.

The resin product was suspended in a mixture of water (0.025 mL), TIPS (0.025 mL) and DCM (1 mL), followed by the addition of TFA (1 mL). The reaction mixture was allowed to stand at ambient temperature for 1 h. The suspension was filtered, washed with DCM (3 mL), and the filterate was evaporated *in vacuo*.

The residual material was triturated with diethyl ether (2 mL) to result an off-white sold. The desired linear peptide was dissolved in water (2 mL) and lyophilized overnight.

(*R*)-Ala^{1}-Thz^{2}-Trp^{3}-Trp^{4}-Gly^{5}-(*R*)-Ala^{6}-Ph(Se)^{7}-Sar^{8}-OH, (46a)

Using Standard protocol A and the Fmoc-Trp-OH (**43a**) the title peptide was assembled as a white solid (54 mg, 56 %, yield, 90 % purity). The linear peptide was used directly in the next cyclisation step without further purification.

RP-HPLC 1-35 % B in 10 min, t_R 10.3 min.

ES-MS *m/z* calcd for $C_{45}H_{51}N_{10}O_8SSe$ 971.2777, found 971.2313 [MH^+].

(*R*)-Ala-Thz-Trp-(5-Br)-Trp-Gly-(*R*)-Ala-Ph(Se)-Sar-OH, (46b)

Using Standard protocol A and the Fmoc-(5-Br)-Trp-OH (**43b**) the title peptide was assembled as a white solid (63 mg, 60 % yield, 69 % purity). The linear peptide was used directly in the next cyclisation step without further purification.

RP-HPLC 1-35 % B in 10 min, t_R 10.6 min.

ES-MS *m/z* calcd for $C_{45}H_{50}BrN_{10}O_8SSe$ 1049.1882, found 1049.1888 [MH^+].

(*R*)-Ala-Thz-Trp-(5-Cl)-Trp-Gly-(*R*)-Ala-Ph(Se)-Sar-OH, (46c)

Using Standard protocol A and the Fmoc-(5-Cl)-Trp-OH (**43c**) the title peptide was assembled as a white solid (56 mg, 56 % yield, 86 % purity). The linear peptide was used directly in the next cyclisation step without further purification.

RP-HPLC 1-35% B in 10 min, t_R 12.1 min.

ES-MS *m/z* calcd for $C_{45}H_{50}ClN_{10}O_8SSe$ 1005.2388, found 1005.2287 [MH^+].

(*R*)-Ala-Thz-Trp-(5-Et)-Trp-Gly-(*R*)-Ala-Ph(Se)-Sar-OH, (46e)

Using Standard protocol A and the Fmoc-(5-Et)-Trp-OH (**43e**) the title peptide was assembled as a white solid (53 mg, 54% yield, 84 % purity). The linear peptide was used directly in the next cyclisation step without further purification.

RP-HPLC 1-35 % B in 10 min, t_R 10.6 min.

ES-MS *m/z* calcd for $C_{47}H_{55}N_{10}O_8SSe$ 999.3090, found 999.2575 [MH^+].

(*R*)-Ala-Thz-Trp-(5-Me)-Trp-Gly-(*R*)-Ala-Ph(Se)-Sar-OH, (46f)

Using Standard protocol A and the Fmoc-(5-Me)-Trp-OH (**43f**), the title peptide was assembled as a white solid (58 mg, 59 % yield, 79 % purity). The linear peptide was used directly in the next cyclisation step without further purification.

RP-HPLC 1-35 % B in 10 min, t_R 11.5 min.

ES-MS *m/z* calcd for $C_{46}H_{53}N_{10}O_8SSe$ 985.2934, found 985.2867 [MH^+].

(*R*)-Ala-Thz-Trp-(5-OMe)-Trp-Gly-(*R*)-Ala-Ph(Se)-Sar-OH, (46g)

Using Standard protocol A and the Fmoc-(5-Me)-Trp-OH (**43g**) the title peptide was assembled as a white solid (64 mg, 64 % yield, 78 % purity). The linear peptide was used directly in the next cyclisation step without further purification.

RP-HPLC 1-35 % B in 10 min, t_R 10.4 min.

ES-MS *m/z* calcd for $C_{46}H_{53}N_{10}O_9SSe$ 1001.2883, found 1001.2643 [MH^+].

(*R*)-Ala-Thz-Trp-(1-Me)-Trp-Gly-(*R*)-Ala-Ph(Se)-Sar-OH, (46i)

Using Standard protocol A and the Fmoc-(1-Me)-Trp-OH (**43i**) the title peptide was assembled as a white solid (84 mg, 86 % yield, 86 % purity). The linear peptide was used directly in the next cyclisation step without further purification.

RP-HPLC 1-35 % B in 10 min, t_R 10.8 min.

ES-MS *m/z* calcd for $C_{46}H_{53}N_{10}O_8SSe$ 985.2934, found 985.2985 [MH^+].

Standard Protocol B for linear peptide synthesis

The derivatised resin **185** (1 eq.) was placed in a reaction column, swollen with DMF/DCM (1 mL) for 12 h, and Fmoc-deprotection was carried out on a continuous flow of 20 % *v/v* piperidine in DMF (2.8 mL min^{-1}, 10 min) using NOVA SYN® GEM manual peptide synthesizer. The reaction was monitored post-column at 355 nm. The resin was then washed with DMF (2.8 mL min^{-1}, 5 min), and the peptide sequence (*R*)-Ala^{1}-Thz^{2}-Trp^{3}-Trp^{4}(X)-Gly^{5}-(*R*)-Ala^{6}-Ph(Se)^{7}-Sar^{8}-OH was assembled manually using NOVA SYN® GEM manual peptide synthesizer.

Sequential acylation reactions were carried out at ambient temperature for 4 h using appropriate N^{α}-Fmoc-protected amino acids (4 eq.) [Fmoc-Ph(Se)-OH (**42**), Fmoc-(*R*)-Ala-OH, Fmoc-Gly-OH, Fmoc-Trp(X)-OH (**43**), Fmoc-Trp-OH, Boc-(*R*)-Ala-Thz-OH (**44**)] and carboxylated-activating reagent, PyOxim(4 eq.) or HATU (3.9 eq.) and DIPEA (8 eq.) in DMF (0.5 mL). Repetitive Fmoc-deprotection was achieved using 20 % *v/v* piperidine in DMF (2.8 mL min^{-1}, 10 min).

After final acylation reaction, the peptidyl-resin directly treated with $NaIO_4$ (4 eq.) in DMF/H_2O (0.5:0.2 mL) and stirred at room temperature for 6 h. The final assembled peptidyl-resin was filtered, washed successively with H_2O, DMF, DCM and hexane, and dried *in vacuo*.

The resin product was suspended in a mixture of water (0.1 mL) and DCM (1 mL), followed by the addition of TFA (1 mL). The reaction mixture was allowed to stand at ambient temperature for 1 h. The suspension was filtered, washed with DCM (3 mL), and the filterate was evaporated *in vacuo*.

The residual material was triturated with diethyl ether (2 mL) to result an off-white sold. The desired linear peptide was dissolved in water (2 mL) and lyophilized overnight.

(*R*)-Ala-Thz-Trp-(6-F)-Trp-Gly-(*R*)-Ala-Dha-Sar-OH, (46d)

Using Standard protocol B and the Fmoc-(6-F)-Trp-OH (**43d**) the title peptide was assembled as a red solid (54 mg, 65 %). The linear peptide was used directly in the next cyclisation step without further purification.

RP-HPLC 1-35 % B in 10 min, t_R 8.2 min.

ES-MS *m/z* calcd for $C_{39}H_{44}FN_{10}O_8S$ 831.3048, found 831.2910 [MH^+].

(*R*)-Ala-Thz-Trp-(4-MeO)-Trp-Gly-(*R*)-Ala-Dha-Sar-OH, (46h)

Using Standard protocol B and the Fmoc-(4-MeO)-Trp-OH (**43h**) the title peptide was assembled as a brown solid (63 mg, 75 %). The linear peptide was used directly in the next cyclisation step without further purification.

RP-HPLC 1-35 % B in 10 min, t_R 7.9 min.

ES-MS *m/z* calcd for $C_{40}H_{47}N_{10}O_9S$ 843.3248, found 843.3193 [MH^+].

(*R*)-Ala-Thz-Trp-(*R*)-Trp-Gly-(*R*)-Ala-Dha-Sar-OH, **(46k)**

Using Standard protocol B and the Fmoc-(*R*)-Trp-OH, the title peptide was assembled as a brown solid (39 mg, 48 %). The linear peptide was used directly in the next cyclisation step without further purification.

RP-HPLC 1-35 % B in 10 min, t_R 8.3 min.

ES-MS *m/z* calcd for $C_{39}H_{45}N_{10}O_8S$ 813.3143, found 813.3288 [MH^+].

***Cyclo*[(*R*)-Ala^1-Thz^2-Trp^3-Trp^4-Gly^5-(*R*)-Ala^6-Ph(Se)^7-Sar^8], (47a)**

Diisopropylethylamine (75 µL, 0.4 mmol) and PyBOP (112 mg, 0.2 mmol) were added successively to a solution of the linear peptide **46a** (70 mg, 0.07 mmol) and HOBt (29 mg, 0.2 mmol) in CH_2Cl_2 (144 mL) at room temperature. The reaction mixture was stirred for 1 day, concentrated and purified by RP-HPLC (Onyx Monolithic C_{18}, 100 x 10 mm) to afford the cyclic peptide **47a** as a white powder (20 mg, 30 % yield).

RP-HPLC 10-60 % B in 12 min, t_R 8.5 min.

ES-MS *m/z* calcd for $C_{45}H_{49}N_{10}O_7SSe$ 953.2672, found 953.2571 [MH^+].

***Cyclo*[(*R*)-Ala^1-Thz^2-Trp^3-(5-Br)-Trp^4-Gly^5-(*R*)-Ala^6-Ph(Se)^7-Sar^8], (47b)**

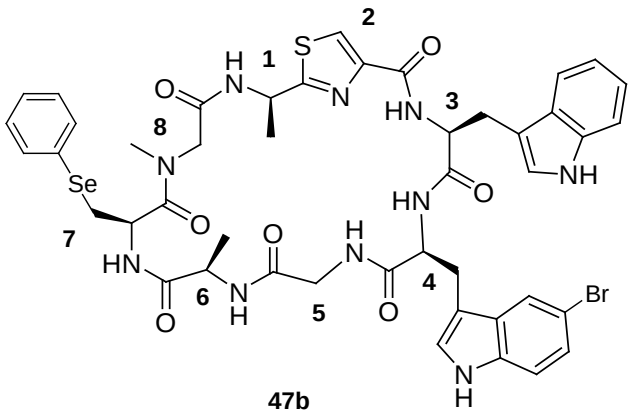

47b

Diisopropylethylamine (92 µL, 0.53 mmol), PyBOP (88 mg, 0.17 mmol) and HOBt (22 mg, 0.1 mmol) were added successively to a solution of the linear peptide **46b** (62 mg, 0.06 mmol) in CH_2Cl_2 (120 mL) at room temperature. The reaction mixture was stirred for 3 days, concentrated and purified by preparative RP-HPLC (Onyx Monolithic C_{18}, 100 x 10 mm) to afford the cyclic peptide **47b** as a white powder (10 mg, 17 % yield).

RP-HPLC 10-60 % B in 12 min, t_R 9.9 min.

^{1}H NMR (400 MHz, DMSO-d_6): δ = 0.65 (d, J = 7 Hz, 3H, 6-CH_3), 1.56 (d, J = 7 Hz, 3H, 1-CH_3), 3.13 (dd, J = 14, 8 Hz, 1H, 4-CH_AH$_B$), 3.22 (s, 3H. 8-CH_3), 3.24 (m, 1H, 4-CH$_A$$H_B$), 3.31 (m, 1H, 5-C$H_AH_B$), 3.34 (m, 1H, 7-C$H_AH_B$), 3.45 (m, 1H, 7-CH$_A$$H_B$), 3.49 (m, 1H, 8-C$H_AH_B$), 3.50 (m, 1H, 3-C$H_AH_B$), 3.67 (m, 1H, 3-CH$_A$$H_B$), 3.74 (m, 1H, 5-CH$_A$$H_B$), 4.13 (q, J = 7 Hz, 1H, 6-α-CH), 4.18 (t, J = 8 Hz, 1H, 4-α-CH), 4.35 (d, J = 17 Hz, 1H, 8-CH$_A$$H_B$), 4.60 (td, J = 7, 4 Hz, 1H, 7-α-CH), 4.78 (td, J = 12, 4 Hz, 1H, 3-α-CH), 5.32 (m, 1H, 1-α-CH), 7.01-7.32 (m, 12H, arom. H), 7.43 (d, J = 3 Hz, 7-NH), 7.56 (m, 2H, arom. H), 7.58 (d, J = 7 Hz, 1H, 1-NH), 7.95 (s, 1H, 2-CH), 8.06 (d, J = 9 Hz, 1H, 6-NH), 8.30 (s, 1H, 4-NH), 8.64 (d, J = 9 Hz, 1H, 3-NH), 8.88 (t, J = 5 Hz, 1H, 5-NH), 10.81 (d, J = 2 Hz, indole-NH), 11.16 (d, J = 2 Hz, indole-NH) ppm.

ES-MS *m/z* calcd for $C_{45}H_{48}N_{10}O_7SSe$ 1031.1777, found 1033.1757 [MH^+].

***Cyclo*[(*R*)-Ala-Thz-Trp-(5-Cl)-Trp-Gly-(*R*)-Ala-Ph(Se)-Sar], (47c)**

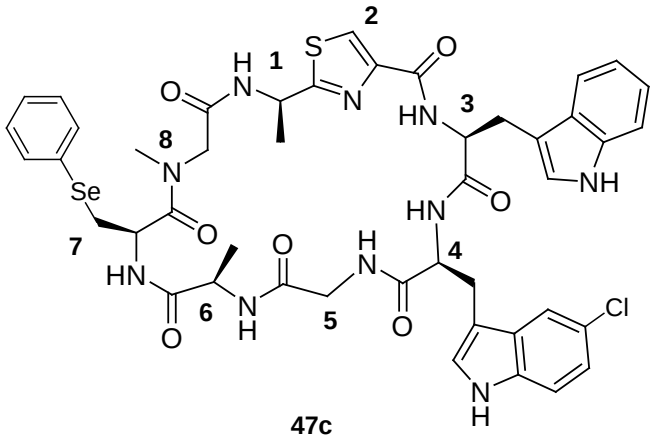

47c

Diisopropylethylamine (87 µL, 0.50 mmol), PyBOP (86 mg, 0.17 mmol) and HOBt (22 mg, 0.17 mmol) were added successively to a solution of the linear peptide **46c** (56 mg, 0.05 mmol) in CH_2Cl_2 (120 mL) at room temperature. The reaction mixture was stirred for 3 days, concentrated and purified by preparative RP-HPLC (Onyx Monolithic C_{18}, 100 x 10 mm) to afford the cyclic peptide **47c** as a white powder (11 mg, 20 % yield).

RP-HPLC 10-60 % B in 12 min, t_R 9.5 min.

^{1}H NMR (400 MHz, DMSO-d_6): δ = 0.65 (d, J = 7 Hz, 3H, 6-CH_3), 1.56 (d, J = 7 Hz, 3H, 1-CH_3), 3.12 (dd, J = 14, 8 Hz, 1H, 4-CH_AH$_B$), 3.22 (s, 3H. 8-CH_3), 3.24 (m, 1H, 4-CH$_A$$H_B$), 3.31 (m, 1H, 5-C$H_AH_B$), 3.34 (m, 1H, 7-C$H_AH_B$), 3.45 (m, 1H, 7-CH$_A$$H_B$), 3.49 (m, 1H, 8-C$H_AH_B$), 3.50 (m, 1H, 3-C$H_AH_B$), 3.67 (m, 1H, 3-CH$_A$$H_B$), 3.74 (m, 1H, 5-CH$_A$$H_B$), 4.13 (q, J = 7 Hz, 1H, 6-α-CH), 4.18 (t, J = 8 Hz, 1H, 4-α-CH), 4.35 (d, J = 17 Hz, 1H, 8-CH$_A$$H_B$), 4.60 (td, J = 7, 4 Hz, 1H, 7-α-CH), 4.78 (td, J = 12, 4 Hz, 1H, 3-α-CH), 5.32 (m, 1H, 1-α-CH), 6.97-7.32 (m, 12H, arom. H), 7.43 (d, J = 3 Hz, 7-NH), 7.56 (m, 2H, arom. H), 7.58 (d, J = 7 Hz, 1H, 1-NH), 7.95 (s, 1H, 2-CH), 8.06 (d, J = 9 Hz, 1H, 6-NH), 8.30 (s, 1H, 4-NH), 8.64 (d, J = 9 Hz, 1H, 3-NH), 8.88 (t, J = 5 Hz, 1H, 5-NH), 10.81 (d, J = 2 Hz, indole-NH), 11.17 (d, J = 2 Hz, indole-NH) ppm.

ES-MS *m/z* calcd for $C_{45}H_{48}N_{10}O_7SSe$ 987.2282, found 987.2104 [MH^+].

***Cyclo*[(*R*)-Ala-Thz-Trp-(7-Et)-Trp-Gly-(*R*)-Ala-Ph(Se)-Sar], (47e)**

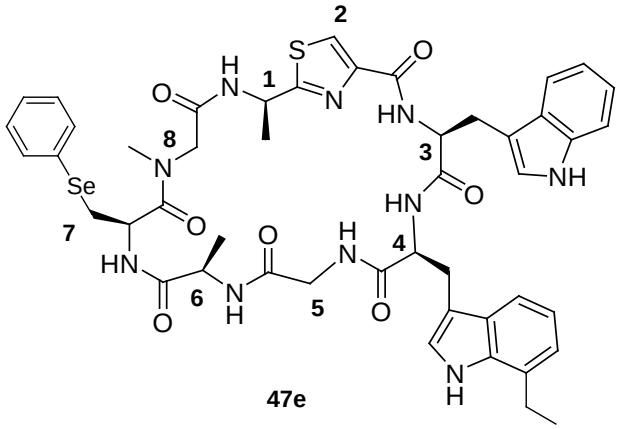

Diisopropylethylamine (80 µL, 0.46 mmol), PyBOP (81 mg, 0.17 mmol) and HOBt (21 mg, 0.16 mmol) were added successively to a solution of the linear peptide **46e** (52 mg, 0.05 mmol) in CH_2Cl_2 (120 mL) at room temperature. The reaction mixture was stirred for 3 days, concentrated and purified by preparative RP-HPLC (Onyx Monolithic C_{18}, 100 x 10 mm) to afford the cyclic peptide **47e** as a white powder (14 mg, 28 % yield).

RP-HPLC 10-60 % B in 12 min, t_R 9.9 min.

^{1}H NMR (400 MHz, DMSO-d_6): δ = 0.65 (d, J = 7 Hz, 3H, 6-CH_3), 1.26 (t, J = 7 Hz, 3H, 4-CH_2CH_3), 1.56 (d, J = 7 Hz, 3H, 1-CH_3), 2.86 (q, J = 7 Hz, 2H, 4-CH_2CH_3), 3.12 (dd, J = 14, 8 Hz, 1H, 4-CH_AH_B), 3.22 (s, 3H, 8-CH_3), 3.24 (m, 1H, 4-CH_AH_B), 3.31 (m, 1H, 5-CH_AH_B), 3.34 (m, 1H, 7-CH_AH_B), 3.45 (m, 1H, 7-CH_AH_B), 3.49 (m, 1H, 8-CH_AH_B), 3.50 (m, 1H, 3-CH_AH_B), 3.67 (m, 1H, 3-CH_AH_B), 3.74 (m, 1H, 5-CH_AH_B), 4.14 (q, J = 7 Hz, 1H, 6-α-CH), 4.22 (t, J = 8 Hz, 1H, 4-α-CH), 4.35 (d, J = 17 Hz, 1H, 8-CH_AH_B), 4.60 (td, J = 7, 4 Hz, 1H, 7-α-CH), 4.78 (td, J = 12, 4 Hz, 1H, 3-α-CH), 5.32 (m, 1H, 1-α-CH), 6.97-7.32 (m, 12H, arom. H), 7.44 (d, J = 3 Hz, 7-NH), 7.56 (m, 2H, arom. H), 7.58 (d, J = 7 Hz, 1H, 1-NH), 7.95 (s, 1H, 2-CH), 8.11 (d, J = 9 Hz, 1H, 6-NH), 8.35 (s, 1H, 4-NH), 8.65 (d, J = 9 Hz, 1H, 3-NH), 8.92 (t, J = 5 Hz, 1H, 5-NH), 10.83 (d, J = 2 Hz, indole-NH), 10.95 (d, J = 2 Hz, indole-NH) ppm.

ES-MS *m/z* calcd for $C_{47}H_{53}N_{10}O_7SSe$ 981.2985, found 981.2607 [MH^+].

***Cyclo*[(*R*)-Ala-Thz-Trp-(5-Me)-Trp-Gly-(*R*)-Ala-Ph(Se)-Sar], (47f)**

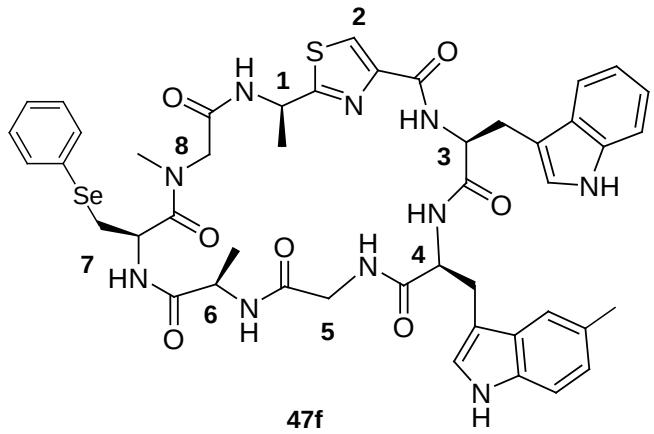

47f

Diisopropylethylamine (89 µL, 0.51 mmol), PyBOP (90 mg, 0.17 mmol) and HOBt (22 mg, 0.17 mmol) were added successively to a solution of the linear peptide **46f** (57 mg, 0.06 mmol) and in CH_2Cl_2 (120 mL) at room temperature. The reaction mixture was stirred for 3 days, concentrated and purified by preparative RP-HPLC (Onyx Monolithic C_{18}, 100 x 10 mm) to afford the cyclic peptide **47f** as a white powder (15 mg, 27 % yield).

RP-HPLC 10-60 % B in 12 min, t_R 9.4 min.

^{1}H NMR (400 MHz, DMSO-d_6): δ = 0.65 (d, J = 7 Hz, 3H, 6-CH_3), 1.56 (d, J = 7 Hz, 3H, 1-CH_3), 2.41 (s, 3H, 4-CH_3), 3.11 (dd, J = 14, 8 Hz, 1H, 4-CH_AH$_B$), 3.22 (s, 3H, 8-CH_3), 3.27 (m, 1H, 4-CH$_A$$H_B$), 3.31 (m, 1H, 5-C$H_AH_B$), 3.34 (m, 1H, 7-C$H_AH_B$), 3.45 (m, 1H, 7-CH$_A$$H_B$), 3.49 (m, 1H, 8-C$H_AH_B$), 3.67 (dd, J = 14, 4 Hz, 1H, 3-CH_AH$_B$), 3.75 (dd, J = 17, 4 Hz,1H, 3-CH$_A$$H_B$), 3.76 (m, 1H, 5-CH$_A$$H_B$), 4.13 (q, J = 7 Hz, 1H, 6-α-CH), 4.20 (t, J = 8 Hz, 1H, 4-α-CH), 4.35 (d, J = 17 Hz, 1H, 8-CH$_A$$H_B$), 4.60 (td, J = 7, 4 Hz, 1H, 7-α-CH), 4.78 (td, J = 12, 4 Hz, 1H, 3-α-CH), 5.32 (m, 1H, 1-α-CH), 6.94-7.56 (m, 12H, arom. H), 7.44 (d, J = 3 Hz, 7-NH), 7.56 (m, 2H, arom. H), 7.58 (d, J = 7 Hz, 1H, 1-NH), 7.95 (s, 1H, 2-CH), 8.09 (d, J = 9 Hz, 1H, 6-NH), 8.28 (s, 1H, 4-NH), 8.64 (d, J = 9 Hz, 1H, 3-NH), 8.85 (t, J = 5 Hz, 1H, 5-NH), 10.78 (d, J = 2 Hz, indole-NH), 10.81 (d, J = 2 Hz, indole-NH) ppm.

ES-MS *m/z* calcd for $C_{46}H_{51}N_{10}O_7SSe$ 967.2828, found 967.2723 [MH^+].

***Cyclo*[(*R*)-Ala-Thz-Trp-(5-OMe)-Trp-Gly-(*R*)-Ala-Ph(Se)-Sar], (47g)**

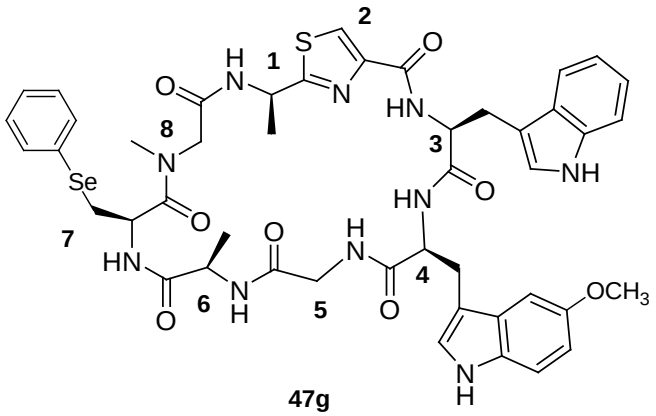

47g

Diisopropylethylamine (186 µL, 1.0 mmol), PyBOP and (185 mg, 0.36 mmol) HOBt (48 mg, 0.36 mmol) were added successively to a solution of the linear peptide **46g** (119 mg, 0.12 mmol) and in CH_2Cl_2 (220 mL) at room temperature. The reaction mixture was stirred for 3 days, concentrated and purified by preparative RP-HPLC (Onyx Monolithic C_{18}, 100 x 10 mm) to afford the cyclic peptide **47g** as a white powder (12 mg, 11 % yield).

RP-HPLC 10-60 % B in 12 min, t_R 8.5 min.

^{1}H NMR (400 MHz, DMSO-d_6): δ = 0.65 (d, J = 7 Hz, 3H, 6-CH_3), 1.56 (d, J = 7 Hz, 3H, 1-CH_3), 3.13 (dd, J = 14, 8 Hz, 1H, 4-CH_AH$_B$), 3.22 (s, 3H. 8-CH_3), 3.24 (m, 1H, 4-CH$_A$$H_B$), 3.31 (m, 1H, 5-C$H_AH_B$), 3.34 (m, 1H, 7-C$H_AH_B$), 3.45 (m, 1H, 7-CH$_A$$H_B$), 3.49 (m, 1H, 8-C$H_AH_B$), 3.50 (m, 1H, 3-C$H_AH_B$), 3.67 (m, 1H, 3-CH$_A$$H_B$), 3.74 (m, 1H, 5-CH$_A$$H_B$), 3.80 (s, 3H, 4-$OCH_3$), 4.13 (q, J = 7 Hz, 1H, 6-α-CH), 4.20 (t, J = 8 Hz, 1H, 4-α-CH), 4.40 (d, J = 17 Hz, 1H, 8-CH$_A$$H_B$), 4.60 (td, J = 7, 4 Hz, 1H, 7-α-CH), 4.79 (td, J = 12, 4 Hz, 1H, 3-α-CH), 5.32 (m, 1H, 1-α-CH), 6.75-7.28 (m, 12H, arom. H), 7.42 (d, J = 3 Hz, 7-NH), 7.56 (m, 2H, arom. H), 7.58 (d, J = 7 Hz, 1H, 1-NH), 7.95 (s, 1H, 2-CH), 8.11 (d, J = 9 Hz, 1H, 6-NH), 8.36 (s, 1H, 4-NH), 8.65 (d, J = 9 Hz, 1H, 3-NH), 8.85 (t, J = 5 Hz, 1H, 5-NH), 10.79 (d, J = 2 Hz, indole-NH), 10.82 (d, J = 2 Hz, indole-NH) ppm.

ES-MS *m/z* calcd for $C_{46}H_{51}N_{10}O_8SSe$ 983.2777, found 983.2693 [MH^+].

***Cyclo*[(*R*)-Ala-Thz-Trp-(1-Me)-Trp-Gly-(*R*)-Ala-Ph(Se)-Sar], (47i)**

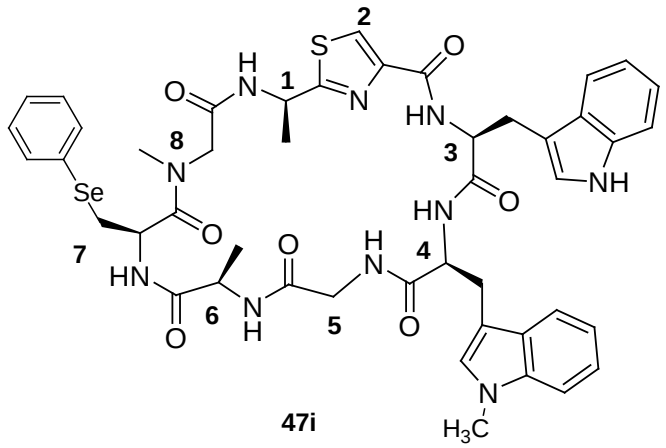

47i

Diisopropylethylamine (133 µL, 0.77 mmol), PyBOP (130 mg, 0.25 mmol) and HOBt (33 mg, 0.25 mmol) were added successively to a solution of the linear peptide **46i** (84 mg, 0.08 mmol) and in CH_2Cl_2 (120 mL) at room temperature. The reaction mixture was stirred for 3 days, concentrated and purified by RP-HPLC (Onyx Monolithic C_{18}, 100 x 10 mm) to afford the cyclic peptide **47i** as a white powder (14 mg, 17 % yield).

RP-HPLC 10-60 % B in 12 min, t_R 8.0 min.

^{1}H NMR (400 MHz, DMSO-d_6): δ = 0.65 (d, J = 7 Hz, 3H, 6-CH_3), 1.56 (d, J = 7 Hz, 3H, 1-CH_3), 3.13 (dd, J = 14, 8 Hz, 1H, 4-CH_AH$_B$), 3.22 (s, 3H. 8-CH_3), 3.24 (m, 1H, 4-CH$_A$$H_B$), 3.31 (m, 1H, 5-C$H_AH_B$), 3.34 (m, 1H, 7-C$H_AH_B$), 3.45 (m, 1H, 7-CH$_A$$H_B$), 3.49 (m, 1H, 8-C$H_AH_B$), 3.50 (m, 1H, 3-C$H_AH_B$), 3.67 (m, 1H, 3-CH$_A$$H_B$), 3.74 (m, 1H, 5-CH$_A$$H_B$), 3.77 (s, 3H, 4-$CH_3$), 4.14 (q, J = 7 Hz, 1H, 6-α-CH), 4.19 (t, J = 8 Hz, 1H, 4-α-CH), 4.33 (d, J = 17 Hz, 1H, 8-CH$_A$$H_B$), 4.61 (td, J = 7, 4 Hz, 1H, 7-α-CH), 4.79 (td, J = 12, 4 Hz, 1H, 3-α-CH), 5.32 (m, 1H, 1-α-CH), 6.75-7.32 (m, 13H, arom. H), 7.42 (d, J = 3 Hz, 7-NH), 7.56 (m, 2H, arom. H), 7.58 (d, J = 7 Hz, 1H, 1-NH), 7.96 (s, 1H, 2-CH), 8.07 (d, J = 9 Hz, 1H, 6-NH), 8.19 (s, 1H, 4-NH), 8.66 (d, J = 9 Hz, 1H, 3-NH), 8.91 (t, J = 5 Hz, 1H, 5-NH), 10.86 (d, J = 2 Hz, indole-NH) ppm.

ES-MS *m/z* calcd for $C_{46}H_{51}N_{10}O_7SSe$ 967.2828, found 967.2866 [MH^+].

General procedure for the preparation of *Cyclo*[(*R*)-Ala[1]-Thz[2]-Trp[3]-Trp[4]-Gly[5]-(*R*)-Ala[6]-Dha[7]-Sar[8]], Argyrin E, (48a)

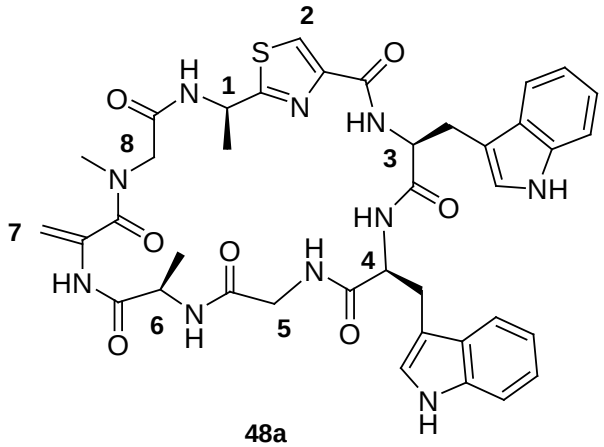

48a

Sodium periodate (3.5 mg, 16 μmol) was added to a solution of cyclic peptide **47a** (4 mg, 4 μmol) in water (2 mL) and acetonitrile (2 mL) at room temperature. The solution was stirred for 2 h. The solvent was removed and the residue was extracted with water (2 mL) and DCM/IPA (7 mL / 2 mL x 2). The organic layers were combined and concentrated. The residue was dissolved in acetonitiles (4 mL) then water (2 mL) and saturated aqueous Na_2CO_3 (2 mL) were added successively. The reaction mixture was stirred for 2 days, diluted with water (4mL) and extracted with DCM/IPA (7 mL/ 2 mL x2). The organic layers were combined, washed with water (5 mL), dried ($MgSO_4$) and concentrated. The residue was purified by preparative RP-HPLC (Onyx Monolithic C_{18}, 100 x 10 mm) to afford the argyrin **48a** as a pale yellow powder (2 mg, 66 % yield).

RP-HPLC 10-60 % B in 12 min, t_R 6.8 min.

^{1}H NMR (400 MHz, DMSO-d_6): δ = 0.87 (d, J = 7 Hz, 3H, 6-CH_3), 1.54 (d, = 7 Hz, 3H, 1-CH_3), 3.08 (s, 3H, 8-CH_3), 3.15 (m, 2H, 4-CH_2), 3.21 (m, 1H, 3-CH_AH$_B$), 3.22(m, 1H, 8-CH_AH$_B$), 3.39 (m, 1H, 5-CH_AH$_B$), 3.44 (m, 1H, 3-CH$_A$$H_B$), 3.80 (d, J = 16 Hz, 1H, 8-CH$_A$$H_B$), 3.88 (dd, J = 16, 8 Hz, 5-CH$_A$$H_B$), 4.24 (m, 1H, 4-α-CH), 4.35 (m, 1H, 6-α-CH), 4.78 (td, J = 12, 4 Hz, 1H, 3-α-CH), 4.89 (s, 1H, 7-CH_AH$_B$), 5.20 (s, 1H, 7-CH$_A$$H_B$), 5.39 (m, 1H, 1-α-CH), 6.90-7.75 (m, 10H, armo. H), 8.03 (s, 1H, 2-CH), 8.12 (d, J = 9 Hz, 1H, 6-NH), 8.29 (d, J = 9 Hz, 1H, 1-NH), 8.52 (d, J = 9 Hz, 1H, 3-NH), 8.57 (s, 1H, 4-NH), 8.79 (t, J = 4 Hz, 1H, 5-NH),

9.39 (s, 1H, 7-NH), 10.84 (d, *J* = 2 Hz, indole-NH), 11.05 (d, *J* = 2 Hz, indole-NH) ppm.

ES-MS *m/z* calcd for $C_{39}H_{43}N_{10}O_7S$ 795.3037, found 795.2959 [MH^+].

***Cyclo*[(*R*)-Ala-Thz-Trp-(5-Br)-Trp-Gly-(*R*)-Ala-Dha-Sar], (48b)**

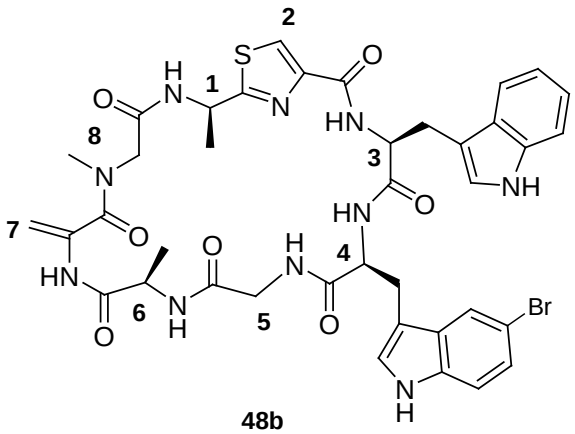

48b

Procedure as described in the general procedure using cyclic peptide **47b** (4 mg, 4 µmol) to afford argyrin **48b** as a sticky solid (2 mg, 58 % yield).

RP-HPLC 10-60 % B in 12 min, t_R 8.0 min.

^{1}H NMR (400 MHz, DMSO-d_6): δ = 0.87 (d, *J* = 7 Hz, 3H, 6-CH_3), 1.54 (d, *J* = 7 Hz, 3H, 1-CH_3), 3.13 (s, 3H, 8-CH_3), 3.15 (m, 2H, 4-CH_2), 3.21 (m, 1H, 3-CH_AH$_B$), 3.22 (m, 1H, 8-CH_AH$_B$), 3.39 (m, 1H, 5-CH_AH$_B$), 3.44 (m, 1H, 3-CH$_A$$H_B$), 3.80 (d, *J* = 16 Hz, 1H, 8-CH$_A$$H_B$), 3.88 (dd, *J* = 16, 8 Hz, 5-CH$_A$$H_B$), 4.24 (m, 1H, 4-α-CH), 4.35 (m, 1H, 6-α-CH), 4.78 (td, *J* = 12, 4 Hz, 1H, 3-α-CH), 4.92 (s, 1H, 7-CH_AH$_B$), 5.16 (s, 1H, 7-CH$_A$$H_B$), 5.39 (m, 1H, 1-α-CH), 6.95-7.77 (m, 9H, arom. H), 8.00 (s, 1H, 2-CH), 8.09 (d, *J* = 9 Hz, 1H, 6-NH), 8.27 (d, *J* = 9 Hz, 1H, 1-NH), 8.40 (s, 1H, 4-NH), 8.56 (d, *J* = 9 Hz, 1H, 3-NH), 8.73 (t, *J* = 4 Hz, 1H, 5-NH), 9.22 (s, 1H, 7-NH), 10.76 (d, *J* = 2 Hz, indole-NH), 11.15 (d, *J* = 2 Hz, indole-NH) ppm.

ES-MS *m/z* calcd for $C_{39}H_{42}N_{10}BrO_7S$ 875.2122, found 875.1877 [MH^+].

***Cyclo*[(*R*)-Ala-Thz-Trp-(5-Cl)-Trp-Gly-(*R*)-Ala-Dha-Sar], (48c)**

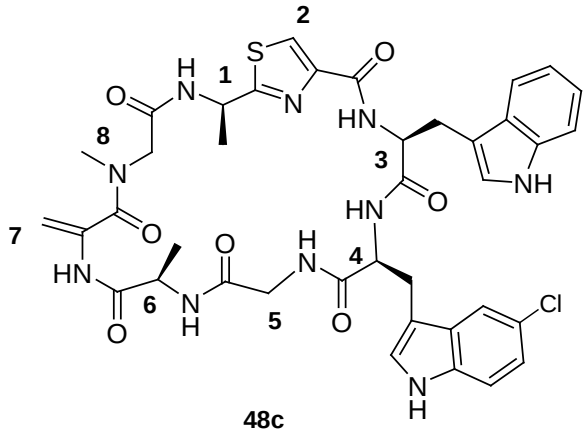

48c

Procedure as described in the general procedure using cyclic peptide **47c** (5 mg, 5 µmol) to afford argyrin **48c** as a sticky solid (3 mg, 67 % yield).

RP-HPLC 10-60 % B in 12 min, t_R 7.5 min

^{1}H NMR (400 MHz, DMSO-d$_6$): δ = 0.87 (d, J = 7 Hz, 3H, 6-CH$_3$), 1.54 (d, J = 7 Hz, 3H, 1-CH$_3$), 3.13 (s, 3H, 8-CH$_3$), 3.15 (m, 2H, 4-CH$_2$), 3.21 (m, 1H, 3-CH_AH$_B$), 3.22 (m, 1H, 8-CH_AH$_B$), 3.39 (m, 1H, 5-CH_AH$_B$), 3.44 (m, 1H, 3-CH$_A$$H_B$), 3.80 (d, J = 16 Hz, 1H, 8-CH$_A$$H_B$), 3.88 (dd, J = 16, 8 Hz, 5-CH$_A$$H_B$), 4.24 (m, 1H, 4-α-CH), 4.35 (m, 1H, 6-α-CH), 4.78 (td, J = 12, 4 Hz, 1H, 3-α-CH), 4.92 (s, 1H, 7-CH_AH$_B$), 5.16 (s, 1H, 7-CH$_A$$H_B$), 5.39 (m, 1H, 1-α-CH), 6.95-7.77 (m, 9H, arom. H), 8.00 (s, 1H, 2-CH), 8.09 (d, J = 9 Hz, 1H, 6-NH), 8.27 (d, J = 9 Hz, 1H, 1-NH), 8.40 (s, 1H, 4-NH), 8.56 (d, J = 9 Hz, 1H, 3-NH), 8.73 (t, J = 4 Hz, 1H, 5-NH), 9.22 (s, 1H, 7-NH), 10.76 (d, J = 2 Hz, indole-NH), 11.15 (d, J = 2 Hz, indole-NH) ppm.

ES-MS *m/z* calcd for $C_{39}H_{42}ClN_{10}O_7S$ 829.2647, found 829.2347 [MH^+].

***Cyclo*[(*R*)-Ala-Thz-Trp-(6-F)-Trp-Gly-(*R*)-Ala-Dha-Sar], (48d)**

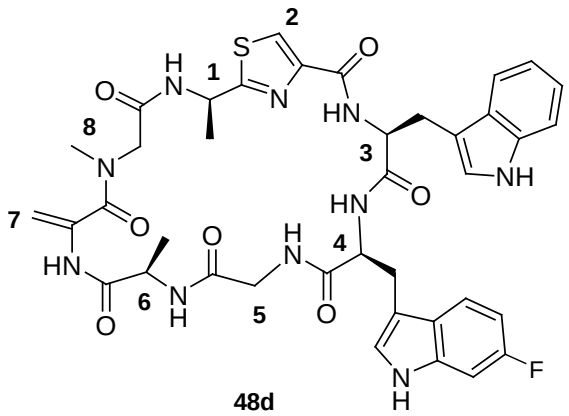

48d

Diisopropylethylamine (101 µL, 0.58 mmol), PyBOP (101 mg, 0.19 mmol) and HOBt (26 mg, 0.19 mmol) were added successively to a solution of the linear peptide **46d** (54 mg, 0.06 mmol) in CH_2Cl_2 (120 mL) at room temperature. The reaction mixture was stirred for 3 days, concentrated and purified by preparative RP-HPLC (Onyx Monolithic C_{18}, 100 x 10 mm) to afford argyrin **48d** as a orange solid (2 mg, 4 % yield).

RP-HPLC 10-60 % B in 12 min, t_R 7.0 min.

^{1}H NMR (400 MHz, DMSO-d_6): δ = 0.87 (d, J = 7 Hz, 3H, 6-CH_3), 1.54 (d, J = 7 Hz, 3H, 1-CH_3), 3.13 (s, 3H, 8-CH_3), 3.15 (m, 2H, 4-CH_2), 3.21 (m, 1H, 3-CH_AH$_B$), 3.22 (m, 1H, 8-CH_AH$_B$), 3.39 (m, 1H, 5-CH_AH$_B$), 3.44 (m, 1H, 3-CH$_A$$H_B$), 3.80 (d, J = 16 Hz, 1H, 8-CH$_A$$H_B$), 3.88 (dd, J = 16, 8 Hz, 5-CH$_A$$H_B$), 4.24 (m, 1H, 4-α-CH), 4.35 (m, 1H, 6-α-CH), 4.78 (td, J = 12, 4 Hz, 1H, 3-α-CH), 4.92 (s, 1H, 7-CH_AH$_B$), 5.16 (s, 1H, 7-CH$_A$$H_B$), 5.39 (m, 1H, 1-α-CH), 6.95-7.77 (m, 9H, arom. H), 8.00 (s, 1H, 2-CH), 8.09 (d, J = 9 Hz, 1H, 6-NH), 8.27 (d, J = 9 Hz, 1H, 1-NH), 8.40 (s, 1H, 4-NH), 8.56 (d, J = 9 Hz, 1H, 3-NH), 8.69 (t, J = 4 Hz, 1H, 5-NH), 9.21 (s, 1H, 7-NH), 10.74 (d, J = 2 Hz, indole-NH), 10.99 (d, J = 2 Hz, indole-NH) ppm.

ES-MS *m/z* calcd for $C_{39}H_{42}FN_{10}O_7S$ 813.2943, found 813.3016 [MH^+].

***Cyclo*[(*R*)-Ala-Thz-Trp-(7-Et)-Trp-Gly-(*R*)-Ala-Dha-Sar], (48e)**

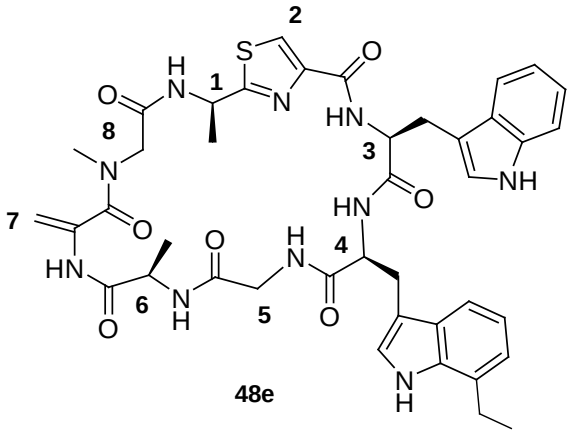

48e

Procedure as described in the general procedure using cyclic peptide **47e** (4 mg, 4 µmol) to afford argyrin **48e** as a sticky solid (2 mg, 52 % yield).

RP-HPLC 10-60 % B in 12 min, t_R 7.9 min.

^{1}H NMR (400 MHz, DMSO-d$_6$): δ = 0.87 (d, J = 7 Hz, 3H, 6-CH$_3$), 1.27 (t, J = 7 Hz, 3H, 4-CH$_2$C*H*$_3$), 1.55 (d, J = 7 Hz, 3H, 1-CH$_3$), 2.85 (q, J = 7 Hz, 2H, 4-C*H*$_2$CH$_3$), 3.12 (s, 3H, 8-CH$_3$), 3.15 (m, 2H, 4-CH$_2$), 3.21 (m, 1H, 3-C*H*$_A$H$_B$), 3.22 (m, 1H, 8-C*H*$_A$H$_B$), 3.39 (m, 1H, 5-C*H*$_A$H$_B$), 3.44 (m, 1H, 3-CH$_A$*H*$_B$), 3.80 (d, J = 16 Hz, 1H, 8-CH$_A$*H*$_B$), 3.88 (dd, J = 16, 8 Hz, 5-CH$_A$*H*$_B$), 4.24 (td, J = 12, 4 Hz, 1H, 4-α-CH), 4.35 (m, 1H, 6-α-CH), 4.78 (td, J = 12, 4 Hz, 1H, 3-α-CH), 4.92 (s, 1H, 7-C*H*$_A$H$_B$), 5.16 (s, 1H, 7-CH$_A$*H*$_B$), 5.39 (m, 1H, 1-α-CH), 6.93-7.76 (m, 9H, arom. H), 8.00 (s, 1H, 2-CH), 8.12 (d, J = 9 Hz, 1H, 6-NH), 8.27 (d, J = 9 Hz, 1H, 1-NH), 8.41 (d, J = 2 Hz, 1H, 4-NH), 8.55 (d, J = 9 Hz, 1H, 3-NH), 8.72 (t, J = 4 Hz, 1H, 5-NH), 9.23 (s, 1H, 7-NH), 10.74 (d, J = 2 Hz, indole-NH), 10.89 (d, J = 2 Hz, indole-NH) ppm.

ES-MS *m/z* calcd for $C_{41}H_{47}N_{10}O_7S$ 823.3350, found 823.3311 [MH^+].

***Cyclo*[(*R*)-Ala-Thz-Trp-(5-Me)-Trp-Gly-(*R*)-Ala-Dha-Sar], (48f)**

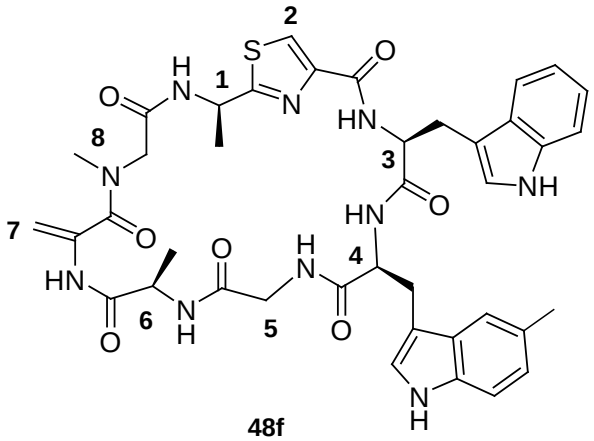

48f

Procedure as described in the general procedure using cyclic peptide **47f** (5 mg, 5 µmol) to afford argyrin **48f** as a sticky solid (3 mg, 66 % yield).

RP-HPLC 10-60 % B in 12 min, t_R 7.3 min

^{1}H NMR (400 MHz, DMSO-d$_6$): δ = 0.87 (d, J = 7 Hz, 3H, 6-CH$_3$), 1.54 (d, J = 7 Hz, 3H, 1-CH$_3$), 2.43 (s, 3H, 4-CH$_3$), 3.13 (s, 3H, 8-CH$_3$), 3.15 (m, 2H, 4-CH$_2$), 3.21 (m, 1H, 3-CH_AH$_B$), 3.22(m, 1H, 8-CH_AH$_B$), 3.39 (m, 1H, 5-CH_AH$_B$), 3.44 (m, 1H, 3-CH$_A$$H_B$), 3.80 (d, J = 16 Hz, 1H, 8-CH$_A$$H_B$), 3.88 (dd, J = 16, 8 Hz, 5-CH$_A$$H_B$), 4.24 (m, 1H, 4-α-CH), 4.35 (m, 1H, 6-α-CH), 4.78 (td, J = 12, 4 Hz, 1H, 3-α-CH), 4.92 (s, 1H, 7-CH_AH$_B$), 5.16 (s, 1H, 7-CH$_A$$H_B$), 5.39 (m, 1H, 1-α-CH), 6.93-7.74 (m, 9H, arom. H), 8.00 (s, 1H, 2-CH), 8.09 (d, J = 9 Hz, 1H, 6-NH), 8.27 (d, J = 9 Hz, 1H, 1-NH), 8.37 (s, 1H, 4-NH), 8.56 (d, J = 9 Hz, 1H, 3-NH), 8.70 (t, J = 4 Hz, 1H, 5-NH), 9.22 (s, 1H, 7-NH), 10.75 (d, J = 2 Hz, indole-NH), 10.76 (d, J = 2 Hz, indole-NH) ppm.

ES-MS *m/z* calcd for $C_{40}H_{45}N_{10}O_8S$ 809.3193, found 809.3016 [MH^+].

***Cyclo*[(*R*)-Ala-Thz-Trp-(5-OMe)-Trp-Gly-(*R*)-Ala-Dha-Sar], (48g)**

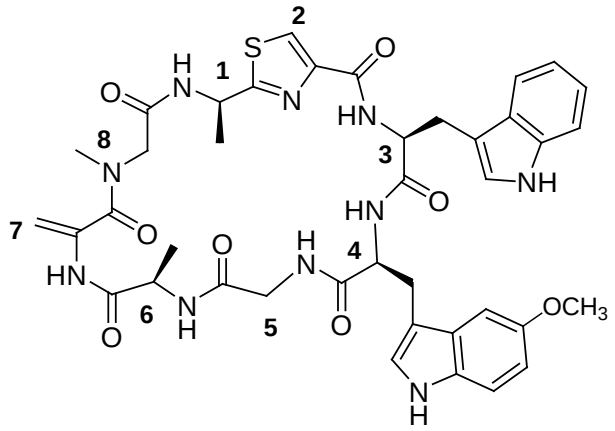

48g

Procedure as described in the general procedure using cyclic peptide **47g** (4 mg, 4 µmol) to afford argyrin **48g** as a sticky solid (2 mg, 58 % yield).

RP-HPLC 10-60 % B in 12 min, t_R 6.5 min.

^{1}H NMR (400 MHz, DMSO-d_6): δ = 0.87 (d, J = 7 Hz, 3H, 6-CH_3), 1.54 (d, J = 7 Hz, 3H, 1-CH_3), 3.08 (s, 3H, 8-CH_3), 3.15 (m, 2H, 4-CH_2), 3.21 (m, 1H, 3-CH_AH$_B$), 3.22 (m, 1H, 8-CH_AH$_B$), 3.39 (m, 1H, 5-CH_AH$_B$), 3.44 (m, 1H, 3-CH$_A$$H_B$), 3.79 (s, 3H, 4-$OCH_3$), 3.80 (d, J = 16 Hz, 1H, 8-CH$_A$$H_B$), 3.88 (dd, J = 16, 8 Hz, 5-CH$_A$$H_B$), 4.22 (m, 1H, 4-α-CH), 4.34 (m, 1H, 6-α-CH), 4.78 (td, J = 12, 4 Hz, 1H, 3-α-CH), 4.93 (s, 1H, 7-CH_AH$_B$), 5.16 (s, 1H, 7-CH$_A$$H_B$), 5.39 (m, 1H, 1-α-CH), 6.90-7.75 (m, 9H, arom. H), 8.00 (s, 1H, 2-CH), 8.12 (d, J = 9 Hz, 1H, 6-NH), 8.27 (d, J = 9 Hz, 1H, 1-NH), 8.42 (s, 1H, 4-NH), 8.56 (d, J = 9 Hz, 1H, 3-NH), 8.69 (t, J = 4 Hz, 1H, 5-NH), 9.24 (s, 1H, 7-NH), 10.75 (d, J = 2 Hz, indole-NH), 10.76 (d, J = 2 Hz, indole-NH) ppm.

ES-MS *m/z* calcd for $C_{40}H_{45}N_{10}O_8S$ 825.3143, found 825.3056 [MH^+].

***Cyclo*[(*R*)-Ala-Thz-Trp-(4-OMe)-Trp-Gly-(*R*)-Ala-Dha-Sar], Argyrin A (48h)**

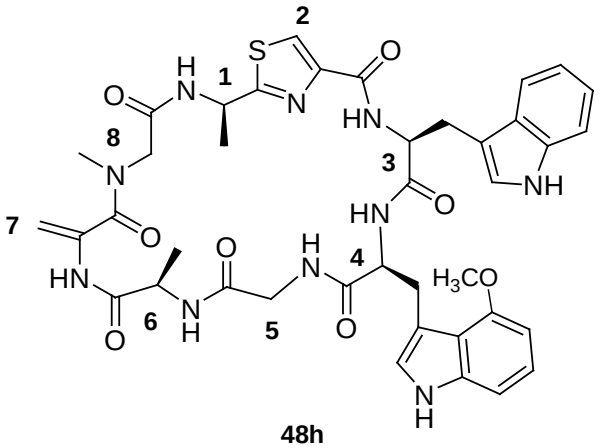

48h

Diisopropylethylamine (94 µL, 0.54 mmol) , PyBOP (93 mg, 0.18 mmol) and HOBt (24 mg, 0.18 mmol) were added successively to a solution of the linear peptide **46h** (60 mg, 0.06 mmol) in CH_2Cl_2 (120 mL) at room temperature. The reaction mixture was stirred for 3 days, concentrated and purified by preparative RP-HPLC (Onyx Monolithic C_{18}, 100 x 10 mm) to afford argyrin **48h** as a sticky solid (2 mg, 6 % yield).

RP-HPLC 10-60 % B in 12 min, t_R 6.6 min

^{1}H NMR (400 MHz, DMSO-d_6): δ = 0.87 (d, J = 7 Hz, 3H, 6-CH_3), 1.54 (d, J = 7 Hz, 3H, 1-CH_3), 3.08 (s, 3H, 8-CH_3), 3.18 (m, 2H, 4-CH_2), 3.22 (m, 1H, 3-CH_AH$_B$), 3.22(m, 1H, 8-CH_AH$_B$), 3.39 (m, 1H, 5-CH_AH$_B$), 3.44 (m, 1H, 3-CH$_A$$H_B$), 3.77 (s, 3H, 4-$OCH_3$), 3.80 (d, J = 16 Hz, 1H, 8-CH$_A$$H_B$), 3.88 (dd, J = 16, 8 Hz, 5-CH$_A$$H_B$), 4.22 (m, 1H, 4-α-CH), 4.34 (m, 1H, 6-α-CH), 4.78 (td, J = 12, 4 Hz, 1H, 3-α-CH), 4.93 (s, 1H, 7-CH_AH$_B$), 5.16 (s, 1H, 7-CH$_A$$H_B$), 5.39 (m, 1H, 1-α-CH), 6.88-7.70 (m, 9H, arom. H), 8.00 (s, 1H, 2-CH), 8.12 (d, J = 9 Hz, 1H, 6-NH), 8.28 (d, J = 9 Hz, 1H, 1-NH), 8.42 (s, 1H, 4-NH), 8.56 (d, J = 9 Hz, 1H, 3-NH), 8.70 (t, J = 4 Hz, 1H, 5-NH), 9.24 (s, 1H, 7-NH), 10.75 (d, J = 2 Hz, indole-NH), 10.78 (d, J = 2 Hz, indole-NH) ppm.

ES-MS *m/z* calcd for $C_{40}H_{45}N_{10}O_8S$ 825.3143, found 825.3092 [MH^+].

***Cyclo*[(*R*)-Ala-Thz-Trp-(*R*)-Trp-Gly-(*R*)-Ala-Dha-Sar], (48k)**

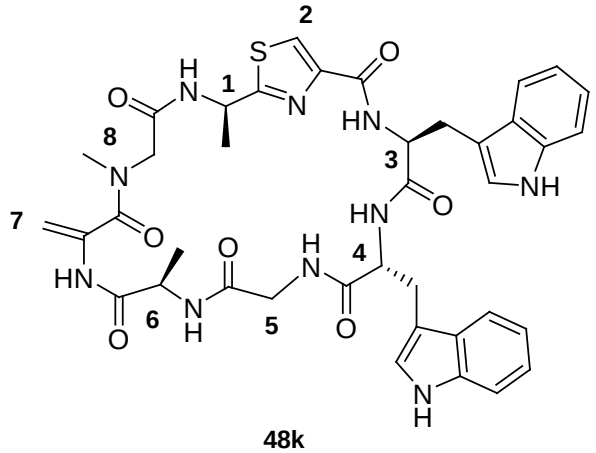

48k

Diisopropylethylamine (75 µL, 0.43 mmol), PyBOP (49 mg, 0.09 mmol) and HOBt (12 mg, 0.09 mmol) were added successively to a solution of the linear peptide **46k** (39 mg, 0.05 mmol) in CH_2Cl_2 (80 mL) at room temperature. The reaction mixture was stirred for 3 days, concentrated and purified by preparative RP-HPLC (Onyx Monolithic C_{18}, 100 x 10 mm) to afford argyrin **48k** as a sticky solid (5 mg, 14 % yield).

RP-HPLC 10-60 % B in 12 min, t_R 5.9 min.

^{1}H NMR (400 MHz, DMSO-d_6): δ = 0.73 (d, J = 7 Hz, 3H, 6-CH_3), 1.48 (d, J = 7 Hz, 3H, 1-CH_3), 3.08 (s, 3H, 8-CH_3), 3.10 (m, 4H, 2-CH_2, 4-CH_2), 3.19 (m, 1H, 8-CH_AH$_B$), 3.40 (m, 1H, 5-CH_AH$_B$), 3.95 (dd, J = 16, 8 Hz, 5-CH$_A$$H_B$), 4.06 (m, 1H, 4-α-CH), 4.49 (m, 1H, 8-CH$_A$$H_B$), 4.61 (s, 1H, 7-C$H_AH_B$), 5.00 (s, 1H, 7-CH$_A$$H_B$), 5.11 (m, 1H, 3-α-CH), 5.43 (m, 1H, 1-α-CH), 6.13-7.46 (m, 8H, arom. H), 7.48 (m, 1H, 6-NH), 7.71 (d, J = 9 Hz, 1H, 3-NH), 7.77 (d, J = 8 Hz, arom. H), 8.27 (s, 1H, 2-CH), 8.32 (d, J = 9 Hz, 1H, 1-NH), 8.85 (m, 2H, 4-NH, 5-NH), 9.75 (s, 1H, 7-NH), 10.67 (d, J = 2 Hz, indole-NH), 11.00 (d, J = 2 Hz, indole-NH) ppm.

ES-MS *m/z* calcd for $C_{39}H_{43}N_{10}O_7S$ 795.3037, found 795.3020 [MH^+].

<u>Methodology Of The In Vitro Cytotoxicity Screen</u>

HCT-116 human colon carcinoma cells were grown in RPMI 1640 medium containing 10% fetal bovine serum and 2 mM glutamine. For the cytotoxicity

screening experiment, cells were inoculated into 96 well microtiter plates in 180 µL at plating densities at 2500 cells per well. Additionally two rows of wells on a separate microtiter plate ('Time 0' plate) received cells as above. After inoculation, both plates were incubated at 37° C, 5 % CO_2, 95 % air and 100 % relative humidity for 24 h prior to T-zero determination and addition of experimental compounds.

At 24 h, MTT assay was performed on the 'Time 0' plate to represent a measurement of the cell population for the cell line at the time of compound addition (Tz). This was done by addition of 50 µL of MTT solution (2 mg/mL in PBS). After incubation for 2 h the supernatant was aspired from each well and the resultant formazan crystals were dissolved in DMSO (150 µL). The absorbance intensity was measured by a micro-plate reader at 550 nm.

Experimental compounds were solubilised in DMSO to achieve a stock concentration of 10 mM and stored frozen prior to use. At the time of compound addition, 20 µL aliquot of frozen solution was thawed and diluted with 180 µL media to achieve a 10 fold the desired final maximum test concentration. Additional five, 10-fold serial dilutions were made to provide a total of six drug concentrations plus control. Aliquots of 20 µl of these different compound dilutions were added to the appropriate microtiter wells already containing 180 µl of medium in quadruplicate, resulting in the required final drug concentrations ranging from 0.1 nM – 10 µM. The final concentration of DMSO in each well is not more than 1%.

Following compound addition, the plates were incubated for an additional 72 h at 37 °C, 5 % CO_2, 95 % air, and 100 % relative humidity. The assay was terminated by the addition of 50 µL of MTT solution (2 mg/mL in PBS). After incubation for 2 h the supernatant was aspired from each well and the resultant formazan crystals were dissolved in DMSO (150 µL). The absorbance intensity was measured by a micro-plate reader at 550 nm.

Determination of GI_{50}

Using the eight absorbance measurements [time zero, (Tz), control growth, (C), and test growth in the presence of compounds at the six concentration levels (Ti)],

the percentage growth was calculated at each of the drug concentration levels. Percentage growth inhibition was calculated as:

[(Ti-Tz)/(C-Tz)] x 100 for concentrations for which Ti >/= Tz

[(Ti-Tz)/Tz] x 100 for concentrations for which Ti < Tz.

50 % Growth inhibition (GI50) was calculated from [(Ti-Tz)/(C-Tz)] x 100 = 50.

References

1. Crawford, L.; Walker, B.; Irvine, A. *J Cell Commun Signal*, 2011, **5**, 101-110.
2. Arendt, S.; Hochstrasser, M. *Proc Natl Acad Sci U S A*, 1997, **94**, 7156-7161.
3. Nickeleit, I.; Zender, S.; Sasse, F.; Geffers, R.; Brandes, G.; Sorensen, I.; Steinmetz, H.; Kubicka, S.; Carlomagno, T.; Menche, D.; Gutgemann, I.; Buer, J.; Gossler, A.; Manns, M. P.; Kalesse, M.; Frank, R.; Malek, N. P. *Cancer Cell*, 2008, **14**, 23-35.
4. Chu, I. M.; Hengst, L.; Slingerland, J. M. *Nat Rev Cancer*, 2008, **8**, 253-267.
5. Cooper, G. M. *The Cell*, 2nd ed., Sinauer Associates, Boston, 2000.
6. Morgan, D. O. *The Cell Cycle: Principles of Control*, 1st ed., Oxford University Press, 2007.
7. Hochhauser, S. J.; Stein, J. L.; Stein, G. S. *Int Rev Cyto*, 1981, **71**, 95-243.
8. Nigg. E. A., *Bioessays*, 1995, **17**, 471-480.
9. Ohtsubo, M.; Theodoras, A. M.; Schumacher, J.; Roberts, J. M.; Pagano, M. *Mol. Cell. Biol.*, 1995, **15**, 2612-2624.
10. Pardee, A. B. *Science*, 1989, **246**, 603-608.

11. Adams, P. D. *Biochim Biophys Acta.*, 2001, **1471**, 123-133.
12. Malumbres, M.; Barbacid, M. *Nat Rev Cancer*, 2001, **1**, 222-231.
13. Connell, M. J.; Walworth, N. C.; Carr, A. M. *Trends Cell Biol.*, 2000, **10**, 296-303.
14. Rudner, A. D.; Murray, A. W. *Curr Opin Cell Biol*, 1996, **8**, 773-780.
15. Zich, J.; Sochaj, A. M.; Syred, H. M.; Milne, L.; Cook, A. G.; Ohkura, H.; Rappsilber, J.; Hardwick, K. G. *Curr Biol*, 2012, **22**, 296-301.
16. Malumbres, M.; Barbacid, M. *Trends Biochem Sci*, 2005, **30**, 630-641.
17. Harper, J. W.; Elledge, S. J. *Genes & Dev.*, 1998, **12**, 285-289.
18. Morgan, D. O. *Nature*, 1995, **374**, 131-133.
19. Ciarallo, S.; Subramaniam, V.; Hung, W.; Lee, J. H.; Kotchetkov, R.; Sandhu, C.; Milic, A.; Slingerland, J. M. *Mol Cell Biol.*, 2002, **22**, 2993-3002.
20. Yuan, C.; Li, J.; Selby, T. L.; Byeon, I. L.; Tsai, M. D. *J Mol Biol*, 1999, **294**, 201-211.
21. Roussel, M. F. *Oncogene*, 1999, **18**, 5311-5317.
22. Polyak, K.; Kato, J. Y.; Solomon, M. J.; Sherr, C. J.; Massague, J.; Rberts, J. M.; Koff, A. *Genes & Dev.*, 1994, **8**, 9-22.
23. Harper, J. W.; Adami, G. R.; Wei, N.; Keyomarsi, K.; Elledge, S. J. *Cell*, 1993, **75**, 805-816.
24. Matsuoka, S.; Edwards, M. C.; Bai, C.; Parker, S.; Zhang, P.; Baldini, A.; Harper, J. W.; Elledge, S. J. *Genes & Dev.*, 1995, **9**, 650-662.
25. Sherr, C. J. *Science*, 1996, **274**, 1672-1677.
26. Boehm, M.; Yoshimoto, T.; Crook, M. F.; Nallamshetty, S.; True, A.; Nabel, G. J.; Nabel, E. G. *EMBO J.*, 2002, **21**, 3390-3401.
27. Deng, X.; Mercer, S. E.; Shah, S.; Ewton, D. Z.; Friedman, E. *J. Biol. Chem.*, 2004, **279**, 22498-22504.
28. Rodier, G. *EMBO J.*, 2001, **20**, 6672-6682.
29. Nakayama, K. I.; Nakayama, K. *Nature Rev. Cancer*, 2006, **6**, 369-381.
30. Shin, I. *Nature Med.*, 2002, **8**, 1145-1152.
31. Motti, M. L.; De Marco, C.; Califano, D.; Fusco, A.; Viglietto, G. *Cell Cycle*, 2004, **3**, e89-e95.
32. Cheng, M. *EMBO J.*, 1999, **18**, 1571-1583.

33. James, M.; Ray, A.; Leznova, D.; Blain, S. W. *Mol. Cell Biol.*, 2008, **28**, 498-510.
34. Cheng, M.; Sexl, V.; Sherr, C. J.; Roussel, M. F. *Proc. Natl Acad. Sci. USA*, 1998, **95**, 1091-1096.
35. Chu, I.; Sun, J.; Arnaout, A.; Kahn, H.; Hanna, W; Narod, S.; Sun, P.; Tan, C. K.; Hengst, L.; Slingerland, J. *Cell*, 2007, **128**, 281-294.
36. Russo, A. A.; Jeffrey, P. D.; Patten, A. K.; Massague, J.; Pavletich, N. P. *Nature*, 1996, **382**, 325-331.
37. Chu, I. *Cell*, 2007, **128**, 281-294.
38. Kaldis, P. *Cell*, 2007, **128**, 241-244.
39. Shin, I.; Rotty, J.; Wu, F. Y.; Arteaga, C. L. *J. Biol. Chem.*, 2005, **280**, 6055-6063.
40. Zeng, Y.; Hirano, K.; Hirano, M.; Nishimura, J.; Kanaide, H. *Biochem. Biophys. Res. Commun.*, 2000, **274**, 37-42.
41. Blain, S. W. *Cell Cycle*, 2008, **7**, 892-898.
42. Hara, T.; Kamura, T.; Nakayama, K.; Oshikawa, K.; Hatakeyama, S.; Nakayama, K. *J Biol Chem.* , 2001, **276**, 48937-48943.
43. Grimmler, M. *Cell*, 2007, **128**, 269-280.
44. Nguyen, H.; Gitig, D. M.; Koff, A. *Mol Cell Biol.*, 1999, **19**, 1190-1201.
45. Slingerland, J.; Pagano, M. *J. Cell Physiol.*, 2000, **183**, 10-17.
46. Bloom, J.; Pagano, M. *Semin. Cancer Biol.*, 2003, **13**, 41-47.
47. Arteaga, C. L.; Baselga, J. *Clin. Cancer Res.*, 2003, **9**, 1579-1589.
48. Sgambato, A.; Cittadini, A, Faraglia, B.; Weinstein, I. B. *J Cell Physiol.*, 2000, **183**, 18-27.
49. Latres, E. *Proc. Natl Acad. Sci. USA*, 2001, **98**, 2515-2520.
50. Hurteau, J. A.; Allison, B. M.; Brutkiewicz, S. A.; Goebl, M. G.; Heilman, D. K.; Bigsby, R. M.; Harrington, M. A. *Gynecol Oncol*, 2001, **83**, 292-298.
51. Baldassarre, G.; Belletti, B.; Bruni, P.; Boccia, A.; Trapasso, F.; Pentimalli, F.; Barone, M. V.; Chiappetta, G.; Vento, M. T.; Spiezia, S.; Fusco, A.; Viglietto, G. *J Clin Invest*, 1999, **104**, 865-874.
52. Hershko, A.; Ciechanover, A. *Annu. Rev. Biochem.*, 1992, **61**, 761-807.
53. Lee, D. H.; Goldberg, A. L. *Trends Cell Biol.*, 1998, **8**, 397-403.
54. Hershko, A.; Leshinsky, E.; Ganoth, D.; Heller, H. *Proc Natl Acad Sci U S A*, 1984, **81**, 1619-1623

55. Glickman, M. H.; Ciechanover, A. *Physiol. Rev.*, 2002, **82**, 373-428.
56. Brooks, P.; Fuertes, G.; Murray, R. Z.; Bose, S.; Knecht, E.; Rechsteiner, M. C.; Hendil, K. B.; Tanaka, K.; Dyson, J.; Rivett, J. *Biochem J*, 2000, **346**, 155-161.
57. Cheng, Y. *Curr. Opin. Struct. Biol*, 2009, **19**, 203-208.
58. Adams, J. *Nat Rev Cancer*, 2004, **4**, 349-360.
59. Verdoes, M.; Florea, B. I.; Van der Marel, G. A.; Overkleef, H. S. *Eur. J. Org. Chem.*, 2009, 3301-3313.
60. Matthews, W.; Driscoll, J.; Tanaka, K.; Ichihara, A.; Goldberg, A. L. *Proc. Natl. Acad. Sci.*, 1989, **8**, 2597.
61. Glotzer, M.; Murray, A. W.; Kirschner, M. W. *Nature*, 1991, **349**, 132-138.
62. Clurman, B. E.; Sheaff, R. J.; Thress, K.; Groudine, M.; Roberts, J. M. *Genes Dev.*, 1996, **10**, 1979-1990.
63. Pagano, M.; Tam, S. W.; Theodoras, A. M.; Beer-Romero, P.; Del Sal, G.; Chau, V.; Yew, P. R.; Draetta, G. F.; Rolfe, M. *Science*, 1995, **269**, 682-685.
64. Koepp, E. M.; Harper, J. W.; Elledge, S. J. *Cell*, 1999, **97**, 431-434.
65. Tanaka, K.; Kawakami, T.; Tateishi, K.; Yashiroda, H.; Chiba, T. *Biochimie*, 2001, **83**, 351-356.
66. Li, C. C.; Dai, H.; Longo, R. M. *Biochem. Biophys. Res. Commun.*, 1995, **215**, 292-301.
67. Karin, M.; Cao, Y.; Greten, F. R.; Li, Z. W. *Nat. Rev. Cancer*, 2002, **2**, 301-130.
68. Fan, X. M.; Chun, B.; Wong, Y. *Int. J. Cancer*, 2001, 481-488.
69. Maki, C. G.; Huibregtse, J. M.; Howley, P. M. *Cancer Res*, 1996, **56**, 2649-2654.
70. Loda, M.; Cukor, B.; Tam, S. W.; Lavin, P.; Fiorentinc, M.; Draetta, G. F.; Jessup, J. M.; Pagano, M. *Nat Med*, 1997, **3**, 231-234.
71. Catzavelos, C.; Bhattacharya, N.; Ung, Y. C.; Wilson, J. A.; Roncari, L.; Sandhu, C.; Shaw, P.; Yeger, H. *Nat Med*, 1997, **3**, 227-230.
72. Hwang, I. Y.; Baguley, B. C.; Ching, L. M.; Gilchrist, C. A. *Cancer Letters*, 2010, **294**, 82-90.
73. Betticher, D. C. *Ann. Oncol.*, 1996, **7**, 223-225.
74. Keyomarsi, K.; Pardee, A. B. *Proc. Natl. Acad. Sci.*, 1993, **90**, 1112-1116.
75. Scagliotti, G. *Crit. Rev. Oncol. Hematol.*, 2006, **58**, 177-189.

76. Loda, M. *Nature Med.*, 1997, **3**, 231-234.
77. Kanai, M.; Yasumoto, M.; Kuriyama, Y.; Inomiy K.; Katsuhara, Y.; Higashiyama, K.; Ishii, A. *Am J Pathol*, 1998, **153**, 505-513.
78. Haupt, Y.; Maya, R.; Kazaz, A.; Oren, M. *Nature*, 1997, **387**, 296-299.
79. Spataro, V.; Norbury, C.; Harris, A. L. *Br J Cancer.* , 1998, **77**, 448-455.
80. Tamatani, T.; Azuma, M.; Aota, K.; Yamashita, T.; Bando, T.; Sato, M. *Cancer Letters*, 2001, **171**, 165-172.
81. Drexler, H. C. A. *Proc. Natl. Acad. Sci*, 1997, **94**, 855-860.
82. Drexler, H. C. A.; Risau, W.; Konerding, M. A. *FASEB J*, 2000, **14**, 65-77.
83. Kudo, Y.; Takata, T.; Ogawa, I.; Kaneda, T.; Sato, S. *Clin Cancer Res*, 2000, **6**, 916-923.
84. Deshaies, R. J. *Annu. Rev. Cell Dev. Biol.*, 1999, 435.
85. Smith, D. M.; Daniel, K. G.; Dou, Q. P. *Lett. Drug Des. Discovery*, 2005, **2**, 74-81.
86. Edelmann, M. J.; Nicholson, B.; Kessler, B. M. *Expert Rev Mol Med.*, 2011, **13**, e35.
87. Mattern, M. R.; Wu, J.; Nicholson, B. *Biochim. Biophys. Acta*, 2012, **1823**, 2041-2021
88. Colland, F. *Biochemical Society Focused Meetings*, 2010, **38**, 137-143.
89. Baumeister, W.; Walz, J.; Zühl, F.; Seemüller, E. *Cell*, 1998, **92**, 367-380.
90. Dick, T. P.; Nussbaum, A. K.; Deeg, M.; Heinemeyer, W. *J. Biol. Chem.*, 1998, **273**, 25637-25646.
91. Brannigan, J. A.; Dodson, G.; Duggleby, H. J.; Moody, P. C.; Smith, J. L.; Tomchick, D. R.; Murzin, A. G. *Nature*, 1995, **378**, 416-419.
92. Seemüller, E.; Lupas, A.; Stock, D.; Löwe, J.; Huber, R.; Baumeister, W. *Science*, 1995, **268**, 579-582.
93. Fenteany, G.; Standaert, R. F.; Lane, W. S.; Choi, S.; Corey, E. J.; Schreiber S. L. *Science*, 1995, **268**, 726-731.
94. Kisselev, A. F.; Goldberg, A. L. *Chem. Biol.*, 2001, **8**, 739-758.
95. Masdehors, P.; Omura, S.; Merle-Béral, H.; Mentz, F.; Cosset, J. M.; Dumont, J.; Magdelénat, H.; Delic J. *Br J Haematol.*, 1999, **105**, 752-757.
96. Ostrowska, H. *Cell Mol. Biol. Lett.*, 2008, **13**, 353-365.
97. Hoeller, D.; Dikic, I. *Nature*, 2009, **458**, 438-444.
98. Drexler, H. C.A.; Risau, W.; Konerding, M. A. *FASEB J.*, 2000, **14**, 65-77.

99. An, B.; Goldfarb, R. H.; Siman, R.; Dou, Q. P. *Cell Death Differ.*, 1998, **5**, 1062-1075.
100. Almond, J. B.; Cohen, G. M. *Leukemia*, 2002, **16**, 433-443.
101. Shah, S. A.; Potter, M. W.; McDada, T. P.; Ricciardi, R.; Perugini, R. A.; Elliott, P. J.; Adams, J.; Callery, M. P. *J Cell Biochem.*, 2001, **82**, 110-122.
102. Russo, S. M.; Tepper, J. E.; Baldwin, A. S.; Liu, R.; Adams, J.; Elliott, P.; Cusack, J. C. *Int J Radiat Oncol Biol Phys.*, 2001, **50**, 183-193.
103. Huber, E. M.; Basler, M.; Schwab, R.; Heinemeyer, W.; Kirk, C. J.; Groettrup, M. *Cell*, 2012, **148**, 727-738.
104. Urru, S. A.; Veglianese, P.; De Luigi, A.; Fumagalli, E.; Erba, E.; Gonella, D. R.; Carrà , A.; Davoli, E.; Borsello, T.; Forloni, G.; Pengo, N.; Monzani, E.; Cascio, P.; Cenci, S.; Sitia, R.; Salmona, M. *J Med Chem.*, 2010, **53**, 7452-7460.
105. Heinemeyer, W.; Fischer, M.; Krimmer, T.; Stachon, U.; Wolf, D. H. *J Biol Chem.*, 1997, **272**, 25200-25209.
106. Arendt, C. S.; Hochstrasser, M. *Proc. Natl. Acad. Sci.*, 1997, **94**, 7156-7161.
107. De Bettignies, G.; Coux, O. *Biochimie.*, 2010, **92**, 1530-1545.
108. Wilk, S.; Orlowski, M. *J Neurochem.*, 1980, **35**, 1172-1182.
109. Vinitsky, A.; Michaud, C.; Powers, J. C.; Orlowski, M. *Biochemistry*, 1992, **31**, 9421-9428.
110. Hines, J.; Groll, M.; Fahnestock, M.; Crews, C. M. *Chem Biol.*, 2008, **15**, 501-512.
111. Momose, I.; Umezawa, Y.; Hirosaws, S.; Iijima, M.; Iinuma, H.; Ikeda, D. *Biosci. Biotechnol. Biochem.*, 2005, **69**, 1733-1742.
112. Lum, R. T.; Nelson, M. G.; Joly, A.; Horsma, A. G.; Meyer, S. M.; Wick, M. M.; Schow, S. R. *Bioorg Med Chem Lett.*, 1998, **8**, 209-214.
113. Chatterjee, S.; Dunn, D.; Mallya, S.; Ator, M. A. *Bioorg. Med. Chem. Lett.*, 1999, **9**, 2603-2606.
114. Bogyo, M.; McMaster, J. S.; Gaczynska, M.; Tortorella, D.; Goldberg, A. L.; Ploegh, H. *Proc. Natl. Acad. Sci*, 1997, **94**, 6629-6634.
115. Ovaa, H.; Van Swieten, P. F.; Kessler, B. M.; Leeuwenburgh, M. A.; Fiebiger, E.; Van den Nieuwendijk, A. M. C. H. *Angew Chem Int Ed Engl*, 2003, **115**, 3754-3757.

116. Adams, J.; Behnke, M.; Chen, S.; Cruickshank, A. A.; Dick, L. R.; Grenier, L.; Klunder, J. M.; Ma, Y. T.; Plamondon, L.; Stein, R. L. *Bioorg Med Chem Lett.*, 1998, **8**, 333-338.

117. Matteson, D.; Sadhu, K. M.; Lienhard, G. E. *J. Am. Chem. Soc.*, 1981, **103**, 5241-5242.

118. Groll, M.; Berkers, C. R.; Ploegh, H. L.; Ovaa, H. *Structure*, 2006, **14**, 451-456.

119. Altun, M.; Galardy, P. J.; Shringarpure, R.; Hideshima, T.; LeBlanc, R.; Anderson, K. C.; Ploegh, H. L.; Kessler, B. M. *Cancer Res.*, 2005, **65**, 7896-7901.

120. Nencioni, A.; Gru¨nebach, F.; Patrone, F.; Ballestrero. A; Brossart, P. *Leukemia*, 2007, **21**, 30-36.

121. Obeng, E. A.; Carlson, L. M.; Gutman, D. M.; Harrington, W. J.; Lee, K. P.; Boise, L. H. *Blood*, 2006, **107**, 4907-4916.

122. Menashe, J. *Community Oncology*, 2007, **4**, 480-484.

123. Kumar, S.; Rajkumar, S. V. *Blood*, 2008, **112**, 2177-2178.

124. Chauhan, D.; Tian, Z.; Zhou, B.; Kuhn, D.; Orlowski, R.; Raje, N.; Richardson, P.; Anderson, K. C. *Clin Cancer Res.*, 2011, **17**, 5311-5321.

125. Piva, R. *Blood*, 2008, **111**, 2765-2775.

126. Dick, L. R.; Fleming, P. E. *Drug Discov. Today*, 2010, **15**, 243-249.

127. Hanada, M.; Sugawara, K.; Kaneta, K.; Toda, S.; Nishiyama, Y.; Tomita, K.; Yamamoto, H.; Konishi, M.; Oki, T. *Antibiot.*, 1992, **45**, 1746-1752.

128. Elofsson, M.; Splittgerber, U.; Myung, J.; Mohan, R.; Crews, C. M. *Chemistry & Biology*, 1999, **6**, 811-822.

129. Verdoes, M.; Willems, L.; Van der Linden, W. A.; Duivervoorden, B. A.; Van der Marel, G. A.; Florea, B. I.; Kisselev, A. F.; Overkleeft, H. S. *Org. Biomol. Chem*, 2010, **8**, 2719-2727.

130. O'Connor, O. A.; Stewart, A. K.; Vallone, M.; Molineaux, C.J.; Kunkel, L. A.; Gerecitano, J. F.; Orlowski, R. Z. *Clin Cancer Res.*, 2009, **15**, 7085-7091.

131. Omura, S.; Fujimoto, T.; Otoguro, K.; Matsuzaki, K.; Moriguchi, R.; Tanaka, H.; Sasaki, Y. *J Antibiot*, 1991, **44**, 117-118.

132. Corey, E. J.; Li, W. Z.; Nagamitsu, T.; Fenteany, G. *Tetrahedron*, 1999, **55**, 3305-3316.

133. Feling, R. H.; Buchanan, G. O.; Mincer, T. J.; Kauffman, C. A.; Jensen, P. R.; Fenical, W. *Angew Chem Int Ed Engl.*, 2003, **42**, 355-357.

134. Groll, M.; Huber, R.; Potts, B. C. *J Am Chem Soc.*, 2006, **128**, 5136-5141.

135. Kisselev, A. F.; Van der Linden, W. A.; Overkleeft, H. S. *Chem Biol.* , 2012, **19**, 99-115.

136. Wäspi, U.; Hassa, P.; Staempfli, A. A.; Molleyres, L. P.; Winkler, T.; Dudler, R. *Microbiol. Res.*, 1999, **154**, 89-93.

137. Oka, M.; Nishiyama, Y.; Ohta, S.; Kamei, H.; Konishi, M.; Miyaki, T.; Oki, T.; Kawaguchi, H. *J Antibiot* 1988, **41**, 1331-1337.

138. Groll, M.; Schellenberg, B.; Bachmann, A. S.; Archer, C. R.; Huber, R.; Powell, T. K.; Lindow, S.; Kaiser, M.; Dudler, R. *Nature*, 2008, **452**, 755-758.

139. Kazi, A.; Smith, D. M.; Daniel, K.; Zhong, S.; Gupta, P.; Bosley, M. E.; Dou, Q. P. *In Vivo.*, 2002, **16**, 397-403.

140. Dou, Q. P.; Landis-Piwowar, K. R.; Chen, D.; Huo, C.; Wan, S. B.; Cahn. T. H. *Inflammopharmacology.*, 2008, **16**, 208-212.

141. Smith, D. M.; Daniel, K. G.; Wang, Z.; Guida, W. C.; Chan, T. H.; Dou, Q. P. *Proteins*, 2004, **54**, 58-70.

142. Messina, M.; Barnes, S. *J Natl Cancer Inst.*, 1991, **83**, 541-546.

143. Kazi, A.; Daniel, K. G.; Smith, D. M.; Kumar, N. B.; Dou, Q. P. *Biochem. Pharmacol.*, 2003, **66**, 965-976.

144. Kohno, J.; Koguchi, Y.; Nishio, M.; Nakao, K.; Kuroda, M.; Shimizu, R.; Ohnuki, T.; Komatsubara, S. *J Org Chem.*, 2000, **65**, 990-995.

145. Albrecht, B. K.; Williams, R. M. *Proc. Natl. Acad. Sci.*, 2004, **101**, 11949-11954.

146. Groll, M.; Koguchi, Y.; Huber, R.; Kohno, J. *J. Mol. Biol.*, 2001, **311**, 543-548.

147. Basse, N.; Piguel, S.; Papapostolou, D.; Ferrier-Berthelot, A.; Richy, N. *J. Med. Chem*, 2007, **50**, 2842-2850.

148. Sasse, F.; Steinmetz, H.; Schupp, T.; Petersen, F.; Memmert, K.; Hofmann, H.; Heusser, C.; Brinkmann, V.; Von Matt, P.; Höfle, G.; Reichenbach, H. *J Antibiot*, 2002, **55**, 543-551.

149. Vollbrecht, L.; Steinmetz, H.; Hofle, G.; Oberer, L.; Rihs, G.; Bovermann, G.; Van Matt, P. *J Antibiot* 2002, **55**, 715-721.

150. Ley, S. V.; Priour, A.; Heusser, C. *Org Lett*, 2002, **4**, 711-714.

151. Bülow, L.; Nickeleit, I.; Girbig, A. K.; Brodmann, T.; Rentsch, A.; Eggert, U.; Sasse, F.; Steinmetz, H.; Frank, R.; Carlomagno, T.; Malek, N. P.; Kalesse, M. *ChemMedChem*, 2010, **5**, 832-836.

152. Wu, W.; Li, Z.; Zhou, G.; Jiang, S. *Tetrahedron Lett.*, 2011, **52**, 2488-2491.

153. Besson, A.; Gurian-West, M.; Schmidt, A.; Hall, A.; Roberts, J. M. *Genes Dev.*, 2004, **18**, 862-876.

154. Davy, D.; Serra, G. *Mar. Drugs* 2010, **8**, 2755-2780.

155. Stauch, B.; Simon, B.; Basile, T.; Schneider, G.; Malek, N. P.; Kalesse, M.; Carlomagno, T.; *Angew Chem Int Ed Engl.*, 2010, **49**, 3934-3938.

156. Van Order, R. B.; Lindwall, H. G. *Chem. Rev.*, 1942, **30**, 69-96

157. Sato, H.; Tsuda, M.; Watanabe, K.; Kobayashi, J. *Tetrahedron*, 1998, **54**, 8687-8690.

158. Matsumoto, K.; Mizowaki, M.; Suchitra, T.; Murakami, Y.; Takayama, H.; Sakai, S.; Aimi, N.; Watanabe, H. *Eur J Pharmacol.*, 1996, **317**, 75-81.

159. Feng, Y.; Davis, R. A.; Sykes, M. L.; Avery, V. M.; Quinn, R, J *Bioorg Med Chem Lett.*, 2012, **22**, 4873-4876

160. Yeh, E.; Garneau, S.; Walsh, C. T. *Proc. Natl. Acad. Sci.*, 2005, **102**, 3960-3965.

161. Allen, M. C.; Brundish, D. E.; Wade, R. *J. Chem. Soc., Perkin Trans. 1*, 1980, 1928-1932.

162. Konda-Yamada, Y.; Okada, C.; Yoshida, K.; Umeda, Y.; Arima, S.; Sato, N,; Kai, T.; Takayanagi, H.; Harigaya. Y. *Tetrahedron*, 2002, **58**, 7851-7861.

163. Yokoyama, Y.; Hikawa, H.; Mitsuhashi, M.; Uyama, A.; Murakami, Y. *Tetrahedron Lett.*, 1999, **40**, 7803-7806.

164. Blaser, G.; Sanderson, J. M.; Batsanov, A. S.; Howards, J. A. K. *Tetrahedron Lett.*, 2008, **49**, 2795-2798.

165. Phillips, R. S. *Tetrahedron: Asymmetry*, 2004, **15**, 2787-2792.

166. Goss, R. J. M.; Newill, P. L. A. *Chem Commun (Camb)*, 2006, 4924-4925.

167. Hengartner, U.; Valentine, D.; Johnson, K. K.; Larscheid, M. E. *J. Org. Chem.*, 1979, **44**, 3741–3747.

168. Bentley, D.; Moody, C. J. *Org. Biomol. Chem*, 2004, **2**, 3545-3547.

169. Ma, J.; Yin, W.; Zhou, H.; Liao, X.; Cook, J. M. *J Org Chem*, 2009, **74**, 264-273.

170. Schöllkopf, U.; Ulrich Groth, D. C.; Deng, C. *Angew Chem Int Ed Engl*, 1981, **20**, 798-799.

171. Ma, C.; Liu, X.; Li, X.; Flippen-Anderson, J.; Yu, S.; Cook, J. M. *J. Org. Chem.*, 2001, **66**, 4525-4542.

172. Jia, Y.; Zhu, J. *J. Org. Chem.*, 2006, **71**, 7826–7834.

173. Kokotos, G.; Padron, J. M.; Martin, T.; Gibbons, W. A.; Martin, V. S. *J. Org. Chem.*, 1998, **63**, 3741-3744.

174. Bayston, D. J. United States, 2001, US Patent 6, 191, 306 B1

175. Vilsmeier, A.; Haack, A. *Ber.*, 1927, **60**, 119.

176. Katritzky, A. R.; Toader, D.; Xie, L. *J Org Chem.*, 1996, **61**, 7571-7577.

177. Aggarwal, V. K.; De Vicente, J.; Pelotier, B.; Holmes, I. P.; Bonner, R. V. *Tetrahedron*, 2000, **41**, 10327-10331.

178. Levine, S. *J. Am. Chem. Soc*, 1958, **80**, 6150.

179. Tam, N. T.; Cho, C. G. *Org. Lett.*, 2007, **9**, 3391-3392.

180. Jeon, S. J.; Chen, Y. K.; Walsh, P. J. *Org. Lett.*, 2005, **7**, 1729-1732.

181. Strecker, A. *Justus Liebigs Annalen der Chemie*, 1850, **75**, 27-45.

182. Byrne, J. J.; Chavarot, M.; Chavant, P. Y.; Vallée, Y. *Tetrahedron Lett.*, 2000, **41**, 873-876.

183. Kobayashi, S.; Ishitani, H. *Chirality*, 2000, **12**, 540-543.

184. Hamashima, Y.; Sawada, D.; Kanai, M.; Shibasaki, M. *J Am Chem Soc*, 1999, **121**, 2641-2642.

185. Groger, H.; *Chem. Rev.*, 2003, **103**, 2795-2827.

186. Chakraborty, T. K.; Hussain, K. A.; Reddy, G. V. *Tetrahedron*, 1995, **51**, 9179-9190.

187. Dave, R. H.; Hosangadi, B. D. *Tetrahedron*, 1999, **55**, 11295-11308.

188. Vincent, S. P.; Schleyer, A.; Wong, C. H. *J Org Chem*, 2000, **65**, 4440-4443.

189. Juaristi, E.; León-Romo, J. L.; Reyes, A.; Escalante, J. *Tetrahedron: Asymmetry*, 1999, **10**, 2441-2495.

190. Speelman, J. C.; Talma, A. G.; Kellogg, R. M.; Meetsma, A.; De Boer, J. L.; Beurskens, P. T.; Boseman, W. P. *J Org Chem*, 1989, **54**, 1055-1062.

191. Vedejs, E.; Kongkittingam, C. *J Org Chem.*, 2001, **66**, 7355-7364.

192. Arasappan, A.; Venkatraman, S.; Padilla, A. I.; Wu, W.; Meng, T.; Jin, Y.; Wong, J.; Prongay, A.; Girijavallabhan, V.; George Njoroge, F. *Tetrahedron Lett.*, 2007, **48**, 6343-6347.

193. Gillman, K. W.; Starrett, J. E.; Parker, M. F.; Xie, K.; Bronson, J. J.; Marcin, L. R.; McElhone, k. E.; Bergstrom, C. P.; Mate, R. A.; Williams, R.; Meredith, J. E.; Burton, C. R.; Barten, D. M.; Toyn, J. H.; Roberts, S. B.; Lentz, K. A.; Houston, J. G.; Zaczek, R.; Albright, C. F.; Decicco, C. P.; Macor, J. E.; Olson, R. E. *Med. Chem. Lett.*, 2010, **1**, 120-124.

194. Steiger, R. E. *Org. Synth.*, 1955, **3**, 84.

195. Ford, J. H. *Org. Synth.*, 1955, **3**, 34.

196. Paris, G.; Lerlinguet, L. Gaudry, R. *Org. Synth.*, 1963, **4**, 496.

197. Lignier, P.; Estager, J.; Kardos, N.; Gravouil, L.; Gazza, J.; Naffrechoux, E.; Draye, M. *Ultrason. Sonochem.*, 2011, **18**, 28-31.

198. Singh, R.; Sharma, R.; Tewari, N.; Geetanjali; Rawat, D. S. *Chemistry & Biodiversity*, 2006, **3**, 1279-1287.

199. Parkins A.W., *Platinum metal review*, 1996, **40**, 169.

200. Katritzky, A. R.; Pilarski, B.; Urogdi, L. *Synthesis*, 1989, **12**, 949.

201. Wiberg, K. B. *J. Am. Chem. Soc.*, 1953, **75**, 3961.

202. Bon, E.; Bigg, D. C. H.; Bertrand, G. *J. Org. Chem.*, 1994, **59**, 1904.

203. Hidalgo-Del Becchio, G.; Oehlschlager, A. C. *J. Org. Chem.*, 1994, **59**, 4853.

204. Kanai, M.; Yasumoto, M.; Kuriyama. Y.; Inomiy, K.; Katsuhara, Y.; Higashiyama, K.; Ishii, A. *Chem. Lett.*, 2004, **33**, 1424.

205. Bernotas, R. C.; Cube, R. V. *Synth. Commun.*, 1990, **20**, 1209-1212.

206. Baltzly, R.; Russell, P. B. *J. Am. Chem. Soc.*, 1953, **75**, 5598.

207. Robinson, B. *Chem. Rev.*, 1969, **69**, 785.

208. Brieger, G.; Nestrick, T. J. *Chem. Rev.* 1974, **74**, 567.

209. El Amin, B.; Anantharamaiah, G. M.; Royer, G. P.; Means, G. E. *J Org. Chem.*, 1979, **44**, 3442-3444.

210. Felix, A. M.; Heimer, E. P.; Lambros, T. J.; Tzougraki, C.; Meienhofer, J. *J Org. Chem.*, 1978, **43**, 4194-4196.

211. Ram, S.; Spicer, L. D. *Tetrahedron Lett.*, 1987, **28**, 515-516.

212. Li, J.; Wang, S.; Crispino, G. A.; Tenhuisen, K.; Singh, A.; Grosso, J. A. *Tetrahedron Lett.*, 2003, **44**, 4041-4043.

213. Quinn, J. F.; Razzano, D. A.; Golden, K. C.; Gregg, B. T. *Tetrahedron Lett.*, 2008, **49**, 6137-6140.

214. Srinivasa, G. R.; Narendra Babu, S. N.; Lakshmi, C.; Channe Gowda, D. *Synth. Commun.*, 2004, **34**, 1831-1837.

215. Kocienski, P. J. *Protecting groups*, Thieme, New York, 2004.

216. Bull, S. D.; Davies, S. G.; Fenton, G.; Mulvaney, A. W.; Prasad, R. S.; Smith, A. D. *J. Chem. Soc., Perkin Trans. 1*, 2000, **1**, 3765.

217. Pérez-Fuertes, Yolanda; Taylor, J. E.; Tickell, D.A.; Mahon, M. F.; Bull, S. D.; James, T. D. *J. Org. Chem.*, 2011, **76**, 6038-6047.

218. Buckle, D. R.; Rockell, C. J. M. *J. Chem. Soc., Perkin Trans. 1*, 1982, 627-630.

219. Zhong, H. M.; Cohen, J. H.; Abdel-Magid, A. F.; Kenney, B. D.; Maryanoff, C. A.; Shah, R. D.; Villani, F. J.; Zhang, F.; Zhang, X. *Tetrahedron Lett.*, 1999, **40**, 7721-7725.

220. Vaughn, H. L.; Robbins, M. D. *J Org. Chem.*, 1975, **40**, 1187.

221. Paquet, A. *Can. J. Chem.*, 1982, **60**, 976-980.

222. Carpino, L. A.; Han, G. Y. *J. Org. Chem.*, 1972, **37**, 3404-3409.

223. Faulkner, D. Y. *Nat. Prod. Rep.*, 1984, **1**, 551-598.

224. Marquez, B. L.; Watts, K. S.; Yokochi, A.; Roberts, M. A.; Verdier-Pinard, P.; Jimenez, J. I.; Hamel, E.; Scheuer, P. L.; Gerwick, W. H. *J. Nat. Prod.*, 2002, **65**, 866-871.

225. Boss, C.; Rasmussen, P. H.; Wartini, A. R.; Waldvogel, S. R. *Tetrahedron Lett.*, 2000, **41**, 6327-6331.

226. Henkel, B.; Beck, B.; Westner, B.; Mejat, B.; Do¨mling, A. *Tetrahedron Lett.*, 2003, **44**, 8947-8950.

227. Hamada, Y.; Shibata, M.; Sugiura, T.; Kato, S.; Shioiri, T. *J. Org. Chem.*, 1987, **52**, 1252-1255.

228. Groarke, M.; Mckervey, M. A.; Moncrieff, H.; Nieuwenhuyzen, M. *Tetrahedron Lett.*, 2000, **41**, 1279-1282.

229. Di Credico, B.; Reginato, G.; Gonsalvi, L.; Peruzzini, M.; Rossin, A. *Tetrahedron*, 2011, **67**, 267-274.

230. Gribble, G. W.; Joule, J. A. *Progress in Heterocyclic Chemistry*, Elsevier, Oxford, 2011.

231. Schmidt, U.; Gleich, P.; Griesser, H.; Utz, R. *Synthesis*, 1986, **12**, 992-998.

232. Sheehan, J. C.; Hess, G. P. *J. Am. Chem. Soc*, 1955, **77**, 1067-1068.

233. Konig, W.; Geiger, R. *Chem. Ber.* , 1970, **103**, 788-798.

234. Lajoie, G.; Lepine, F.; Maziak, L, Belleau, B *Tetrahedron Lett.*, 1983, **24**, 3815-3818.

235. Cava, M. P.; Levinson, M. I. *Tetrahedron*, 1985, **41**, 5061-5087.

236. Curphey, T. J. *J. Org. Chem.*, 2002, **67**, 6461-6473.

237. Holzapfel, C. W.; Pettit, G. R. *J. Org. Chem.*, 1985, **50**, 2323-2327.

238. Aguilar, E.; Meyers, A. I. *Tetrahedron Lett.*, 1994, **35**, 2473-2476.

239. Parker, D. *Chem. Rev.*, 1991, **91**, 1441-1457.

240. Allenmark, S. G. *Chromatographic Enantioseparation: Methods and Applications*, Ellis Horwood, Chester, 1988.

241. Raban, M.; Mislow, K. *Tetrahedron Lett.*, 1965, **48**, 4929-4253.

242. Pirkle, W. H.; Sikkenga, D. L.; Pavlin, M. S. *J. Org. Chem.*, 1977, **42**, 384-387.

243. Anderson, R. C.; Shapiro, M. J. *J. Org. Chem.*, 1984, **49**, 1304-1305.

244. Dale, J. A.; Dull, D. L.; Mosher, H. S. *J. Org. Chem.* 1969, **34**, 2543-2549.

245. Giddens, A. C.; Boshoff, H. I.M.; Franzblau, S. G.; Barry, C. E.; Copp, B. R. *Tetrahedron Lett.*, 2005, **46**, 7355-7357.

246. Pettit, G. R.; Hogan, F.; Xu, J. P.; Tan, R.; Nogawa, T.; Cichacz, Z.; Pettit, R. K.; Du, J.; Ye, Q. H.; Cragg, G. M.; Herald, C. L.; Hoard, M. S.; Goswami, A.; Searcy, J.; Tackett, L.; Doubek, D. L.; Williams, L.; Hooper, J. N.; Schimide, J. M.; Chapuis, J. C.; Tackett, D. N.; Craciunescu, F. *J. Nat. Prod.* , 2008, **71**, 438-444.

247. N'Diaye, I.; Guella, G.; Mancini, I.; Pietra, F.; Almazole, D. *Tetrahedron Lett.*, 1996, **37**, 3049-3050.

248. Roy, R. S.; Gehring, A. M.; Milne, J. C.; Belshaw, P. J.; Walsh, C. T. *Nat. Prod. Rep.*, 1999, **16**, 249-263

249. Vaccaro, H. A.; Levy, D. E.; Sawabe, A.; Jaetsch, T.; Masamune, S.; *Tetrahedron Lett.*, 1992, **33**, 1937-1940.

250. Wipf, P.; Willer, C. P. *Tetrahedron Lett.*, 1992, **33**, 6267-6270.

251. Nakamura, M.; Shibata, T.; Nakane, K.; Nemoto, T.; Ojika, M.; Yamada, K. *Tetrahedron Lett.*, 1995, **36**, 5059-5062.

252. Wipf, P.; Willer, C. P. *Tetrahedron Lett.*, 1992, **33**, 907-910.

253. Khapli, S.; Dey, S.; Mal, D. *J. Indian Inst. Sci.*, 2001, **81**, 461-176.

254. Kigoshi, H.; Yamada, S. *Tetrahedron*, 1999, **55**, 12301-12308.

255. Brain, C. T.; Paul, J. M.; Loong, Y.; Oakley, P. J. *Tetrahedron Lett.*, 1999, **40**, 3275-3278.

256. Meyers, A. I.; Tavares, F. *Tetrahedron Lett.*, 1994, **35**, 2481-2484.

257. Mink, D.; Mecozzi, S.; Rebek, J. *Tetrahedron Lett.*, 1998, **39**, 5709-5712.

258. Meyers, A. I.; Tavares, F. X. *J. Org. Chem.*, 1996, **61**, 8207-8215.

259. Williams, D. R.; Lowder, P. D.; Gu, Y. G.; Brooks, D. A. *Tetrahedron Lett.*, 1997, **38**, 331-334.

260. Viehe, H. G.; Janousek, Z.; Merenyi, R.; Stella, L *Acc. Chem. Res.*, 1985, **18**, 148-154.

261. Carmichael, W. W. *J. Appl. Bacteriol.*, 1992, **72**, 445-459.

262. Porse, B. T.; Leviev, I,; Mankin, A. S.; Garrett, R. A. *J. Mol. Biol.*, 1998, **276**, 391-404.

263. Palmer, D. E.; Pattaroni, C.; Nunami, K.; Chadha, R. K.; Goodman, M.; Wakamiya, T.; Fukase, K.; Horimoto, S.; Kitazawa, M. *J. Am. Chem. Soc*, 1992, **114**, 5634-5642.

264. Carbery, D. R. *Org. Biomol. Chem.*, 2008, **6**, 3455-3460.

265. Terada, M.; Sorimachi, K. *J. Am. Chem. Soc.*, 2007, **129**, 292-239.

266. Naidu, B. N.; Sorenson, M. E.; Connolly, T. P.; Ueda, Y. *J Org Chem*, 2003, **68**, 10098-10102

267. Ferreira, P. M. T.; Maia, H. L. S.; Monteiro, L. S.; Sacramento, J. *J. Chem. Soc., Perkin Trans. 1*, 2001, 3167-3173.

268. Ranganathan, D.; Shah, K.; Vaish, N. *J. Chem. Soc., Chem. Commun.*, 1992, 1145.

269. Burrage, S.; Raynham, T.; Williams, G.; Essex, J. W.; Allen, C.; Cardno, M.; Swali, V.; Bradley, M. *Chem. Eur. J*, 2000, **6**, 1455-1466.

270. Okeley, N. M.; Zhu, Y.; Van der Donk, W. A. *Org Lett*, 2000, **2**, 3603-3606.

271. Strumeyer, D. H.; White, W. N.; Koshland, D. E. *Proc. Natl. Acad. Sci.*, 1963, **50**, 931-935.

272. Okawa, K.; Kinutani, T.; Sakai, K. *Bull. Chem. Soc. Jpn.*, 1968, **41**, 1353.

273. Burrage, S. A.; Raynham, T.; Bradley, M. *Tetrahedron Lett.*, 1998, **39**, 2831-2834.

274. Rich, D. H.; Tam. J. P. *J. Org. Chem.*, 1977, **42**, 3815.

275. Yamada, M.; Miyajima, T.; Horikawa, H. *Tetrahedron Lett.*, 1998, **39**, 289-292.
276. Delaet, N. G. J.; Tsuchida, T. *Lett. Pept. Sci.*, 1995, **2**, 325-331.
277. Alter, R.; Roy, J. *J. Org. Chem.*, 1971, **36**, 1971.
278. Hashimoto, K.; Sakai, M.; Okuno, T.; Shirahama, H. *Chem Commun.*, 1996, 1139-1140.
279. Sakai, M.; Hashimoto, K.; Shirahama, H. *Heterocycles*, 1997, **44**, 319.
280. But, T. Y. S.; Toy, P. H. *Chemistry An Asian Journal*, 2007, **2**, 1340-1355.
281. Nelson, S. G.; Spencer, K. L.; Cheung, W. S.; Mamie, S. J. *Tetrahedron*, 2002, **58**, 7081-7091
282. Stahl, G. L.; Walter, R.; Smith, C. W. *J. Org. Chem.*, 1978, **43**, 2285-2287.
283. Goodacre, J.; Ponsford, H. J.; Stirling, I. *Tetrahedron Lett.*, 1975, **16**, 3609-3612.
284. Greene, T. W.; Wuts, P. G. M.,3rd ed., *Protective Groups in Organic Synthesis*, John Wiley & Sons, New York, 1999.
285. Merrifield, R. B. *J. Am. Chem. Soc.*, 1963, **85**, 2149-2154.
286. Atherton, E.; Fox, H.; Harkiss, D.; Sheppard, R. C. *J. Chem. Soc., Chem. Commun.*, 1978, 539-540.
287. Atherton, E.; Logan, C. J.; Sheppard, R. C. *J. Chem. Soc., Perkin Trans. 1*, 1981, 538-546.
288. Merrifield, R. B. *Science*, 1986, **232**, 341-347.
289. Bayer, E.; Rapp, W. *Chemistry of peptides and Proteins*, 1986, **3**, 3-8.
290. Barany, G.; Sole, N. A.; Van Abel, R. J.; Albericio, F.; Selsted, M. E. *Innovations and Perspectives in Solid Phase Synthesis*, 1992, 29-38.
291. Chan, W. C.; White, P. D. Oxford University press, 2000
292. Barlos, K.; Gatos, D.; Kallitsis, J.; Papaphotiu, G.; Sotiriu, P.; Wenqing, Y.; Schäfer, W. *Tetrahedron Lett.*, 1989, **30**, 3943-3946.
293. Han, S.; Kim, Y. *Tetrahedron*, 2004, **60**, 2447-2467.
294. Coste, J.; Le-Nguyen, D.; Castro, B. *Tetrahedron lett.*, 1990, **31**, 205-208.
295. Subirós-Funosas, R.; Prohens, R.; Barbas, R.; El-Faham, A.; Albericio, F. *Chemistry*, 2009, **15**, 9394-9403.
296. Albericio, F.; Bofill, J. M.; El-Faham, A.; Kates, S. A. *J. Org. Chem.*, 1998, **63**, 9678-9683.

297. Dourtoglou, V.; Ziegler, J. C.; Gross, B. *Tetrahedron letter*., 1978, **19**, 1269-1272.

298. Carpino, L. A.; El-Faham, A.; Albericio, F. *Tetrahedron Lett.*, 1994, **35**, 2279-2282.

299. Jiang, S.; Li, Z.; Ding, K.; Roller, P. P. *Curr. Org. Chem.*, 2008, **12**, 1502-1542.

300. Olga Chatzi, L. B.; Gatos, D.; Stavroloilos, G. *Int. J. Peptide Protein Res.*, 1991, **37**, 513-520.

301. Davies, J. S. *J. Pep. Sci*., 2003, **9**, 471-501.

302. Mosmann, T. *Journal of Immunological Methods*, 1983, **65**, 55-63.

303. Hernandes, M. Z.; Cavalcanti, S. M.; Moreira, D. R.; De Azevedo, J. W. F.; Leite, A. C. *Curr. Drug. Targets*, 2010, **11**, 303-314.

304. Hrib, N. J. *Drugs Future*, 2000, **25**, 587-611.

305. Auffinger, P.; Hays, F. A.; Westhof, E.; Ho, P. S. *Proc. Natl. Acad. Sci*, 2004, **101**, 16789-16794.

306. Kraus, M.; Rückrich, T.; Reich, M.; Gogel, J.; Beck, A.; Kammer, W.; Berkers, C. R.; Burg, D.; Overkleeft, H.; Ovaa, H.; Driessen, C. *Leukemia*, 2007, **21**, 84-92.

307. Burkett, B. A.; Chai, C. L. L., *Tetrahedron Lett.*, 2000, **41**, 6661-6664.

308. Phillips, A.; Uto, Y.; Wipf, P.; Reno, M. J.; Williams, D. R. *Org. Lett.*, 2000, **2**, 1165-1168.

309. Xia, Z.; Smith, C. D. *J. Org. Chem.*, 2001, **66**, 3459-3466.